UNIVERSITE DE BOURGOGNE
Unité Mixte de Recherche
Procédés Alimentaires et Microbiologiques

UNIVERSITY OF BALAMAND
Faculty of Sciences
Department of Chemistry

Proton-Transfer-Reaction Mass-Spectrometry (PTR-MS) for the Study of the Aromatic Potential of Bakery Starter Strains

A THESIS

Submitted in Fulfillment of the Requirements for the Degree of

Docteur
De l'Université de Bourgogne
Discipline: Sciences de l'alimentation

Doctor of Philosophy
From the University of Balamand
Discipline: Chemistry

BY

SALIM SAMIR MAKHOUL

Defended on January 18, 2016

Thesis Director
Mr. Jean Guzzo

Thesis Co-director
Mr. Hanna El-Nakat

Jury

Mr. Jean Guzzo, Professor, Université de Bourgogne, Co-director
Mr. Hanna El-Nakat, Professor, University of Balamand, Co-director
Mr. Ibrahim Bou Malham, Professor, Lebanese University, Rapporteur and Chairman of the Jury
Mrs. Jacqueline Maalouly, Professor, Lebanese University, Rapporteur
Mr. Giuseppe Spano, Professor, University of Foggia, Member
Mrs. Stéphanie Weidmann, Maître de Conférences, Université de Bourgogne, Member and
Mr. Franco Biasioli, Doctor, Fondazione Edmund Mach, Member

UNIVERSITE DE BOURGOGNE
UMR-Procédés Alimentaires et Microbiologiques

UNIVERSITE DE BALAMAND
Faculté des Sciences

THÈSE

Pour obtenir le grade de

Docteur de l'Université de Bourgogne
Discipline : Sc. alimentation

Docteur de l'Université de Balamand
Discipline : Chimie

par

Salim Samir Makhoul

Soutenue le 18 Janvier 2016

Proton-Transfer-Reaction Mass-Spectrometry (PTR-MS) for the Study of the Aromatic Potential of Bakery Starter Strains

Directeur de thèse

M. Jean Guzzo

Co-directeur de thèse

M. Hanna El-Nakat

Jury

Prof. Guzzo, Jean, Université de Bourgogne, Co-directeur
Prof. El-Nakat, Hanna, Université de Balamand, Co-directeur
Prof. Bou Malham, Ibrahim, Université Libanaise, Rapporteur et Président du Jury
Prof. Maalouly, Jacqueline, Université Libanaise, Rapporteur
Prof. Spano, Giuseppe, Université de Foggia, Membre,
Dr. Stéphanie Weidmann, Université de Bourgogne, Membre et
Dr. Biasioli, Franco, Fondazione Edmund Mach, Membre

To Samir and Guilda,

Who brought me to this world!

To You, Nathalia,

My Love, my Life, my entire World!

To all those who Prayed

For me, from all over the World...

“It is Finished...”

Glory to God, the Creator of this World!

ACKNOWLEDGEMENTS

I always wondered whether I would ever reach the stage where I would be writing this part of my thesis, acknowledging all the people who helped me in fulfilling what was once a dream, later an ambition, and today a prideful reality. I thought it would be easy compared to the hours and days I spent, over the last three years of my PhD studies, trying to understand complicated matrices using novel analytical techniques... But instead, as I started to think of all the people who helped me, I stood in awe, and realized that whatever I say, I would never be able to thank you all and thank you enough!

It all started with one person who trusted me, chose me among hundreds of candidates for this scholarship position and this project, worked with me as a leader and never as a boss; guiding me, sharing with me his tremendous experience in PTR-MS and in life, understanding me, and listening to all the difficulties I was facing, not only as a researcher scientist, but also as a Lebanese guy working abroad, away from my family, my church and my suffering country. Dr. Franco Biasioli, not a single day will pass without me acknowledging that if I ever became a '*Doctor*' myself, it is thanks to you! I gratefully thank you and I hope that you really '*made the right choice*'.

Of course, my FEM supervisor Dr. Biasioli who is also the head of the Volatile Compounds facility at the *Research and Innovation Center* of the *Fondazione Edmund Mach*, couldn't have developed and carried out this project with me, without the support of the Foundation, its FIRS>T PhD school, and the Autonomous Province of Trento. I extend my thanks to all of them, and in particular for Dr. Roberto Viola, Dr. Alessandro Gretter, Dr. Elisabetta Perini, Mrs. Tiziana Gramazio and Dr. Flavia Zanon.

From January 2013, FEM became my second family, I started working in Italy with people whose experience promoted me to a higher level of maturity, professionalism and international scientific achievement. I specially thank Dr. Luca Cappellin with whom we accomplished the '*Ethylene*' project, at the early stages of my thesis; your genius and devotion has always inspired me. I deeply thank Dr. Andrea Romano for following each and every step of the '*ProBake'* project later on, from the experimental design, to the statistical data analyses, the presentations, the papers... You were always there when I needed you, with your expertise, your modesty and your sense of humor. Thank you! Since October 2014, I have been carrying

out the last part of my thesis under the assistance of Dr. Vittorio Capozzi, who kept me thinking, planning, working, discussing, yet laughing, while learning and learning a lot from him. I admire your humbleness and your dedication, and thank you for your continuous support.

My family abroad also consisted of many Doctors, technicians, colleagues and PhD students with whom I worked, lived, laughed, discussed my worries, defied many obstacles, shared the joy of many '*successes*', and the delights of my country whenever I came back from a visit to Lebanon, or whenever we had our delicious lunch-meetings. Thank you Dr. Flavia Gasperi, Dr. Eugenio Aprea, Dr. Isabella Endrizzi, Dr. Maria-Luisa Demattè, Dr. José Sànchez del Pulgar, Dr. Maria-Laura Corollaro, Dr. Brian Farneti, Dr. Valentina Ting, Dr. Mattéo Lanza, Mrs. Loredana Frizzera, Dr. Cristiano Vernesi, Mrs. Jessica Zambanini, Miss Emanuela Betta, as well as all the PhD students: Iulia Khomenko, Alberto Algarra Alarcon, Hugo Campbell Sills, Elisabetta Benozzi, Matteo Bergamaschi, Samiya Abdul Samad, Mastaneh Ahrar, Lama Wehbe, all the members of the Francophone Community at FEM and all the PhD students and Post-Docs in the open-space, in CRI and at FEM in general... I will forever cherish your help and kindness and the wonderful time we spent together... *Grazie per tutti*!

Moreover, I benefitted from the experience of many Professors from outside the Fondazione, whose contribution in my PhD is highly valued and appreciated, namely Professor Tilmann Märk, the Rector of the University of Innsbruck, Professor Matteo Scampicchio from the Free University of Bolzano, and Professor Giuseppe Spano from the University of Foggia.

Finally, I come to Marin Tudoroiu, my Romanian flatmate; thank you for the long cheerful talks we used to have, thank you for your company, your concern, and your friendship. Another important person who was there for me from day one: Dr. Mathilde-Clémence Charles. Dear Mathilde, your care and encouragement brought warmth to my heart and hope to my soul, from your words, your wisdom and even your silence I learned a lot! Merci! And last but not least, I extend my words of gratitude and appreciation for Sine Yener, my colleague, my lab partner, my "kitchen-mate", my shoulder to cry on, my best friend from Antioch! Sine, no words can describe how thankful I am for having you in my life, day in day out, as a sister and true friend! '*teşekkür ederim*' or should I say '*Choukran'* in Arabic!

It is true that spending my research years in Italy pulled me away from my family and my church, but miraculously, I found myself surrounded by angels whose prayers and love kept my days blissfully running. In this regard, I cannot but mention '*Likaat Rouhie*', its founder Archimandrite Evyenius Aranki and all my brothers and sisters with whom I prayed on Skype

every single night for the past three years. You were my strength and you will always be in my prayers, keep me in yours!

A researcher in Italy, but also a PhD student in France and Lebanon. Dr. Biasioli and Dr. Romano worked on choosing the most suitable partner universities for my project and my future plans, and only few months after receiving the FIRS>T PhD scholarship, and publishing our first paper, a cotutelle agreement was signed between the University of Burgundy in Dijon-France, and the University of Balamand in El-Kourah-Lebanon. In this context, I thank all the employees at both universities and doctoral schools who made sure that this convention was being respected despite all the obstacles. In particular, I would like to thank Prof. Jean Guzzo, my PhD advisor in France for according me trust, autonomy and continuous guidance and support. Your perpetual appreciation for my approach and my work kept me aiming for more, and thus achieving much more! It was my honor to be your PhD student!

Flying back to Lebanon brought me to the welcoming arms of my mother-University, the University of Balamand, where I learned the meaning of '*the truth that will set me free*'. I am grateful for its President Dr. Elie Salem, the Vice-President Dr. Georges Nahas and the dean of the Faculty of Sciences Dr. Jihad Attieh for their care and support throughout these years, without forgetting the blessings of His Beatitude Patriarch John X, His eminence Metropolitan Spiridon El-Khouy and the prayers of the Very Reverend Father Georges Maalouf (my beloved spiritual father), and the Very Reverend Father Mikhail El Khoury. Furthermore, I thank all the fathers and friends at the St. John of Damascus Institute of Theology and the St. Georges Orthodox Church in Hoch el Omara for their prayers, as well as all my colleagues in the Chemistry Department, in particular Mrs. Amal Aoun El-Murr, Miss Dima Moussa, Miss Sherine Saliba, Miss Aida Younes and especially Dr. Mira Younes Mitri whose continuous support made these hard years much easier. This all brings me to the Chairman of the Chemistry Department, Prof. Hanna El-Nakat, my advisor and mentor. I always looked up for you as a role model grasping from your experience, your virtues, your achievements, your vision, your commitment... You believed in me, and this work today is the fruit of your trust, and the root for more '*successes*' in the future, if God permits.

I also extend my regards to the two reporters who evaluated my thesis, Prof. Jacqueline Maalouly and Prof. Ibrahim Bou Malham. Thank you for taking the time to read my work, and for your positive and constructive feedback.

On a more personal level, and from Lebanon, many '*Besties'* never missed a day without expressing their care and support, I cannot thank you enough Maria and Antoine Bechwaty,

Rana Ahdab, Kamal Akl and family, Cynthia Assaf, Elie Issa, Bianca Salloum, Rabia Osseis, Chafic and Siham Abou Fayçal, Camil Baz and family, Chafic and Sarah Chebib, my theology classmates and schoolmates, the Nabhan family... And last but not least, I thank Nelly Bitar for spicing up my days, in 'her own way' with infinite affection and endless care, as well as Ronald Jabbour, who blessed my life by being part of it, and taught me the meaning of having a true friend, a real 'best man', and a lifetime brother. '*Cheers to a success we weaved altogether!*' With this toast, I also thank my in-laws, El-Haber family: Michel and Rafka, their daughters Dr. Dina and her husband Dr. Naji Salibi, Carla, Denise, Myriam and her husband Tony Freiha, '*Jeddo Amin*', Uncles Antoine, Issam, Nassib, Jean and their families. As for my '*second in-laws'*, Nada and Yara Antoun, I love you so much, and Gaby, your memory shall be eternal!

My thoughts go now to my own big family, my grandmothers Georgette and Gloria, my aunts Najwa, Leina and Sylvie, my uncles Antoine, Mourad and Georges, and all their families along with those who rested in the Lord: my grandfather Salim, Uncle Joseph and '*Jeddo Jean*', I miss you! I come to you Ola, my sister and idol; with your husband Jamil, you were my inspiration and my refuge in times of trouble, your guidance and personal experience gave me strength, hope and confidence that distance never kills true love and that hard work always pays off! As for you Nour, my younger sister and princess, you always knew how to raise me up, with your words, affection and sense of humor, and the prayers and wisdom of your husband, Father Youhanna, and the joy brought to my heart by your children, Maximos and Paraskévi; '*Mim loves you, khalo!*' At this moment, all that comes to my mind are the words of my late father, Samir, to my pious mother, Guilda, he told her once: '*I am not afraid, Salim can make it no matter what...*' Yes dad, I could only make it thanks to you, my guardian angel, and to my mom, my true wonder woman, my superhero! I hope I made you proud...

At the end, the flaming motive behind this achievement is you Nathalia, my wife, the Love of my life, the color of my life, my life itself! If I used words to thank all the others for their tremendous support, in front of yours, I stand in silence, praying to God to grant me all what it takes to compensate for the suffering I caused by being away from you, and to live up to the unconditional love you keep pouring in our relationship. '*I have loved you for a thousand years, I'll love you for a thousand more!*' and much more!

O Holy Trinity, I did '*Cast my cares on You'*, and through the intercessions of Your Mother, the most Holy Theotokos, my Patron-Saint Stefanos, and the prayers and support of all those I have just mentioned, You sustained me and I am sure You will keep doing so... Glory be to Your name, Amen!

TABLE OF CONTENTS

LIST OF TABLES

LIST OF FIGURES

LIST OF APPENDICES

"The kingdom of heaven is like yeast
that a woman took and mixed
into about three measures of flour
until it worked all through the dough"

MATTHEW 13:33

Introduction

1. Introduction (in French)

La bio-préservation des matières premières comestibles et périssables à travers le processus de fermentation représente la première application biotechnologique et l'une des premières formes de traitement alimentaire dans l'histoire humaine. La saveur demeure un des facteurs qui caractérise principalement le degré de la typicité des produits fermentés et influence l'acceptabilité des consommateurs. Un grand nombre de composés organiques volatils (COV) responsables de la perception de la saveur (et du mauvais goût des aliments) sont d'origine microbienne. Par conséquent, les composés organiques volatils microbiens, influençant la qualité des aliments, affectent les préférences des consommateurs concernant les aliments fermentés, le pain dans notre cas. Le grand nombre de variables géographiques, microbiologiques et technologiques souligne l'ample nécessité de développer des technologies bien adaptées en vue d'améliorer l'acceptation de ces aliments fermentés traditionnels par les consommateurs.

Les technologies de Spectroscopie de Masse par Injection Directe (SMID), associant la résolution temporelle avec la grande sensibilité et la robustesse, offrent des aperçus intéressants dans le domaine. La Réaction de Transfert Protonique, combinée à un Spectromètre de Masse à temps de vol (PTR-ToF-MS) est une approche analytique basée sur l'ionisation chimique et qui appartient aux technologies SMID. Ces techniques ont consenti la détermination rapide des Composés Organiques Volatils dans les échantillons, assurant une haute sensibilité et précision. En général, PTR-MS ne nécessite pas de préparation de l'échantillon ni la destruction de l'échantillon, ce qui permet l'analyse des échantillons d'une façon non invasive et en temps réel. Les Caractéristiques de la PTR-MS sont exploitées dans de nombreux domaines, de la chimie de l'environnement, à la chimie atmosphérique, aux sciences médicales et biologiques.

Dans les dernières années, PTR-ToF-MS a été également appliquée en sciences et technologies des aliments, englobant des études telles que la comparaison des COV dans

l'espace libre par rapport à l'espace nasal, la simulation des conditions in vivo (par exemple la simulation de la bouche humaine), la réalisation des empreintes complètes des COV comme une méthodologie de profilage, l'étude des COV associés aux différents producteurs, l'analyse de l'impact des différents procédés technologiques sur la teneur en COV, ainsi que le suivi en ligne des COV libérés lors de la fermentation des aliments.

Dans cette thèse, les améliorations les plus récentes que nous avons introduites sur cette technique, pour la première fois, sont discutées et validées. En fait, après avoir testé la méthode des Ions Réactifs Commutables pour étudier une molécule simple d'éthylène, nous avons développé une méthodologie analytique fondée sur le couplage de PTR-ToF-MS avec un échantillonneur automatique et suivie d'outils avancés d'analyse de données, afin d'augmenter le degré de l'automatisation et, par conséquent, d'accroître le potentiel de cette technique. Cette approche a permis l'analyse de séries d'échantillons plus vastes et plus complexes (par exemple la fermentation de la pâte), pour étudier plusieurs modes expérimentaux (par exemple différents types de farine, différentes levures, différentes heures d'incubation), afin de surveiller le bioprocédé de panification en termes de la teneur en COV. Dans ce projet, les résultats de notre approche sur le modèle simple choisi (*c.à.d.* l'éthylène) sont présentés. Ensuite, cette méthodologie est appliquée sur une matrice complexe qui n'a jamais été étudiée avant avec cette technique: la pâte, le levain et le pain cuit (recette traditionnelle adaptée du Sud de l'Italie). Par conséquent, nous révélons: i) la détection des COV libérés pendant la fermentation alcoolique de la pâte (étude en ligne du bioprocédé de panification), ii) l'étude de l'interaction entre les différents ingrédients, iii) l'élution des COV résultants de la cuisson, iv) ainsi que le profil volatile d'un modèle de levain basé sur la réalisation des volatomes complets de *Saccharomyces cerevisiae* et *Lactobacillus sanfranciscensis.*

L'objectif général de ce projet est de concevoir des approches "sur mesure" pour comprendre profondément le bioprocédé étudié, améliorer la préservation de l'authenticité et la

gestion de l'innovation dans le domaine des aliments fermentés traditionnels, un secteur fascinant de l'industrie alimentaire pertinente pour l'économie et pour la nutrition humaine. En outre, les techniques SMID, et en particulier la PTR-MS, offertes comme des outils rapides et à haut débit pour l'analyse des aliments, représentent une occasion pour la formulation de nouvelles hypothèses en science alimentaire et nutrition, en particulier à la lumière de l’attention qui a été récemment attribuée aux aliments fermentés comme de précieux modèles d'écosystèmes microbiens.

1. Introduction (in English)

The bio-preservation of perishable edible raw materials through fermentations represents the first biotechnological application and one of the first forms of food processing in human history. Flavor is one of the factors which mainly characterizes the degree of typicality of fermented products and influences consumers' acceptability. Many Volatile Organic Compounds (VOCs) responsible for flavor (and off-flavor) perception are of microbial origin. Hence, microbial Volatile Organic Compounds (mVOCs), influencing the quality of food, affect consumer preference on fermented food, bread in our case. The huge number of geographical, compositional, microbiological and technological variables highlights the important need for tailored technologies to improve consumer acceptance of these traditional fermented foods.

Direct-Injection Mass Spectrometric (DIMS) technologies, associating time resolution with high sensitivity and robustness, offer interesting insights in the field. Proton-Transfer-Reaction (PTR), combined to a Time-of-Flight (ToF) Mass Spectrometer (MS) is an analytical approach based on chemical ionization which belongs to the DIMS technologies. These techniques consented the rapid determination of VOCs in samples, assuring high sensitivity and accuracy. In general, PTR-MS doesn't require neither sample preparation nor sample destruction, which allows real time and non-invasive analysis. PTR-MS features are exploited in many fields, from environmental and atmospheric chemistry to medical and biological sciences. In the last years, PTR-ToF-MS has been also applied in food science and technology, encompassing studies such as comparison of headspace versus nose-space VOC analysis, simulated in vivo conditions (e.g. simulating human mouth), VOC fingerprinting as a profiling methodology, VOCs associated with different producers, impact of different technological processes on VOC content, as well as the on-line monitoring of VOCs released during food processing.

In this thesis, the recent upgrades we introduced on this technique, for the first time, are discussed and validated. In fact, in addition to the Switchable-Reagent-Ion tested to study a simple Ethylene molecule, we developed an analytical methodology based on the coupling of PTR-ToF-MS with an autosampler and tailored data analysis tools, in order to increase the degree of automation and, consequently, to enhance the potential of this technique. This approach, permitted the screening of larger and more complex sample sets (*i.e.* fermenting dough), to analyze several experimental modes (*e.g.* different flour types, different yeast starters, different incubation hours), in order to monitor the bread-making bioprocess in terms of VOC content. In this work, the results of our approach on the simple chosen model are reported. Afterwards, this methodology is applied on a complex matrix which has never been studied before using this technique: dough, sourdough and baked bread (a traditional recipe adapted from Southern Italy). Hence, we report: i) the detection of VOCs released during alcoholic fermentation of the dough (on-line bioprocess monitoring), ii) the study of the interaction between different ingredients, iii) the monitoring of VOCs arising upon baking, iv) as well as the volatile profile of a sourdough model based on the realization of the complete volatomes of *Saccharomyces cerevisiae* and *Lactobacillus sanfranciscensis*.

The general aim of this project is to conceive 'tailored' approaches to improve authenticity preservation and innovation management in the field of traditional fermented foods, a fascinating sector of the food industry relevant for the economy and for human nutrition. In addition, DIMS techniques, and especially PTR-MS, if considered high-throughput and rapid applications in 'foodomics' analysis, represent an intriguingly opportunity for the formulation of new hypotheses in food science and nutrition, particularly in the light of the recent attention attributed to fermented foods as valuable models of microbial ecosystems.

Bibliography

2. Bibliography

2.1 Volatile Organic Compounds

2.1.1 Definition and origins

The World Health Organization (WHO), as cited in ISO 16000-6, defined as a Volatile Organic Compound (VOC) any organic compound whose boiling point is in the range from (50 °C to 100 °C) to (240 °C to 260 °C), corresponding to having saturation vapor pressures at 25 °C greater than 100 kPa ("ISO 16000-6:2011 - Indoor air -- Part 6: Determination of volatile organic compounds in indoor and test chamber air by active sampling on Tenax TA sorbent, thermal desorption and gas chromatography using MS or MS-FID,").

Other definitions of VOCs are influenced by the concerned field of study. For instance, in 1993, H.W. Art defined VOCs as "hydrocarbon compounds that have low boiling points, usually less than 100ºC, and therefore evaporate readily. Some are gases at room temperature. Propane, benzene, and other components of gasoline are all volatile organic compounds" (Art, 1993). In their turn, Lincoln et al. stated that "Volatile Organic Compounds are released into the atmosphere by anthropogenic and natural emissions which are important because of their involvement in photochemical pollution" (Lincoln, Boxshall, & Clark, 1998). Later, in 2006, Zogorski et al. defined them as "ground-water contaminants of concern because of very large environmental releases, human toxicity, and a tendency for some compounds to persist in and migrate with ground-water to drinking-water supply well … In general, VOCs have high vapor pressures, low-to-medium water solubilities, and low molecular weights. Some VOCs may occur naturally in the environment, other compounds occur only as a result of manmade activities, and some compounds have both origins" (Zogorski et al., 2006).

Finally, the U.S Geological Survey defined VOCs as "organic compounds that can be isolated from the water phase of a sample by purging the water sample with inert gas, such as

helium, and, subsequently, analyzed by gas chromatography. Many VOCs are human-made chemicals that are used and produced in the manufacture of paints, adhesives, petroleum products, pharmaceuticals, and refrigerants. They often are compounds of fuels, solvents, hydraulic fluids, paint thinners, and dry-cleaning agents commonly used in urban settings. VOC contamination of drinking water supplies is a human-health concern because many are toxic and are known or suspected human carcinogens" (Survey).

From these various yet close definitions, one can infer that VOCs are organic hydrocarbons with high vapor pressure and low boiling point, which causes large numbers of molecules to evaporate or sublimate from the liquid or solid form of the compound and enter the surrounding air. In addition, the origin of VOCs can be either biogenic (produced naturally by living organisms) or anthropogenic (produced directly by human activities); hence, many hundreds of these compounds are present in the atmosphere and spaces surrounding any process namely headspace, nose-space, etc.

In more details, and without considering microbes, natural biogenic sources include the emission of organic gases by living species, both plants and animals (summarized in **Figure 1**). A well-known example, discussed in a review by Blake et al., is the emission of a variety of gaseous organic compounds in the breath of animals, which are released from both the digestive system and the lungs. Plants are also major sources of organic gases, as is the decay of dead animal and plant matter. Subsequent photochemistry can add further compounds to the mixture. Consequently, even without contributions from humans, ambient air from the Earth's atmosphere would consist of a complex mixture of VOCs. On the other hand, anthropogenic sources of VOCs include emissions from the extraction and refining of fossil fuels, the incomplete burning of fossil fuels by motorized transport and by heat and electrical power

generators, the evaporation of solvents employed in industrial and domestic operations, and the leakage of gases from landfill sites (Blake et al., 2009).

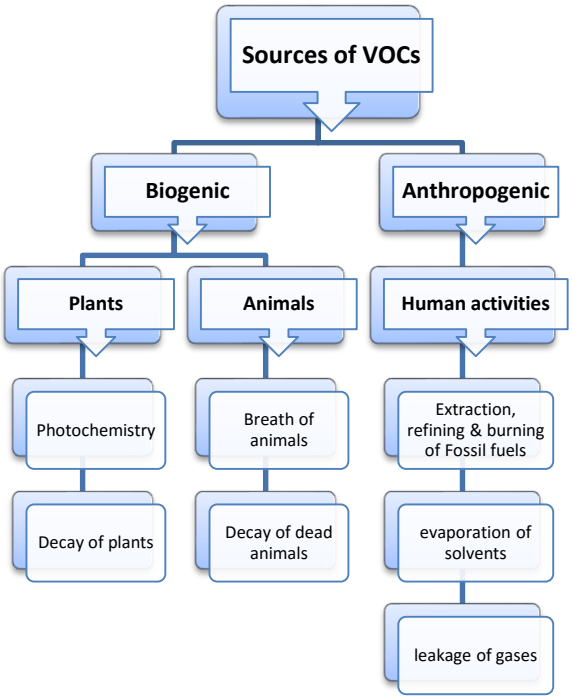

Figure 1. A summary of the origins of VOCs with some given examples (Blake, Monks, & Ellis, 2009)

By far, the most common organic compound found in the Earth's atmosphere is methane (CH_4), but even this compound is only present at an average level of around 2 parts per million by volume (2 ppmV). After methane, the most abundant VOCs include ethane, propane, isoprene, acetone, and methanol, but typical mixing ratios for these compounds are in the region of a few parts per billion by volume (ppbV) (Blake et al., 2009).

2.1.2 Applications and Importance of VOCs

Whether released from biological or technological processes, and even at very low concentrations, VOCs are ubiquitous and deemed important in several fields including

environmental and atmospheric chemistry, plant biology and medical sciences (Cappellin et al., 2013).

They also play a most relevant role in agro-industrial processes, and food science and technology. The principal reason is that they are at the origin of both the aroma and flavor of food and hence control human sensory perception of food (Biasioli, Gasperi, Yeretzian, & Märk, 2011). Thus, amelioration in food quality must also consider its complex flavor profile, the origin of this profile, its evolution in time and the interaction with people (Klee, 2010). A second reason for the relevance of VOCs in food science is that they are produced and released in most stages of the food-production chain ‘‘from farm to fork’’ (*i.e.* from plants and crops, during fruit ripening and maturation, in food processing and storage and, eventually, during food consumption). They also create an interesting link to atmospheric studies because, in several regions, Biogenic VOC (BVOC) emissions are, at least for certain species, dominated by emissions from crops (M. Karl, Guenther, Köble, Leip, & Seufert, 2009). Direct BOVC monitoring is therefore an important non-invasive tool for product characterization and process monitoring in agro-industrial applications. Given this, it does not come as a surprise that there is a huge literature on VOCs in food, mostly of biogenic origin. A general reference for technical aspects, not limited to foods, mentioned in a recent review (Biasioli, Gasperi, et al., 2011), is the book edited by Berger which also includes interesting chapters on biogenic precursors of flavor compounds and bioprocessing (Berger, 2007). Two additional references in this context are a recently edited book by Taylor and Linforth (A. Taylor, 2010), and the review of Ross on studies related to sensory analysis and instrumental characterization of food (C. F. Ross, 2009). It is therefore clear that the success of future research in this field will also depend on the available methods to identify, to quantify and to monitor the olfactory stimuli (*i.e.* VOCs) (Biasioli, Gasperi, et al., 2011).

In more general terms, according to Cappellin et al., an efficient monitoring of VOCs needs analytical techniques that are capable of dealing with challenging issues:

1. the need to separate and quantify VOCs in complex gas mixtures;
2. the need to detect a wide range of concentrations, from trace levels to parts per million or more;
3. the need to track concentrations that rapidly change in time.

Because of these experimental constraints, the ideal methodology for VOC monitoring should be highly selective, with high sensitivity and dynamic range, and high time resolution. “Fulfilling all requirements is still a challenge” (Cappellin et al., 2013).

2.2 Detection techniques

Numerous analytical and sensory techniques have been developed to study VOCs. These techniques include liquid/liquid extraction (Weurman, 1969), simultaneous steam distillation and liquid extraction (Nickerson & Likens, 1966), static (Chialva, Gabri, Liddle, & Ulian, 1982) and dynamic headspace analysis (Werkhoff & Bretschneider, 1987), capillary gas chromatography with mass spectrometry (GC-MS) coupled with olfactometric detection (Grimm, Lloyd, Miller, & Spanier, 1997; Marsili, 1999a), solid-phase micro-extraction followed by GC-MS (Arthur & Pawliszyn, 1990). VOCs can also be detected using Direct-Injection Mass Spectrometric (DIMS) techniques. These represent a class of analytical instrumental approaches which offers considerable mass and time resolution with high sensitivity and robustness, allowing the quick detection and quantification of (VOCs) (Biasioli, Yeretzian, Märk, Dewulf, & Van Langenhove, 2011). To this category belong, among others, Atmospheric-Pressure Chemical Ionization Mass Spectrometry (APCI-MS), MS-electronic-nose detection (Marsili, 1999b; Zohora, Khan, Srivastava, & Hundewale, 2013), Atmospheric

Pressure Chemical Ionization-MS (APCI-MS) (Berchtold, Bosilkovska, Daali, Walder, & Zenobi, 2014), as well as Ion Mobility Spectrometry, the Flowing Afterglow technique, Secondary Electrospray Ionization Mass Spectrometry (SESI-MS), and Selected Ion-Flow-Tube Mass Spectrometry (SIFT-MS) (Ellis & Mayhew, 2013).

Many reviews discussed the advantages and limitations of these techniques; For instance, MS-e-noses, by simulating the behavior of human olfaction, provide a digital fingerprint of the analyzed product, with good prospect for the large sample sets screening (Ballabio, Cosio, Mannino, & Todeschini, 2006; Biasioli, Yeretzian, et al., 2011), but with possible disadvantages such as high sensitivity to moisture, poor linearity, and poor reproducibility. APCI, performing ionization at atmospheric pressure, lessens any loss of volatiles addressable to an inefficient transport of neutral molecules into the vacuum, considered to be robust, sensitive, and reproducible in flavor-release applications (Berchtold et al., 2014; Biasioli, Yeretzian, et al., 2011). However, APCI ionization is quite complex due to the presence of many possible ionization agents (Ellis & Mayhew, 2013).

Among all these techniques, there is no doubt that GC-MS remains the most established for identification and quantification of VOCs (Biasioli, Gasperi, et al., 2011; Cappellin et al., 2013). GC-MS systems have high precision and, if coupled with pretreatment and pre-concentration stages, they can reach detection limits as low as 0.1 pptv. GC-MS is, therefore, the ‘gold standard’ for trace gas analysis (Ellis & Mayhew, 2013); nevertheless, even this technique, as discussed in the next section, suffers from a relatively low time resolution and risk of artefacts (Cappellin et al., 2013).

2.2.1 Gas Chromatography and its Limitations

2.2.1.1 Basic GC Principles

The basic principle behind GC is that the constituents of a flowing gas mixture (the mobile phase) can be separated by passage over a suitable liquid or solid (the stationary phase). Partitioning between the mobile and stationary phases can lead to different retention times for different compounds due to differences in the way each compound in the gas interacts with the stationary phase. This difference in retention times characterizes GC detection (Pecsok, 1959).

As illustrated in **Figure 2**, the sample is injected into the injection point and is carried by the mobile gas into the column. Inside the column, the components get separated by differential partition in between the mobile phase gas and stationary phase liquid. The component that partitioned into gas comes out of the column first and is detected by detector. The one partitioned into liquid phase comes out later and is also detected. The recordings are displayed as a plot onto a computer software. Such a plot is known as a gas chromatogram. From the peaks on the chromatogram one can identify the components and also their concentration.

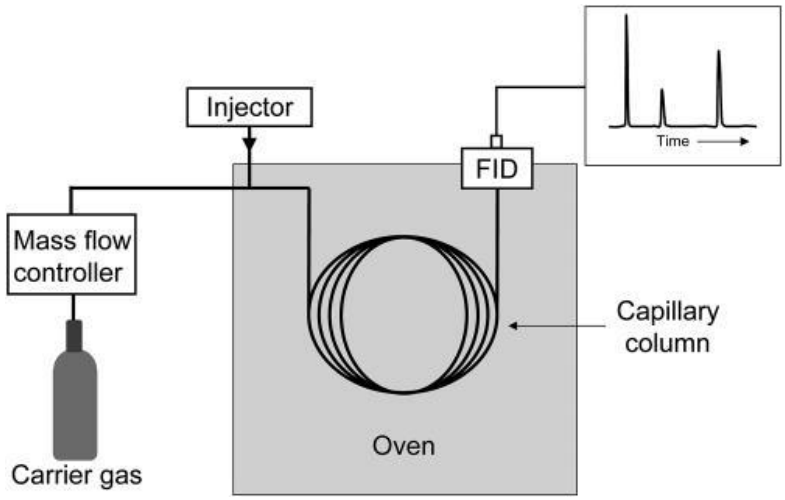

Figure 2. Schematic diagram of a GC instrument with a flame ionization detector (FID). An analyte gas is injected into a flow of inert carrier gas at the injector. The gradual separation of compounds in the column leads to elution of distinct compounds at different (retention) times, as measured by the FID, leading to a chromatogram such as that shown in the upper right of the diagram. (Ellis & Mayhew, 2013)

2.2.1.2 Types of GC Detectors

There are several types of detectors which can be coupled to a gas chromatograph. One example is the flame ionization detector (FID) which works best for compounds such as hydrocarbons and is therefore not a universal detector. Other types of well-known GC detectors include the electron capture detector (ECD) and the thermal conductivity detector (TCD), and as with FID these alternatives also have their strengths and weaknesses (Karasek & Clement, 2012).

Another limitation is compound identification, since there is always the possibility, particularly with complex mixtures, that two or more compounds may have very similar retention times and therefore cannot be distinguished in this way. To get around these limitations, the FID, ECD or TCD can be replaced with a mass spectrometer (MS) equipped with an electron impact ionization source. In most cases, the mass spectrometer is of the quadrupole variety.

The instrument works by recording a whole series of mass spectra, one after the other, as the analyte elutes through the column. In this way, important analytical information is obtained from both the retention time and the mass spectrum. The mass spectrum recorded for a particular GC peak can be compared with those stored in a library on the control computer, which usually allows compound identification. GC–MS is an extremely valuable analytical tool, but it suffers from a lower detection sensitivity than GC-FID because of the scanning time of the mass spectrometer, and so for air analysis it is often used more for compound identification than for quantification (Ellis & Mayhew, 2013).

From the description above, some of the limitations with GC and its variants become clear. It is not a universal technique, since the choice of trap and column will affect the sensitivity and accuracy towards certain classes of compounds. Another particularly serious matter in GC analysis is the speed of measurement which, because of the need for sample

collection and also some degree of pre-concentration, is often limited to a single measurement every few minutes, at best. Consequently, if rapidly evolving gas systems are being explored, GC is still a time-consuming procedure (López-Feria, Cárdenas, & Valcárcel, 2008).

In conclusion, from a technical point of view, GC is the reference method for the analysis of VOCs. But there is also a growing need to develop rapid, simpler methods to overcome its main limitations. In fact, there is genuine interest in the development of methods for rapid, non-invasive and very sensitive monitoring of volatile compounds emitted (Biasioli, Gasperi, et al., 2011). Among the various possibilities proposed and investigated for rapid identification and quantification of VOCs is Proton-Transfer-Reaction Mass Spectrometry (PTR-MS) which is considered to allow rapid, direct and highly sensitive on-line monitoring of VOCs (Biasioli, Gasperi, et al., 2011; Buhr, van Ruth, & Delahunty, 2002; Cappellin et al., 2013; Jordan, Haidacher, Hanel, Hartungen, Märk, et al., 2009; W. Lindinger, Hansel, & Jordan, 1998).

2.2.2 Proton-Transfer-Reaction Mass Spectrometry (PTR-MS)

Before going deeper into the history, principles and upgrades of this technique, it is important to summarize the basics of mass spectrometry in general, as well as the most common ionization techniques currently applied.

2.2.2.1 Basic principles of Mass Spectrometry

2.2.2.1.1 Main components of a mass spectrometer

The main components of a mass spectrometer are (**Figure 3**) (Agarwal, 2012):

(1) The ion source: produces ions from the studied samples.

(2) The mass analyzer: separates ions according to their mass-to-charge ratio.

(3) The ion detector: detects the ions, providing the relative abundance of each of the resolved ionic species.

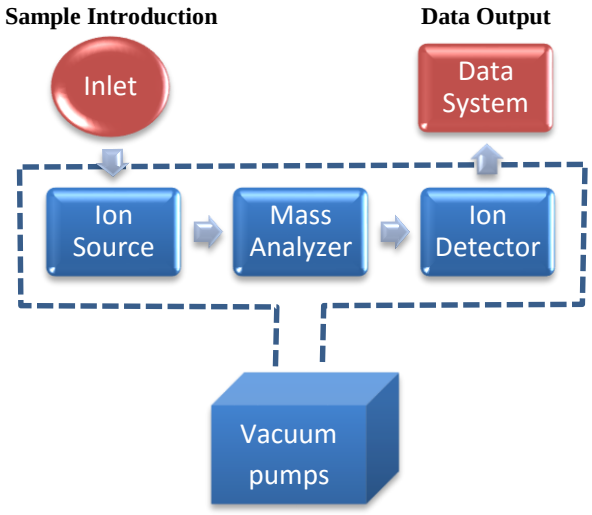

Figure 3. Schematic representation of the basic components of a mass spectrometer

The number and the relative abundance of the produced ions is mainly related to the ionization technique, which therefore plays a key role in determining which types of samples may be analyzed with a specific mass spectrometer.

2.2.2.1.2 Ionization Techniques

The most commonly used ionization techniques are electron ionization and chemical ionization:

(1) Electron ionization (EI) is produced by the impact of an energetic electron carrying usually 70 eV of kinetic energy with a neutral. If the energy transferred in the collision reaction exceeds the ionization energy (IE) of the neutral, then ionization occurs, generating a positive ion, which can be singly, doubly or even triply charged. Since high energy is usually involved in this process, fragmentation of the produced ions often occurs, thus making this a “hard” ionization technique (Harrison, 1992).

(2) Chemical ionization (CI) is used to produce ionized species by interaction of gaseous molecules with ions. The reaction may involve the transfer of an electron, proton or

other charged species between the reactants. Less energy is involved in this process, resulting in a lower fragmentation of the produced ions. This technique is considered as a "soft" ionization process (Harrison, 1992). A technique which produces less fragment ions is often preferred because of the possibility of obtaining mass spectra with a higher ion yield of the charged parent molecule. This leads both to an easier interpretation of the mass spectra, especially in case of mixtures, and an easier quantification of the analyte molecules (Lanza et al., 2015).

This brings us to the detection technique defended in this thesis as an optimal combination between many desired features: Proton-Transfer-Reaction Mass Spectrometry (PTR-MS). In fact, PTR-MS focuses on sensitivity and, thanks to the recent implementation of high-resolution mass analyzers, on chemical information. The further coupling with automated sampling systems and tailored data analysis tools constitutes a complete set-up which is suitable both for the identification of very small quantities of VOCs and real-time monitoring of VOCs without sample preparation (Makhoul, Romano, Cappellin, Spano, Capozzi, Benozzi, Märk, Aprea, Gasperi, & El-Nakat, 2014; Romano, Capozzi, Spano, & Biasioli, 2015b; Romano et al., 2014; Yener et al., 2014).

2.2.2.2 Historical Developments of PTR-MS

The development of the proton transfer technology started with first studies on the reaction kinetics in the gas phase. In the 1960s, Ferguson et al. developed the Flowing Afterglow (FA) technique (Ferguson, 1992). This technique represented a first effective tool for the study of reaction kinetics under varying conditions (*e.g.* temperature) and reaction partners (Bohme, Dunkin, Fehsenfeld, & Ferguson, 1969). Reactant ions are produced by an ion source and are then carried and thermalized to room temperature through a Pyrex, quartz,

or stainless steel flow tube by a buffer gas (typically helium). The sample is introduced at some point into the flow tube and allowed to react with the reagent ions. The resulting swarm of ions is carried to the end of the flow tube by the buffer gas (Watson, 2009).

Together with these positive aspects, which enabled tremendous progress in the understanding of ion-molecule reaction kinetics, some negative ones had to be taken into account. The technique was, indeed, not thought for and not suitable for gas analysis, because of a too long residence time of the gas in the drift tube. The consequence of the latter has been the desorption of impurities from the walls and, therefore, a high background signal (Werner Lindinger, Fall, & Karl, 2001). However, even in the case of a low background signal, the lack of an ion selection system prior to the reactor made the interpretation or the resulting mass spectra particularly difficult, especially in the case of complex molecules, where numerous secondary ions could be produced (Blake et al., 2009; Bohme et al., 1969).

The successive step was the development of the so-called Selected Ion Flow Tube (SIFT) mass spectrometry (Adams & Smith, 1976). Similar to the FA, ions were produced by an electrical discharge, but a quadrupole mass filter was used to select the reagent ions prior to injection in the reaction section. A detailed study of the reactions between the selected ion and the analytes was, therefore, possible (Adams & Smith, 1976; Smith & Adams, 1987). More recently, this technique has been used for trace gas detection, selecting NO^+, O_2^+ and H_3O^+ as the reagent ions (Spanel & Smith, 1997; Španěl & Smith, 1998).

Before developing the modern PTR-MS technology, W. Lindinger et al. performed some experiments using a Selected Ion Flow Drift Tube-Mass Spectrometry (SIFDT-MS) instrument (Blake et al., 2009; Lagg, Taucher, Hansel, & Lindinger, 1994). In their work, an electric field was used together with the carrier gas flow, to increase the kinetic energy of the ion-molecule reaction and, consequently, the average collision velocity and the reaction probability of the ions with the buffer gas.

In 1995, the same group developed the modern PTR-MS technology at the University of Innsbruck, in Austria (Hansel et al., 1995; W. Lindinger et al., 1998). The major differences to SIFDT-MS were:

1. The replacement of the ion source with a hollow-cathode ion source, able to generate H_3O^+ primary ions at a very high purity level (> 99.5 %), thus making the use of a mass filter obsolete;
2. The use of a shorter drift tube, where sample air was used as the carrier gas. The components of air (e.g. oxygen, nitrogen) do not react with the reagent ion because of a lower proton affinity than water (PA= 691 kJ mol^{-1} or 165 kcal mol^{-1} (W. Lindinger et al., 1998)).

The resulting overall instrument is characterized by a much higher sensitivity (Blake et al., 2009).

2.2.2.3 Configuration of the PTR-MS instrument

The apparatus required to perform Proton-Transfer-Reaction Mass Spectrometry (PTR-MS) (illustrated schematically in **Figures 4 and 5**) includes the following (Ellis & Mayhew, 2013):

1. An ion source.
2. A drift tube.
3. A mass spectrometer.
4. An ion detector.
5. An instrumental control system.

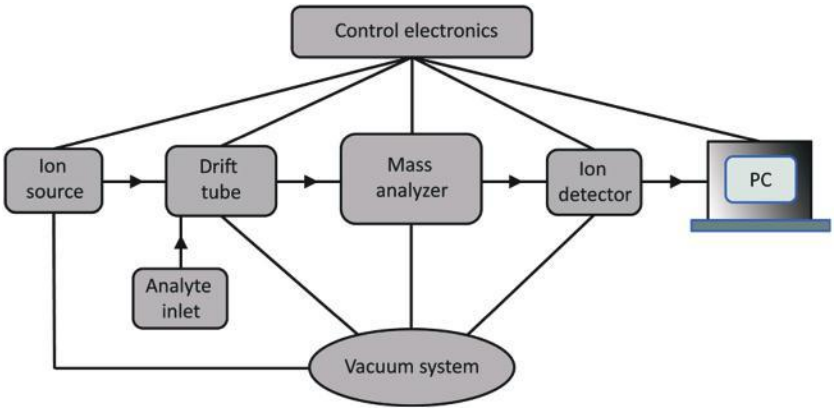

Figure 4. Simplified representation of the main constituents of a PTR-MS instrument.(Ellis & Mayhew, 2013)

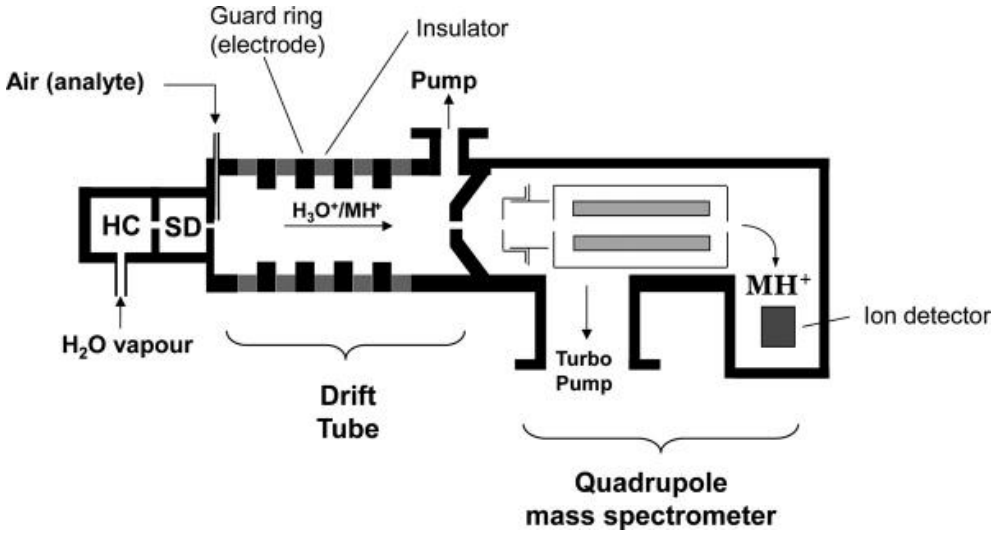

Figure 5. Schematic representation of a PTR-MS instrument, where in this case the mass spectrometer is a quadrupole device. HC signifies a hollow cathode discharge ion source and SD is known as the source drift region. (Ellis & Mayhew, 2013)

2.2.2.3.1 The Ion Source: Since H_3O^+ is normally used as the proton transfer reagent in PTR-MS, a source which generates this ion in high yield with little contamination from other ions is essential. The ion source of a typical PTR-MS system consists of a hollow cathode discharge source. This can be divided in three main regions, *i.e.* cathode, cathode fall and negative glow. High energy electrons undergo ionizing collisions with the neutrals in the source (*e.g.* water vapor, N_2 or O_2). This process takes place while electrons emitted from the

cathode through a mechanism of field emission move to the negative glow region, which is axial to the cylindrical cathode, between two anodes and close to anode potential. In case of water vapor, for example, several positive ions (*e.g.* OH^+, H^+. H_2^+, H_2O^+) are produced and, subsequently, are attracted to the cathode (Hansel et al., 1995). Secondary electrons are emitted when the produced positive ions hit the cathode's surface with a kinetic energy greater than its work function (*i.e.* the minimum energy required to remove an electron from a solid to a point in the vacuum immediately outside the solid surface). However, in the source drift region, most of the positive ions undergo secondary reactions with water producing H_3O^+ (**Reactions 1-12**). In addition, the secondary electrons traverse the cathode fall ionizing again neutral molecules. The result of all of these processes is the production of a plasma that is a highly ionized gas, with a relatively high density, in which the number of free electrons and cations is equivalent (House, 2009). In order to ignite the plasma discharge, a certain potential (approx. 500 V) applied to the two electrodes is needed. When operating in H_3O^+ mode, water vapor is fed to the ion source with a flow between 5 and 8 sccm (standard cubic centimeters per minute) and undergoes the following reactions (reactions 1-12) (Hansel et al., 1995; House, 2009):

$$e^- + H_2O \rightarrow H_2O^+ + 2e^- \quad (1)$$

$$e^- + H_2O \rightarrow H_2^+ + O + 2e^- \quad (2)$$

$$e^- + H_2O \rightarrow H^+ + OH + 2e^- \quad (3)$$

$$e^- + H_2O \rightarrow O^+ + 2H + 2e^- \quad (4)$$

$$e^- + H_2O \rightarrow OH^+ + H + 2e^- \quad (5)$$

$$O^+ + H_2O \rightarrow H_2O^+ + O \quad (6)$$

$$H^+ + H_2O \rightarrow H_2O^+ + H \quad (7)$$

$$H_2^+ + H_2O \rightarrow H_3O^+ + H \quad (8)$$

$$H_2^+ + H_2O \rightarrow H_2O^+ + H_2 \quad (9)$$

$$OH^+ + H_2O \rightarrow H_3O^+ + O \quad (10)$$

$$OH^+ + H_2O \rightarrow H_2O^+ + OH \quad (11)$$

$$H_2O^+ + H_2O \rightarrow H_3O^+ + OH \quad (12)$$

2.2.2.3.2 The Drift Tube: this second part has two purposes (Ellis & Mayhew, 2013):

a. It provides a reaction zone of fixed length, which is important for quantitative analysis;
b. The electric field, E, along the drift tube raises the kinetic energies of the ions relative to the neutral gas molecules. The resulting drift velocity of the positive ions, which is dependent on the ratio of E to the gas number density, N, in the drift tube, helps to prevent the formation of cluster ions such as $H_3O^+(H_2O)$ and $MH^+(H_2O)$ through moderately energetic collisional dissociation with neutral molecules, where M represents an analyte molecule.

When reacting with H_3O^+, analyte molecules undergo proton transfer reaction only if their proton affinity is greater than that of water (691 KJ mol^{-1}) (Jordan, Haidacher, Hanel, Hartungen, Herbig, et al., 2009) (**Appendix 1** provides an extensive list of studied VOCs along with their proton affinity, mass and protonated mass). The interaction taking place in the drift tube when using H_3O^+ as the reagent ion may result in proton transfer reactions of two types: non-dissociative (**Reaction 13**) or dissociative (**Reaction 14**):

Non dissociative: $H_3O^+ + A \rightarrow AH^+ + H_2O$ (Reaction 13)

Dissociative: $H_3O^+ + A \rightarrow (AH^+)^* + H_2O$

$$(AH^+)^* \rightarrow F^+ + N \qquad \text{(Reaction 14)}$$

where AH^+ is the protonated parent molecule, F^+ a fragment ion and N a neutral fragment (Ellis & Mayhew, 2013).

As already mentioned, if the PA of the molecule is greater than that of water, this reaction is energetically permitted. When the proton affinities of the reactants are close to each other, like in the case of formaldehyde for instance (Wisthaler et al., 2008), a considerable amount of protonated molecules might undergo the backward reaction, especially if the humidity in the drift tube is high. The formation of water clusters when operating at low E/N values represents an additional issue, because they may also react with the analyte molecules via proton transfer or ligand switching reactions (**Reactions 15-16**). The proton affinity of these ions is, however, higher than that of water (e.g. PA $_{(H_2O)_2}$ = 833.6 kJ mol^{-1}) (Kawai, Yamaguchi, Okada, & TAKEUCHI, 2004)

$$H_3O^+ \cdot H_2O + A \rightarrow AH^+ + 2H_2O \qquad \text{(Reaction 15)}$$

$$H_3O^+ \cdot H_2O + A \rightarrow AH^+ \cdot H_2O + H_2O \qquad \text{(Reaction 16)}$$

These kinds of reactions are more common for polar molecules containing a dipole moment, like acetaldehyde (Blake et al., 2009). The $AH^+.H_2O$ species may undergo further dissociation steps, depending on the stability of the formed cluster.

On the other hand, in case of O_2^+, or NO^+ as the reagent ions, other reactions may take place, i.e. charge transfer or hydride ion abstraction (Cappellin et al., 2014). These reactions are discussed in detail in section 2.2.2.6.2.

2.2.2.3.3 The Mass Spectrometer: this third part provides a means for separating ions according to their mass/charge ratio, m/z. Quadrupole (Quad) and time-of-flight (ToF) mass spectrometers have been employed in PTR-MS instruments.

Quad-MS: The Quad mass filter was the type of mass analyzer used in the earliest PTR-MS instruments and it is still the most popular choice at the time of writing. The popularity of the Quad-MS stems from its relatively compact size and reasonable price. A Quad-MS system contains four parallel metal rods positioned equidistant from the center, inside a vacuum chamber (**Figure 6**). A voltage in the Z-direction is used to accelerate ions into the system. Ions passing through the quadrupole are separated using an electric field, generated using a combination of direct current voltage U and high-frequency alternating current voltage V$\cos\omega$t (where ω is the frequency and t is the time). Opposite rods have an applied voltage of the same polarity. The result of this combination is the oscillation of the ions in the X and Y directions, while only ions of a specific m/z ratio are in resonance with this oscillation and thus, are able to pass through the quadrupole and reach the detector ("SHIMADZU CORPORATION,").

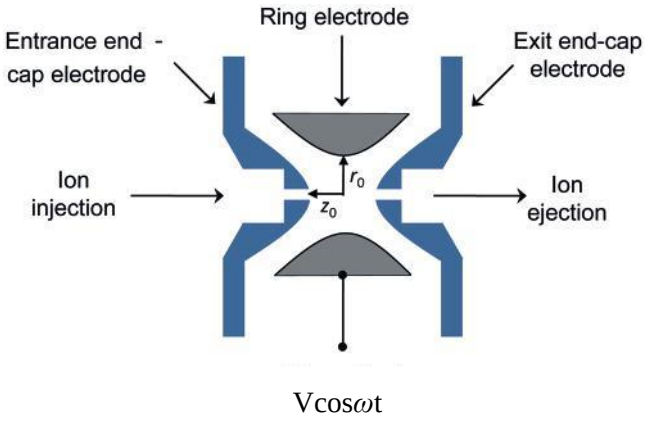

Figure 6. Cross-sectional view of a quadrupole ion trap. An appropriate voltage is applied to the incoming end-cap electrode to allow ions to enter. The outgoing end-cap electrode is then switched to a potential to slow this batch of ions down so that they can be kept inside the trap. A radiofrequency voltage is applied to the ring electrode to trap and then select/eject ions of the desired m/z. (Ellis & Mayhew, 2013)

ToF-MS: The simplest version of a TOF-MS (**Figure 7**) consists of a relatively short ion acceleration region and a much longer part known as the flight tube. Ions may be generated within the ion acceleration region (e.g. by electron impact or by photoionization) but in the case of PTR-MS the ions are generated externally by Chemical Ionization in a drift tube, which is coupled to the TOF-MS. These ions enter into the acceleration region along a direction perpendicular to the long axis of the flight tube, as shown in **Figure 7**, which will be referred to as the x direction: such an arrangement is known as orthogonal acceleration TOF-MS. The acceleration region is formed by two electrodes, known as the repeller and extractor electrodes. The extractor electrode is a high transmission grid to allow the majority of incident ions to pass through into the flight tube. The flight tube has no electrical field and therefore the velocity delivered to the ions in the acceleration region is maintained once they enter the flight tube. Initially, the repeller and extractor electrodes are kept at the same electrical potential in order to prevent deflection of the incoming ions. To obtain a mass spectrum, this voltage state is then altered rapidly such that the voltage on the repeller is higher than on the extractor. This potential gradient is used to send a pulse of ions into the flight tube and if a detector with sufficient sensitivity and sufficient speed of response is located near the end of the flight tube the arrival times of ions in the extracted packet can be determined. Heavier ions will take longer to reach the detector than lighter ions, and so measurement of the time-of-flight provides the basis for recording a mass spectrum (Ellis & Mayhew, 2013).

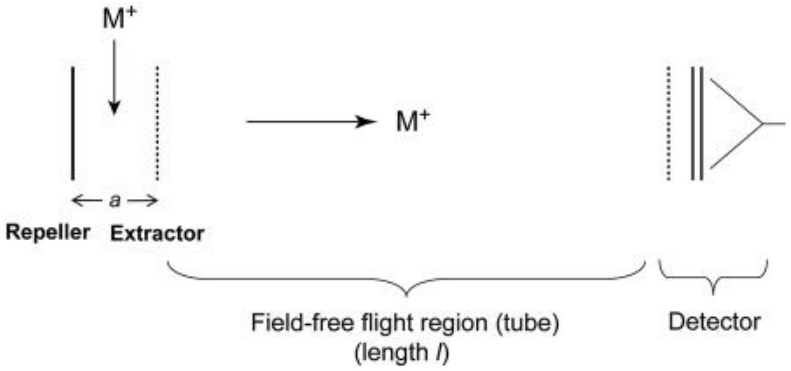

Figure 7. Simplest possible arrangement for a time-of-flight mass spectrometer. The broken lines indicate fine mesh electrodes, which allow good ion transmission while also giving well defined electrical potentials (Ellis & Mayhew, 2013)

To be effective, collisions with background gases need to be avoided and so a good vacuum in the flight tube, and preferably $<10^{-5}$ mbar, is essential (Inomata, Tanimoto, Aoki, Hirokawa, & Sadanaga, 2006).

2.2.2.3.4 The Ion Detector: A sensitive ion detector and associated data acquisition electronics is critical to achieve the requisite overall detection sensitivity in PTR-MS.

Secondary Electron Multiplier (SEM): The SEM belongs to the group of discrete dynode electron multipliers, characterized by the emission of secondary electrons after impact of energetic particles on a metal or semiconductor's surface (Gross, 2011).

Arc-shaped dynodes are coated with a layer of, *e.g.* Be-Cu or Ag-Mg, with a low work function. An ion or an electron generates multiple secondary electrons upon striking this layer, depending on its kinetic energy. If successive stages are connected in series, an avalanche of electrons is produced from a single ion. A positive voltage of approximately 100 V is applied between each couple of dynodes to accelerate the electrons. The most common setup includes the supply of a high voltage (usually about 3000 V) to the whole SEM, with the individual dynodes being connected to the taps of this voltage. The positive high-voltage pole is grounded to keep the escaping electrons at approximately ground potential (**Figure 8**). These types of arrangements produce current amplification factors of

about 10^7 ("Vacuum Technology & Vacuum Pumps from the leading manufacturer Pfeiffer Vacuum,").

The gain of the SEM is mass dependent and it usually decreases as the mass increases. The emission on the first dynode is, indeed, velocity dependent and the latter decreases with the mass of the ions. The SEM has a high sensitivity, a good signal-to-noise (S/N) ratio and the average life time ranges between months and years, depending on the vacuum and the number of ions reaching the detector (Gross, 2011).

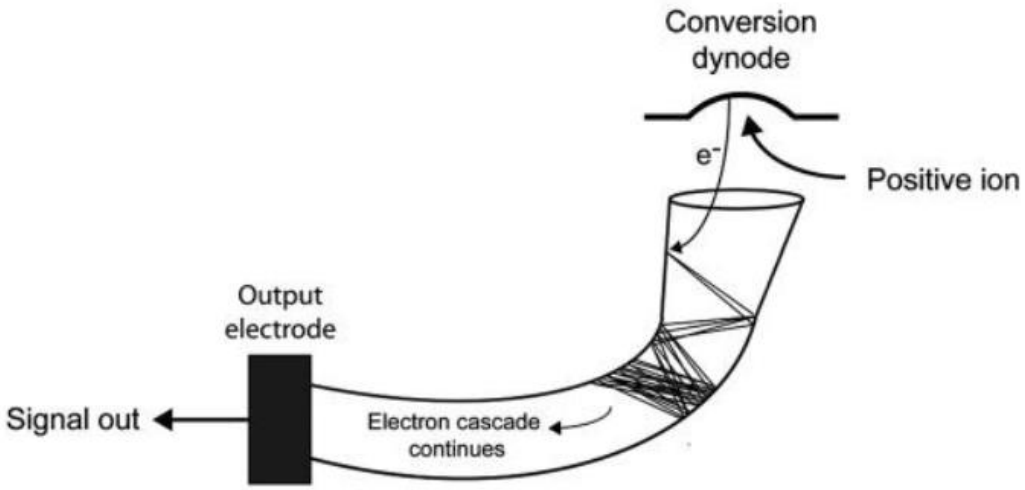

Figure 8. Schematic diagram of an electron multiplier (Ellis & Mayhew, 2013)

Micro Channel Plate (MCP): The MCP contains a series of tiny channels (3 to 20 μm diameter). Every channel is a continuous-dynode electron multiplier, covered with semiconducting material, where electrons are multiplied under the presence of a strong electric field (**Figure 9**). The channels are usually inclined to guarantee the impact of the ion on the surface (Wiza, 1979). After the cascade, the MCP needs a recovery (or recharge) time before being able of detecting another ion (Guilhaus, 1995).

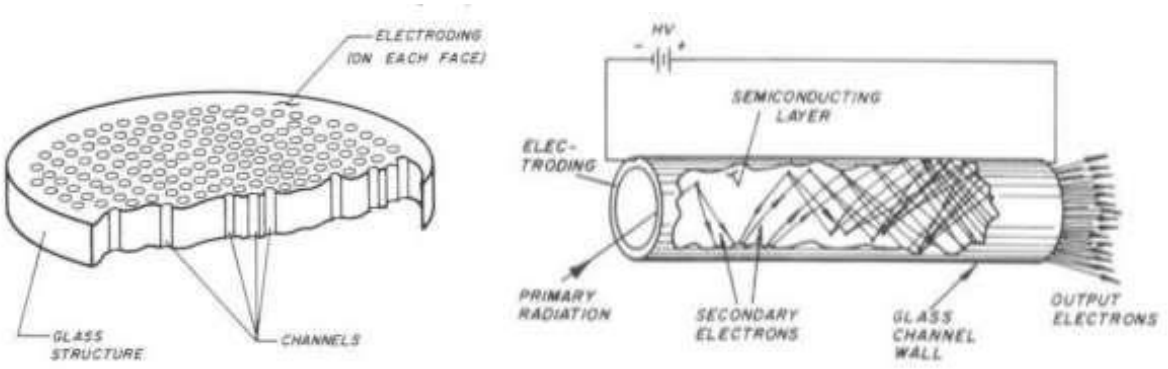

Figure 9. Cutaway views of the MCP detector (left hand side) and a single channel (right hand side) (Wiza, 1979)

A single MCP detector provides a gain of 10^3, which is much lower than the value obtained when using a SEM detector. In addition, an unwanted signal, called "dark current" originates either from (i) electric field emission from the channel walls; (ii) Ionization of residual gases; (iii) local discharge by a high electric field and; (iv) photoelectron emission by photons produced by electric field scintillation of the MCP support parts. Both optimized fabrication conditions and an improved assembling structure are used to eliminate sources of dark current caused by local discharge (Hamamatsu). In addition, two MCPs are usually put together in a geometry which is called "Chevron plate", to catch those ions having an incident trajectory parallel to the surfaces of the channels (Wiza, 1979). Using this geometry also results in a gain of 10^7-10^8 as amplification factor.

2.2.2.3.5 The Instrumental Control System: A computer is used to collect and display data and for overall control of the instrument. The software used to perform measurements throughout this work was TofDaqRecorder (Tofwerk, Switzerland). This software allows data to be saved as hd5 files (large amount of data recordable). In addition, the TOF and detector system may be controlled using the TPS controller (Tofwerk, Switzerland).

2.2.2.4 Sample Spectrum Obtained by PTR-ToF-MS

Figure 10 shows a typical spectrum which can be obtained using PTR-ToF-MS, in less than one second (depending on the acquisition rate), the highest peak reflects the primary ion (H_3O^+ at m/z = 21.0221) in this case. The ToF analyzer allows the separation of compounds having the same nominal mass, this is exemplified at the top right side of the figure.

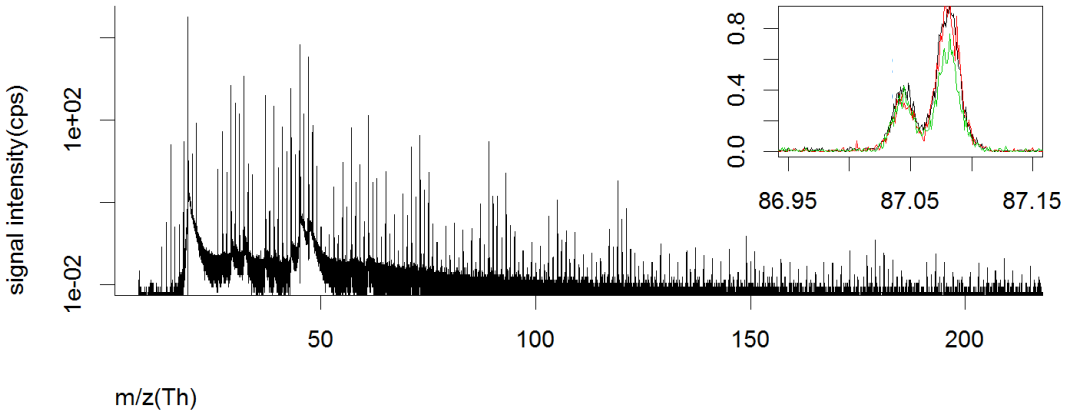

Figure 10. Average mass spectra of a dough sample. The top right insets shows the detail for nominal mass m/z 87. Spectra were obtained by averaging over 150-750s of measurement. (Makhoul, Romano, Cappellin, Spano, Capozzi, Benozzi, Märk, Aprea, Gasperi, & El-Nakat, 2014)

2.2.2.5 PTR-ToF-MS 8000 Apparatus from Ionicon Analytik

Figure 11. PTR-ToF-MS 8000 Apparatus from Ionicon Analytik (to the left) and a schematic view of its components (to the right) ("Ionicon website,").

In the series of experiments presented in this work, a PTR-ToF-MS 8000 apparatus from Ionicon Analytik GmbH (Innsbruck, Austria) was used in its standard V mode configuration (**Figure 11**). This is a trace gas analyzer, able to determine VOCs in real time (response time of 100 ms) with a high sensitivity and low limit of detection (pptv within 1 min). Its high mass resolution is up to 8000 m/Δm. Technical specifications are provided in **Table 1**.

Table 1. Technical specifications of the PTR-ToF-MS 8000 used in this study ("Ionicon website,")

Max. mass resolution	>5000 m/Δm (FHWM) up to 8000 m/Δm (FWHM)
Response time	100 ms
Sensitivity	> 150 cps/ppbv for Benzene @ 60 kHz > 100 cps/ppbv for Benzene @ 40 kHz > 240 cps/ppbv for m/z 181 @ 40 kHz
Detection limit (1 min)	< 5 pptv for Benzene < 5 pptv for m/z 181
Linearity range	5 pptv – 1 ppmv
Pulse frequency	Up to 80 kHz
Adjustable inlet flow	50 – 1000 sccm
Inlet system heating range	Up to 180 °C
Reaction chamber heating range	40 – 120 °C
Dimensions (w x h x d)	56 x 130 x 78 cm
Weight	170 kg

2.2.2.6 Latest Achievements

2.2.2.6.1 The Autosampler

In order to operate the PTR-MS analyses in an automated fashion, thus increasing the number of samples analyzed under the same conditions, a GC autosampler (Gerstel, Mülheim am Main, Germany, see **Figure 12**) was specially mounted and adapted to the PTR apparatus, by the *Composti Volatili group* at the Fondazione Edmund Mach in 2013 (Makhoul, Romano, Cappellin, Spano, Capozzi, Benozzi, Märk, Aprea, Gasperi, & El-Nakat, 2014).

Figure 12. The GC autosampler specially adapted to PTR-ToF-MS analyses

At the beginning of the experiment, the robotic arm would move the sample from a cooling tray to the incubation tray. Vials are then moved to the temperature-controlled purging site, connected to the PTR-ToF-MS inlet, and where the headspace analysis takes place with a pre-defined acquisition rate. After measurement, the vial is moved to the incubation tray and the cycle is repeated on the following sample. This allowed to monitor long bioprocesses namely the fermentation process, discussed in this thesis, while minimizing random human errors.

2.2.2.6.2 Switchable-Reagent-Ion Mass Spectrometry (SRI-MS)

As we previously discussed, most PTR-MS instruments employed use an ion source consisting of a hollow cathode (HC) discharge in water vapor which provides an intense source of proton donor H_3O^+ ions. However, some VOCs have proton affinities (PA) below that of H_2O, hence they cannot be ionized and detected (Jordan, Haidacher, Hanel, Hartungen, Herbig, et al., 2009). In order to solve this issue, other reagent ions can be used, namely NO^+ and O_2^+, and the device is no more a PTR-MS but rather a Switchable Reagent-Ion Mass Spectrometer (SRI-MS) (Cappellin et al., 2014; Jordan, Haidacher, Hanel, Hartungen, Herbig, et al., 2009). NO^+ and O_2^+ are produced using pure O_2, charcoal filtered air (or, alternatively, pure N_2 and O_2) (Sulzer et al., 2012). A high purity of the produced primary ions (> 98%) is guaranteed even in this case (Edtbauer et al., 2014). The main impurities are (i) H_3O^+, NO^+ and NO_2^+ in the case of O_2^+ as the reagent ion; (ii) H_3O^+, O_2^+ and NO_2^+, in the case of NO^+ as the reagent ion.

When using O_2^+ as the reagent ion, the dominant reaction which occurs in the drift tube is Electron Transfer Reaction (ETR). The reaction may be either non-dissociative (**Reaction 17**) or dissociative (**Reaction 18**), with the latter usually predominating (high energies involved in the reaction) [45]. The ETR is energetically permitted when the ionization energy (IE) of the analyte molecules is lower than the recombination energy of O_2 (12.07 eV) (Sulzer et al., 2012).

Non dissociative: $X^+ + A \rightarrow A^+ + X$ (Reaction 17)

Dissociative: $X^+ + A \rightarrow (A^+)^* + X$

$(A^+)^* \rightarrow F^+ + N$ (Reaction 18)

Where X^+ is the reagent ion, F^+ is a fragment ion and N a neutral fragment. An example is the case of ethylene (C_2H_4). The PA of this molecule is 680.2 $kJ.mol^{-1}$ which is lower than that of

water, whilst the IE is 10.5 eV thus making it ionizable when using O_2^+ as the reagent ion (Cappellin et al., 2014). This case is discussed in details in section 3.1.

Different reaction pathways may take place when using NO^+ as the reagent ion. The analyte molecules may undergo either ETR, hydride (H^-) or hydroxyl (OH^-) ion abstraction (**Reaction19**) or both of them. In addition, NO^+ may form a cluster with the analyte (**Reaction 20**), if a third partner (generally a buffer gas) stabilizes the formed cluster (Cappellin et al., 2014).

$$NO^+ + A \rightarrow [A - X]^+ + \mathrm{XNO} \qquad \text{(Reaction 19)}$$

$$\mathrm{NO}^+ + A + B \rightarrow A \cdot NO^+ + B \qquad \text{(Reaction 20)}$$

As in the case of O_2^+, ETR is energetically permitted if the IE of the analyte molecules is lower than the RE of NO^+ (9.26 eV) (Sulzer et al., 2012). However, the energy involved in this process is lower than in case of O_2^+, thus making this a soft ionization technique, able to provide mass spectra with a very low percentage of fragment ions (Agarwal, 2012; Ellis & Mayhew, 2013; T. Karl et al., 2012; Sulzer et al., 2012).

2.2.2.6.3 The FastGC Add-on

The latest add-on introduced by Ionicon on PTR-MS, is fastGC (**Figure 13**). This add-on enriches the data with another dimension of chemical information, allowing to separate isomeric compounds, while maintaining fast spectral runs ("Ionicon website,"). In 2014, Romano et al. proved the success of this pre-treatment technique to analyze wine samples (Romano et al., 2014). The complete setup, consisted of a short (3.5 m) nonpolar pure dimethyl polysiloxane GC column, a custom-made valve block, a flow controller, and a heating controller. The whole system is built into the PTR-ToF-MS and uses the same sample inlet. The column is resistively heated by applying a current, which allows for fast heating rates (>10

°C/s). The low thermal mass of the heating module also ensures fast cooling rates (from 200 °C to 50 °C in less than 20 s.).

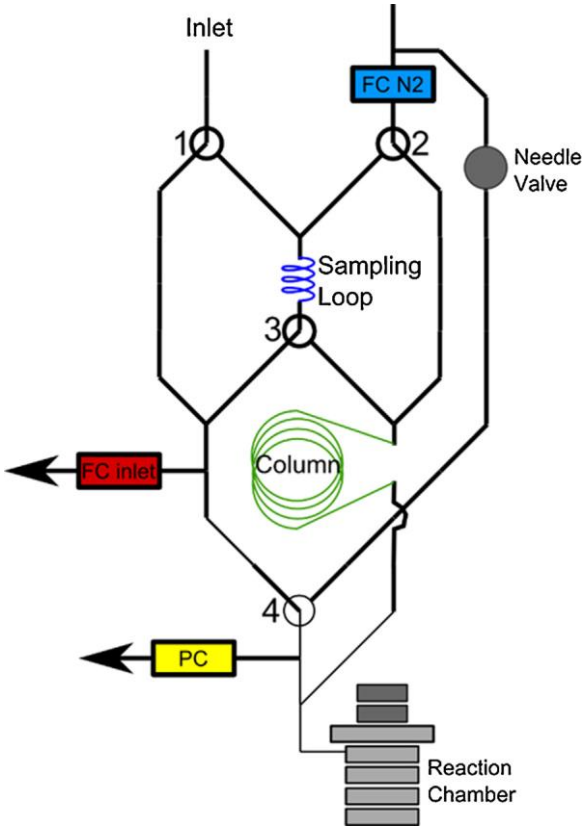

Figure 13. Schematic drawing of a PTR-ToF-MS inlet system with a FastGC setup, including the additional components valves 1–4, and the flow controller (FC N_2). The valves are depicted in their NO (normally open) state, as they are when FastGC is disabled. (Romano et al., 2014)

2.2.2.7 Data Analysis

Upon combining all the characteristics of PTR Mass spectrometers along with the various upgrades and add-ons previously discussed, we obtain an instrument of higher mass range, faster measuring time (a complete mass spectrum in a split second) and higher mass resolution, which multiply the analytical information contained in the spectra (Cappellin et al., 2011). However, such advantages come at the expense of having to deal with larger and more complex spectra. Hence arises the necessity to develop new procedures to extract manageable datasets, which can be employed in preliminary data visualization and analysis or as inputs for data

mining procedures (Cappellin et al., 2011). In their works, Cappellin et al. suggest up-to-date data mining methods; these start with the internal calibration of PTR-TOF-MS spectral data (Cappellin et al., 2010), followed by data pre-processing, such as denoising and baseline removal. A semi-automatic method for peak identification and peak area extraction was also developed by the same research group using using MATLAB (MathWorks, Natick, MA) (Matlab, 1999) in order to produce data matrices for preliminary data exploration or to feed data mining algorithms. **Figure 14** summarizes the data analysis scheme suggested.

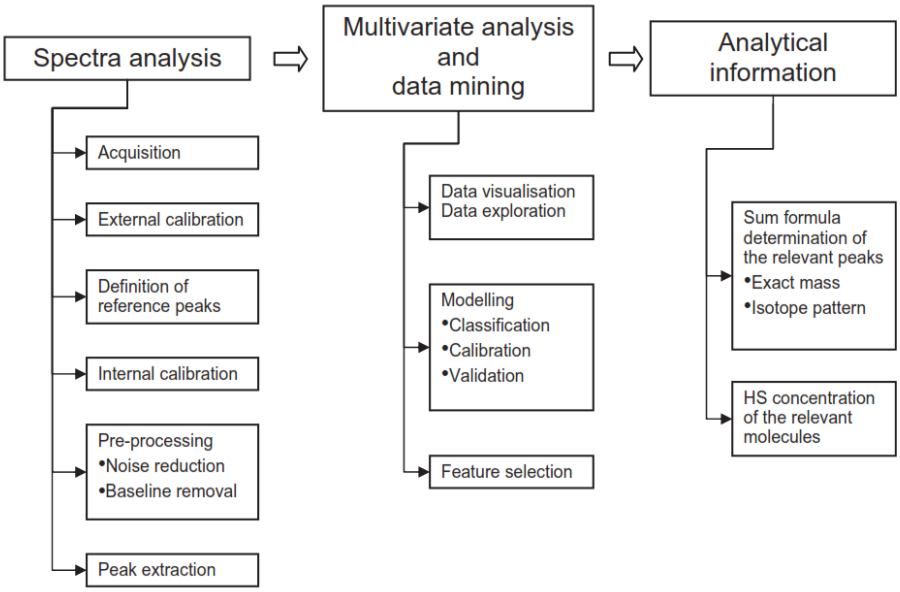

Figure 14. Schematics of the data analysis methodology presented (Cappellin et al., 2011)

The same approach will be carried out in our work and deep investigations via multivariate tests will be performed using in-house developed scripts written in R programming language (R Foundation for Statistical Computing, Vienna, Austria) (Team, 2014). These will be discussed in detail in each of the presented papers (see Chapter 3). But before moving to the applications, it is necessary to introduce the matrix and field of study where we suggest to apply this technique: food bioprocesses and specifically the bread-making process.

2.3 Food Bioprocesses[1]

2.3.1 Food Fermentation

Food fermentation is one of the first forms of food preservation (and processing) in human history (Hutkins, 2008). The bio-preservation/processing of perishable/edible raw materials through fermentations is also known as the 'oldest biotechnology' (Leroy & De Vuyst, 2004). Without knowing the existence of microscopic forms of life, our ancestors used the metabolic activities associated with 'virtuous' microorganisms development to transform, for example, milk into cheese and must into wine (Steinkraus, 2002).

This historic, cultural, and transdisciplinary significance explains well the relevance of fermented foods in the important sector of traditional, typical, and artisanal foods and beverages (Capozzi, Russo, & Spano, 2012; Capozzi, Spano, & Fiocco, 2012). For instance, without considering wines, fermented products represent more than 80% of the EU Geographical Indications (GIs; "GI is a sign used on goods that have a specific geographical origin and possess qualities, reputation, or characteristics that are essentially attributable to that place of origin" (WIPO 2015)) (37% cheeses, 20% beer, 16% meat products, 4% fruit and vegetables, 4% bakery products, biscuits, confectionery (Capozzi & Spano, 2011)). The result is a field of food market where most products, even when produced on an industrial scale (*e.g.*, yoghurt production (Arena et al., 2015)) are a traditional production developed by millenary human cultures. Nowadays, we find this millenary tradition on the shelves of the food industry and declined in many geographical contexts by reason of the differences in raw materials, environmental conditions and in traditional knowledge, leading to surprising breadth of different fermented typical products. Considering microbial resources associated with these manufactures, traditionally, food fermentations rely on naturally selected microbial consortia;

[1] Note that parts of this section have been accepted for publication, as a commentary chapter in the book entitled: *Fermented Foods: Sources, Consumption and Health Benefits*, by NOVA publishers, currently at press.

however, large scale production usually standardizes safety and quality of the final products by means of the ‘starter cultures’ regiment (R. P. Ross, Morgan, & Hill, 2002), where starter culture can be defined as “a microbial preparation of large numbers of cells of at least one microbial species to be added to a raw material to produce a fermented food by accelerating and steering its fermentation process” (Leroy & De Vuyst, 2004).

2.3.2 The importance of microbial Volatile Organic Compounds (mVOCs) in food fermentation

Encompassing the exploitation of micro-organisms and/or microbial enzymes which led to desirable biochemical changes and substantial variation to the food matrices, five are the main desired activities of microorganisms in fermented foods (Caplice & Fitzgerald, 1999; Capozzi, Russo, Dueñas, López, & Spano, 2012; Capozzi, Russo, Ladero, et al., 2012; Russo et al., 2014; Steinkraus, 2002):

1. enhancing the human dietary by means of improved/new flavors, aromas and textures,
2. increasing the shelf life and microbiological safety (lactic acid, alcoholic, acetic acid, alkaline fermentations and high salt fermentations),
3. enriching foods in vitamins, protein, essential amino acids and essential fatty acids,
4. reducing the toxicity of the substrate,
5. decreasing cooking times and fuel requirements.

Besides, fermentations might lead to more digestible foods and improve the functional content of final products (Arena et al., 2014; Caplice & Fitzgerald, 1999). The preservation and the improvement of aroma, flavor and texture connected with microbial resources are key drivers of consumers acceptance and choice (C Borresen, J Henderson, Kumar, L Weir, & P

Ryan, 2012). Microbial associated volatile organic compounds (mVOCs) provide the molecular basis of aroma/flavor perception. In fact, many microbial metabolites are VOCs since they fit the definition we provided in section 1.1.1, by being organic compounds characterized by low water solubility, and a vapor pressure of at least 0.01 kPa at 20°C (Pagans, Font, & Sánchez, 2006). In pursuance thereof characteristics, this peculiar class of metabolites is usually able to diffuse across the membranes of microbial cells and be released into the food matrix.

2.3.2.1 Previous studies on mVOCs

In 1921, Zoller and Clark (1921) described for the first time the production of volatiles by bacteria (formic and butyric acid) (Zoller & Clark, 1921). Schulz and Dickschat (2007), studying the chemistry of a panel of bacterial strains grown on defined artificial media, demonstrated the high heterogeneity of contribution in terms of bacterial volatiles (75 fatty acid derivatives, 50 aromatic compounds, 74 nitrogen-containing compounds, 30 sulfur compounds, 96 terpenoids, and 18 halogenated, selenium, tellurium, or other metalloid compounds) (Schulz & Dickschat, 2007), while Dickschat et al. (2005) and Kai et al. (2007) demonstrated the importance of species/strains contribution (Dickschat, Martens, Brinkhoff, Simon, & Schulz, 2005; Kai, Effmert, Berg, & Piechulla, 2007) (*e.g.,* Kai et al. (2007) reported up to 60 compounds per strain). The correlations between flavor properties and mVOCs provide the basis for making qualified decisions in producing quality fermented foods, a subject of relevant economic and social importance. For example, it is noteworthy to consider that:

1. only GIs agro-food market size is approximately $50 billion (Capozzi & Spano, 2011) and,
2. fermented foods and beverages represent a relevant part of human diet, accounting for approximately one-third of the global food intake (Campbell-Platt, 1994) (in fact, traditional fermented foods are diffused staple food for most of developing

countries and also the crucial healthy foodstuff for developed countries (Yang, Xu, Song, & Wang, 2010).

2.3.2.2 Release of mVOCs in traditional fermented food and beverages: a multifaceted problem:

Contrary to other areas of standardization and innovation of sensory quality in the food industry, the optimization of mVOCs in traditional fermented foods is a broad and heterogeneous sector by reason of the many geographical, compositional, microbiological and technological variables which have been reported in many recent review papers: traditional Indian fermented foods (Satish Kumar et al., 2013), fermented fruits and vegetables of Asia (Swain, Anandharaj, Ray, & Parveen Rani, 2014), African fermented foods (Franz et al., 2014), cereal based functional food of Indian subcontinent (Das, Raychaudhuri, & Chakraborty, 2012), traditional healthful fermented products of Japan (Murooka & Yamshita, 2008), traditional fermented plant foods and beverages in Eastern Europe (Sõukand et al., 2015), traditional fermented foods and beverages of Turkey (Kabak & Dobson, 2011), cereal fermentations in Africa and Asia (Nout, 2009).

In each geographical region, fermented foods are produced from different raw materials (justifying important differences addressable to chemical composition): cereal products, dairy products, fish products, fruit and vegetable products, legumes, and meat products (Campbell-Platt, 1987). In each of these categories, and for each geographical region, we might encounter hundreds of different productions. See, for instance, the quote attributed to Charles De Gaulle *"How can you govern a country that makes five hundred different cheeses?"* (Rudduck, Harris, & Wallace, 1994). Further differences are induced by fermentation activities: fermentations producing textured vegetable (*e.g.,* Indonesian tempe and ontjom), high salt sauce and paste fermentations (*e.g.,* Chinese soy sauce and Japanese miso), lactic acid fermentations (*e.g.,*

Russian kefir and sauerkraut), alcoholic fermentations (*e.g.*, Egyptian bouza and Ethiopian tej), acetic acid fermentations (*e.g.*, wine vinegars in the West and coconut water vinegar in the Philippines), alkaline fermentations (*e.g.*, Nigerian dawadawa and Indian kenima) (according to the classification reported by (Steinkraus, 2002), with minor modifications). For each kind of fermentation, the biochemical changes are associated to a complex microbiota, in which several species might have protechnological properties.

Finally, it is worth to stress the intraspecific diversity (Bisson, 2012) and the related fundamental strain-dependent protechnological characters. Given the huge number of interconnected variables there is a clear need for innovative analytical approaches that can manage the complexity of this sector which is relevant for both the economy and the nutrition and, in particular, for analytical techniques suitable for on-line monitoring without destroying the analyzed sample (*e.g.*, in dry-cured or dry-fermented food as Turkish sausages (Kaban, 2013) or dough and bread as in our case (Makhoul et al., 2015; Makhoul, Romano, Cappellin, Spano, Capozzi, Benozzi, Märk, Aprea, Gasperi, & El-Nakat, 2014)).

2.3.2.3 The needs for suitable approaches for mVOCs monitoring

The recent and fast growing development of Direct-Injection Mass Spectrometric (DIMS) technologies for VOCs analysis opens new opportunities for the rapid monitoring and quantification of VOCs. This class of techniques embraces different approaches including MS-e-noses, APCI-MS, SESI-MS, SIFT-MS, and of course PTR-MS (Bean, Mellors, Zhu, & Hill, 2015; Biasioli, Yeretzian, et al., 2011). This panel of instrumental analytical systems can nowadays combine considerable mass and time resolution with high sensitivity and robustness (Biasioli, Yeretzian, et al., 2011).

As discussed in the previous section, each approach has peculiar strengths and weaknesses, as a function of:

i) the instrumental design,

ii) Ionization conditions,

iii) The analysis approach. (For reviews, refer to (Berchtold et al., 2014; Biasioli, Yeretzian, et al., 2011)).

In general, the option of switching between different precursor ions, together with the enhanced design of time-of-flight-based instruments, allows the effective detection of most VOCs of interest by DIMS (Biasioli, Yeretzian, et al., 2011). Several recent uses of the DIMS technologies for the rapid monitoring and quantification of VOCs in fermented foods testify the wide range of application of the existing analytical methods (Table 2).

Table 2. Exemplificative list of scientific studies applying Direct-Injection Mass Spectrometric (DIMS) technologies to monitor VOCs' content in fermented food/beverage matrices

Fermented foods and beverages matrices	Fermentation monitored (Y/N)	DIMS technologies	References
Cheese	N	APCI-MS	(A. Taylor, Linforth, Harvey, & Blake, 2000)
Cheese	N	MS-eNOSE	(Pérès, Begnaud, & Berdagué, 2002)
Cheese	N	PTR-MS	(Boscaini, Van Ruth, Biasioli, Gasperi, & Märk, 2003)
Cheese	N	PTR-MS	(Bovolenta et al., 2008)
Cheese	N	MS-eNOSE	(Botre, Gharpure, Shaligram, & Sadistap, 2009)
Cheese	N	PTR-ToF-MS	(Fabris et al., 2010)
Cheese	N	PTR-ToF-MS	(Galle et al., 2011)
Cheese	N	SIFT-MS	(Langford et al., 2012)
Cheese	N	SIFT-MS	(K. Taylor, Wick, Castada, Kent, & Harper, 2013)
Cheese	N	SIFT-MS	(Castada, Wick, Taylor, & Harper, 2014)
Cheese	N	PTR-ToF-MS	(Bergamaschi et al., 2015)
Cheese	N	SESI-MS	(Bean et al., 2015)

Dry Fermented Sausage	N	SIFT-MS	(Olivares et al., 2011)
Fermented Whey	Y (LAF)	PTR-MS	(F. J. Gallardo-Escamilla, Kelly, & Delahunty, 2005)
Fermented Whey	N	PTR-MS	(F. Gallardo-Escamilla, Kelly, & Delahunty, 2007)
Sourdough	Y (LAF, AF)	SIFT-MS	(Van Kerrebroeck, Vercammen, Wuyts, & De Vuyst, 2015)
Wine	N	MS-eNOSE	(Vera, Mestres, Boqué, Busto, & Guasch, 2010)
Wine	N	PTR-ToF-MS	(Romano et al., 2014)
Yogurt	N	PTR-MS	(Mei, Reineccius, Knighton, & Grimsrud, 2004)
Yogurt	N	APCI-MS	(Saint-Eve et al., 2006)
Yogurt	Y (LAF)	PTR-ToF-MS	(Soukoulis et al., 2010)
Yogurt	N	PTR-ToF-MS	(Soukoulis et al., 2010)
Yogurt	Y (LAF)	PTR-ToF-MS	(Tsevdou et al., 2013)
Yogurt	Y (LAF)	PTR-ToF-MS	(Benozzi et al., 2015)

Direct-injection mass spectrometric (DIMS); Proton Transfer Reaction-Mass Spectrometry (PTR-ToF-MS); Selected Ion Flow Tube-Mass Spectrometry (SIFT-MS); Secondary Electrospray Ionization-Mass Spectrometry (SESI-MS), Atmospheric Pressure Chemical Ionization-Mass Spectrometry (APCI-MS); Lactic Acid Fermentation (LAF); Alcoholic fermentation (AF); Yes (Y); Not (N).

2.3.3 The Bread-making Process: A bioprocess which was has never been studied by DIMS techniques before

Bread is the most popular baked product made from Bread wheat (*Triticum aestivum* L.) which provides approximately 20% of calories consumed by humans (Pfeifer et al., 2014). Because of its nutritional quality and its sensory and textural properties (Patel, Waniska, & Seetharaman, 2005; Poinot et al., 2008), bread is consumed almost daily all over the world. This gives it an important socio-economic status in human nutrition, providing important amounts of nutrients, such as starch, dietary fiber, proteins, lipids, vitamins and minerals…

(Paraskevopoulou, Chrysanthou, & Koutidou, 2012). First, a dough is prepared from starting ingredients, it undergoes a so-called leavening or resting process, and finally it is baked at a certain high temperature in order to obtain the final product. These three steps (preparation, leavening and baking) are discussed briefly in the following subsections and thoroughly in the papers.

2.3.3.1 The recipe

The main ingredient in bread is flour obtained after the grinding and milling of soft or durum wheat (Hui, 2008). Historically, household recipes for bread fermentation were often based on natural microflora of hydrated flour (flour + water). Such a fermentation process is due to the presence of yeasts and of bacteria (especially lactic acid bacteria, LAB) on the surface of cereal berries. Leavening (yeasts and LAB), acidification (LAB), and flavor formation (LAB and yeasts) result in a fermented dough called sourdough (**Figure 15**), a model of which is presented in section 3.4 of this manuscript.

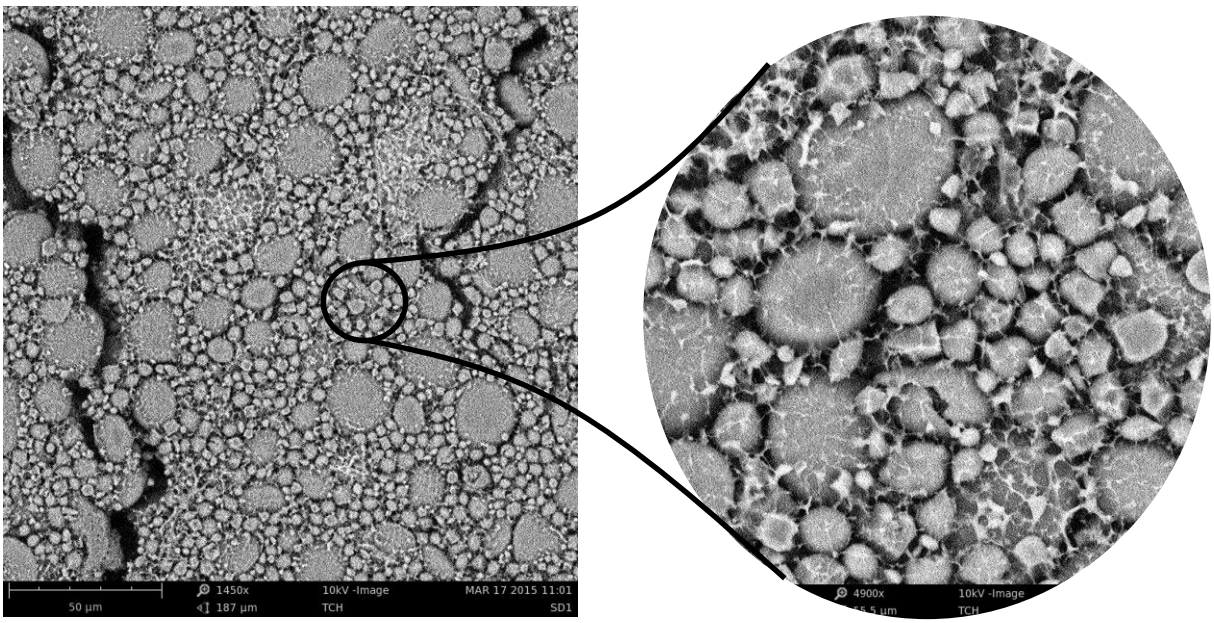

Figure 15. Pictures of a sourdough model taken by a Scanning Electron Microscope

Nevertheless, in the industrial food production, the necessary amount of selected strains added to a raw material to accelerate and steer a fermentation process, also known as starter cultures, is usually used to ensure standardization, consistency, safety, and quality of the final product (Frédéric Leroy, 2004). Hence, commercial baker's yeasts (Hui, 2008) started to be used, often in combination with bacterial starters; Commonly, baker's yeast is made by strains belonging to *Saccharomyces cerevisiae* (**Figure 16**), the most common species in bread-making (Reale et al., 2013). It is responsible for the leavening of the dough, as well as for the formation of desired sensorial characteristics.

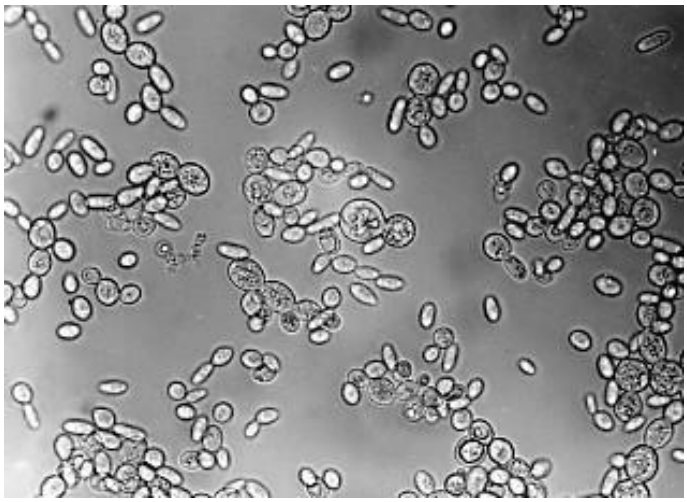

Figure 16. Microscopic picture of *Saccharomyces cerevisiae,* retrieved online *("Budding Yeast,")*

Saccharomyces cerevisiae, also known as the "budding yeast", is the common yeast used in baking ("baker's yeast") and brewing ("brewer's yeast"). This unicellular eukaryote, whose genome is entirely known, can be cultured easily and grows rapidly ("Budding Yeast,"). Through a process called alcoholic fermentation, these leavening agents produce gases mainly CO_2, according to the reaction:

$$C_6H_{12}O_6 \rightarrow 2C_2H_5OH + 2CO_2 \qquad \text{(Reaction 21)}$$

Glucose ethyl alcohol carbon dioxide

In addition to flour, water, sugar (glucose) and yeast, other ingredients may include salt (NaCl), animal fat and ascorbic acid (Capozzi et al., 2011), in order to provide a rich matrix for the leavening process. **Figure 17** pictures the ingredients used in this project's recipe, which consists of an adapted version of the AACC 10-10B procedure, approved by the American Association of Cereal Chemists (Capozzi et al., 2011).

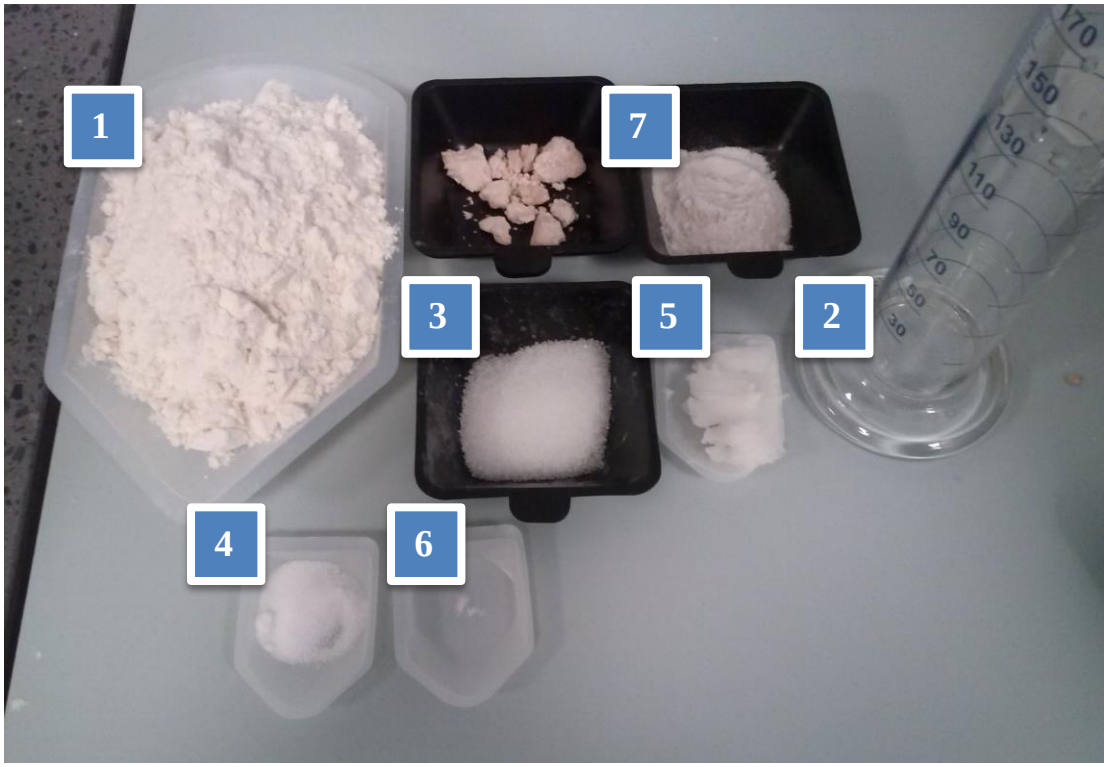

Figure 17. The ingredients of the bread recipe used in this project. According to an adapted version of the AACC 10-10B procedure, these ingredients include flour (1), water (2), sugar (3), salt (4), animal fat (5), ascorbic acid (6), and yeast preparations (7) (Capozzi et al., 2011)

2.3.3.2 The leavening process

Prior to baking, the dough has to undergo a leavening phase which is essential for the production and incorporation of gases in the baked product to increase the volume and produce the shape and the crumb texture (an example is provided in **Figure 18**). It is in this phase that (Reaction 21) takes place, and also in this phase, pleasant flavors and aroma precursors (aldehydes, ketones, and other volatile organic compounds) take shape, partly due to the biochemical activity of these agents (Salim ur, Paterson, & Piggott, 2006).

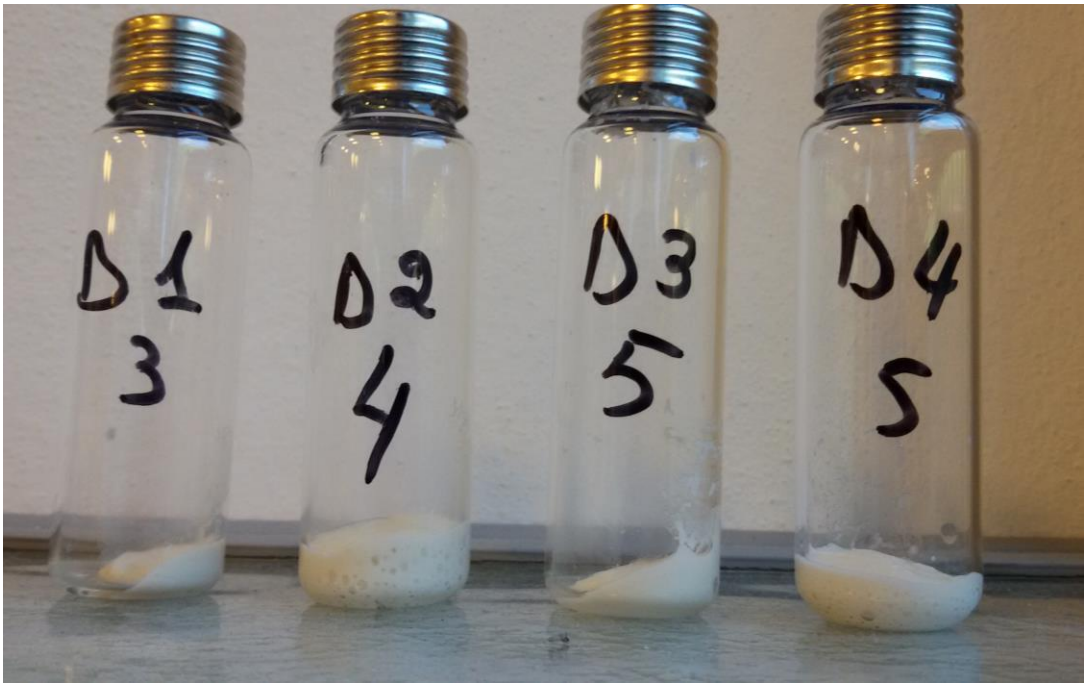

Figure 18. An example of the leavening of four different types of Dough (D1-D4) prepared in one of our projects (Makhoul, Romano, Cappellin, Spano, Capozzi, Benozzi, Märk, Aprea, Gasperi, El-Nakat, et al., 2014). A clear difference is observed in D2 which shows a maximal expansion volume.

2.3.3.3 The baking process and Maillard reactions

Upon baking, and around 170°C, an important biochemical process occurs. At this roasting stage, specific aromas are produced upon condensation reactions, called Maillard reactions (exemplified in **Figure 19**). These reactions take place between amino acids and sugars creating flavor, aroma and color of the bread crust (Cho & Peterson, 2010).

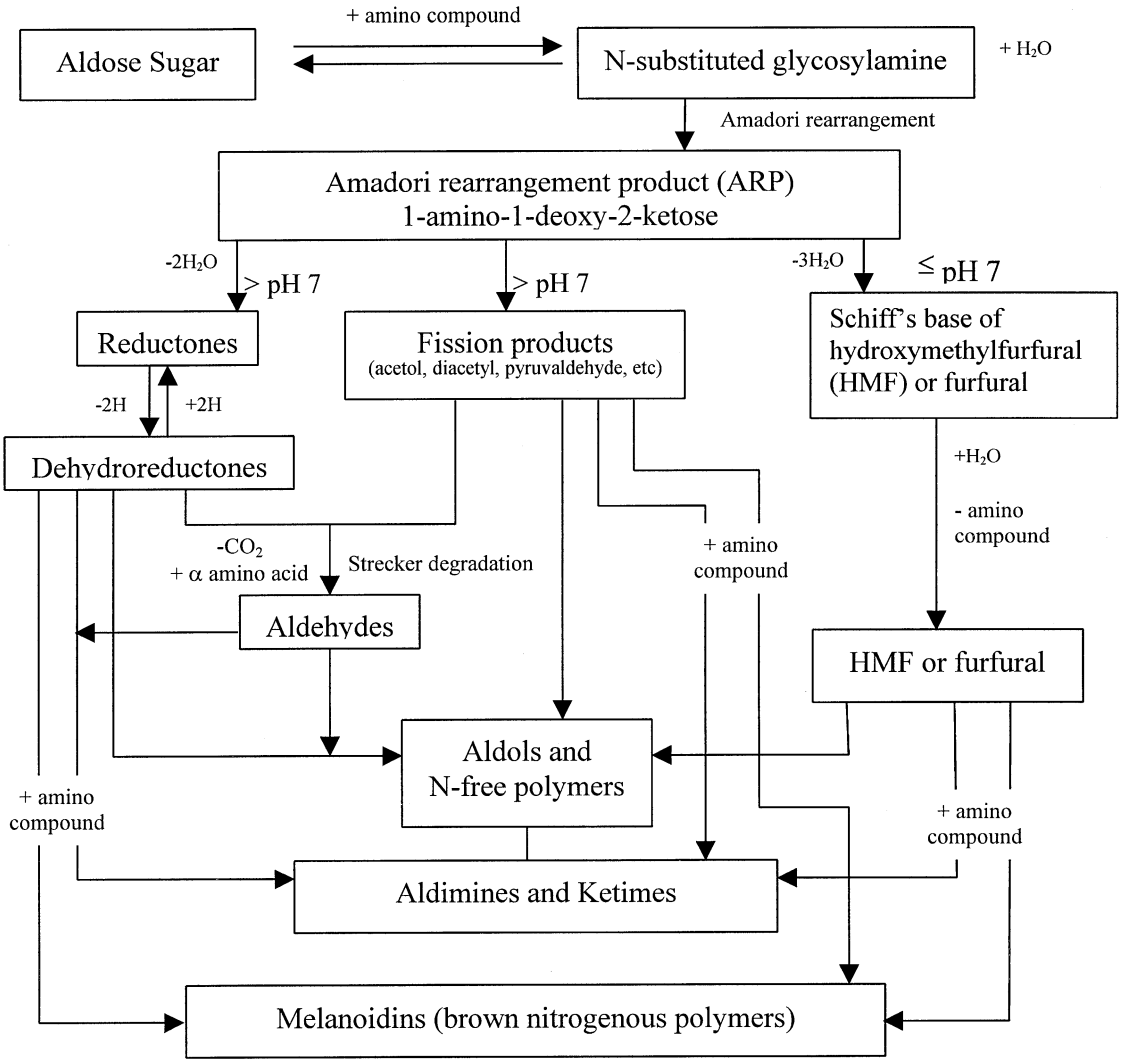

Figure 19. A Maillard reaction scheme (Martins, Jongen, & van Boekel, 2000)

The effectiveness of this final step depends on the nature and amount of aromatic precursors (alcohols, esters, carbonyls, carboxylic acids and other VOCs (Gassenmeier & Schieberle, 1995)) formed during the leavening process (Martins et al., 2000). It is important to note that the yeast metabolism yields not only some of these precursors, but also other volatiles that will remain in the baked bread and contribute to the aromatic profile of the final product **(Figure 20)**.

Figure 20. An example of bread "micro-loaves" obtained upon baking.

2.3.4 Our Approach

In this project, we aim at demonstrating the applicability of our comprehensive methodology (automatic sampling, PTR-ToF-MS analysis and tailored data handling and analysis) to study *Saccharomyces cerevisiae* VOCs released during alcoholic fermentations involved in the bread-making bioprocess (Vittorio Capozzi et al., 2015). In particular, after successfully testing the methodological applicability of PTR-ToF-MS on a simple model (*i.e.* ethylene, in section 3.1) we will use this approach on a complex matrix (*i.e.* dough, bread and sourdough in sections 3.2, 3.3 and 3.4) in order to:

1. Monitor on-line the leavening process, in an automated fashion, for the first time
2. differentiate bakery yeast starter cultures in reason of their release of VOCs and
3. analyze the effect on VOCs productivity as a function of:
    a. different bakery yeast starter cultures/flour combinations,
    b. the interaction between *S. cerevisiae* and *Lactobacillus sanfranciscensis* (an example of LAB) as model microorganisms in the sourdough environment.

Results

3. Results

3.1 Ethylene: Absolute real-time high-sensitivity detection with PTR/SRI-MS. The example of fruits, leaves and bacteria

Before testing the methodology we developed on the complex dough and bread matrix chosen in this PhD thesis, we had to understand and solve the limitations of the PTR-ToF-MS technique using a simple model molecule, the reason why we opted for the ethylene molecule as a starting point. In this project, the Switchable-Reagent-Ions upgrade (also known as Selective-Reagent Ionization) was tested, compared to other techniques and evaluated.

Ethylene (**Figure 21**) is the simplest alkene which has the molecular formula C_2H_4. It is a colorless flammable gas with a faint "sweet and musky" odor when pure. This hydrocarbon has four hydrogen atoms bound to a pair of carbon atoms that are connected by a double bond. The Ethylene is relatively rigid, but being a simple molecule, it is spectroscopically simple, hence it is used as a test for many theoretical and analytical methods (Booth & Campbell, 1929).

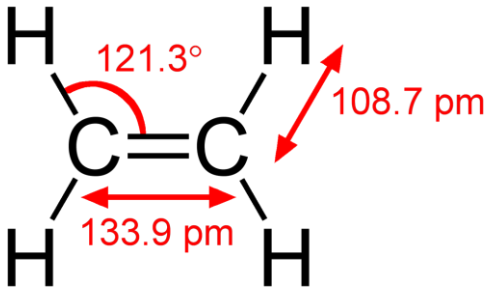

Figure 21. Chemical structure of Ethylene (Booth & Campbell, 1929)

In the following paper (Cappellin et al., 2014), ethylene is tested for the first time using this DIMS technique. We concluded that among the explored instrumental set-ups, the preferable one for ethylene detection with SRI-ToF-MS is O_2^+ mode. We finally showed that SRI-MS is a powerful tool for ethylene investigations in biological samples.

International Journal of Mass Spectrometry 365–366 (2014) 33–41

Contents lists available at ScienceDirect

International Journal of Mass Spectrometry

journal homepage: www.elsevier.com/locate/ijms

Ethylene: Absolute real-time high-sensitivity detection with PTR/SRI-MS. The example of fruits, leaves and bacteria

Luca Cappellin[a,*], Salim Makhoul[a], Erna Schuhfried[b], Andrea Romano[a], José Sanchez del Pulgar[a], Eugenio Aprea[a], Brian Farneti[a], Fabrizio Costa[a], Flavia Gasperi[a], Franco Biasioli[a]

[a] Research and Innovation Centre, Fondazione Edmund Mach, Via E. Mach, 1, 38010 S. Michele a/A, Italy
[b] Institut für Ionenphysik und Angewandte Physik, Leopold Franzens Universität Innsbruck, Technikerstr. 25, A-6020 Innsbruck, Austria

ARTICLE INFO

Article history:
Received 18 October 2013
Received in revised form 7 December 2013
Accepted 9 December 2013
Available online 17 December 2013

Dedicated to Tilmann D. Märk on the occasion of his 70th birthday.

Keywords:
PTR-MS
SRI-MS
Time-of-flight
Ethylene
Volatile organic compounds

ABSTRACT

Ethylene is a gaseous hormone playing a fundamental role in many systems and its detection and quantification is often crucial for several research fields. In the present work we investigated the possibility to employ Proton Transfer Reaction-Mass Spectrometry (PTR-MS) instruments modified by a Selective Reagent Ionization (SRI) upgrade to detect ethylene in real time with high sensitivity. Compared to commercial laser-based instruments the performance of SRI-MS is similar in terms of detection limits and superior as far as response time and dynamic range are concerned. We showed that, with SRI coupled to a time-of-flight (ToF) mass analyzer, absolute ethylene determination is possible. We experimentally determined the reaction rate coefficients for ethylene reactions with H_3O^+, O_2^+ and NO^+ as primary ions in the SRI-MS drift tube and proved that in the case of O_2^+ such reaction proceeds at collision rate, while in the case of H_3O^+ and NO^+ the reaction is less efficient. Reaction product yields and their eventual dependence on the buffer gas were investigated. New product ions that were not previously reported were found. We concluded that among the explored instrumental set-ups, the preferable one for ethylene detection with SRI-ToF-MS is O_2^+ mode, considering the $C_2H_4^+$ ion signal at m/z 28.0307. We finally showed that SRI-MS is a powerful tool for ethylene investigations in biological samples.

1. Introduction

Ethylene, the simplest unsaturated hydrocarbon, is a volatile compound of importance in many fields, in particular, as a plant hormone. This volatile compound is emitted by higher plants in order to trigger and control several physiological mechanisms including plant growth [1], host–plant interactions [2], fruit ripening [3] and programmed cell death [4]. Mechanisms for ethylene biosynthesis [5], signalling [6] and detection have been deeply investigated.

Current techniques to detect ethylene include gas chromatography (GC), optical devices and electrochemical devices. GC is a well established technique to detect volatile compounds and it is in many cases the gold standard thanks to its analytical power. In early studies, GC was employed to measure ethylene in apples [7,8]. GC coupled with a TDC achieved detection limits in the order of tens of ppmv (or equivalently μL/L). In more recent times GC columns coupled with adsorption–desorption devices [9] have been shown to achieve a detection limit lower by 1000 times over a measurement time of about 10 min. In order to improve time resolution some companies manufactured fast and compact GC systems able to achieve response times of a few minutes at the expense of a poorer detection limit. However, in order to study physiological processes involving ethylene, a detection limit at ppbv or sub-ppbv level should be achieved and the preconcentration of ethylene, necessary to achieve a better sensitivity and a more efficient GC measurement, should be avoided.

Optical sensors go in this direction by providing high time resolution (from seconds to minutes) and detection limits in the low ppbv and in some cases in the sub-ppbv region. They build upon the observation that ethylene has specific absorption properties, displaying the highest absorption in the mid-infrared region with a peak at 10 μm. There exist laser-based sensors coupled to photoacoustic spectroscopy. Recently such instruments have become commercially available providing a nominal detection limit of 0.3 ppbv within a 5 s measuring time [10]. Due to the internal volume and due to gas flow constraints (up to 5 L/h), the response time of the ETD-300 ranges from tens of seconds to minutes. Other optical sensors employ quantum cascade lasers [11] or coupled diode lasers to cavity ring-down spectroscopy or cavity-enhanced absorption spectroscopy [12]. Detection limits are in the low ppbv region for a few seconds of measurement time [12,13]. There also

* Corresponding author. Tel.: +39 0461 615189.
E-mail address: luca.cappellin@fmach.it (L. Cappellin).

1387-3806/$ – see front matter © 2013 Elsevier B.V. All rights reserved.
http://dx.doi.org/10.1016/j.ijms.2013.12.004

exist non-dispersive sensors that consider a broadband source without resolving the absorption spectrum [14]. They may suffer interferences from gases other than ethylene and achieve detection limits of hundreds of ppbv.

A different approach for ethylene detection is provided by electrochemical sensors. There are chemoresistive [15], capacitive [16] and amperometric [17] sensors. They reach detection limits of tens of ppbv but are sensitive to interfering gases and to temperature and humidity changes. We refer to the reviews on the subject (e.g. [18]) for further details.

Our recent studies related to fruit ripening physiology [19,20] suggested the possibility to monitor ethylene by using Proton Transfer Reaction-Mass Spectrometry (PTR-MS). PTR-MS is an established direct injection-mass spectrometric technique allowing real-time monitoring of most volatile organic compounds (VOCs) with low detection limits, typically a few pptv [21]. PTR-MS was firstly introduced in 1993 [22,23] and combined chemical ionization presented by Munson and Field in the 60s [24] with the swarm technique described by Ferguson and co-workers [25,26]. Thanks to its high time resolution, its high sensitivity and its non-invasive detection properties, it has cutting-edge applications in many fields including plant biology, environmental science, food science and technology and medicine [27].

In PTR-MS, neutral VOCs are ionized by reacting with a primary ion, typically H_3O^+, within the PTR-MS drift tube. PTR-MS instruments have been recently equipped with systems that allow to switch from H_3O^+ to other primary ions, such as, for instance, NO^+, O_2^+, Kr^+ and Xe^+ [21,28]. This widens the number of compounds that are detectable, including important VOCs such as CO, CO_2, N_2O, SO_2, and in some cases allows to separate isomeric compounds [28–30]. Such new generation instruments are generally called Selective Reagent Ionization-Mass Spectrometry (SRI-MS) instruments. The trace gas molecules, after undergoing ionization, are accelerated by the electric field in the drift tube and can be detected by a mass analyzer. Originally, PTR-MS instruments were equipped with a quadrupole mass spectrometer [23] providing good sensitivity and response time but a mass resolution limited to the nominal mass. Recently PTR-MS has been coupled with ion trap [31,32] and time-of-flight (ToF) mass analysers [33,34]. The latter provides higher time (20 Hz) and mass ($m/\Delta m = 7000$) resolution and a wider mass range [33].

In this work we use H_3O^+, NO^+ and O_2^+ ion chemistry to explore the possibility to detect ethylene with SRI-ToF-MS technology. We also show that SRI-ToF-MS with O_2^+ as primary ion is suitable for ethylene detection in practical applications and we test the agreement with another technique based on an optical sensor.

2. Materials and methods

2.1. Reagents and standards

Oxygen and nitrogen were 5.0 purity grade. Ethylene standards were supplied at concentrations of 10,000 and 100 ppbV in nitrogen (5.0 purity grade). All gaseous samples were provided by Rivoira (Milano, Italy). Whenever air was employed as diluting gas, this was supplied in the form of "zero air" by means of a Gas Calibration Unit (GCU, Ionicon Analytik GmBH, Innsbruck, Austria). All other chemicals were of the highest available purity grade and were all supplied by Sigma–Aldrich (St. Louis, MO).

2.2. SRI-ToF-MS

Measurements were performed with a commercial PTR-TOF 8000 apparatus from Ionicon Analytik GmbH, Innsbruck (Austria) [21]. The instrument was equipped with a system allowing for primary ion switching and could be operated in either H_3O^+ mode (PTR-ToF-MS) or O_2^+ mode or NO^+ mode. The conditions in the drift tube were the following: 110 °C drift tube temperature, 2.3 mbar drift pressure, 480 V drift voltage. This leads to an E/N ratio of about 120 Townsend (Td) (E corresponding to the electric field strength and N to the gas number density; $1\,Td = 10^{-17}\,Vcm^2$). During calibration experiments the drift voltage was changed to obtain E/N ratios of about 94 Td and 151 Td. The ions exiting the drift tube were detected using a time-of-fight (ToF) mass analyzer operated in its standard configuration (V mode). The sampling time per channel of ToF acquisition was 0.1 ns, amounting to 350,000 channels for a mass spectrum ranging up to $m/z = 400$. Every single spectrum is the sum of about 28.600 acquisitions lasting 35 μs each, resulting in a time resolution of 1 s.

2.2.1. SRI-ToF-MS in H_3O^+ mode: PTR-ToF-MS

The operational mode for H_3O^+ ion chemistry has been extensively reviewed by De Gouw and Warneke [35] and by Blake et al. [27]. We therefore refer to the literature on the subject for details.

The SRI-TOF-MS instrument employed in the present work is equipped with a dynamically adjustable source valve, which allows to control the gas exchange rate in the ion-source via a differential pumping stage [21]. In H_3O^+ mode, the source valve was set to 40% and the ion current to 5.0 mA. During the measurements the purity of the H_3O^+ ions from the ion source was above 97%. The fraction of O_2^+ and NO^+ were 0.02–3% and 0.4–0.6%, respectively, relative to the H_3O^+ signal. Most parasitic O_2^+ ions originated from the oxygen present in the analyte gas mixture and indeed a fraction of 0.02% relative to H_3O^+ was achieved when the analyte gas contained no oxygen.

Proton transfer from H_3O^+ to the analyte molecule in the drift tube efficiently proceeds when the molecule has higher proton affinity (more precisely, Gibbs energies, corresponding to gas phase basicities) than water and the difference in proton affinities is larger than about 35 kJ mol^{-1} [36]. The reaction reads

$$H_3O^+ + A \xrightarrow{k_1} AH^+ + H_2O \quad (1a)$$

Dissociative proton transfer reaction may also occur (see e.g. [37])

$$H_3O^+ + AB \xrightarrow{k_2} AH^+ + B + H_2O \quad (1b)$$

For proton transfer from H_3O^+ to proceed, the proton affinity of the reactant has to be above that of water. As can be seen from Table 1, the proton affinity for ethylene is even below that of water, which is much too low for the protonation reaction to proceed efficiently. When the proton affinity is endothermic or close to that of water, association reactions may occur,

$$H_3O^+ + A \xrightarrow{k_3} (H_3O^+) \cdot A \quad (1c)$$

as has been reported for ethylene in Selected Ion Flow Tube (SIFT) [38], a technique related to PTR-MS.

2.2.2. SRI-ToF-MS in O_2^+ mode

In O_2^+ mode, the hollow cathode in the ion-source was supplied with oxygen in the primary ion production region for O_2^+, leading to the following ionization reaction:

$$O^+ + O_2 \rightarrow O_2^+ + O \quad (2)$$

The source valve was set to 100%, and the ion current to 5.0 mA. During the measurements the fraction of NO^+, NO_2^+ and H_3O^+ were 3–15%, 0.1–0.4% and 0.4–1.2%, respectively, relative to the O_2^+ signal.

Table 1
Ion energetics data for ethylene and the precursor ions H_3O^+, O_2^+, NO^+.

Compound	Ionization energy (eV)	Proton affinity (kJ mol^{-1})	Gas phase basicity (kJ mol^{-1})
Ethylene	10.5138[a]	680.5[d]	651.5[d]
O_2	12.0697[b]		
NO	9.2642[c]		
H_2O		691[d]	660.0[d]

[a] Ref. [53].
[b] Ref. [59]
[c] Ref. [60].
[d] Ref. [61], evaluated values retrieved via the NIST WebBook.

O_2^+ ions entering the drift tube region collide with trace gases present in the analyte air [21]. Previous ion chemistry studies [38,39] identified charge transfer reactions

$$O_2^+ + A \xrightarrow{k_4} A^+ + O_2 \quad (3a)$$

and dissociative charge transfer reactions

$$O_2^+ + AB \xrightarrow{k_5} A^+ + B + O_2, \quad (3b)$$

as main pathways of analyte ionization, although other channels have also been found [40].

Charge transfer requires that the ionization energy of the primary ion is larger than that of the analyte molecule. See Table 1 for a list of ionization energies. Concerning ionization energies, ethylene lies between NO and O_2. This means that charge transfer from ethylene to O_2^+ is energetically allowed.

2.2.3. SRI-ToF-MS in NO^+ mode

In NO^+ mode, two flow controllers are used to tune the relative quantity of oxygen and nitrogen entering the primary ion generation region for NO^+. The following ionization reactions occur [29]:

$$N^+ + O_2 \rightarrow NO^+ + O \quad (4)$$

$$N_2^+ + O_2 \rightarrow O_2^+ + N_2 \quad (5)$$

$$O^+ + N_2 \rightarrow NO^+ + N \quad (6)$$

$$O_2^+ + NO \rightarrow NO^+ + O_2 \quad (7)$$

As pointed out by Federer et al. [41], reactions (4) and (7) occur at about collision rate, while reactions (5) and (6) are strongly suppressed. The source valve was set to 40% and the ion current to 5.0 mA. During the measurements the fraction of NO_2^+, O_2^+ and H_3O^+ were 2.8–3.3%, 0.5–1.2% and 0.03–0.18%, respectively, relative to the NO^+ signal. High purity of NO^+ production has been observed by Knighton et al. [42] who moreover showed that NO_2^+ formation can be largely limited by tuning the ion source extraction voltage.

Using NO^+ as primary ion, previous ion chemistry studies [21,39,42,43] identified four dominant reaction pathways, including

$$\text{charge transfer}: \quad NO^+ + AH \xrightarrow{k_6} AH^+ + NO, \quad (8a)$$

$$\text{hydride ion transfer}: \quad NO^+ + AH \xrightarrow{k_7} A^+ + HNO, \quad (8b)$$

$$\text{hydroxide ion transfer}: \quad NO^+ + AOH \xrightarrow{k_8} A^+ + HNO_2, \quad (8c)$$

and

three body association reactions :

$$NO^+ + A + N_2 \xrightarrow{k_9} (NO^+) \cdot A + N_2, \quad (8d)$$

The ionization potential of NO (see Table 1) is much lower than that for many VOCs, as for instance ethylene. Hence reaction (8a) does not proceed for many VOCs.

2.2.4. Fragmentation

Even though SRI-TOF-MS, in particular when used in its H_3O^+ mode, is a very soft ionization technique, fragmentation of the product ion may occur. The intensity of fragmentation can be influenced by the parameter E/N, i.e. the field strength E to number density N ratio, which is controlled by the pressure and temperature in the drift tube and the voltages applied to the drift tube [44]. Higher E/N values increase the energy the ions experience, and hence the likeliness of fragmentation [44]. The operational range of SRI-TOF-MS is typically at an E/N 80–155 Td, roughly corresponding to the range employed in this study. A cut-off at 2% of the most abundant ion is applied when reporting ion products.

2.3. Data analysis

2.3.1. Analysis of ToF spectra

Count losses due to the detector dead time were corrected offline via a procedure based on Poisson statistics [45,46]. Since the external calibration automatically provided by the acquisition software did not lead to a good mass accuracy, internal calibration was performed according to a procedure described elsewhere [47]. Such a method generally allows reaching a mass accuracy better than 0.001 Th, which is sufficient for sum formula determination in our case. We performed baseline removal and peak area extraction according to Cappellin et al. [48], using modified Gaussians to fit the data.

2.3.2. Absolute ethylene concentration determination

In principle, with SRI-TOF-MS it is possible to perform absolute determination of the concentration of a volatile compound without the need of calibrating the instrument, provided the compound underlying the signal, its reaction rate coefficient with the primary ion and the branching ratios are known [49]. For example, considering O_2^+ as primary ion and a reaction described by Eq. (3a), it follows in a first order approximation, that the concentration of the analyte volatile compound A is retrieved from the ion signals measured in the mass spectrometer via the equation [23]

$$[A] = \frac{1}{k_4 \tau} \frac{[A^+]}{[O_2^+]} \quad (9)$$

where k_4 is the rate coefficient of the charge transfer reaction governing Eq. (3a), τ is the residence time of the ion in the drift tube, $[A^+]$ and $[O_2^+]$ are the ion concentrations. Prerequisites for Eq. (9) to be valid are that there is an excess amount of O_2^+, with $[O_2^+] \gg [M^+]$, and that the concentration of precursor ion O_2^+ remains constant in the drift tube. Values of τ for a standard SRI-TOF-MS are close to 100 μs. A proper determination of τ may be carried out experimentally [50] or theoretically [49].

The $[A^+]/[O_2^+]$ ratio does not coincide with the ratio of the ion count rates detected directly with the mass spectrometer. Indeed, there is an important caveat, that is the mass discrimination of the detector must be taken into account. For SRI-ToF-MS a very simple

Table 2
Calculated collision rates k for the reaction of ethylene with various precursor ions.

Precursor ion	k (10^{-9} cm^3/s)
H_3O^+	1.4
O_2^+	1.2
NO^+	1.3

theoretical approach is also possible, leading to transforming Eq. (9) into [49]

$$[A] = \frac{1}{k_4 \tau} \frac{[A^+]_{measured}}{[O_2^+]_{measured}} \frac{\sqrt{(m/z)_{O_2^+}}}{\sqrt{(m/z)_{A^+}}} \quad (10)$$

where now $[A^+]_{measured}$ and $[O_2^+]_{measured}$ are the ion count rates measured with the mass spectrometer. $[O_2^+]_{measured}$ can be estimated from the signal of the isotope of O_2^+ at $m/z = 33.997$ Th. In this case $\sqrt{(m/z)_{O_2^+}}$ must be replaced by $\sqrt{33.997}$.

Since fragmentation of the charged VOC may occur, in order to properly estimate VOC concentrations, the branching ratios must be employed or equivalently Eq. (10) must be used for all fragments separately and their results subsequently summed up. More details on the described method can be found in [49].

In practical applications it is convenient to employ collision rate k_{col} for reaction rate coefficients [49]. This means replacing k_4 in Eq. (10) with k_{col}. Such a procedure is correct if k_4 is close to collision rate. If several reaction pathways are present, Eq. (10) must be used for all products separately and their results subsequently summed up. Values for collision rates of ethylene with primary ions are reported in Table 2. They have been calculated according to [49]. Since ethylene is a non-polar molecule, the collision rates do not vary with the energy conditions in the drift tube and are hence uniform for all E/N values.

2.4. Calibration setup

A custom built calibration system was used to dilute ethylene standards. A 10,000 ppbv Rivoira ethylene canister was employed for ethylene concentrations larger than 10 ppbv, while a 100 ppbv Rivoira ethylene canister was used for lower concentrations. Gas standards were selectively connected to flow controllers (MKS, Andover, MA) with 200 sccm or 20 sccm maximum flow. A mass flow controller with 2000 sccm maximum flow was used to supply the dilution gas. This was either nitrogen or zero air (generated by a Gas Calibration Unit, Ionicon Analytik GmbH). The outflow from both flow controllers was mixed via PEEK and Teflon fittings thus allowing for a dynamic dilution range between 1/1000 and 1. The uncertainty related to the dynamic dilution system is estimated to be ±10%, leading to a combined uncertainty of ±15%. The mixed flow was split to allow parallel measurements by a SRI-ToF-MS and a ETD-300 ethylene detector.

2.5. Ethylene determination by photoacustics

Since to date laser-induced methods represent the benchmark for ethylene determination an ETD-300 ethylene detector (Sensorsense BV, Nijmegen, the Netherlands) was used throughout the experimentation and employed as reference. The theoretical basis of the technique has been extensively discussed elsewhere [51]. Measurements and standardization were performed as recommended by the producer: briefly, analytical standards or headspace from biological samples were supplied at a constant known flow rate directly to the detector. Before reaching the detector samples were addressed through an NaOH and a $CaCl_2$ scrubber for the removal of CO_2 and water vapour, respectively. The instrument was calibrated using an ethylene mixture in nitrogen, supplied at a concentration of 500 ppbv.

2.6. Setup for ethylene emission measurements from fruits

In order to measure the ethylene emission from fruits, the different samples were put in hermetically closed glass jars and incubated in a water bath for 30 min at 30 °C [52]. Each jar was then connected to the GCU zero air provider and a two-way outlet divided the exiting flow between the SRI-ToF-MS and the ETD-300 ethylene detector, the latter receiving a flow of 3 L/h.

2.7. Setup for leaf and bacteria headspace ethylene measurements

Disks of 0.8 cm diameter were cut from leaves of plants of the species *Arundo donax*. Each disc was suspended in a 0.1 mM $NaHCO_3$ solution and transferred into 20 ml glass vials equipped with PTFE/silicone septa (Agilent, Cernusco sul Naviglio, Italy). Samples were incubated at 25 °C for 30 min before analysis.

During measurements 100 sccm of zero air was continuously injected into the vial through a needle heated to 40 °C and the outflow going through a second heated needle was split and delivered via Teflon fittings to the SRI-ToF-MS and to the ETD 300 Ethylene Detector. Each measurements lasted for 20 min and automatic switching of vials was done using an adapted GC autosampler (MPS Multipurpose Sampler, GERSTEL). The SRI-ToF-MS was used in O_2^+ mode at a E/N of 120 Td. Vials containing the buffer solution were used as blank.

A similar setup was also reproduced to evaluate the headspace ethylene concentration of bacterial cultures containing different strains of the Gram-negative bacterium *Pseudomonas syringae pv. actinidiae*. For this purpose vials containing 5 ml of bacterial culture were analyzed, along with non inoculated culture media, employed as blank.

3. Results and discussion

3.1. Ethylene-ion reactions in the drift tube

3.1.1. Reactions of ethylene with O_2^+

The results of the ethylene reactions with O_2^+ can be seen in Table 3, which reports ions down to a 2% cutoff level of the amount of the predominant ion. The efficient reaction of ethylene with O_2^+ at collisional rate and the formation of $C_2H_4^+$ has previously been reported in the literature [38] in a Selected Ion Flow Tube (SIFT) study, SIFT being a technique related to PTR-MS but deploying ambient temperature reactions, whereas PTR-MS deploys higher energy reactions (typically about 0.1–0.2 eV).

In the ion branching pattern the main ions are $C_2H_4^+$ and $C_2H_2^+$, consistently with the reactions described by Eqs. (3a) and (3b). $C_2H_2^+$ becomes predominant in N_2 at high E/N. When comparing the reaction products of ethylene diluted in N_2, to those of ethylene diluted in zero-air, the ion branching pattern changes. In particular, the resulting ion product at m/z 26.016 ($C_2H_2^+$) has lower branching ratio in zero-air while there is an increase in the branching ratios of the product ions at m/z 42.010 ($C_2H_2O^+$) and 43.018 ($C_2H_3O^+$). To the best of our knowledge, the latter two ion products have not been previously reported for O_2^+ reactions with ethylene. The presence of such ion products was attributed to ethylene reactions since it is unlikely that they originated from contaminants in the standard gas and moreover they are consistently present in the expected amount in the ethylene emission measurements of the considered biological samples.

The main difference between N_2 and zero-air is the presence of ca 21% oxygen in zero-air, besides some minor gases and the main constituent N_2. Thus, seemingly, the increased presence of oxygen,

Table 3
Reactions of ethylene with primary ions in SRI-MS used in O_2^+ mode, consisting typically of reactions with O_2^+, with ions reported at the 2% cutoff level and in percent of the most abundant ion. Iso stands for isotopologue.

Measured Ion	Sum formula (actual m/z)	Ion abundance [in % of highest]			Primary ion
E/N [Td]		94 Td	121 Td	155 Td	
Ethylene in pure N_2					
m/z 26.016	$C_2H_2^+$ (26.0151)	2.8	32.8	100.0	O_2^+
m/z 27.023	$C_2H_3^+$ (27.0229), $C_2H_2^+$ iso(27.0185)	1	3.1	9.9	O_2^+
m/z 28.032	$C_2H_4^+$ (28.0307)	100.0	100.0	39.7	O_2^+
m/z 29.035	$C_2H_4^+$ iso (29.0342)	2.6	2.8	1.4	O_2^+
m/z 42.008	$C_2H_2O^+$ (42.0100)	0.2	1.1	4.4	O_2^+
Ethylene in zero-air					
m/z 15.022	CH_3^+ (15.0229)	0.4	2.3	5.7	O_2^+
m/z 26.016	$C_2H_2^+$ (26.0151)	0.6	11.3	51.4	O_2^+
m/z 28.031	$C_2H_4^+$ (28.0307)	100.0	100.0	100.0	O_2^+
m/z 29.035	$C_2H_4^+$ iso (29.0342)	2.3	2.1	2.2	O_2^+
m/z 42.010	$C_2H_2O^+$ (42.0100)	0.4	9.9	77.9	O_2^+
m/z 43.018	$C_2H_3O^+$ (43.0178), $C_2H_2O^+$ iso (43.0134)	4.0	9.2	15.7	O_2^+

in particular when the energy is increased in the drift tube, results in a reduced amount of $C_2H_2^+$ and increased amounts of $C_2H_2O^+$ and $C_2H_3O^+$.

Table 4 reports calibration factors for the reaction of ethylene with O_2^+. We define the calibration factor for a particular ion product as the ratio between the actual ethylene concentration and the corresponding estimation via Eq. (10) using the rate coefficient reported in Table 2. As explained by Cappellin and co-workers [49], the sum of the calibration factors of all product ions also provides an experimental estimation of the reaction rate coefficient between ethylene and the primary ion O_2^+. In fact, a value of 1 in Table 4 (considering the rows related to the sum of all peaks in the ion branching pattern) would imply a perfect agreement between the theoretical value reported in Table 2 and the corresponding experimental estimation. The relevant values reported in Table 4 range between 0.84 and 1.01, which leads to conclude that the experimental reaction rate coefficient is between 1.01×10^{-9} cm^3/s and 1.21×10^{-9} cm^3/s, thus confirming that the reaction proceeds at collision rate (1.2×10^{-9} cm^3/s), as expected.

Interestingly, the calibration factor of m/z 28.031 ($C_2H_4^+$) basically remains the same (see Table 4) when comparing N_2 to zero-air and hence this would, in principle, allow for a calibration for ethylene based on the ion $C_2H_4^+$, independently of dilution gas. In fact, as implied by the values in Table 4, the difference between the fraction of $C_2H_4^+$ between N_2 and zero air are 7%, 0%, 4% for 94 Td, 121 Td, 151 Td, respectively.

An important caveat is the fact that the same is not true for other ions present in the fragmentation pattern. For instance, the fraction of $C_2H_2^+$ and $C_2H_2O^+$ in the resulting spectrum strongly depends on the dilution gas (Table 3) and in particular on the amount of oxygen. Therefore, particular care must be devoted in order to employ one of these ions to assess the concentration of ethylene in the analyte air. Comparison of the calibration factors obtained between N_2 and zero-air can be important when performing calibration measurements from N_2, but sample measurements from zero-air. In that case, the calibration factors must be comparable. These considerations suggest that it is preferable to employ $C_2H_4^+$ for ethylene concentration estimation when using SRI-ToF-MS with O_2^+ as primary ion.

Table 4
Measured calibration factors for the reaction of ethylene with O_2^+ in SRI-MS operated in O_2^+ mode, reported for N_2 and zero-air, for an E/N range of 94–155 Td and considering a collision rate of 1.2×10^{-9} cm^3/s (see Table 2).

Calibration factor of	Ethylene diluted in	E/N [Td]		
		94	121	155
total sum[a]	pure N_2	0.84	0.90	1.01
$C_2H_4^+$ (m/z 28)	pure N_2	0.79	0.65	0.25
total sum[a]	zero-air	0.92	0.87	–
$C_2H_4^+$ (m/z 28)	zero-air	0.85	0.65	0.24

[a] Total sum of calibration factors of reported product ions and fragments.

3.1.2. Reactions of ethylene with NO^+

Reactions of ethylene with NO^+ are very inefficient. The ionization energy of NO is much lower than that of ethylene and therefore reaction (8a) is strongly suppressed. SIFT data report as single product ion from the reaction, $C_2H_4{\cdot}NO^+$, and a rate coefficient <0.001 [53]. Even though we do see this association product, its abundance is below 0.2% of the highest ion abundance, and we detect it with SRI-MS in NO^+ mode only for the lowest E/N, well below the threshold we use for reporting ions. We also confirm a reaction rate <0.001 between NO^+ and ethylene (data not displayed).

The main ions are $C_2H_4^+$ and $C_2H_2^+$, which are not related to a reaction with NO^+ but rather to a reaction with parasitic O_2^+ ions which are present in the drift tube even in NO^+ mode, as previously described. Reactions performed with zero-air as dilution gas, and hence in the presence of additional oxygen, yield $C_2H_2O^+$ and $C_2H_3O^+$, which are expected from reactions with O_2^+, and their branching ratio are consistent with Table 3.

In conclusion, SRI-MS in NO^+ mode is not suitable for ethylene detection. In this operational mode ethylene may be detected at a lower sensitivity compared to O_2^+ mode by considering the ion products (in particular $C_2H_4^+$) of the reactions with the primary ion O_2^+ if present in a relevant amount as parasitic ion in the drift tube. In this case, the $C_2H_4^+$ calibration factors in Table 4 and Eq. (10) may be used for absolute ethylene concentration estimation, considering O_2^+ as primary ion.

3.1.3. Reactions of ethylene with H_3O^+

The reactions of H_3O^+ with ethylene are reported in Table 5, and the corresponding observed reaction rates can be found in Table 6. The main reaction products are $C_2H_4{\cdot}H^+$, $C_2H_2{\cdot}H^+$ and $C_2H_4{\cdot}H_3O^+$, consistently with the reactions described in Eqs. (1a)–(1c).

For the reaction of H_3O^+ with ethylene, SIFT literature reports, next to proton transfer according to Eq. (1a) leading to the formation of $C_2H_5^+$, the formation of an association product, $C_2H_4{\cdot}H_3O^+$. We observe this association product as well. The branching ratio of $C_2H_4{\cdot}H_3O^+$ varies from 2 to 84% of the product ion $C_2H_4{\cdot}H^+$, depending on the E/N, as expected (see Table 5) and this is compatible with literature [38].

Due to the presence of parasitic O_2^+ ions in the drift tube, the detected ions reported in Table 5 are the products of the ethylene reactions with both, O_2^+ and H_3O^+. While the former proceeds at

Table 5
Reactions of ethylene in SRI-MS operated in H_3O^+ mode. Ions are reported at the 2% cutoff level and in percent of the most abundant ion. The primary ion is also reported. Iso stands for isotopologue. Ions likely produced in reaction with parasitic O_2^+ primary ions are reported in grey.

Measured Ion	Tentative compound (actual m/z)	Ion abundance [in % of highest]			Primary ion
E/N [Td]		94 Td	121 Td	155 Td	
Ethylene in pure N_2					
m/z 26.016	$C_2H_2^+$ (26.0151)	0.9	1.5	3.2	H_3O^+, O_2^+
m/z 27.024	$C_2H_3^+$ (27.0229)	1.9	3.0	19.8	H_3O^+
m/z 28.031	$C_2H_4^+$ (28.0307)	4.2	1.9	0.2	O_2^+
m/z 29.040	$C_2H_4{\cdot}H^+$ (29.0386)	100.0	100.0	100.0	H_3O^+
m/z 30.042	$C_2H_4{\cdot}H^+$ iso (30.0420)	2.3	2.4	2.4	H_3O^+
m/z 47.050	$C_2H_4{\cdot}H_3O^+$ (47.0497)	84.0	10.6	2.4	H_3O^+
m/z 48.053	$C_2H_4{\cdot}H_3O^+$ iso (48.0526)	2.0	0.3	0.1	H_3O^+
Ethylene in zero-air					
m/z 26.016	$C_2H_2^+$ (26.0151)	1.2	10.8	38.7	H_3O^+, O_2^+
m/z 27.024	$C_2H_3^+$ (27.0229), $C_2H_2^+$ iso (27.0185)	1.0	1.5	9.2	H_3O^+, O_2^+
m/z 28.031	$C_2H_4^+$ (28.0307)	100.0	100.0	76.3	O_2^+
m/z 29.038	$C_2H_4{\cdot}H^+$ (29.0386), $C_2H_4^+$ iso (29.0342)	24.7	40.9	100.0	H_3O^+, O_2^+
m/z 42.010	$C_2H_2O^+$ (42.0100)	0.5	7.9	49.8	O_2^+
m/z 47.050	$C_2H_4{\cdot}H_3O^+$ (47.0497)	33.3	7.6	3.7	H_3O^+

collision rate, as confirmed in the previous section, the latter has been reported to be less efficient, proceeding at a few percents of collision rate [37,38,54–56]. Table 5 reports the product ions, branching ratios and the most likely primary ion, on the basis of all available data.

The calibration factors are displayed in Table 6. We recall that a value of 1 in Table 6 (considering the rows related to the sum of the calibration factors of all products ions of the reactions with H_3O^+) would imply a perfect agreement between the theoretical value reported in Table 2 and the corresponding experimental estimation. The relevant values reported in Table 6 range between 0.010 and 0.024, which leads to conclude that the experimental reaction rate coefficient is between 0.014×10^{-9} cm^3/s and 0.034×10^{-9} cm^3/s, thus the reaction of H_3O^+ with ethylene proceeds far below the collision rate (1.4×10^{-9} cm^3/s). This indicates that the reaction of ethylene with H_3O^+ is very inefficient, as would be expected because of the (quasi) endothermal reaction energies involved (see Table 1).

Interestingly, the calibration factors for $C_2H_4{\cdot}H_3O^+$ (m/z 47.050) remains about the same (see Table 6) when comparing N_2 to zero-air as dilution gases. This is not the case for $C_2H_4{\cdot}H^+$ and $C_2H_2{\cdot}H^+$, as can be inferred from Table 5. In conclusion, when employing SRI-MS in H_3O^+ mode (i.e. PTR-MS), for ethylene quantification it is preferable to consider either $C_2H_4^+$ ions resulting from reactions with the parasitic O_2^+, if present in sufficient amount, or $C_2H_4{\cdot}H_3O^+$ ions resulting from the reaction with H_3O^+ in case the O_2^+ ions are too low.

Reactions in pure N_2 suffer from the low abundance of O_2^+ as reagent ion and therefore $C_2H_4^+$ products are scarce. Reactions with zero air as dilution gas do not have this disadvantage. In particular, reactions at a mid-range E/N of 121 Td agree well within ±3.5% when comparing calibration factors in H_3O^+ and O_2^+ mode. This is a further indication that the product ion $C_2H_4^+$ found in H_3O^+ mode is mostly derived from an O_2^+ reaction, and moreover, that absolute ethylene quantification in zero-air based on the concentration of O_2^+ and $C_2H_4^+$ is possible.

Table 6
Measured calibration factors for the reactions of ethylene with H_3O^+ in SRI-MS operated in H_3O^+ mode, reported for N_2 and zero-air, for an E/N range of 94–155 Td and considering a collision rate of 1.4×10^{-9} cm^3/s (see Table 2).

Calibration factor of	Sample diluted in	E/N [Td]		
		94	121	155
total sum[a]	pure N_2	0.014	0.014	0.021
$C_2H_4{\cdot}H_3O^+$ (m/z 47)	zero-air	0.004	0.001	0.0002
total sum[a]	zero-air	0.010	0.007	0.010
$C_2H_4{\cdot}H_3O^+$ (m/z 47)	zero-air	0.005	0.001	0.0002

[a] Total sum of calibration factors of reported product ions and fragments related to reactions with H_3O^+.

3.2. Absolute ethylene concentration determination with SRI-ToF-MS

Based on the results of Section 3.1, absolute ethylene concentration with SRI-ToF-MS can be achieved considering O_2^+ as primary ion and $C_2H_4^+$ as product and using Eq. (10) and the calibration factors in Table 4. Fig. 1 reports an exemplary calibration curve for ethylene detection with SRI-ToF-MS using O_2^+ as primary ion. In the considered dynamic range, the PTR-MS instrument shows a linear response. For comparison, the figure also reports a calibration curve for a laser-based ethylene detector (ETD-300 Sensorsense BV) that has been used to assess ethylene concentration in parallel with SRI-ToF-MS. Absolute ethylene concentrations have been calculated according to Eq. (10) considering the peak at m/z 28.031 ($C_2H_4^+$), the reaction rate coefficient displayed in Table 2 and the calibration factors reported in Table 4. ETD-300 does not provide a linear response above 5 ppmv of ethylene, while SRI-ToF-MS has a much broader dynamic range [45].

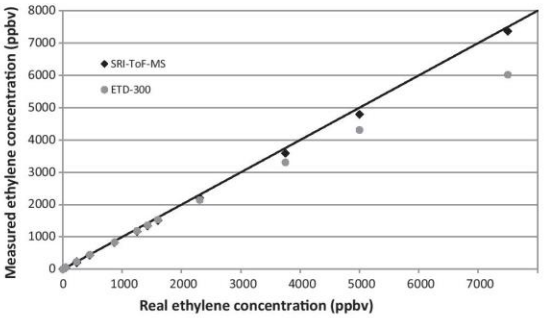

Fig. 1. Example of calibration curves for ethylene detection with SRI-ToF-MS and ETD-300 Ethylene Detector compared to ethylene standard concentrations. The solid line represents the ideal values.

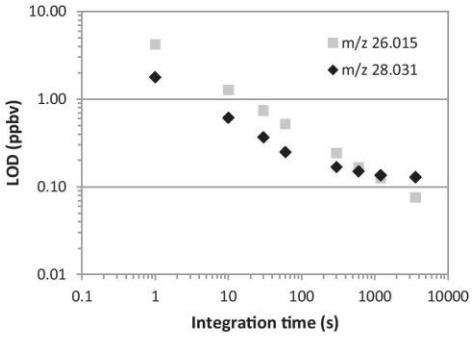

Fig. 2. Limit of detection for ethylene with SRI-ToF-MS in O_2^+ mode and $E/N = 120$ Td at different time resolutions. At the selected instrumental conditions, monitoring the $C_2H_4^+$ ion peak (m/z 28.031) provides a higher sensitivity.

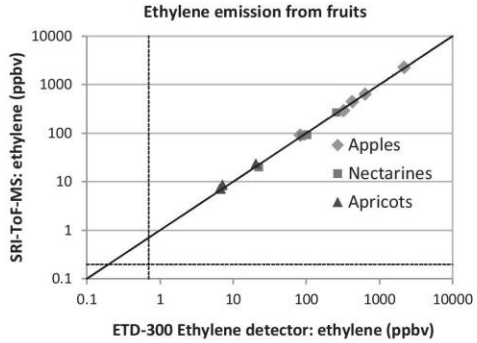

Fig. 3. Ethylene emission from fruits. Comparison between SRI-ToF-MS and ETD-300. The dotted lines indicate the instrument limit of detection at the selected instrumental conditions.

The instrument limit of detection (LOD) has been evaluated for various time resolutions between 1 s and 1 h using a statistical method:

$$\mathrm{LOD} = \frac{3 \times \mathrm{SD}_{\mathrm{background}}}{\mathrm{sensitivity}}$$

where $SD_{background}$ is the standard deviation of the background (expressed e.g. in cps) and the sensitivity is expressed e.g. in cps/ppbv.

The results in the case of $E/N = 120$ Td are reported in Fig. 2. Considering $C_2H_4^+$ ions, at 1 s acquisition time, the LOD is 1.8 ppbv, while at 20 min it is as low as 0.14 ppbv. The latter value was also verified during the calibration experiments using an ethylene standard gas at 0.1 and 0.2 ppbv of ethylene. The corresponding measured values were 0.18 and 0.08 ppbv, respectively, for SRI-ToF-MS in O_2^+ mode considering a time resolution of 20 min, while with the ETD-300 laser-based ethylene detector no ethylene was detected in either case. For SRI-ToF-MS, in general the LOD is inversely proportional to the amount of primary ion O_2^+ in the drift tube, which was about 1.8×10^6 cps (before duty cycle correction [57]) in our measurements. This dependence results from the fact that in general the ion counts in a ToF channel can be described by a random process [57], and thus the uncertainty of N counts is proportional to $\sqrt{N}$. From this observation it is straightforward to show that under the above hypothesis the LOD should be inversely proportional to the square root of the integration time. In fact, this dependence is found for $C_2H_2^+$ and for low integration times also for $C_2H_4^+$, see Fig. 2. The peak of interest for ethylene measurements, namely the one corresponding to $C_2H_4^+$, is close to other peaks as for instance the peak related to N_2^+ at m/z 28.0056. Therefore, it is clear that a good strategy [48,58] to disentangle the different peaks is mandatory for a good ethylene quantification. This provides a further uncertainty to the estimated ion counts for $C_2H_4^+$ and it is likely the reason of the LOD behaviour at high integration times for $C_2H_4^+$.

3.3. Ethylene detection in the headspace of fruits, bacteria and cut leaves

SRI-ToF-MS was employed in ethylene determination on real biological samples. We assessed the ethylene emission from different types of fruits, using both SRI -ToF-MS and ETD-300 Ethylene Detector. The comparison is reported in Fig. 3. A very good agreement (below 17% disagreement) is found for all measured apples, apricots and nectarines. It must be pointed out that, in principles, when considering a completely new matrix, interferences with the $C_2H_4^+$ peak from fragments of higher molecular compounds cannot be excluded a priori. Therefore, it is recommended to check if all other peaks related to ethylene (see Section 3.1.1) are also consistently present in the spectrum at the expected intensity. This was the case for the considered fruits.

The ethylene in the headspace of bacterial cultures and leaf disc was also measured after an accumulation period. Again, a SRI-ToF-MS and an ETD-300 ethylene detector were employed for simultaneous measurements. The response of SRI-ToF-MS is extremely fast (1–2 s in our setting), while the response of the ETD-300 ethylene detector is longer (about 120 s in the considered settings, see Fig. 4). With SRI-ToF-MS the headspace concentration

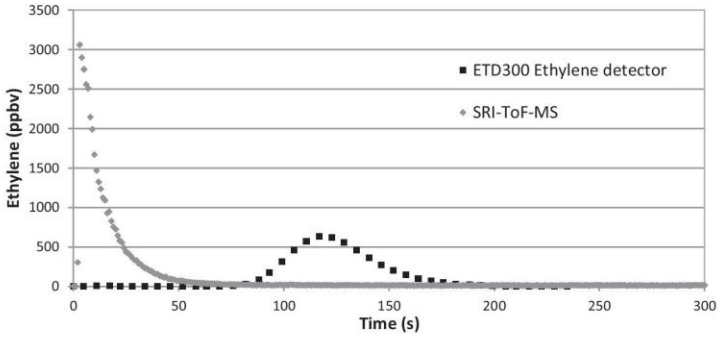

Fig. 4. Example of ethylene detection in bacteria headspace. SRI-ToF-MS depicts the actual time-dependent concentration of ethylene, while the ETD300 fails to do so and moreover displays an artificial peak due to the internal setup of the instrument.

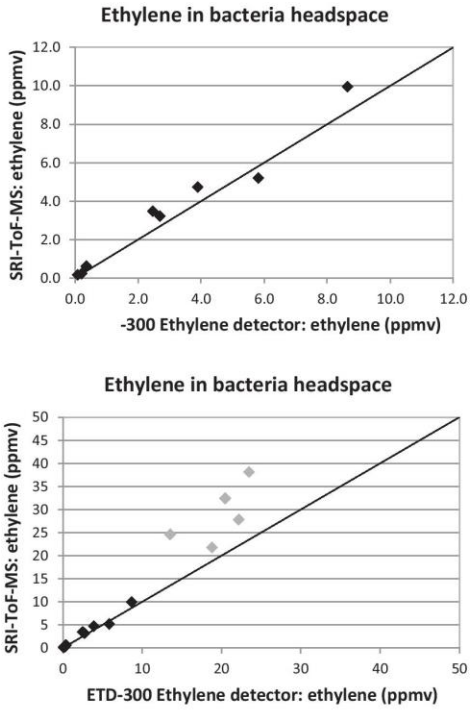

Fig. 5. Ethylene in bacteria headspace. Comparison between SRI-ToF-MS and ETD-300 (black squares). At high headspace concentrations (grey squares) only SRI-ToF-MS provides a linear response.

can be evaluated in virtually a few seconds by considering the concentration after the response time or, alternatively, in some minutes by depleting the sample headspace and calculating the total amount of ethylene that passes through the instrument. As far as the ETD-300 ethylene detector is concerned, only the latter method can be employed since the internal circuit spreads the ethylene over subsequent measurement points and therefore the integrated signal must be considered. The total ethylene is calculated by summing up all (instantaneous) concentrations weighted by the corresponding (instantaneous) flux. The comparison between the results of the two instruments is displayed in Fig. 5. Agreement within 29% is found. As the ETD-300 ethylene detector can only measure ethylene concentrations up to 5 ppmv, it fails to provide the right response for higher concentrations, see Fig. 5. In contrast, as shown in Fig. 1, the response of SRI-ToF-MS is still linear at higher concentrations. Analogously to the case of bacteria, for the ethylene in the headspace of leaves the two instruments provided similar results (Fig. 6, agreement within 18%).

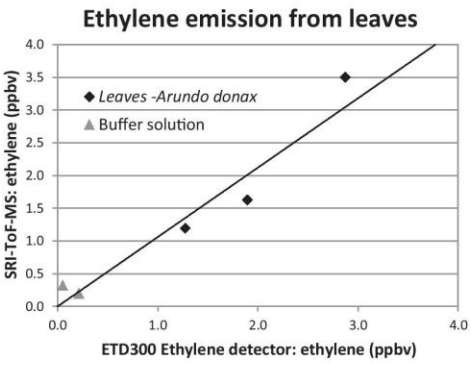

Fig. 6. Ethylene in leaf headspace. Comparison between SRI-ToF-MS and ETD-300.

4. Conclusions

We proved that SRI-ToF-MS is a very useful tool to detect and quantify ethylene concentrations in real time. We showed that with SRI-ToF-MS it is possible to absolutely determine ethylene concentration even without the need of previous calibration of the instrument. Currently the cutting-edge instruments for ethylene detection available in the market are in particular laser-based tools [18]. Compared to latter, the performance of SRI-ToF-MS are comparable in terms of detection limits and superior in terms of response time and dynamic range. A further advantage of SRI-ToF-MS is the simultaneous detection of many other volatile compounds. Moreover, ethylene was detected with SRI-ToF-MS without additional scrubbers. A limitation of SRI-ToF-MS is potentially the lack of specificity, especially in the presence of complex matrices when other compounds may interfere with the signals for ethylene in the spectrometer. However, it must be pointed out that we did not face this problem in all considered practical applications and that ion branching ratios can be used to confirm the compound identity. An advantage of SRI-ToF-MS over other available instruments for ethylene detection is the fact that with SRI-ToF-MS it is possible to absolutely determine ethylene concentration without the need of calibrating with an external standard. We explored the possibility of operating SRI-ToF-MS in O_2^+, NO^+ and H_3O^+ mode. We experimentally determined the reaction rate coefficients for reactions of these primary ions with ethylene. In the case of O_2^+, such reactions proceeds at collision rate, while in the case of H_3O^+ and NO^+ the reaction is less efficient. Using pure nitrogen and zero-air as dilution gases we showed that the product yields of the above reactions do not depend on the buffer gas for some products, namely $C_2H_4^+$ for ethylene reactions with O_2^+ and $C_2H_4{\cdot}H_3O^+$ for reactions with H_3O^+; while for other products the reaction yield depended on the buffer gas. We conclude that among the explored instrumental conditions the preferable setup for ethylene detection with SRI-ToF-MS is O_2^+ mode, considering $C_2H_4^+$ ion signal. Hence, SRI-ToF-MS is a fast and sensitive tool for the detection of ethylene.

Acknowledgments

Work partially supported by PAT (Provincia Autonoma di Trento, AP 2013). José Sánchez del Pulgar was beneficiary of a grant from the Fundación Alfonso Martín Escudero (Spain). Salim Makhoul was supported by the FIRS>T doctoral school of Fondazione Edmund Mach.

References

[1] F.B. Abeles, P.W. Morgan, M.E.S. Saltveit Jr., Ethylene in Plant Biology, Academic Press, San Diego, CA, 1992.
[2] N. Kavroulakis, S. Ntougias, G.I. Zervakis, C. Ehaliotis, K. Haralampidis, K.K. Papadopoulou, Role of ethylene in the protection of tomato plants against soil-borne fungal pathogens conferred by an endophytic *Fusarium solani* strain, J. Exp. Bot. 58 (2007) 3853–3864.
[3] A.B. Bleecker, H. Kende, Ethylene. A gaseous signal molecule in plants, Annu. Rev. Cell Dev. Biol. 16 (2000) 1–18.
[4] S.F. Yang, N.E. Hoffman, Ethylene biosynthesis and its regulation in higher plants, Annu. Rev. Plant Physiol. 35 (1984) 155–189.
[5] T.I. Zarembinski, A. Theologis, Ethylene biosynthesis and action: a case of conservation, Plant Mol. Biol. 26 (1994) 1579–1597.
[6] C. Chang, The ethylene signal transduction pathway in Arabidopsis: an emerging paradigm? Trends Biochem. Sci. 21 (1996) 129–133.

[7] S.P. Burg, J.a.J. Stolwijk, A highly sensitive katharometer and its application to the measurement of ethylene and other gases of biological importance, J. Biochem. Microbiol. Technol. Eng. 1 (1959) 245–259.
[8] F.E. Huelin, B.H. Kennett, Nature of the olefines produced by apples, Nature 184 (1959) 996.
[9] A. Segal, T. Górecki, P. Mussche, J. Lips, J. Pawliszyn, Development of membrane extraction with a sorbent interface-micro gas chromatography system for field analysis, J. Chromatogr. A 873 (2000) 13–27.
[10] F.J.M. Harren, G. Cotti, J. Oomens, S.L. Hekkert, Photoacoustic spectroscopy in trace gas monitoring, in: Encyclopedia of Analytical Chemistry, John Wiley & Sons Ltd., Chichester, 2006.
[11] D. Weidmann, A.A. Kosterev, C. Roller, R.F. Curl, M.P. Fraser, F.K. Tittel, Monitoring of ethylene by a pulsed quantum cascade laser, Appl. Opt. 43 (2004) 3329.
[12] E. Wahl, S. Tan, S. Koulikov, B. Kharlamov, C. Rella, E. Crosson, D. Biswell, B. Paldus, Ultra-sensitive ethylene post-harvest monitor based on cavity ring-down spectroscopy, Opt. Express 14 (2006) 1673.
[13] J. Manne, A. Lim, W. Jäger, J. Tulip, Off-axis cavity enhanced spectroscopy based on a pulsed quantum cascade laser for sensitive detection of ammonia and ethylene, Appl. Opt. 49 (2010) 5302–5308.
[14] Y.-H. Pao, Optoacoustic Spectroscopy and Detection, Elsevier, New York, 2012.
[15] B. Esser, J.M. Schnorr, T.M. Swager, Selective detection of ethylene gas using carbon nanotube-based devices: utility in determination of fruit ripeness, Angew. Chem. Int. Ed. 51 (2012) 5752–5756.
[16] B.B. Straumal, S.G. Protasova, A.A. Mazilkin, A.A. Myatiev, P.B. Straumal, G. Schütz, E. Goering, B. Baretzky, Ferromagnetic properties of the Mn-doped nanograined ZnO films, J. Appl. Phys. 108 (2010) 073923.
[17] V.M. Schmidt, E. Pastor, Adsorption and oxidation of acetylene and ethylene on gold electrodes, J. Electroanal. Chem. 376 (1994) 65–72.
[18] S.M. Cristescu, J. Mandon, D. Arslanov, J.D. Pessemier, C. Hermans, F.J.M. Harren, Current methods for detecting ethylene in plants, Ann. Bot. (2012), http://dx.doi.org/10.1093/aob/mcs259.
[19] C. Soukoulis, L. Cappellin, E. Aprea, F. Costa, R. Viola, T.D. Märk, F. Gasperi, F. Biasioli, PTR-ToF-MS, a novel, rapid, high sensitivity and non-invasive tool to monitor volatile compound release during fruit post-harvest storage: the case study of apple ripening, Food Bioprocess Technol. 6 (2013) 2831–2843.
[20] F. Costa, L. Cappellin, E. Zini, A. Patocchi, M. Kellerhals, M. Komjanc, C. Gessler, F. Biasioli, QTL validation and stability for volatile organic compounds (VOCs) in apple, Plant Sci. 211 (2013) 1–7.
[21] A. Jordan, S. Haidacher, G. Hanel, E. Hartungen, J. Herbig, L. Märk, R. Schottkowsky, H. Seehauser, P. Sulzer, T.D. Märk, An online ultra-high sensitivity proton-transfer-reaction mass-spectrometer combined with switchable reagent ion capability (PTR+SRI-MS), Int. J. Mass Spectrom. 286 (2009) 32–38.
[22] A. Hansel, A. Jordan, R. Holzinger, P. Prazeller, W. Vogel, W. Lindinger, Proton transfer reaction mass spectrometry: on-line trace gas analysis at the ppb level, Int. J. Mass Spectrom. Ion Processes 149–150 (1995) 609–619.
[23] W. Lindinger, A. Hansel, A. Jordan, On-line monitoring of volatile organic compounds at pptv levels by means of proton-transfer-reaction mass spectrometry (PTR-MS) medical applications, food control and environmental research, Int. J. Mass Spectrom. Ion Processes 173 (1998) 191–241.
[24] M.S.B. Munson, F.H. Field, Chemical ionization mass spectrometry. I. General introduction, J. Am. Chem. Soc. 88 (1966) 2621–2630.
[25] F.C. Fehsenfeld, A.L. Schmeltekopf, E.E. Ferguson, Thermal energy ion-neutral reaction rates. IV. Nitrogen ion charge-transfer reactions with CO and CO_2, J. Chem. Phys. 44 (1966) 4537–4538.
[26] E.E. Ferguson, F.C. Fehsenfeld, A.L. Schmeltekopf, Flowing afterglow measurements of ion-neutral reactions, in: D.R. Bates, I Estermann (Eds.), Advances in Atomic and Molecular Physics, Academic Press, New York, 1969, pp. 1–56, http://dx.doi.org/10.1016/S0065-2199(08)60154-2.
[27] R. Blake, P. Monks, A. Ellis, Proton-transfer reaction mass spectrometry, Chem. Rev. 109 (2009) 861–896.
[28] P. Sulzer, A. Edtbauer, E. Hartungen, S. Jürschik, A. Jordan, G. Hanel, S. Feil, S. Jaksch, L. Märk, T.D. Märk, From conventional proton-transfer-reaction mass spectrometry (PTR-MS) to universal trace gas analysis, Int. J. Mass Spectrom. 321–322 (2012) 66–70.
[29] T. Karl, A. Hansel, L. Cappellin, L. Kaser, I. Herdlinger-Blatt, W. Jud, Selective measurements of isoprene and 2-methyl-3-buten-2-ol based on NO^+ ionization mass spectrometry, Atmos. Chem. Phys. 12 (2012) 11877–11884.
[30] Y.J. Liu, I. Herdlinger-Blatt, K.A. McKinney, S.T. Martin, Production of methyl vinyl ketone and methacrolein via the hydroperoxyl pathway of isoprene oxidation, Atmos. Chem. Phys. Discuss. 12 (2012) 33323–33358.
[31] P. Prazeller, P.T. Palmer, E. Boscaini, T. Jobson, M. Alexander, Proton transfer reaction ion trap mass spectrometer, Rapid Commun. Mass Spectrom. 17 (2003) 1593–1599.
[32] L.H. Mielke, D.E. Erickson, S.A. McLuckey, M. Muller, A. Wisthaler, A. Hansel, P.B. Shepson, Development of a proton-transfer reaction-linear ion trap mass spectrometer for quantitative determination of volatile organic compounds, Anal. Chem. 80 (2008) 8171–8177.
[33] A. Jordan, S. Haidacher, G. Hanel, E. Hartungen, L. Mark, H. Seehauser, R. Schottkowsky, P. Sulzer, T. Mark, A high resolution and high sensitivity proton-transfer-reaction time-of-flight mass spectrometer (PTR-TOF-MS), Int. J. Mass Spectrom. 286 (2009) 122–128.
[34] M. Graus, M. Müller, A. Hansel, High resolution PTR-TOF: quantification and formula confirmation of VOC in real time, J. Am. Soc. Mass Spectrom. 21 (2010) 1037–1044.
[35] J. de Gouw, C. Warneke, Measurements of volatile organic compounds in the earths atmosphere using proton-transfer-reaction mass spectrometry, Mass Spectrom. Rev. 26 (2007) 223–257.
[36] G. Bouchoux, J.Y. Salpin, D. Leblanc, A relationship between the kinetics and thermochemistry of proton transfer reactions in the gas phase, Int. J. Mass Spectrom. Ion Processes 153 (1996) 37–48.
[37] D.B. Milligan, P.F. Wilson, C.G. Freeman, M. Meot-Ner, M.J. McEwan, Dissociative proton transfer reactions of H_3^+, N_2H^+, and H_3O^+ with acyclic cyclic, and aromatic hydrocarbons and nitrogen compounds, and astrochemical implications, J. Phys. Chem. A 106 (2002) 9745–9755.
[38] P.F. Wilson, C.G. Freeman, M.J. McEwan, Reactions of small hydrocarbons with H_3O^+, O_2^+ and NO^+ ions, Int. J. Mass Spectrom. 229 (2003) 143–149.
[39] P. Spanel, D. Smith, Selected ion flow tube studies of the reactions of H_3O^+ NO^+, and O-2(+) with several aromatic and aliphatic hydrocarbons, Int. J. Mass Spectrom. 181 (1998) 1–10.
[40] I. Dotan, A.A. Viggiano, Kinetics of the reaction of O_2^+ with CH_4 from 500 to 1400 K: a case for state specific chemistry, J. Chem. Phys. 114 (2001) 6112.
[41] W. Federer, W. Dobler, F. Howorka, W. Lindinger, M. Durup-Ferguson, E.E. Ferguson, Collisional relaxation of vibrationally excited NO+(v) ions, J. Chem. Phys. 83 (1985) 1032–1038.
[42] W.B. Knighton, E.C. Fortner, S.C. Herndon, E.C. Wood, R.C. Miake-Lye, Adaptation of a proton transfer reaction mass spectrometer instrument to employ NO^+ as reagent ion for the detection of 1,3-butadiene in the ambient atmosphere, Rapid Commun. Mass Spectrom. 23 (2009) 3301–3308.
[43] C. Amelynck, N. Schoon, T. Kuppens, P. Bultinck, E. Arijs, A selected ion flow tube study of the reactions of H_3O^+, NO^+ and O_2^+ with some oxygenated biogenic volatile organic compounds, Int. J. Mass Spectrom. 247 (2005) 1–9.
[44] W. Lindinger, A. Jordan, Proton-transfer-reaction mass spectrometry (PTR-MS): on-line monitoring of volatile organic compounds at pptv levels, Chem. Soc. Rev. 27 (1998) 347–375.
[45] L. Cappellin, F. Biasioli, E. Schuhfried, C. Soukoulis, T.D. Märk, F. Gasperi, Extending the dynamic range of proton transfer reaction time-of-flight mass spectrometers by a novel dead time correction, Rapid Commun. Mass Spectrom. 25 (2011) 179–183.
[46] T. Titzmann, M. Graus, M. Müller, A. Hansel, A. Ostermann, Improved peak analysis of signals based on counting systems: illustrated for proton-transfer-reaction time-of-flight mass spectrometry, Int. J. Mass Spectrom. 295 (2010) 72–77.
[47] L. Cappellin, F. Biasioli, A. Fabris, E. Schuhfried, C. Soukoulis, T. Mark, F. Gasperi, Improved mass accuracy in PTR-TOF-MS: another step towards better compound identification in PTR-MS, Int. J. Mass Spectrom. 290 (2010) 60–63.
[48] L. Cappellin, F. Biasioli, P.M. Granitto, E. Schuhfried, C. Soukoulis, F. Costa, T.D. Märk, F. Gasperi, On data analysis in PTR-TOF-MS: from raw spectra to data mining, Sens. Actuators B 155 (2011) 183–190.
[49] L. Cappellin, T. Karl, M. Probst, O. Ismailova, P.M. Winkler, C. Soukoulis, E. Aprea, T.D. Märk, F. Gasperi, F. Biasioli, On quantitative determination of volatile organic compound concentrations using proton transfer reaction time-of-flight mass spectrometry, Environ. Sci. Technol. 46 (2012) 2283–2290.
[50] C. Warneke, C. van der Veen, S. Luxembourg, J.A. de Gouw, A. Kok, Measurements of benzene and toluene in ambient air using proton-transfer-reaction mass spectrometry: calibration, humidity dependence, and field intercomparison, Int. J. Mass Spectrom. 207 (2001) 167–182.
[51] S.M. Cristescu, S.T. Persijn, S. te, L. Hekkert, F.J.M. Harren, Laser-based systems for trace gas detection in life sciences, Appl. Phys. B 92 (2008) 343–349.
[52] L. Cappellin, C. Soukoulis, E. Aprea, P. Granitto, N. Dallabetta, F. Costa, R. Viola, T.D. Märk, F. Gasperi, F. Biasioli, PTR-ToF-MS and data mining methods: a new tool for fruit metabolomics, Metabolomics 8 (2012) 761–770.
[53] B.A. Williams, T.A. Cool, Two-photon spectroscopy of Rydberg states of jet-cooled C_2H_4 and C_2D_4, J. Chem. Phys. 94 (1991) 6358–6366.
[54] D.K. Bohme, G.I. Mackay, Gas-phase proton affinities for water, ethylene, and ethane, J. Am. Chem. Soc. 103 (1981) 2173–2175.
[55] D.A. Fairley, G.B.I. Scott, C.G. Freeman, R.G.A.R. Maclagan, M.J. McEwan, $C_2H_7O^+$ potential surface and ion-molecule association between H_3O^+ and C_2H_4, J. Phys. Chem. A 101 (1997) 2848–2851.
[56] K.K. Matthews, N.G. Adams, N.D. Fisher, Isomeric forms of the products of the collisional associations of CH_3^+ with CH_3OH and H_3O^+ with C_2H_4, J. Phys. Chem. A 101 (1997) 2841–2847.
[57] I.V. Chernushevich, A.V. Loboda, B.A. Thomson, An introduction to quadrupole-time-of-flight mass spectrometry, J. Mass Spectrom. 36 (2001) 849–865.
[58] M. Müller, T. Mikoviny, W. Jud, B. D'Anna, A. Wisthaler, A new software tool for the analysis of high resolution PTR-TOF mass spectra, Chemom. Intell. Lab. Syst. 127 (2013) 158–165.
[59] R.G. Tonkyn, J.W. Winniczek, M.G. White, Rotationally resolved photoionization of O_2^+ near threshold, Chem. Phys. Lett. 164 (1989) 137–142.
[60] T. Ebata, Y. Anezaki, M. Fujii, N. Mikami, M. Ito, High Rydberg states of nitric oxide studied by two-color multiphoton spectroscopy, J. Phys. Chem. 87 (1983) 4773–4776.
[61] E.P.L. Hunter, S.G. Lias, Evaluated gas phase basicities and proton affinities of molecules: an update, J. Phys. Chem. Ref. Data 27 (1998) 413–656.

3.2 Proton-Transfer-Reaction mass spectrometry for the study of the production of volatile compounds by bakery yeast starters

After elucidating the advantages of the PTR-MS technique in terms of sensitivity and resolution, it was time to move to a more complex matrix. The acronym chosen for the study of bakery starters using Proton-Transfer-Reaction Mass Spectrometry was '*ProBake*'. As discussed earlier, the *ProBake* project will try to resolve many aspects which have never been done before, in an attempt at maximizing the PTR-MS potential to monitor such a complicated bioprocess.

In this first paper (Makhoul, Romano, Cappellin, Spano, Capozzi, Benozzi, Märk, Aprea, Gasperi, & El-Nakat, 2014), we tested the autosampler add-on specially adapted by our group to the PTR-ToF-MS 8000 apparatus used at the Fondazione Edmund Mach. This step aims at achieving the online monitoring of VOCs in an automated fashion throughout the leavening process and upon baking. Moreover, the dataset was subjected to a series of multivariate data analyses developed in-house, in order to create a fingerprint of the VOCs involved in this bioprocess. Finally, the overall productivity as well as the kinetics of VOC production were studied and compared, and the effect of various yeast starters was evaluated.

The conditions of the PTR device as well all the materials and methods applied are discussed in the paper. It is important to comment on the huge dataset which results from such a study, with more than 400 peaks detected and quantified in ppbv (parts per billion by volume) via the formula described by Lindinger et al. (W. Lindinger et al., 1998), using the appropriate reaction rate coefficient or a constant value for the reaction rate coefficient ($k = 2.10^{-9}$ cm^3 s^{-1}), when the underlying compound is not known. The latter introduces a systematic error of up to 30 % that can be accounted for the actual rate if the coefficient is known (Cappellin, Soukoulis, et al., 2012).

Research article

Journal of MASS SPECTROMETRY

Received: 24 February 2014 Revised: 4 June 2014 Accepted: 22 June 2014 Published online in Wiley Online Library

(wileyonlinelibrary.com) DOI 10.1002/jms.3421

Proton-transfer-reaction mass spectrometry for the study of the production of volatile compounds by bakery yeast starters†

Salim Makhoul,[a,b,c] Andrea Romano,[a]* Luca Cappellin,[a] Giuseppe Spano,[d] Vittorio Capozzi,[d] Elisabetta Benozzi,[a,e] Tilmann D. Märk,[e] Eugenio Aprea,[a] Flavia Gasperi,[a] Hanna El-Nakat,[b] Jean Guzzo[c] and Franco Biasioli[a]

The aromatic impact of bakery yeast starters is currently receiving considerable attention. The flavor characteristics of the dough and the finished products are usually evaluated by gas chromatography and sensory analysis. The limit of both techniques resides in their low-throughput character. In the present work, proton-transfer-reaction mass spectrometry (PTR-MS), coupled to a time-of-flight mass analyzer, was employed, for the first time, to measure the volatile fractions of dough and bread, and to monitor *Saccharomyces cerevisiae* volatile production in a fermented food matrix. Leavening was performed on small-scale (1 g) dough samples inoculated with different commercial yeast strains. The leavened doughs were then baked, and volatile profiles were determined during leavening and after baking. The experimental setup included a multifunctional autosampler, which permitted the follow-up of the leavening process on a small scale with a typical throughput of 500 distinct data points in 16 h. The system allowed to pinpoint differences between starter yeast strains in terms of volatile emission kinetics, with repercussions on the final product (i.e. the corresponding micro-loaves). This work demonstrates the applicability of PTR-MS for the study of volatile organic compound production during bread-making, for the automated and online real-time monitoring of the leavening process, and for the characterization and selection of bakery yeast starters in view of their production of volatile compounds. Copyright © 2014 John Wiley & Sons, Ltd.

Keywords: bakery; PTR-MS; leavening; yeast; VOCs

Introduction

Bread is consumed almost daily all over the world, which gives it an important socio-economic status in human nutrition, providing important amounts of nutrients, such as carbohydrates, dietary fiber, proteins, lipids, vitamins and minerals. Among the various stages of bread-making, and prior to baking, the dough has to undergo a leavening phase. This phase is essential for the production and incorporation of gases in the baked product by increasing the volume and producing the shape and the crumb texture,[1] as well as defining the taste of the final product.[2] Historically, household recipes for bread fermentation were often based on virtuous natural microflora of hydrated flour in addition to the yeasts and bacteria present in the food preparation area. Such a fermentation process is due to the presence of yeasts and of bacteria (especially lactic acid bacteria, LAB) that naturally contaminate the flour. Leavening (yeasts and LAB), acidification (LAB) and flavor formation (LAB and yeasts) result in a fermented dough called sourdough.[3,4] In the industrial food production, the necessary amount of selected strains (starter cultures) added to a raw material to accelerate and steer a fermentation process is usually used to ensure standardization, consistency, safety and quality of the final product.[5,6] Hence, commercial baker's yeasts [7] started to be used, often in combination with bacterial starters; these leavening agents produce gases, mainly CO_2, according to the reaction:

$$C_6H_{12}O_6 \rightarrow 2C_2H_5OH + 2CO_2$$

Glucose (from matrix) ethyl alcohol carbon dioxide (Reaction1)[8]

In this phase, pleasant flavors and aroma precursors (aldehydes, ketones and other volatile organic compounds

* Correspondence to: Andrea Romano, Department of Food Quality and Nutrition, Research and Innovation Centre, Fondazione Edmund Mach (FEM), via E. Mach 1, 38010 San Michele all'Adige, TN, Italy. E-mail: andrea.romano@fmach.it

† This article is part of the Journal of Mass Spectrometry special issue entitled "3rd MS Food Day" edited by Gianluca Giorgi.

a Department of Food Quality and Nutrition, Research and Innovation Centre, Fondazione Edmund Mach (FEM), via E. Mach 1, 38010 San Michele all'Adige, TN, Italy

b Department of Chemistry, University of Balamand, P. O. Box 100, Tripoli, Lebanon

c MR PAM—équipe VALMIS, IUVV, 1 rue Claude Ladrey, 21078 Dijon Cedex, France

d Department of Agriculture, Food and Environment Sciences, University of Foggia, via Napoli 25, 71122 Foggia, Italy

e Institut für Ionenphysik und Angewandte Physik, Leopold-Franzens Universit t Innsbruck, Technikerstr. 25, 6020 Innsbruck, Austria

(VOCs)) take shape, partly due to the biochemical activity of these agents.[2]

Upon baking/cooking, (around 170–230 °C), an important biochemical process occurs: specific aromas are produced upon condensation reactions, called Maillard reactions, which take place between amino acids and sugars creating flavor, aroma and color of the bread crust.[9] The effectiveness of this final step depends on the nature and amount of aromatic precursors (alcohols, esters, carbonyls, carboxylic acids and other VOCs [10]) formed during the leavening process.[11] It is important to note that the yeast metabolism yields provide not only some of these precursors but also other volatiles that will remain in the baked bread and contribute to the aromatic characteristics of the final product.[9]

The aim of this work is to study the profile of all these volatiles produced during the leavening of the dough and upon baking, by means of an analytical technique that will provide better results than the usually applied ones. So far, bread volatiles have been analyzed by means of gas chromatography (GC). GC protocols, though sometimes lengthy and time-consuming, represent the standard reference for the analysis of bread flavor compounds. In a series of papers, Schierberle and Grosch reported the identification of more than 250 VOCs in bread, mostly focusing on the crust profile, since it strongly influences the acceptance of the bread by the consumer.[12–14] In 2008, dynamic headspace extraction technique coupled to the GC–mass spectrometry analysis was applied [15] to characterize volatile compounds of both crust and crumb of Italian durum wheat sourdough bread, leading to the characterization of 89 volatiles belonging to different chemical classes. More recently, and for the same purpose, headspace solid-phase microextraction technique coupled to the GC–MS analysis was applied by Paraskevopoulou *et al.* [16] (2012) on lupin proteins isolated from enriched wheat flour bread.

In a recent review, more than 540 bread volatiles have been reported, most of them being alcohols, esters, ketones, acids, pyrazines, pyrrolines, and also furans, hydrocarbons and lactones,[9] mainly isolated from various crusts and crumbs of sourdough bread [17] or various specialty breads (wheat bread,[10] rye bread [13] and chestnut flour-based bread [18]). However, little is known about the aromatic impact of industrial bakery starter cultures, which are mostly selected on the basis of their technological properties. The fermentation properties and genetic diversity of industrial starters were studied in 2013 by Birch *et al.* [19] and Reale *et al.*,[20] and fermentation kinetics could be monitored by high throughput techniques, such as 2D-fluorescence spectroscopy (Grote *et al.*, 2014 [21]), but no light has ever been shed on volatile compound production and evolution. Even though Birch *et al.* [22] demonstrated that temperature and starter culture amount have an influence on the volatile profile of bread (measured by GC), neither the effect of different starters nor the online monitoring of volatiles was ever studied.

Proton-transfer-reaction time-of-flight mass spectrometry (PTR-ToF-MS) delivers a high analytical throughput, whereas mild ionization by means of a pure beam of hydronium ions and the high mass resolution granted by the ToF mass analyzer provide cutting-edge sensitivity and mass spectra with a high informational content.[23] The technique has found several applications in the field of food science [24,25] and, among others, it was successfully applied in the monitoring of VOCs formed or depleted during lactic acid fermentation of milk.[26,27] In the present work, PTR-ToF-MS was used, for the first time and in a fully automated fashion, to study the production of VOCs by bakery starter strains, focusing on the evolution of the production and depletion of VOCs, and their relative kinetics during the leavening process and upon baking of dough samples supplemented with different commercial yeast preparations.

Materials and methods

Sample preparation

The procedure described in the American Association of Cereal Chemists AACC 10-10B was applied (Approved Methods of the AACC, 10th ed.; American Association of Cereal Chemists: St. Paul, MN, 2000), with minor modifications (Capozzi *et al.*, 2011), in order to prepare the dough and bread samples [28]. Thus, the basic dough was obtained by mixing 200 g of wheat flour (Coop Italia, Casalecchio di Reno, Italy), 3 g of sodium chloride, 12 g of sucrose, 6 g of animal fat (Casa Modena, Modena, Italy), 8 mg of ascorbic acid and 120 ml of distilled water. The preparation was carried out using a bread homemaker machine (Princess Household Appliances, Lainate, Italia). The basic dough preparations were supplemented with four different commercial yeast preparations, labeled from Y1 to Y4. Preparations Y1 (Lessaffre, Parma, Italy), Y2 (Lessaffre, Parma, Italy) and Y3 (Pakmaya, Istanbul, Turkey) were single selected strains, while Y4 (Italmill, Cologne, Italia) was a 'natural' yeast preparation. Yeast preparations were added in different amounts (30 g/kg of flour—Y1 and Y2, 10 g/kg of flour—Y3 and 100 g/kg of flour—Y4) following the manufacturers' recommendations. In addition to that, and following a pre-existing manufacturing practice (Vittorio Capozzi, personal communication), some dough samples were inoculated with a mixture of Y1 and Y4 (30 g/kg and 50 g/kg of flour, respectively). Finally, some dough samples were left non inoculated and served as blank controls. The dough was divided into little pieces (1.0 g each) and put in 20-ml vials (Supleco, Bellefonte, PA). During preparation, the dough was kept at 4 °C in order to slow down the process of fermentation, and then the samples were transferred at 30 °C for the whole duration of the experiment. Five replicates of each dough sample were analyzed (along with two empty vials resulting in a total of 32 vials), and the entire experiment was repeated twice.

For baked bread analysis, the same experiment was repeated with Y1, Y2 and Y3 yeast preparations. After 2 h and 42 min of leavening (corresponding to three analytical cycles, see below), the fermentation was stopped, and the vials were taken out of the autosampler. Caps were removed, and vials were transferred to a kitchen oven at 220 °C. Doughs were baked for 8 min, until a golden crust was formed.

PTR-TOF-MS analysis

Measurements of the headspace of the dough and bread samples were performed with a commercial PTR-TOF 8000 apparatus from Ionicon Analytik GmbH (Innsbruck, Austria), in its standard configuration (V mode). The ionization conditions in the drift tube involved 110 °C drift tube temperature, 2.30-mbar drift pressure and 550-V drift voltage. This led to an E/N ratio of about 140 Townsend (1 Td = 10^{-17} cm^2 V^{-1} s^{-1}). The inlet line consisted of a PEEK capillary tube (internal diameter 0.04 inches) heated at 110 °C. The inlet flow was set at 120 sccm and 40 sccm for dough and bread measurements, respectively.

The leavening experiments were carried out in automated fashion using a GC autosampler (Gestel, Mulheim am Main, Germany) especially adapted to PTR-MS analysis. At the beginning of the experiment, the robotic arm moved the sample from a cooling tray where it was kept at 4 °C, to the incubation tray, whose temperature was set at 30 °C. Vials were then moved to the temperature-controlled (30 °C) purging site, connected to the PTR-ToF-MS inlet, and where the headspace analysis took place for 30 s with an acquisition rate of one spectrum per second. After measurement, the vial was moved to the incubation tray, and the cycle was repeated on the following sample. This allowed to perform a scan of the tray (32 samples) in approximately 1 h (1 cycle = 54 min). During leavening, the scan was repeated 16 to 20 times, in order to monitor the fermentation process. Due to the presence of relevant amounts of ethanol (an average of 20 ppmv) in the headspace of the samples during leavening, an inert gas dilution was applied in an inert gas to sample ratio of 2:1. This permitted to prevent primary ion depletion and formation of ethanol clusters which might affect the final quantification of volatiles.

The headspace of micro-loaves was measured in the same instrumental conditions and with the aid of the autosampler. Prior to analysis, samples were flushed with a stream of non-preheated Zero air (200 ml/min for 30 s), humidified at 80% and generated by a Gas Calibration Unit apparatus (Ionicon Analytik GmbH), then incubated at 30 °C for 30 minand finally analyzed for 30 s at one spectrum per second. No dilution of the headspace was required in this case.

Data analysis

Dead time correction, internal calibration of mass spectral data and peak extraction were performed according to a procedure described elsewhere,[29,30] using a modified Gaussian peak shape. Peak intensity in ppbv was estimated using the formula described in literature,[31] using a constant value for the reaction rate constant coefficient ($k = 2 \times 10^{-9}\ cm^3\ s^{-1}$). This introduces a systematic error for the absolute concentration for each compound that is in most cases below 30% and could be accounted for if the actual rate constant coefficient is available.[32]

All data detected and recorded by the PTR-TOF-MS were processed and analyzed using MATLAB (MathWorks, Natick, MA) and R (R Foundation for Statistical Computing, Vienna, Austria).

Results and discussion

Automated monitoring of the leavening process

After preparing the dough samples supplemented with the different yeast preparations, and setting up both, the PTR-ToF-MS and the autosampler, the leavening process was launched in an automated fashion. This allowed the samples to be incubated at 30 °C for 30 min, and then their headspace was analyzed every 54 min. This generated up to 20 time points during the course of a typical leavening experiment. The whole data set consisted of ten replicates for each experimental mode, obtained upon combining the results of two distinct biological replicates. The results of the

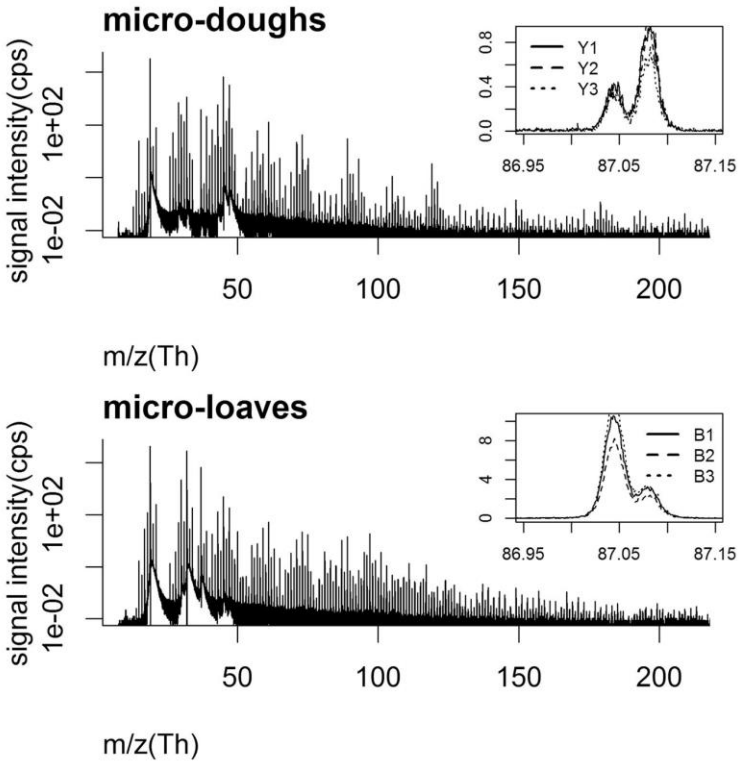

Figure 1. Average mass spectra of dough and bread. The top right insets show the detail for nominal mass *m/z* 87 and the three yeast starters (and resulting micro-loaves). Spectra were obtained by averaging over 150–750 s of measurement.

dough samples supplemented with the mixture of Y1 and the 'natural' yeast preparation (Y4) showed no difference compared to the results of Y1 alone; in addition, the blank controls and the doughs supplemented with Y4 showed a limited production of volatiles and slow fermentation kinetics (data not shown). In the case of non-inoculated dough, the virtuous microflora naturally presented in the flour,[33] in addition to the microorganisms present in the surrounding preparation area, requires several days, with frequent backslopping, to reach a sufficient concentration to perform an efficient sourdough fermentation. Furthermore, the limited VOC production detected with Y4 preparation could be explained by the particular formulation of this starter culture: while Y1, Y2 and Y3 preparations consisted of *Saccharomyces cerevisiae* biomass, Y4 was a dried natural sourdough used as starter culture in sourdough-based bread production. Giving that sourdoughs generally contain yeast/LAB [34] in a 1:100 ratio, they probably require several hours to reach the classical leavening power obtained using yeast concentrated biomass (Y1, Y2 and Y3) as starter culture. For these reasons, data analysis in this paper is restricted to dough samples supplemented with Y1, Y2 or Y3, and the results of other samples were not shown.

The typical mass spectrum of dough (Fig. 1) displayed more than 400 distinct peaks. In spite of the dilution of the headspace, ethanol (peak at nominal mass 47) was the second highest peak in terms of relative abundance, and ethanol-related mass peaks (*m/z* 65, 75 and 93 among others) were also well represented. However, it is important to notice that no depletion of the primary ion (monitored using peak at *m/z* 21) was observed.

It was observed that, out of the 400 mass peaks detected in the dough headspace, those with average concentrations below 1 ppbv showed little or no difference across the different experimental modes. The data set was thus filtered using a minimum threshold of 1-ppbv average concentration. This filtering yielded a subset of 72 mass peaks. The timepoint corresponding to cycle 3 (obtained at 2 h and 42 min of leavening) corresponded to the maximum expansion and was therefore selected for further analysis.

The results obtained for the three yeast preparations (Y1, Y2 and Y3) were visualized by means of principal component analysis (PCA), with each point representing a distinct sampling (Fig. 2). All three yeast preparations were able to perform fermentation (as shown by the evident increase in dough volume) and displayed a clear evolution of the VOC profile. The score plots for the first two principal components, which comprised 76.1% of the overall variability, had different starting and ending points, and the shading consistently varied over time. The elbow-like disposition of the points in the PCA reflects the fact that the different VOCs reached the top productivity at different time points along the course of the experiment (see further). The results were repeatable also between the two distinct biological replicates, and an overall time evolution which sums up the various kinetics showed similar overall trends, with yeast Y3 appearing to behave slightly differently from Y1 and Y2.

In-depth analysis of the leavening data

One of the advantages of the PTR-ToF-MS technique relies in the ability to discriminate between different peaks in one nominal mass. This is well exemplified by the insets in Fig. 1, showing the details for nominal mass 87 and the three yeast starters (and resulting micro-loaves). In the aforementioned example, the high mass resolution provided by the ToF mass analyzer

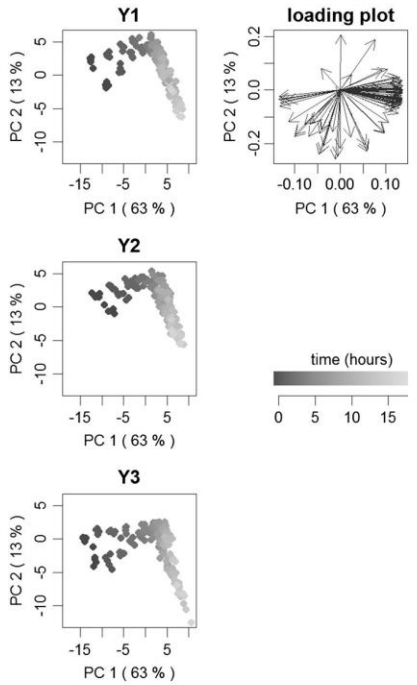

Figure 2. Volatile emission during leavening: principal component analysis of the autoscaled data. A loading plot and score plots for the first two principal components for three different yeasts are depicted ($n = 10$). Different shadings represent time evolution.

allowed to discriminate between masses *m/z* 87.044 (diacetyl) and *m/z* 87.081 (a C5 aldehyde or ketone.

The subset of 72 peaks obtained after filtration based upon concentration was further examined. Following a calibration procedure reported elsewhere,[29] exact masses could be estimated with three decimal places, thus reducing the range of error in peak identification. Upon treatment of the PTR-ToF-MS data, and elimination of peaks belonging to ^{13}C and ^{18}O isotopologues, water and ethanol clusters, 46 remaining mass peaks were further examined. Table 1 depicts the significantly different results, expressed in terms of productivity in ppbv per hour. Thirty-five of these 46 peaks could be assigned to a sum formula and based upon literature data 26 of these formulas could be tentatively assigned to one or more compounds. These tentatively identified compounds belong to various chemical classes including hydrocarbons (alkenes), carbonyls (esters, aldehydes, ketones), alcohols, carboxylic acids, in addition to some furan derivatives and sulfur compounds. They originate mainly from yeast metabolism [2] and are likely to contribute to the desirable aroma and odor properties of the baked product,[19] especially after undergoing further chemical reactions upon heating (e.g. Maillard reactions). One-way analysis of variance (ANOVA) ($p < 0.05$) showed differences between experimental modes for 16 relevant peaks, indicating a clear impact of the starter preparation on the volatile profile of the fermented dough. Y3 showed a lower productivity in 14 out of these 16 peaks, and a higher productivity rate in 2 out of 12 peaks. Since the chosen timepoint corresponded to the maximum in volume expansion for all the preparations (Y1, Y2 and Y3), therefore the leavening performances (a function of metabolic activity) were similar.

Table 1. Main volatiles detected in dough at maximum volume expansion. Whenever possible, mass peaks are associated to sum formulas and tentative identifications. For yeast starters Y1, Y2, and Y3 mean concentrations and standard deviations are reported. Statistically significant differences between experimental modes are established by means of one-way ANOVA ($p < 0.05$) and Tukey's *post-hoc* test and represented by means of superscript letter annotations

Meas. mass	Theor. mass	Sum formula	Concentration (ppbV)									*p*-value	Tentative identification	Ref.
			Y1			Y2			Y3					
41.039	41.039	$C_3H_5^+$	453.1	±	86.0 [ab]	487.3	±	79.2 [b]	388.8	±	56.0 [a]	**0.021**	Alkylic fragment (diverse origin)	
42.010	n.a.	Non identified	123.4	±	7.3 [a]	126.8	±	6.0 [a]	121.6	±	7.8 [a]	0.270		
43.017	43.018	$C_2H_3O^+$	3987.3	±	385.2 [a]	4108.1	±	81.4 [a]	3990.8	±	535.0 [a]	0.775	Ester fragment	[36]
43.054	43.054	$C_3H_7^+$	253.9	±	56.5 [a]	234.8	±	62.8 [a]	264.8	±	61.6 [a]	0.372	Alkylic fragment (diverse origin)	
43.150	n.a.	Non identified	3.3	±	0.5 [a]	3.2	±	0.3 [a]	3.2	±	0.4 [a]	0.796		
44.008	n.a.	Non identified	8.9	±	6.8 [a]	6.7	±	5.1 [a]	11.2	±	9.1 [a]	0.398		
45.032	45.033	$C_2H_5O^+$	36 251.7	±	11 356.7 [a]	33 393.0	±	8868.3 [a]	39 171.3	±	15 314.0 [a]	0.574	Acetaldehyde	[16]
47.014	47.013	$CH_3O_2^+$	26.2	±	1.4 [a]	29.4	±	2.6 [b]	24.9	±	2.0 [a]	**0.001**	Formic acid	
47.047	47.049	$C_2H_7O^+$	20 787.1	±	4741.3 [ab]	22 420.0	±	4898.7 [b]	17 363.0	±	3319.8 [a]	**0.045**	Ethanol	[16,37]
53.007	n.a.	Non identified	5.1	±	0.9 [a]	5.2	±	0.9 [a]	4.7	±	0.9 [a]	0.409		
53.038	n.a.	Non identified	16.0	±	0.9 [a]	16.6	±	1.1 [a]	16.1	±	0.7 [a]	0.100		
55.018	n.a.	Non identified	2.9	±	0.3 [a]	2.9	±	0.3 [a]	2.7	±	0.2 [a]	0.438		
55.054	55.054	$C_4H_7^+$	67.4	±	1.7 [a]	68.2	±	3.7 [a]	69.2	±	3.4 [a]	0.192	Fragment (butenal)	[36]
57.033	57.033	$C_3H_5O^+$	9.2	±	2.2 [b]	10.1	±	2.5 [b]	7.3	±	1.2 [a]	**0.017**		
57.070	57.070	$C_4H_9^+$	388.4	±	88.7 [a]	416.2	±	78.5 [a]	343.9	±	52.8 [a]	0.113	Fragment (butanal)	[36]
59.049	59.049	$C_3H_7O^+$	49.1	±	7.7 [a]	50.9	±	7.4 [a]	56.1	±	4.2 [a]	0.065	Acetone	[38]
61.028	61.028	$C_2H_5O_2^+$	779.6	±	182.2 [a]	860.7	±	198.6 [a]	677.1	±	114.4 [a]	0.069	Acetic acid/acetate esters	[16,39]
63.008	n.a.	Non identified	9.6	±	3.3 [ab]	10.9	±	3.1 [b]	7.0	±	2.6 [a]	**0.024**		
63.029	63.026	$C_2H_7S^+$	25.4	±	8.1 [a]	28.0	±	8.3 [a]	21.3	±	4.0 [a]	0.126	Dimethyl-sulfide	
65.040	n.a.	Non identified	1.2	±	0.8 [a]	1.4	±	0.5 [a]	1.0	±	0.5 [a]	0.229		
67.055	67.054	$C_5H_7^+$	3.1	±	0.7 [b]	3.3	±	0.8 [b]	2.4	±	0.5 [a]	**0.008**	Fragment (pentenal)	[36]
69.070	69.070	$C_5H_9^+$	12.5	±	1.0 [b]	13.0	±	1.4 [b]	6.8	±	0.9 [a]	**0.001**	Fragment (pentanal; generic aldehyde or terpene fragment)	[36]
71.050	71.049	$C_4H_7O^+$	20.6	±	1.3 [b]	17.1	±	0.8 [a]	22.8	±	2.7 [c]	**0.001**	Butenal	[16]
71.085	71.086	$C_5H_{11}^+$	131.0	±	33.7 [b]	143.1	±	36.3 [b]	89.6	±	19.2 [a]	**0.001**	Fragment (pentanol; generic alkylic fragment)	[36]
73.034	n.a.	Non identified	3.4	±	1.0 [a]	3.4	±	1.2 [a]	3.5	±	1.1 [a]	0.980		
73.065	73.065	$C_4H_9O^+$	278.3	±	20.0 [a]	285.1	±	22.3 [a]	304.5	±	19.0 [b]	**0.031**	n-Butyraldehyde/ methylpropanal	[16,38]
75.024	n.a.	Non identified	2.5	±	0.5 [a]	2.4	±	0.3 [a]	2.7	±	0.4 [a]	0.206		
75.044	75.044	$C_3H_7O_2^+$	6.0	±	1.1 [b]	6.8	±	1.3 [b]	4.6	±	0.5 [a]	**0.001**	Propionic acid and propanoate esters	[39,40]
75.080	75.080	$C_4H_{11}O^+$	27.2	±	11.4 [ab]	31.9	±	12.8 [b]	18.7	±	6.7 [a]	**0.030**	n-Butanol/methylpropanol	[16,37,40]

Journal of MASS SPECTROMETRY

79.054	79.054	$C_6H_7^+$	1.3	±	0.5	a	1.3	±	0.5	a	1.3	±	0.4	a	0.968		
81.070	81.070	$C_6H_9^+$	1.9	±	0.4	a	1.7	±	0.3	a	1.8	±	0.2	a	0.898	Fragment (hexenal)	[36]
83.049	83.049	$C_5H_7O^+$	1.0	±	0.4	a	1.0	±	0.3	a	1.0	±	0.4	a	0.999	2-Methylfuran	[16]
85.102	85.101	$C_6H_{13}^+$	1.0	±	0.3	a	1.1	±	0.3	a	1.2	±	0.4	a	0.548	Fragment (hexanal)	[36]
87.044	87.044	$C_4H_7O_2^+$	2.5	±	0.4	b	2.1	±	0.2	a	2.3	±	0.3	ab	**0.039**	Diacetyl	[12,16,37,40]
87.081	87.080	$C_5H_{11}O^+$	6.0	±	0.4	b	6.3	±	0.8	b	4.1	±	0.5	a	**0.001**	Isovaleraldehyde /2-methylbutanal/ pentanal	[12,16,38]
89.060	89.060	$C_4H_9O_2^+$	166.2	±	42.0	a	180.7	±	45.9	a	143.2	±	21.0	a	0.102	2-Methyl -propanoic acid/ethyl acetate	[16,37]
91.056	91.058	$C_4H_{11}S^+$	6.1	±	3.1	a	5.4	±	2.4	a	5.4	±	2.5	a	0.789		
91.075	91.075	$C_4H_{11}O_2^+$	5.3	±	0.8	a	5.6	±	0.9	a	5.4	±	0.4	a	0.639		
93.067	93.070	$C_7H_9^+$	1.7	±	0.6	a	1.7	±	0.2	a	1.6	±	0.6	a	0.734		
95.090	95.086	$C_7H_{11}^+$	1.1	±	0.3	a	1.0	±	0.3	a	1.0	±	0.2	a	0.624		
103.076	103.075	$C_5H_{11}O_2^+$	2.6	±	1.5	b	2.3	±	0.7	b	1.4	±	0.4	a	**0.024**	2-Methyl-butanoic acid/pentanoic acid/ethylpropionate	[16,39,40]
105.071	105.070	$C_8H_9^+$	6.7	±	2.2	b	6.9	±	1.9	b	4.2	±	1.8	a	**0.009**		
117.092	117.091	$C_6H_{13}O_2^+$	1.1	±	0.4	a	1.2	±	0.3	a	0.9	±	0.2	a	0.140	Hexanoic acid/ methylpropyl-acetate/ ethyl esters	[16,37,39]
119.087	119.086	$C_9H_{11}^+$	14.5	±	9.2	a	12.6	±	7.3	a	13.6	±	8.3	a	0.874		
121.067	121.065	$C_8H_9O^+$	2.4	±	1.3	a	2.4	±	1.2	a	2.5	±	1.4	a	0.971	Phenylacetaldehyde/ acetophenone	[12,16,40]
121.107	n.a.	Non identified	3.0	±	2.6	a	2.0	±	1.4	a	2.2	±	1.7	a	0.473		

Journal of MASS SPECTROMETRY

Supposedly, differences in VOCs profile could be more related to differences at the strain level than to the kind of yeast formulation. In fact, Y3 is produced by a different company, while Y1 and Y2 are both produced by Lessaffre; no scientific information is provided regarding differences between strains present in Y1 and Y2 formulations; however, given that they belong to the same company, it is possible that they are genetically and metabolically similar, and different from Y3. A clear example of such variations is peak *m/z* 87.081, tentatively assigned to a C5 aldehyde or ketone. Table 1 shows that Y1 and Y2 produced more of this product than Y3. The same trend can be seen for 14 other peaks, which can be attributed to fragments of metabolic aldehydes, alcohols, carboxylic acids and esters, all molecules with a contribution to the aromatic profile. On the other hand, peaks 71.050 and 73.065 (tentatively identified as butenal and n-butyraldehyde or methylpropanal, respectively) were produced more by Y3 than Y1 and Y2.

Yeast starters Y1 and Y2, in spite of being relatively close in terms of VOC production, displayed differences for mass peaks *m/z* 47.014, 71.050 and 87.044, tentatively identified as formic acid, butenal and diacetyl, respectively. Y1 had a smaller emission for the first peak and a greater one for the other two. This shows the efficiency of the applied method in clearly depicting minor differences also among yeasts having very similar metabolic behaviors.

Figure 3 depicts the evolution of three selected peaks, corresponding to mass peaks *m/z* 63.029, 71.050 and 103.076 and tentatively assigned to a sulfur compound, a carbonyl and a carboxylic acid or an ester (Table 1). This test shed light on statistical differences among the yeasts confirming previous analyses, in terms of yeast 3 (Y3) being different from the first two. While for some peaks (i.e. *m/z* 63.029 Th), the evolution is similar, for other peaks, yeast 3 has either a higher (i.e. *m/z* 71.05 Th) or a lower (i.e. *m/z* 103.0758 Th) production. Figure 3 also exemplifies how, depending on the mass peak, different kinetic processes can be noticed:

i. Fast production until the third leavening cycle, followed by a slow increase, an absolute maximum around the fifth cycle (obtained at 4 h and 30 min of leavening), then the volatile productivity starts to decrease (Fig. 3.a).
ii. A bimodal pattern consisting in a decreasing productivity rate followed by an increasing one, with an absolute minimum around the fifth cycle (Fig. 3.b).
iii. An accumulation trend with a slow increase in the volatile concentration (Fig. 3.c).

As mentioned earlier among all time points, the third cycle was selected as optimum because it corresponds to the maximum expansion of the dough. These results suggest that, thanks to the possibility to monitor VOC productivity in real time and simultaneously on multiple dough samples, PTR-MS would possibly allow to find alternative time optima for the fermentation process, based upon criteria other than expansion alone (i.e. defined to optimize certain aromatic contents).

Determination of the evolution of the VOCs after baking

A separate experiment was carried out with the aim to ascertain the impact of the starter metabolic activity during leavening on the VOC profile of the final product. The previous experiment had demonstrated the limited impact of the dried natural sourdough (i.e. Y4) in terms of VOC production during leavening. Therefore, in the present experiment, the doughs were supplemented with Y1, Y2 or Y3 only. At the third cycle of leavening the fermentation process was stopped, and the samples were baked for 8 min at 220 °C. This led to produce small-scale bread samples originating from the three different yeast preparations, and hence called B1, B2 and B3.

The comparison of top and bottom panels in Fig. 1 already provides an overview of the overall change in relative abundance of mass peaks that takes place upon baking of the samples. This is further exemplified by the comparison between the corresponding insets, displaying an inversion between peaks *m/z* 87.044 and 87.081 in terms of relative abundance.

Bread mass spectral data yielded about 400 mass peaks overall. Similar to the dough analysis, the data set was submitted to filtering based on a 1-ppbv concentration threshold, obtaining 64 mass peaks. Elimination of isotopers and clusters gave 35 peaks, 8 of which revealed statistically significant (one-way ANOVA, $p < 0.05$) differences among experimental modes. Again, it can be noticed that B3 showed a different volatile profile from B1

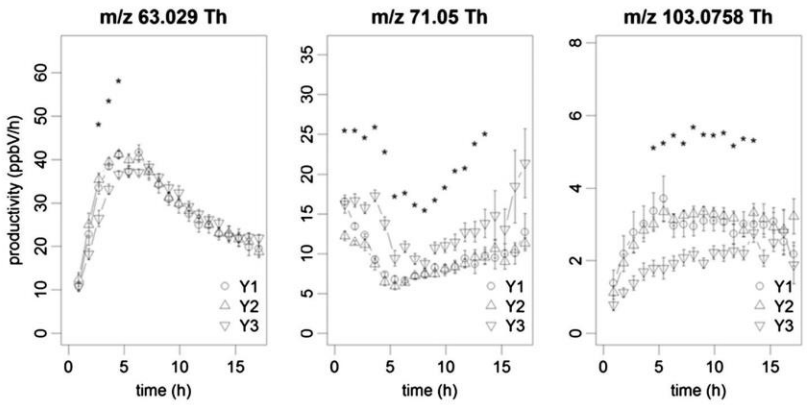

Figure 3. Volatile emission during leavening: time evolution of three selected mass peaks and three yeasts. Points represent average productivity values ($n = 10$), and error bars depict standard errors. Whenever a statistically significant difference between yeasts is encountered (one-way ANOVA, $p < 0.05$), this is indicated by an asterisk.

Table 2. Main volatiles detected in bread obtained with three different yeast starters. Whenever possible, mass peaks are associated to sum formulas and tentative identifications. For bread B1, B2, and B3 mean concentrations and standard deviations are reported. Statistically significant differences between experimental modes are established by means of one-way ANOVA ($p < 0.05$) and Tukey's *post-hoc* test and represented by means of superscript letter annotations

Meas. mass	Theor. mass	Sum formula	Concentration (ppb)										*p*-value	Tentative identification	Ref.
			B1				B2			B3					
41.039	41.039	$C_3H_5^+$	19.8	±	1.7	a	17.0	±	6.0	a	20.9	±	2.2	a	0.121	Alkylic fragment (diverse origin)	
43.018	43.018	$C_2H_3O^+$	131.4	±	27.3	a	106.6	±	40.4	a	174.3	±	44.1	b	0.016	Ester fragment	[36]
43.055	43.054	$C_3H_7^+$	8.5	±	0.6	a	7.4	±	2.5	a	8.7	±	0.9	a	0.118	Alkylic fragment (diverse origin)	
45.033	45.033	$C_2H_5O^+$	474.7	±	179.8	a	370.1	±	195.0	a	539.6	±	231.9	a	0.188	Acetaldehyde	[16]
47.013	47.013	$CH_3O_2^+$	16.5	±	2.6	a	13.8	±	4.7	a	16.8	±	2.3	a	0.284	Formic acid	
47.049	47.049	$C_2H_7O^+$	219.8	±	166.6	a	137.4	±	77.5	a	228.9	±	158.7	a	0.286	Ethanol	[16,37]
49.011	49.011	CH_5S^+	2.2	±	0.3	a	1.5	±	0.9	a	2.6	±	0.7	a	0.166	Methanethiol	
55.054	55.054	$C_4H_7^+$	5.6	±	0.4	a	5.1	±	1.2	a	5.8	±	0.6	a	0.309	Fragment (butenal)	[36]
55.935	n.a.	Non identified	2.2	±	0.1	a	2.3	±	0.1	a	2.2	±	0.1	a	0.148		
57.034	57.033	$C_3H_5O^+$	8.3	±	2.2	a	6.4	±	2.8	a	9.6	±	2.7	a	0.097		
57.070	57.070	$C_4H_9^+$	8.3	±	0.7	a	7.2	±	2.8	a	8.1	±	1.4	a	0.132	Fragment (butanal)	[36]
59.049	59.049	$C_3H_7O^+$	34.7	±	12.8	ab	25.9	±	8.6	a	39.4	±	13.0	b	**0.040**	Acetone	[38]
61.028	61.028	$C_2H_5O_2^+$	49.5	±	11.6	a	45.9	±	17.7	a	72.9	±	20.0	a	0.068	Acetic acid	[16]
63.026	63.026	$C_2H_7S^+$	5.9	±	0.2	a	5.8	±	0.2	a	5.9	±	0.4	a	0.614	Dimethyl-sulfide	
69.033	69.033	$C_4H_5O^+$	3.0	±	0.8	a	2.1	±	1.1	a	3.5	±	1.0	a	0.116		
69.070	69.070	$C_5H_9^+$	3.9	±	0.6	a	3.3	±	1.1	a	4.0	±	0.4	a	0.127	Fragment (pentenol. pentanal)	[36]
71.049	71.049	$C_4H_7O^+$	11.0	±	2.2	a	9.9	±	3.7	a	16.0	±	3.4	b	**0.015**	butenal	[16]
71.086	71.086	$C_5H_{11}^+$	2.9	±	0.4	a	2.5	±	1.2	a	2.5	±	0.7	a	0.354	Pentanol fragment	[36]
73.065	73.065	$C_4H_9O^+$	25.4	±	3.7	a	20.8	±	9.2	a	28.1	±	4.8	a	0.129	n-Butyraldehyde/methylpropanal	[16,38]
81.034	81.033	$C_5H_5O^+$	4.5	±	1.1	a	3.3	±	1.7	a	5.0	±	1.2	a	0.502		
83.049	83.049	$C_5H_7O^+$	2.0	±	0.6	a	1.5	±	0.6	a	2.3	±	0.6	a	0.279	Methylfuran	[16]
83.086	83.086	$C_6H_{11}^+$	1.2	±	0.1	a	1.2	±	0.1	a	1.3	±	0.1	a	0.388	Hexanol fragment	[36]
85.028	85.028	$C_4H_5O_2^+$	1.2	±	0.3	a	1.0	±	0.3	a	1.3	±	0.3	a	0.364	2-(5H)-furanone	[16]
87.045	87.044	$C_4H_7O_2^+$	11.8	±	2.7	ab	8.7	±	3.7	a	13.7	±	3.3	b	**0.050**	Diacetyl	[12,16,37,40]
87.081	87.080	$C_5H_{11}O^+$	3.3	±	0.6	a	2.5	±	1.4	a	3.5	±	0.4	a	0.084	Isovaleraldehyde/ 2-methylbutanal/pentanal	[12,16,38]
89.060	89.060	$C_4H_9O_2^+$	14.8	±	2.6	a	13.6	±	5.1	a	20.6	±	3.6	b	**0.016**	Methyl-propanoic acid/ethyl acetate	[16,37]
95.014	95.016	$C_2H_7O_2S^+$	4.2	±	0.8	ab	3.1	±	1.4	a	5.2	±	1.4	b	**0.013**		
95.060	95.060	$C_5H_7N_2^+$	1.6	±	0.2	a	1.3	±	0.5	a	1.7	±	0.2	a	0.406	Methylpyrazine	[16]
96.021	n.a.	non identified	3.1	±	0.7	ab	2.2	±	1.2	a	3.9	±	1.2	b	**0.008**		
97.029	97.028	$C_5H_5O_2^+$	21.3	±	5.1	a	15.0	±	8.2	a	26.5	±	8.2	b	**0.006**	Furfural	[12,16,40]
99.045	99.044	$C_5H_7O_2^+$	2.2	±	0.4	a	1.7	±	0.7	a	2.4	±	0.6	b	**0.001**	Furanmethanol	[16]
101.060	101.060	$C_5H_9O_2^+$	4.4	±	0.7	a	3.3	±	1.5	a	4.7	±	0.7	a	0.161	2-3-Pentanedione/	[16]
103.076	103.075	$C_5H_{11}O_2^+$	1.4	±	0.3	a	1.4	±	0.5	a	0.9	±	0.3	a	0.173	methyl-butanoic acid/ pentanoic acid/ethylpropionate	[16,40]
111.046	111.044	$C_6H_7O_2^+$	1.6	±	0.3	a	1.3	±	0.6	a	1.9	±	0.6	a	0.882	Acetyl-furan/methylfurfural	[16]
117.073	117.073	$C_6H_{13}S^+$	1.5	±	0.1	a	1.4	±	0.3	a	1.6	±	0.1	a	0.147		

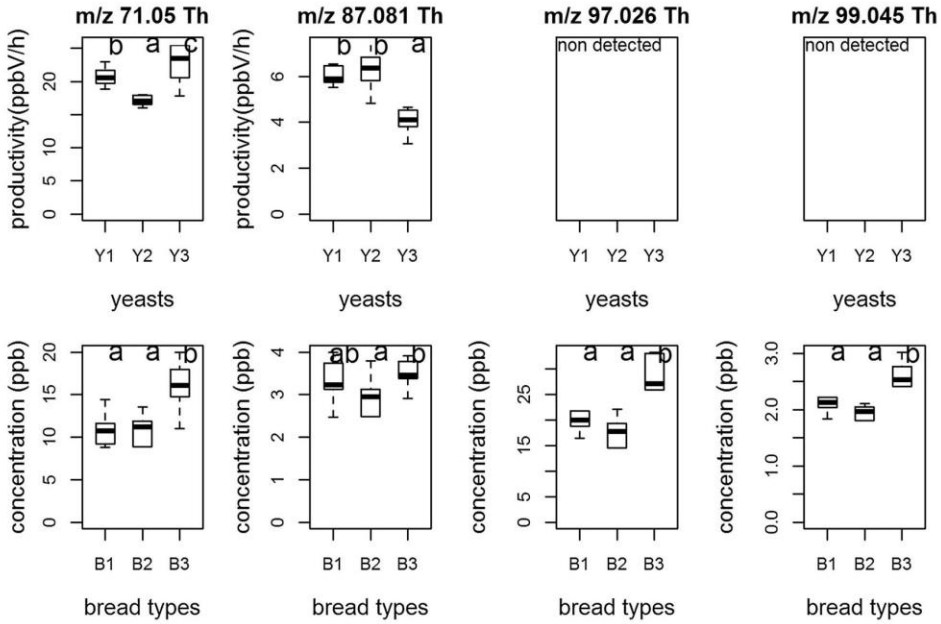

Figure 4. Selected volatiles emitted from dough after about 3 h of fermentation (top) and the corresponding micro-loaves (bottom): boxplots represent medians, upper and lower quartile, maximum and minimum for selected masses ($n = 10$ and $n = 5$ for dough and bread, respectively). Labels depict statistically significant differences (one-way ANOVA, $p < 0.05$ and Tukey's test).

and B2, producing more VOCs for all seven peaks and confirming the effect of the type of yeast initially used. These peaks (Table 2) can be attributed to compounds of several chemical classes including esters (e.g. peaks *m/z* 43.018 and *m/z* 101.060), ketones (e.g. peak *m/z* 59.049), aldehydes (e.g. peaks *m/z* 45.033 and *m/z* 71.049), alcohols (e.g. peak *m/z* 47.049), carboxylic acids (e.g. peaks *m/z* 61.028, and *m/z* 89.060) and furan derivatives (e.g. peaks *m/z* 97.029 and *m/z* 99.045). These peaks were identified in previous works [9] and can be attributed various characteristic aromatic properties.

The comparison of VOC emission in dough and bread is further exemplified by Fig. 4: sometimes, differences in doughs were reflected by bread (mass peak *m/z* 71.049) and sometimes not (mass peak *m/z* 87.081). Also, the analysis of the so-called 'micro-loaves' showed that some volatiles (24 mass peaks in total) were consumed upon baking; hence, the concentration of the peak either decreased or became below threshold. Other compounds (corresponding to 13 mass peaks overall) were absent during the leavening process of the bread but arose after the baking of the samples, proving the thermal effect of baking in enhancing the formation of new VOCs that will potentially affect the flavor of the baked product. In this group, we can also notice differences among yeasts, an example of which are mass peaks *m/z* 97.026 and *m/z* 99.045: these can be assigned to the furan derivatives furfural and 2-furanmethanol, respectively, which are mainly the result of the Maillard reaction which takes place upon baking.[9]

Conclusion

In this work, PTR-ToF-MS was used for the online study of *S. cerevisiae* volatile production during the fermentation of a food matrix: an interesting field of study, given the fact that *S. cerevisiae* domesticated strains have been used to make bread, beer and wine for thousands of years.[35] Moreover, this is the first experimental work that employs PTR-ToF-MS to assess (1) VOC release during bread-making and (2) the VOC production of different bakery starters. The system allowed for a fast, automated and real-time monitoring of the leavening process of bread; three types of yeast preparations exhibited the capability of performing the leavening process under the conditions applied with clear differences among them, in terms of VOC concentrations and kinetics. The overall course of the reaction was reproducible and enabled us to track the evolution of the production or depletion of a large number of VOCs as well as to discriminate between the different types of yeast preparations; this technique also allowed to tentatively identify major VOCs related to yeast metabolic activity or arising upon baking and more importantly, to point out differences in terms of volatile production and evolution kinetics either with time, between yeasts, and even before and after baking. Unexpectedly, the 'natural' yeast preparation (referred to as Y4), displayed scarce aromatic impact during leavening and therefore was not investigated in detail. The development of *ad hoc* protocols for the monitoring of dough fermentations by other types of bakery starters, along with further analytical verification on selected dough and bread samples by means of GC, will be addressed during the course of future research work.

References

[1] S.P. Cauvain, L.S. Young. Baking Problems Solved, Woodhead Publishing: Cambridge, UK, **2001**.
[2] S. Ur-Rehman, A. Paterson, J.R. Piggott. Flavour in sourdough breads: a review. *Trends in Food Science & Technology* **2006**, *17*, 557–566.

[3] L. De Vuyst, G. Vrancken, F. Ravyts, T. Rimaux, S. Weckx. Biodiversity, ecological determinants, and metabolic exploitation of sourdough microbiota. *Food Microbiology* **2009**, *26*, 666–675.
[4] V. Capozzi, P. Russo, M. Fragasso, P. De Vita, D. Fiocco, G. Spano. Biotechnology and pasta-making: lactic Acid bacteria as a new driver of innovation. *Frontiers in microbiology* **2012**, *3*, 94.
[5] L. De Vuyst, F. Leroy. Lactic acid bacteria as functional starter cultures for the food fermentation industry. *Trends in Food Science & Technology* **2004**, *15*, 67–78.
[6] V. Capozzi, G. Spano. Food Microbial Biodiversity and "Microbes of Protected Origin". *Frontiers in Microbiology* **2011**, *2*, 237.
[7] Y.H. Hui. Bakery Products: Science and Technology. John Wiley & Sons: Chichester, UK, **2008**.
[8] M.T. Madigan, J.M. Martinko, J. Parker, T.D. Brock. Biology of microorganisms. Prentice hall: Upper Saddle River, NJ, **1997**.
[9] I. Cho, D. Peterson. Chemistry of bread aroma: A review. *Food Science and Biotechnology* **2010**, *19*, 575–582.
[10] K. Gassenmeier, P. Schieberle. Potent aromatic compounds in the crumb of wheat bread (French-type) â€" influence of pre-ferments and studies on the formation of key odorants during dough processing. *Zeitschrift fÃ¼r Lebensmittel-Untersuchung und Forschung* **1995**, *201*, 241–248.
[11] S.I.F.S. Martins, W.M.F. Jongen, M.A.J.S. van Boekel. A review of Maillard reaction in food and implications to kinetic modelling. *Trends in Food Science & Technology* **2000**, *11*, 364–373.
[12] P. Schieberle, W. Grosch. Identification of the volatile flavour compounds of wheat bread crust â€" comparison with rye bread crust. *Zeitschrift fÃ¼r Lebensmittel-Untersuchung und Forschung* **1985**, 180, 474–478.
[13] P. Schieberle, W. Grosch. Quantitative analysis of aroma compounds in wheat and rye bread crusts using a stable isotope dilution assay. *Journal of Agricultural and Food Chemistry* **1987**, *35*, 252–257.
[14] P. Schieberle, W. Grosch. Evaluation of the flavour of wheat and rye bread crusts by aroma extract dilution analysis. *Zeitschrift fÃ¼r Lebensmittel-Untersuchung und Forschung* **1987**, *185*, 111–113.
[15] F. Bianchi, M. Careri, E. Chiavaro, M. Musci, E. Vittadini. Gas chromatographicâ€"mass spectrometric characterisation of the Italian Protected Designation of Origin â€œAltamuraâ€ bread volatile profile. *Food Chemistry* **2008**, *110*, 787–793.
[16] A. Paraskevopoulou, A. Chrysanthou, M. Koutidou. Characterisation of volatile compounds of lupin protein isolate-enriched wheat flour bread. *Food Research International* **2012**, *48*, 568–577.
[17] A. Hansen, P. Schieberle. Generation of aroma compounds during sourdough fermentation: applied and fundamental aspects. *Trends in Food Science & Technology* **2005**, *16*, 85–94.
[18] M. Aponte, F. Boscaino, A. Sorrentino, R. Coppola, P. Masi, A. Romano. Volatile compounds and bacterial community dynamics of chestnut-flour-based sourdoughs. *Food Chemistry* **2013**, *141*, 2394–2404.
[19] A.N. Birch, M.A. Petersen, Å.S. Hansen. The aroma profile of wheat bread crumb influenced by yeast concentration and fermentation temperature. *LWT - Food Science and Technology* **2013**, *50*, 480–488.
[20] A. Reale, T. Di Renzo, M. Succi, P. Tremonte, R. Coppola, E. Sorrentino. Microbiological and Fermentative Properties of Baker's Yeast Starter Used in Breadmaking. *Journal of Food Science* **2013**, *78*, M1224–M1231.
[21] B. Grote, T. Zense, B. Hitzmann. 2D-fluorescence and multivariate data analysis for monitoring of sourdough fermentation process. *Food Control* **2014**, *38*, 8–18.
[22] A.N. Birch, F.W.J. van den Berg, Å.S. Hansen. Expansion profiles of wheat doughs fermented by seven commercial baker's yeasts. *Journal of Cereal Science* **2013**, *58*, 318–323.
[23] A. Jordan, S. Haidacher, G. Hanel, E. Hartungen, L. MÄ¤rk, H. Seehauser, R. Schottkowsky, P. Sulzer, T.D. MÄ¤rk. A high resolution and high sensitivity proton-transfer-reaction time-of-flight mass spectrometer (PTR-TOF-MS). *International Journal of Mass Spectrometry* **2009**, *286*, 122–128.
[24] F. Biasioli, F. Gasperi, C. Yeretzian, T.D. MÄ¤rk. PTR-MS monitoring of VOCs and BVOCs in food science and technology. *TrAC Trends in Analytical Chemistry* **2011**, *30*, 968–977.
[25] S.P. Heenan, J.-P. Dufour, N. Hamid, W. Harvey, C.M. Delahunty. Characterisation of fresh bread flavour: Relationships between sensory characteristics and volatile composition. *Food Chemistry* **2009**, *116*, 249–257.
[26] C. Soukoulis, E. Aprea, F. Biasioli, L. Cappellin, E. Schuhfried, T.D. MÄ¤rk, F. Gasperi. Proton transfer reaction time-of-flight mass spectrometry monitoring of the evolution of volatile compounds during lactic acid fermentation of milk. *Rapid Communications in Mass Spectrometry* **2010**, *24*, 2127–2134.
[27] F.J. Gallardo-Escamilla, A.L. Kelly, C.M. Delahunty. Influence of Starter Culture on Flavor and Headspace Volatile Profiles of Fermented Whey and Whey Produced from Fermented Milk. *Journal of dairy science* **2005**, *88*, 3745–3753.
[28] V. Capozzi, V. Menga, A.M. DigesÃ1, P. De Vita, D. van Sinderen, L. Cattivelli, C. Fares, G. Spano. Biotechnological Production of Vitamin B2-Enriched Bread and Pasta. *Journal of Agricultural and Food Chemistry* **2011**, *59*, 8013–8020.
[29] L. Cappellin, F. Biasioli, A. Fabris, E. Schuhfried, C. Soukoulis, T.D. MÄ¤rk, F. Gasperi. Improved mass accuracy in PTR-TOF-MS: Another step towards better compound identification in PTR-MS. *International Journal of Mass Spectrometry* **2010**, *290*, 60–63.
[30] L. Cappellin, F. Biasioli, P.M. Granitto, E. Schuhfried, C. Soukoulis, F. Costa, T.D. MÄ¤rk, F. Gasperi. On data analysis in PTR-TOF-MS: From raw spectra to data mining. *Sensors and Actuators B: Chemical* **2011**, *155*, 183–190.
[31] W. Lindinger, A. Hansel, A. Jordan. On-line monitoring of volatile organic compounds at pptv levels by means of proton-transfer-reaction mass spectrometry (PTR-MS) medical applications, food control and environmental research. *International Journal of Mass Spectrometry and Ion Processes* **1998**, *173*, 191–241.
[32] L. Cappellin, T. Karl, M. Probst, O. Ismailova, P.M. Winkler, C. Soukoulis, E. Aprea, T.D. MÄ¤rk, F. Gasperi, F. Biasioli. On Quantitative Determination of Volatile Organic Compound Concentrations Using Proton Transfer Reaction Time-of-Flight Mass Spectrometry. *Environmental Science & Technology* **2012**, *46*, 2283–2290.
[33] L. De Vuyst, P. Neysens. The sourdough microflora: biodiversity and metabolic interactions. *Trends in Food Science & Technology* **2005**, *16*, 43–56.
[34] M. Gobbetti, A. Corsetti, F. La Rosa, S. De Vincenzi. Identification and clustering of lactic acid bacteria and yeasts from wheat sourdoughs of central Italy. *Italian J Food Sci* **1994**, *1*, 85–94.
[35] J.C. Fay, J.A. Benavides. Evidence for domesticated and wild populations of Saccharomyces cerevisiae. *PLoS genetics* **2005**, *1*, 66–71.
[36] K. Buhr, S. van Ruth, C. Delahunty. Analysis of volatile flavour compounds by Proton Transfer Reaction-Mass Spectrometry: fragmentation patterns and discrimination between isobaric and isomeric compounds. *International Journal of Mass Spectrometry* **2002**, *221*, 1–7.
[37] B. Hansen, Å. Hansen. Volatile compounds in wheat sourdoughs produced by lactic acid bacteria and sourdough yeasts. *Zeitschrift für Lebensmittel-Untersuchung und Forschung* **1994**, *198*, 202–209.
[38] F.E. Kohn, L. Wiseblatt, L.S. Fosdick. Some Volatile Carbonyl Compounds Arising During Panary Fermentation. American Institute of Baking: Chicago, Illinois, **1960**.
[39] E. Aprea, F. Biasioli, T.D. Märk, F. Gasperi. PTR-MS study of esters in water and water/ethanol solutions: Fragmentation patterns and partition coefficients. *International Journal of Mass Spectrometry* **2007**, *262*, 114–121.
[40] N.T. Annan, L. Poll, S. Sefa-Dedeh, W.A. Plahar, M. Jakobsen. Volatile compounds produced by Lactobacillus fermentum, Saccharomyces cerevisiae and Candida krusei in single starter culture fermentations of Ghanaian maize dough. *Journal of Applied Microbiology* **2003**, *94*, 462–474.

3.3 Volatile Compound Production during the Bread-Making Process: Effect of Flour, Yeast and Their Interaction

In the first *ProBake* paper, we showed that this technique allowed the automated online monitoring of VOCs as well as the tentative identification of major VOCs related to yeast metabolic activity or arising upon baking. More importantly, we were able to point out differences in terms of volatile production and evolution kinetics either with time, between yeasts, and even before and after baking. After this first step, we were interested in studying the effect of each ingredient as well as the possible ingredient/microbe interaction. Hence, in this second *ProBake* paper, further investigation was conducted on the main ingredient in the bread recipe: flour. It is commonly known among locals and bread-makers that flour has the most noticeable influence on the final aroma of the baked product (Annett, Spaner, & Wismer, 2007). PTR-ToF-MS was applied to test this hypothesis.

In parallel, the contribution of yeast to the final properties was assessed as well. The comparison of both studies lead to the conclusion that yeast has a more pronounced effect. However, a cycle-by-cycle monitoring of the leavening process revealed a third dimension, proving a kind of synergistic and/or disruptive interaction between flour and yeast affecting the productivity of VOCs.

As mentioned in the paper, “such findings shed a new light on the selection of ingredients for each bread recipe depending on the desired volatile profile of the baked product and on the potential of PTR-MS in analyzing protechnological microbes/matrix interaction during food fermentations” (Makhoul et al., 2015).

Note that supplementary material, available only for the online version of this paper, are attached at the end of this thesis (**Appendix 2**). They include two extended tables, the loadings plot, the PC variance table, the variation of Principal Components plot, as well as the plot of the Cumulative Variation of Principle Components.

Food Bioprocess Technol (2015) 8:1925–1937
DOI 10.1007/s11947-015-1549-1

ORIGINAL PAPER

Volatile Compound Production During the Bread-Making Process: Effect of Flour, Yeast and Their Interaction

Salim Makhoul[1,2,3] · Andrea Romano[1,4] · Vittorio Capozzi[1,4] · Giuseppe Spano[5] · Eugenio Aprea[1] · Luca Cappellin[1] · Elisabetta Benozzi[1,6] · Matteo Scampicchio[4] · Tilmann D. Märk[6] · Flavia Gasperi[1] · Hanna El-Nakat[2] · Jean Guzzo[3] · Franco Biasioli[1]

Received: 19 March 2015 / Accepted: 15 June 2015 / Published online: 7 July 2015

Abstract Bread is one of the most consumed products around the world, justifying the continuous research and development activities on how to improve its sensory, chemical and industrial characteristics. Volatile organic compounds (VOCs) play a key role in this regard because they take shape during the leavening process and are enhanced upon baking. In this study, proton-transfer reaction mass spectrometry (PTR-MS), coupled to a time-of-flight (ToF) mass analyser, was undertaken in order to analyse the effects of *Saccharomyces cerevisiae* strains as well as the type of wheat flour used in the bread-making process on VOC production. The results showed a greater impact of yeast strains over the expected flour influence. This observation was confirmed when the leavened dough samples were baked and the volatile profiles determined. However, the peak-by-peak monitoring, followed by a tailored statistical approach, revealed not only the effect of changing ingredients but also different kinds of yeast/flour interaction. Such findings shed a new light on the selection of ingredients for each bread recipe depending on the desired volatile profile of the baked product and on the potential of PTR-MS in analysing protechnological microbes/matrix interaction during food fermentations.

Keywords PTR-MS · VOCs · Bread · Yeast · Flour · Aroma · Interaction

Electronic supplementary material The online version of this article (doi:10.1007/s11947-015-1549-1) contains supplementary material, which is available to authorized users.

✉ Franco Biasioli
franco.biasioli@fmach.it

[1] Department of Food Quality and Nutrition, Research and Innovation Centre, Fondazione Edmund Mach (FEM), via E. Mach 1, 38010 San Michele all'Adige, TN, Italy

[2] Department of Chemistry, University of Balamand, P. O. Box 100, Tripoli, Lebanon

[3] UMR PAM—équipe VALMIS, IUVV, 1 rue Claude Ladrey, 21078 Dijon Cedex, France

[4] Faculty of Science and Technology, Free University of Bolzano, 39100 Bolzano, Italy

[5] Department of Agriculture, Food and Environmental Sciences, University of Foggia, via Napoli 25, 71122 Foggia, Italy

[6] Institut für Ionenphysik und Angewandte Physik, Leopold-Franzens Universität Innsbruck, Technikerstr. 25, 6020 Innsbruck, Austria

Introduction

Bread wheat (*Triticum aestivum* L.) provides approximately 20 % of calories consumed by humans (Feldman et al. 2012) under the form of an articulate variety of baked products. Among these, bread is the most popular because of its nutritional quality and its sensory and textural properties (Patel et al. 2005; Poinot et al. 2008). The main ingredient in bread is flour obtained after the grinding and milling of soft or durum wheat (Hui 2008). Wheat is one of the most ancient of domesticated crops, with archaeological evidence of its use also in combination with yeast and bacteria in staple food (Shevchenko et al. 2014).

Bread aroma is formed during the three main steps, namely kneading, fermentation and baking, each strongly affected by the time and temperature used. Fermentation comes after the incorporation of yeasts in the dough. In this phase, secondary metabolic activities by microorganisms lead to the release of a variety of VOCs. Finally, during baking, the precursor compounds previously formed lead to a number of volatile compounds resulting from two non-enzymatic browning reactions, known as the Maillard reactions and caramelization,

two phenomena rapidly observable at temperature higher than 140 °C, in addition to the flour lipids oxidation. In particular, VOCs in bread crumb mainly arise from the yeast fermentative performances, from flour lipid oxidation and to a lower extent from Maillard reactions (Birch et al. 2013b), while the aroma of bread crust is mostly due to Maillard reactions (Purlis and Salvadori 2009).

Flour has always been considered a crucial ingredient in the determination of the chemical, physical and sensory properties of bakery products (Annett et al. 2007; Hansen and Hansen 1994), including texture, volume and flavour, the latter being central to consumer acceptability and product recognition (Heenan et al. 2009). Salovaara and Valjakka (1987), studying the effects of the type of wheat flour, fermentation temperature and origin of starter on acid production and bread properties, concluded that the type of flour was the most important factor (Salovaara and Valjakka 1987). In effect, apart from starch that represents its major constituent, wheat flour also contains many other types of substances (e.g. gluten, non-starch polysaccharides, lipids) with relevant influence on the bread quality (Goesaert et al. 2005); among these, while a different content in reducing sugars and protease may directly impact on bread flavour (Goesaert et al. 2005; Mathewson 2000), all other components potentially influence bread aroma in reason of their influence on the microbial fermentation performances (Vernocchi et al. 2008; Birch et al. 2013b).

With this concern, while spontaneous fermentations, backslopping practices and traditional recipes have historically been used, with the development of the industrial processes in the 1930s, it became achievable to manufacture high-quality baker's yeast at a low price (Gélinas 2012). A considerable number of new ingredients, processing aids and additives were also introduced in bread making. Obliviously, together with flour characteristics, any modifications of the bread-making process or recipe also leads to changes in the quality of bread (Paraskevopoulou et al. 2012). For instance, Birch et al. (2013c) have recently reported that the dough expansion depends on several factors besides the type of wheat flour such as yeast concentration, additives (including lactic acid, fat, sugar and sodium chloride) and process variables (relative humidity, fermentation temperature and mixing duration) (Birch et al. 2013c). Recently, an increasing attention of both consumers and the bakery industry has been focused on aroma as a quality criterion (Birch et al. 2013a). To explain the importance of bread flavour from various flour types, different extraction methods (solvent extraction, SPME etc.) and analytical techniques have been developed along with olfactometric techniques (dilution, intensity, detection frequency methods) so that the most important bread aroma compounds, belonging to VOCs, are arranged in order of their flavour significance (Paraskevopoulou et al. 2012).

The development and the use of baker's yeast was a crucial phase of modern baking technology and an important factor in bread quality perception (Randez-Gil et al. 2013). During bread fermentations, the yeast *Saccharomyces cerevisiae* uses simple carbohydrates to produce ethanol and carbon dioxide as the primary products. In addition, baker's yeast also releases secondary metabolites (higher alcohols, aldehydes, sulphur-containing compounds, esters, phenols, carbonyl compounds and organic acids) that have a marked effect on the product's sensory quality (Steensels et al. 2014). This quantitative release of aroma-active compounds is a yeast strain-dependent character (Steensels et al. 2014). Recently, Makhoul et al. studied the VOC production of different bakery starters, showing the importance of online monitoring of yeast in volatile production during the leavening process of the dough and upon baking, using for the first time proton-transfer-reaction time-of-flight mass spectrometry (PTR-ToF-MS) to monitor this food bioprocess (Makhoul et al. 2014),whereas a previous study defined a PTR-MS-based protocol only for simulating bread aroma during mastication (Onishi et al. 2012). PTR-MS is a direct injection mass spectrometry technique, based upon mild ionization by means of a pure beam of hydronium ions (Romano et al. 2015). This characteristic, along with the coupling to a time-of-flight (ToF) mass analyser, provides cutting-edge sensitivity and mass spectra with a high informational content (Jordan et al. 2009) also allowing to monitor VOCs in a direct, fast and sensitive way (Biasioli et al. 2011; Soukoulis et al. 2013). Furthermore, among other applications, PTR-ToF-MS was proven successful not only in studying the volatile organic compound production during bread making but also in characterizing and selecting bakery commercial starter cultures in view of their production of volatile compounds (Makhoul et al. 2014). However, the effect of different starters with respect to diverse flours has never been studied before.

In fact, the yeast aroma contribution to baked products has been receiving increasing interest as testified by recent applied studies (Birch et al. 2013b; Paraskevopoulou et al. 2012), breeding and selection efforts (Steensels et al. 2014; Dueñas-Sánchez et al. 2014) and by the number of patented strains with enhanced aroma performances (Gelinas 2009). The impact of different starter cultures and or diverse fermentation temperatures is usually considered in terms of bread aroma. Nevertheless, several relevant factors on bread making need major insights. For instance, the effect of yeast strains on bread aroma is far to be understood (Birch et al. 2013a) while the interaction between flour types and baking yeast strains has never been investigated. Therefore, in order to monitor online the leavening process and to employ a technique useful to identify VOCs originating from the interaction between starter cultures and food matrices, the approach recently described by Makhoul et al. was adopted (Makhoul et al. 2014). Compared to 'traditional' techniques, often time-consuming and limited (Sauer et al. 2004; Gelinas and Lachance 1995), PTR-ToF-MS is suggested for or the automated and online

real-time monitoring of the leavening process (Makhoul et al. 2014). Concerning the range of flours used in this study, our aim was to represent the main types of raw matrices used in bread making such as bread flour (extensively used for a wide range of baked products), Manitoba flour (well known for high performances in dough characteristics) and durum flour (mainly used for Italian pasta but also for relevant typical bread in the Mediterranean region). With regard to yeast addition and in order to increase the applicative significance of the study, commercial yeast preparations, purchased from different manufactures and following bread-makers instructions, were chosen.

Therefore, in this study, we evaluate the impact of using various flour types on the VOCs evolved during leavening and upon baking. Moreover, the effect of bakery starter cultures and the importance of interaction between flour and yeast on VOCs production were evaluated. For the first time, we report PTR-MS as a practical high-throughput tool to study the effect of interaction of protechnological microbes with the raw matrices on VOC production in fermented food manufacture.

Materials and Methods

Sample Preparation

The experimental plan was conceived to test the effect of flour, yeast and their interaction on bread volatile organic compounds. Four different types of flour and two different yeast preparations were used to obtain eight different dough samples, prepared according to the procedure described in AACC 10-10B (approved methods of the AACC, 10th ed.; American Association of Cereal Chemists: St. Paul, MN, 2000), with minor modifications (Capozzi et al. 2011). Our experimental design considered four independent biological intra-day replicates and two independent biological inter-day replicates (overall eight independent biological replicates for each tested condition). Each dough was obtained by mixing 200 g of F1 flour (durum wheat, Divella, Italy), F2 flour (bread wheat type '00', Granoro, Italy), F3 flour (bread wheat type '0', Antico Molino Rosso, Italy) and F4 Manitoba flour (Molino Spadoni, Italy), 3 g of sodium chloride (Sigma Aldrich, St. Louis, MO), 12 g of sucrose (Sigma Aldrich), 6 g of animal fat (Casa Modena, Modena, Italy), 8 mg of ascorbic acid (Sigma Aldrich) and 120 mL of distilled water. The preparation was carried out using a bread homemaker machine (Princess Household Appliances, Lainate, Italy). The dough samples were supplemented with one of these two yeast preparations, either Y1 (Lesaffre, Parma, Italy) or Y2 (Pakmaya, Istanbul, Turkey) which consisted in single *S. cerevisiae* strain. The yeast preparations were added in different amounts (30 g/kg of flour Y1, 10 g/kg of flour Y2) following the manufacturer's recommendations. The dough was divided into 1.0 g pieces (stored in 22-mL vials). During preparation, the dough was kept at 4 °C in order to reduce the fermentation process. Then, the samples were transferred at 30 °C for the whole duration of the experiment (approximately 16 h). Four replicates of each dough sample were analysed (resulting in a total of 32 vials) and the entire experiment was repeated twice.

For baked bread analysis, the same experiment was repeated with F1, F2, F3 and F4 flours inoculated with either Y1 or Y2 yeast preparations. After 2 h and 42 min of leavening, the vials were taken out. Caps were removed and vials were transferred to a kitchen oven and baked for 8 min at 220 °C. Around this temperature, Maillard reactions, condensation reactions, take place between amino acids and sugars creating flavour, aroma and colour of the bread crust. Thus, it is considered an important biochemical process (Cho and Peterson 2010). It is important to note that prior to the analysis, we accurately cleaned the oven and turned it on for 1 h with ventilation to be sure to avoid residual VOCs from other preparations. To confirm the absence of residual VOCs, an empty vial was introduced in the oven during baking and later used as a blank control.

Yeast Count

One gram of baker's yeast was suspended in 9 mL of sterile physiological saline (8.5 g NaCl, g/L). Serial decimal dilutions were prepared in sterile physiological saline, and 0.1 mL samples of appropriate dilutions were spread on sterile YPG agar plates (20 g/L glucose, 20 g/L yeast extract, 10 g/L peptone and 20 g agar, pH 5.5). The plates were incubated at 26 °C for 48 h before counting the yeast colony forming units (CFU).

PTR-TOF-MS Analysis

In order to measure the headspace of the dough and bread samples, a commercial PTR-TOF-MS 8000 apparatus from Ionicon Analytik GmbH (Innsbruck, Austria), was used in its standard configuration (V mode). The ionization conditions in the drift tube were the following: 110 °C drift tube temperature, 2.30 mbar drift pressure and 550 V drift voltage. This led to an E/N ratio of about 140 Townsend (1 Td = 10^{-17} cm^2 V^{-1} s^{-1}). The inlet line consisted of a PEEK capillary tube (internal diameter 0.40 mm) heated at 110 °C. The inlet flow was set at 120 and 40 sccm for dough and bread measurements, respectively.

The automation used for the leavening experiments was the same as the one described in previous works by Makhoul et al. (2014) using an autosampler (Gerstel, Mulheim am Main, Germany) especially adapted to PTR-MS analyses. After setting up both the PTR-ToF-MS and the autosampler, the leavening process was launched, allowing the samples to be

incubated at 30 °C for 30 min, and then their headspace was analysed every 54 min. This generated up to twenty time points during the course of a typical leavening experiment. The whole dataset consisted of ten replicates for each experimental mode, obtained aggregating two distinct biological replicates. At the beginning of the experiment, the robotic arm moved the sample from a cooling tray where it was kept at 4 °C, to the incubation tray, whose temperature was set at 30 °C. Vials were then moved to the temperature-controlled purging site, connected to the PTR-ToF-MS inlet, and where the headspace analysis took place for 30 s with an acquisition rate of one spectrum per second. After measurement, the vial was moved to the incubation tray and the cycle was repeated on the following sample. This allowed to perform a scan of the tray (32 samples) in approximately 1 h (1 cycle = 54 min). During leavening, the scan was repeated 16 to 20 times, in order to monitor the fermentation process. Due to the presence of relevant amounts of ethanol (an average of 20 ppmv of ethanol) in the headspace of the samples during leavening, an inert gas dilution was applied in an inert gas to sample ratio of 2:1. This permitted to prevent primary ion depletion and formation of ethanol clusters which might affect the final quantification of volatiles (Aprea et al. 2007). In fact, at all times, the ionization should be carried out by the H_3O^+ primary ions. If at any point, the levels of ethanol or ethanol clusters exceed that of H_3O^+, the latter will not remain the primary ionizing ion which will lead to errors in data analysis afterwards.

The headspace of micro-loaves obtained after baking was measured as before. Prior to analysis, samples were flushed with a stream of clean air (200 mL/min for 30 s), as generated by a gas calibration unit apparatus (Ionicon Analytik GmbH), then incubated at 30 °C for 30 min and finally analysed for 30 s at one spectrum per second. No dilution of the headspace was required in this case.

Data and Statistical Analyses

Dead time correction, internal calibration of mass spectral data and peak extraction were performed according to a procedure described in the works of Cappellin et al. (Cappellin et al. 2010; Cappellin et al. 2011), using a modified Gaussian peak shape. Peak intensity in ppbV was estimated using the formula described in literature (Lindinger et al. 1998), using a constant value for the reaction rate constant coefficient ($k = 2.10^{-9}$ cm^3 s^{-1}). This introduces a systematic error for the absolute concentration for each compound that is in most cases below 30 % and could be accounted for if the actual rate constant coefficient is available (Cappellin et al. 2012).

All data detected and recorded by the PTR-TOF-MS were processed and analysed using MATLAB (MathWorks, Natick, MA) and in-house developed scripts written in R programming language (R Foundation for Statistical Computing, Vienna, Austria).

Principal component analysis (PCA) was applied to visualize the entire evolution of the leavening process and the effect of changing each ingredient. Analysis of variances (ANOVA, $p < 0.05$) along with post hoc statistical tests was applied to identify significant differences and interactions between different groups (flour types and yeasts).

Results

Automated Monitoring of the Leavening Process

More than 400 peaks were detected during this leavening process, showing a number of ethanol (peak 47.049) and ethanol-related peaks (e.g. peaks 65.059, 75.080 and 93.091) (Aprea et al. 2007). Upon filtering the results based on a 1-ppbV concentration threshold, under which peaks have no or poor contribution to the experimental modes, a subset of 45 mass peaks was obtained. The time point corresponding to cycle 3 (obtained at 2 h and 42 min of leavening) corresponded to the maximum in volume expansion of the dough and was therefore selected for further analysis.

After analysis of the volatile profile of the leavening process of the dough and upon treatment of the PTR-ToF-MS data, and elimination of peaks belonging to isotopes, 24 mass peaks were kept. Table 1 depicts the significantly different results, expressed in terms of productivity in ppbV per hour. If we consider the flour as the changing factor, one-way ANOVA ($p < 0.05$) shows differences between experimental modes for 6 relevant peaks. In one case, F1 (durum wheat) is different than the rest of flours and in another case F2 (bread wheat type 00) is different. In all other cases, all types of flour exhibited the same volatile profile. On the other hand, if we consider the yeast as the changing factor, differences are now observed for 23 different peaks. In 15 out of these 23 peaks, Y1 produced more than Y2 and less for the remaining 8 peaks. We did not observe any difference in yeast count between the two preparations (data not shown). The observations in VOC changes reported for the dough have a particular relevance if we consider that the production of dehydrated dough/sourdoughs is a business having worldwide diffusion, as these are generally added as ingredient to several bakery productions (Kulp and Lorenz 2003).

Volatile Profile of the Baked Samples

The volatile profile of baked samples resulted in no less than 500 peaks. After setting a threshold of 1 ppbV, 89 mass peaks remained, and upon treatment of the PTR-ToF-MS data, including the elimination of peaks belonging to isotopes, 28 mass peaks were kept. Table 2 depicts the statistically

Table 1 Main volatiles detected in dough at maximum volume expansion

Meas.Mass	Theor.Mass	Sum Formula	Flour Types					Yeasts		
			Concentration (ppb)				*p*-value	Concentration (ppb)		*p*-value
			F1	F2	F3	F4		Y1	Y2	
39.965			1.0±0.1	1.1±0.1	1.1±0.1	1.1±0.2	0.195	1.0±0.1	1.2±0.1	*0.000*
40.027			8.8±2.5	8.5±1.7	8.9±1.8	8.2±2.2	0.575	9.3±2.1	7.9±1.8	*0.001*
40.972			56.4±4.9	58.4±3.1	58.0±4.4	58.2±4.7	0.402	54.6±3.5	60.9±2.3	*0.000*
41.039	41.039	$C_3H_5^+$	35.9±10.5	33.4±6.8	35.4±7.3	32.4±9.5	0.436	37.5±8.7	31.0±7.3	*0.000*
42.010	n.a.	non identified	23.2±6.0	22.0±3.7	23.9±4.9	22.2±6.1	0.566	26.6±4.4	19.0±2.7	*0.000*
43.018	43.018	$C_2H_3O^+$	466.9±64.5^a	467.9±66.4^a	528.4±72.7^b	484.6±69.0^{ab}	*0.007*	462.1±67.2	511.7±67.9	*0.001*
43.055	43.054	$C_3H_7^+$	16.9±4.6	16.4±4.0	17.1±3.5	16.0±4.8	0.788	19.0±4.3	14.2±2.3	*0.000*
44.975	44.997	CO_2H^+	4.0±0.5	3.9±0.7	4.2±0.9	4.0±0.6	0.311	3.6±0.5	4.4±0.7	*0.000*
45.033	45.033	$C_2H_5O^+$	8496.5±1278.5	8399.1±1612.3	9279.0±1744.4	8533.1±1356.8	0.166	7649.0±1040.6	9704.9±1213.4	*0.000*
45.075	n.a.	non identified	6.1±1.8^b	4.7±0.8^a	5.3±1.2^{ab}	4.9±1.2^a	*0.003*	6.1±1.4	4.4±0.7	*0.000*
45.182	n.a.	non identified	14.2±1.8	13.9±2.3	15.3±2.5	14.4±1.9	0.167	12.9±1.5	15.9±1.6	*0.000*
47.049	47.049	$C_2H_7O^+$	635.1±316.9	517.0±179.5	615.2±259.6	560.6±309.0	0.428	797.7±217.9	366.3±80.9	*0.000*
53.006	n.a.	non identified	2.1±0.5	2.0±0.4	2.2±0.5	2.0±0.6	0.669	2.3±0.5	1.8±0.3	*0.000*
57.070	57.070	$C_4H_9^+$	27.7±9.4	24.9±6.2	26.1±6.3	22.8±8.0	0.157	27.1±7.6	23.6±7.4	*0.024*
61.029	61.028	$C_2H_5O_2^+$	33.4±20.7	33.5±18.1	43.1±23.1	37.7±27.3	0.399	54.1±19.8	19.7±5.8	*0.000*
63.008	n.a.	non identified	1.5±1.3	0.9±0.7	1.3±0.9	1.0±0.9	0.141	1.9±0.9	0.4±0.2	*0.000*
71.086	71.086	$C_5H_{11}^+$	5.4±1.4	5.4±1.1	5.8±1.1	5.2±1.4	0.535	5.9±1.3	5.0±1.0	*0.000*
73.065	73.065	$C_4H_9O^+$	28.9±6.6	30.1±3.3	30.9±3.7	29.9±3.3	0.502	28.6±4.7	31.4±3.7	*0.002*
75.027	75.026	$C_3H_7S^+$	1.1±0.2	1.2±0.1	1.1±0.1	1.2±0.1	0.810	1.1±0.1	1.2±0.2	*0.000*
89.060	89.060	$C_4H_9O_2^+$	4.3±2.5	4.0±1.9	5.2±2.6	4.4±3.0	0.410	6.4±2.2	2.6±0.7	*0.000*

For flour types F1, F2, F3 and F4 and yeast starters Y1 and Y2 mean concentrations and standard deviations are reported. Statistically significant differences between experimental modes are established by means of one-way ANOVA (when $p<0.05$, the p value is shown in italics) and Tukey's post hoc test and represented by means of superscript letter annotations. Only statistically different peaks are represented

Table 2 Main volatiles detected in bread obtained with four different flour types and two different yeast starters

Meas. Mass	Theor. Mass	Sum Formula	Flour Types					Yeasts		
			Concentration (ppb)				*p*-value	Concentration (ppb)		*p*-value
			F1	F2	F3	F4		Y1	Y2	
41.038	41.039	$C_3H_5^+$	92.1±26.1	87.1±25.8	88.8±23.7	104.1±42.9	0.693	81.2±17.4	105.9±35.6	*0.020*
42.010	n.a.	non identified	4.0±2.1	3.7±2.2	3.1±1.8	2.8±1.6	0.574	4.1±1.9	2.8±1.7	0.061
42.043	n.a.	non identified	3.6±1.3	3.4±0.9	3.5±1.0	4.1±1.6	0.635	3.1±0.7	4.2±1.4	*0.011*
47.013	47.013	$CH_3O_2^+$	28.3±5.4	37.9±19.0	32.5±11.0	27.2±12.1	0.354	38.9±13.9	23.5±4.7	*0.000*
51.940	n.a.	non identified	1.8±0.1	1.8±0.1	1.8±0.1	1.9±0.1	0.301	1.8±0.1	1.9±0.1	*0.013*
53.038	n.a.	non identified	1.9±0.3	2.1±0.3	2.3±0.6	2.5±0.8	0.147	2.0±0.3	2.5±0.7	*0.028*
55.054	55.054	$C_4H_7^+$	18.8±5.8	18.2±6.8	22.8±10.1	29.0±15.3	0.154	17.3±5.7	27.4±12.3	*0.006*
55.934	n.a.	non identified	5.0±0.3	5.1±0.3	5.2±0.3	5.3±0.3	0.231	5.1±0.3	5.3±0.3	0.063
58.040	n.a.	non identified	2.9±1.0	3.4±1.5	4.4±2.3	6.5±4.7	0.074	2.9±1.1	5.8±3.6	*0.005*
59.049	59.049	$C_3H_7O^+$	104.6±37.1	142.9±51.1	125.3±59.7	136.7±64.0	0.512	136.5±65.4	117.8±35.7	0.339
61.028	61.028	$C_2H_5O_2^+$	244.3±27.4	279.0±45.2	329.2±88.4	283.0±65.7	0.079	272.4±44.2	293.1±80.7	0.379
67.055	67.054	$C_5H_7^+$	1.2±0.5	1.2±0.6	1.5±0.7	2.1±1.5	0.198	1.1±0.5	1.9±1.2	*0.012*
69.070	69.070	$C_5H_9^+$	21.5±11.6	22.1±20.3	26.6±14.1	25.5±13.4	0.891	17.1±11.0	31.1±14.9	0.006
71.049	71.049	$C_4H_7O^+$	$142.3±33.2^b$	$122.8±15.4^b$	$110.1±13.1^{ab}$	$88.5±23.0^a$	*0.001*	122.8±24.6	109.0±33.6	0.197
73.065	73.065	$C_4H_9O^+$	213.8±70.3	201.7±76.8	230.4±105.3	252.7±107.3	0.705	181.7±69.6	270.0±85.2	*0.004*
81.069	81.070	$C_6H_9^+$	1.3±0.2	1.3±0.2	1.4±0.1	1.2±0.1	0.154	1.2±0.1	1.3±0.2	*0.020*
83.086	83.086	$C_6H_{11}^+$	$1.8±0.5^a$	$1.5±0.5^a$	$2.9±1.1^b$	$2.3±0.6^{ab}$	*0.002*	2.1±0.7	2.1±1.0	0.966
85.065	n.a.	$C_5H_9O^+$	1.9±0.5	2.1±0.7	2.1±0.6	2.1±0.6	0.947	2.3±0.7	1.8±0.4	*0.041*
87.081	87.080	$C_5H_{11}O^+$	20.2±12.4	21.2±17.5	29.0±19.7	49.6±45.0	0.132	16.2±10.7	44.8±33.9	*0.003*
89.060	89.060	$C_4H_9O_2^+$	$200.0±46.5^b$	$172.7±19.2^b$	$157.0±18.3^{ab}$	$126.2±35.4^a$	*0.001*	176.3±33.1	151.3±46.3	0.094
103.076	103.075	$C_5H_{11}O_2^+$	5.5±2.1	4.8±2.1	5.8±1.4	5.9±2.4	0.765	6.8±1.6	4.1±1.4	*0.000*

For the obtained bread samples, mean concentrations and standard deviations are reported. Statistically significant differences between experimental modes are established by means of one-way ANOVA (when $p < 0.05$, the p value is shown in italics) and Tukey's post hoc test and represented by means of superscript letter annotations. Only statistically different peaks are represented

significant results, expressed in terms of concentration in ppbV per hour. Again, if we consider flour to be the changing factor, one-way ANOVA ($p < 0.05$) shows differences between experimental modes for 10 relevant peaks: F3 (bread wheat flour type 0) different for one peak, F4 (Manitoba flour) different for 2 peaks, and F1 (durum wheat flour) different for one peak. While if we consider yeast to be the changing factor, the test reveals 15 significant peaks with Y2 producing more volatiles than Y1 for 5 peaks.

In-Depth Analysis of the Influence of Changing Ingredients

Differences between the effect of flour and yeast throughout the entire process were observed by means of principal component analysis (PCA), with each point representing a distinct sampling point (Fig. 1). It was clear that all eight preparations were able to perform fermentation (an evident increase in dough volume was observed) and displayed a clear evolution of the VOC profiles. The score plots for the first two principal components, which comprised 81.7 % of the overall variability, had different starting and ending points as shown by the shading varying along the first dimension. The results were repeatable between the two distinct biological replicates, and an overall time evolution, which sums up the various kinetics, was visible having similar overall trends. We can notice differences when a different yeast preparation was applied, more than when the flour type was changed. In addition, it is possible to observe for Y2, after a VOC production relatively constant during the first phases of the leavening (darker points), a volatile release pattern that seems to be driven by the different flours. Upon baking, the score plots for the first two principal components, which comprised 54.2 % of the overall variability and 48.7 % for the first and third components (Fig. 2), show a clear separation of the samples based on the type of yeast added, more than the type of flour. Only F1 (durum wheat flour) which belongs to a different wheat species can be separated from the remaining types of flour.

These differences were also denoted when evolution plots of each peak were drawn, showing a clear grouping based on

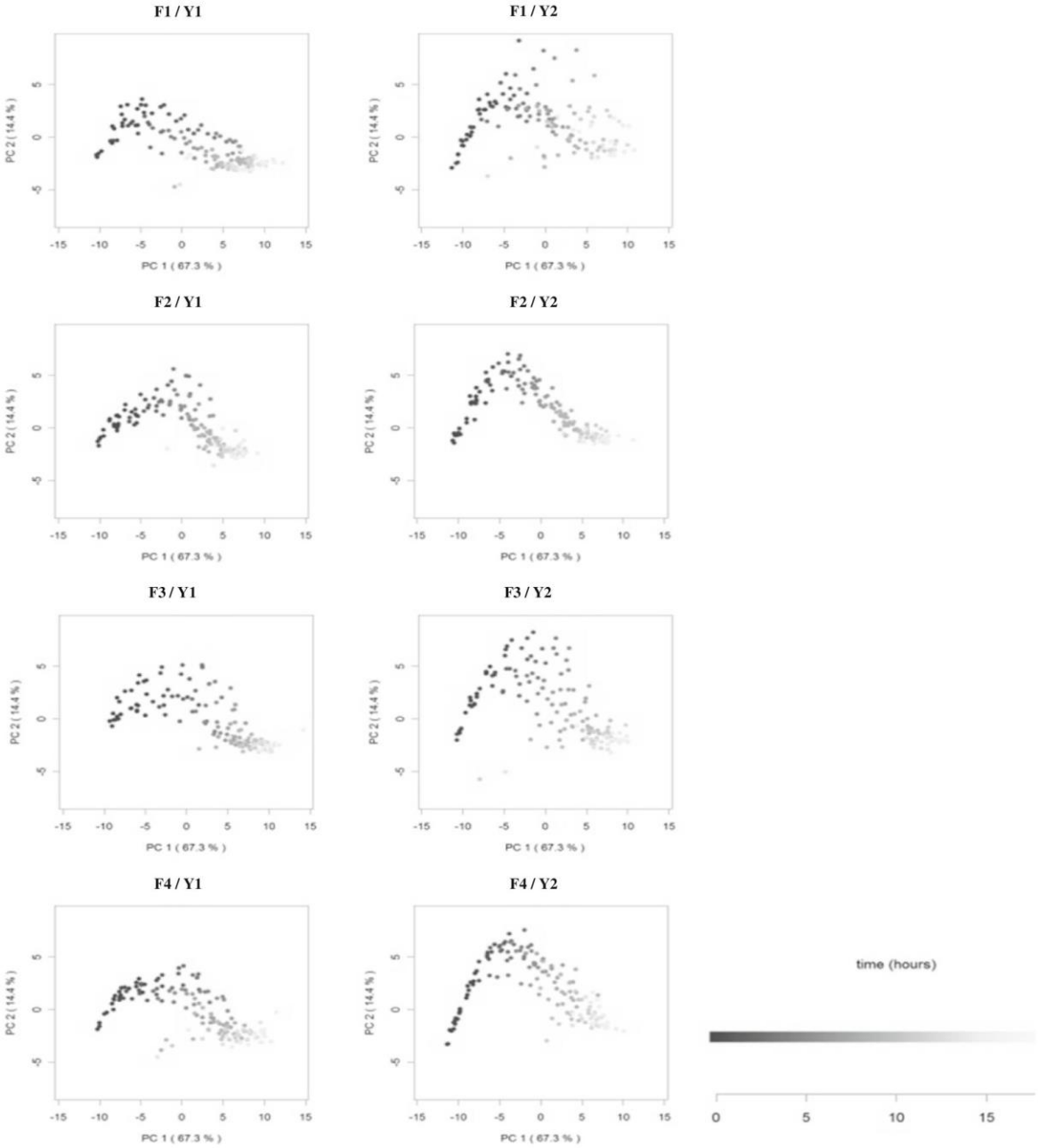

Fig. 1 Volatile emission during leavening: Principal component analysis of the autoscaled data. Score plots for the first two principal components for four different flour types inoculated with two different yeasts are depicted and separated in eight different plots for a better visualization. *Different shadings* represent time evolution

the yeast factor, as observed in the chosen peaks (Fig. 3). Changing the flour type had little impact on the volatile production compared to the effect of changing the yeast preparation.

Flour-Yeast Interaction

However, another question was addressed upon the analysis of the results and dealt with a possible interaction between the

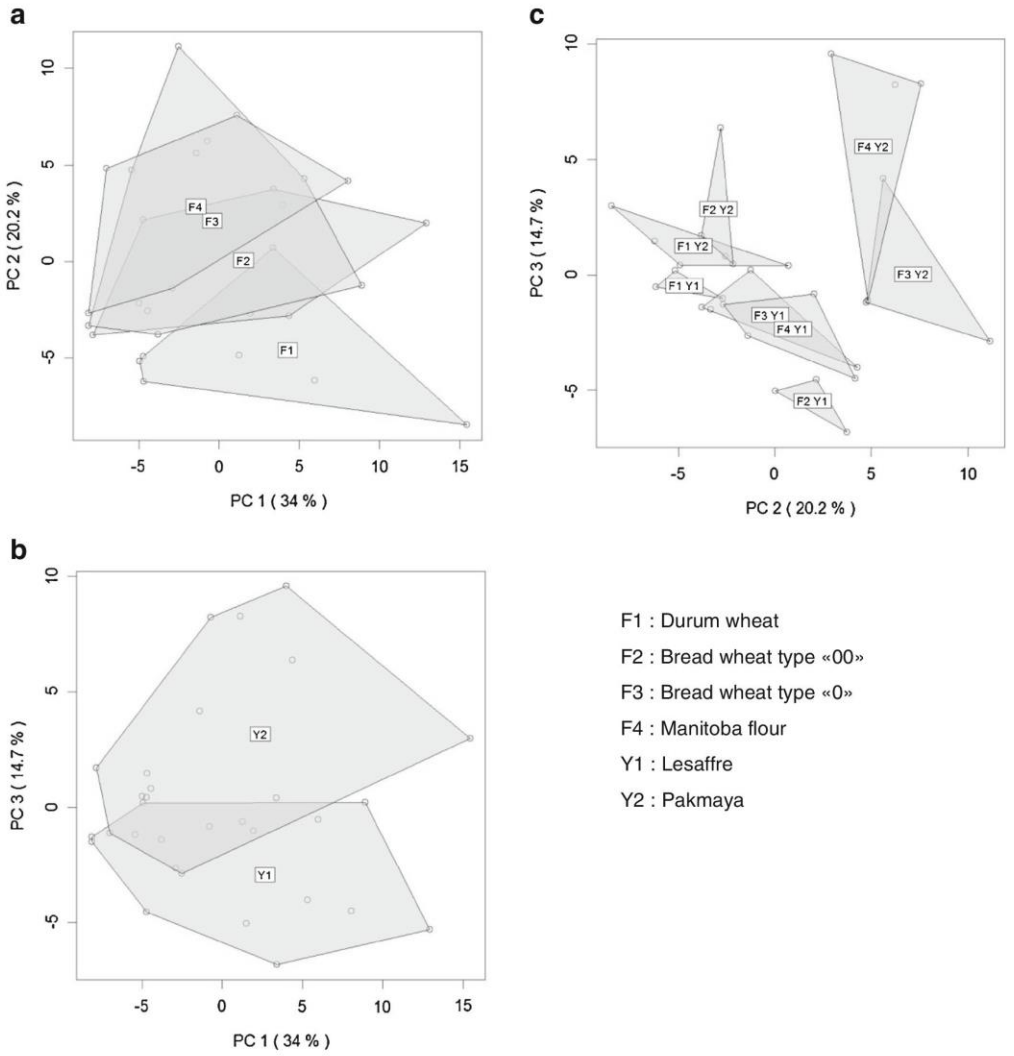

Fig. 2 Volatile emission upon baking: Principal component analysis of the autoscaled data. Score plots for the first two principal components (*2.a*) the first and the third (*2.b*) and the second and the third principal components (*2.c*) for four different flour types inoculated with two different yeasts are depicted

two parameters which might lead to a clearer understanding of the situation. The statistical 'F test' applied to the dough and bread matrices was able to depict a synergistic interaction between Y1 and F3 (bread wheat type 0) in peak 47.014, tentatively identified as formic acid (Fig. 4). In fact, an amplified production of the peak is observed only when these two types are combined, while for the other three combinations, the response is intrinsically the same. Van Boekel and Brands reported formic acid as one of the main degradation components for the Maillard reaction of glucose and fructose (Van Boekel and Brands 1998), hence highlighting its importance in the final profile of the baked product (Martins et al. 2000).

On the other hand, many examples of disruptive interactions can be given (Fig. 5), during which changing one component results in an inverse response. For instance, the productivity of mass peak 97.028, tentatively identified as furfural, characterized as an odour active compound (Rega et al. 2009), clearly depends on the yeast-flour combination, for Y1 interacts better with F1 (durum wheat) than F3 (bread wheat type 0) which, inversely, yields more furfural when combined with Y2. The same results are observed with peaks 61.028 (tentatively identified as acetic acid or acetate ester, another main component of the Maillard reaction of glucose and fructose (Van Boekel and Brands 1998)), 75.044 (propionic acid or

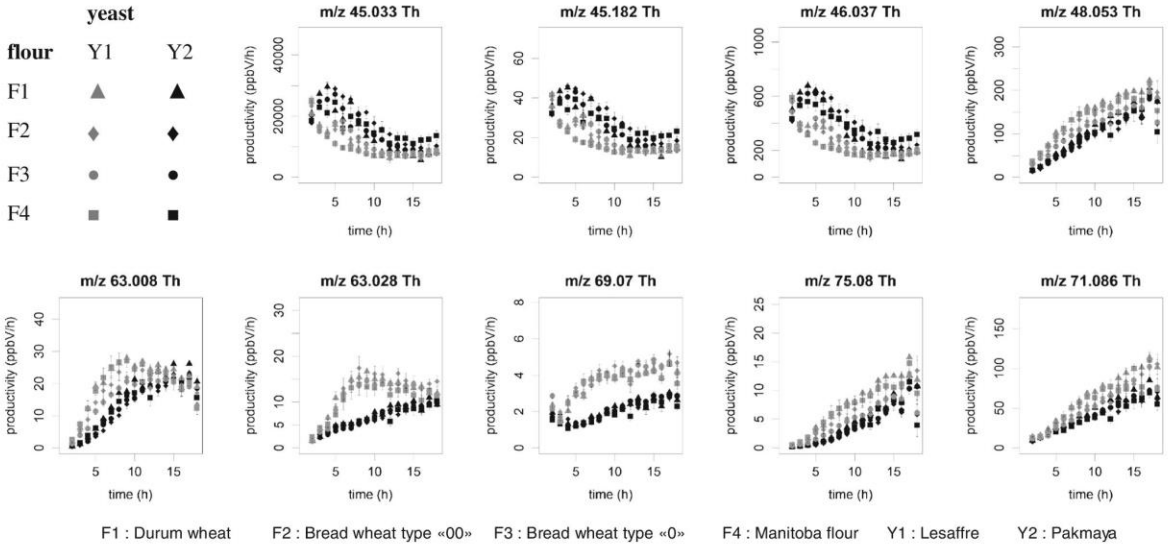

Fig. 3 Volatile emission during leavening: time evolution of selected mass peaks. *Points* represent average productivity values. *Different signs* represent different types of flour and *different colours* represent different yeasts

propanoate ester), 81.069 (a fragment of hexanal) and 117.091 (hexanoic acid or methylpropyl acetate). These compounds, among others, were reported as being important aroma precursors and odour active compounds affecting the quality and aromatic profile of the final baked product (Gassenmeier and Schieberle 1995; Rega et al. 2009; Salovaara and Valjakka 1987).

Discussion

Our results are in general agreement with what was previously observed by Makhoul et al. (2014) and by Birch et al. (Birch et al. 2013a) concerning the VOC production by different baking yeast cultures. In fact, considering that we add the same yeast amount (CFU per grams), the differences are

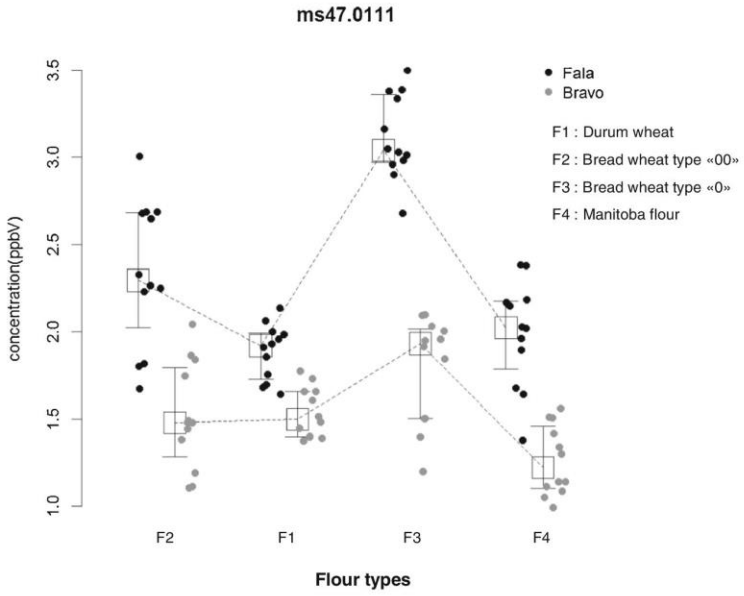

Fig. 4 Synergistic interaction between flour and yeast for peak 47.011 tentatively identified as formic acid showing an amplified volatile productivity upon changing one component

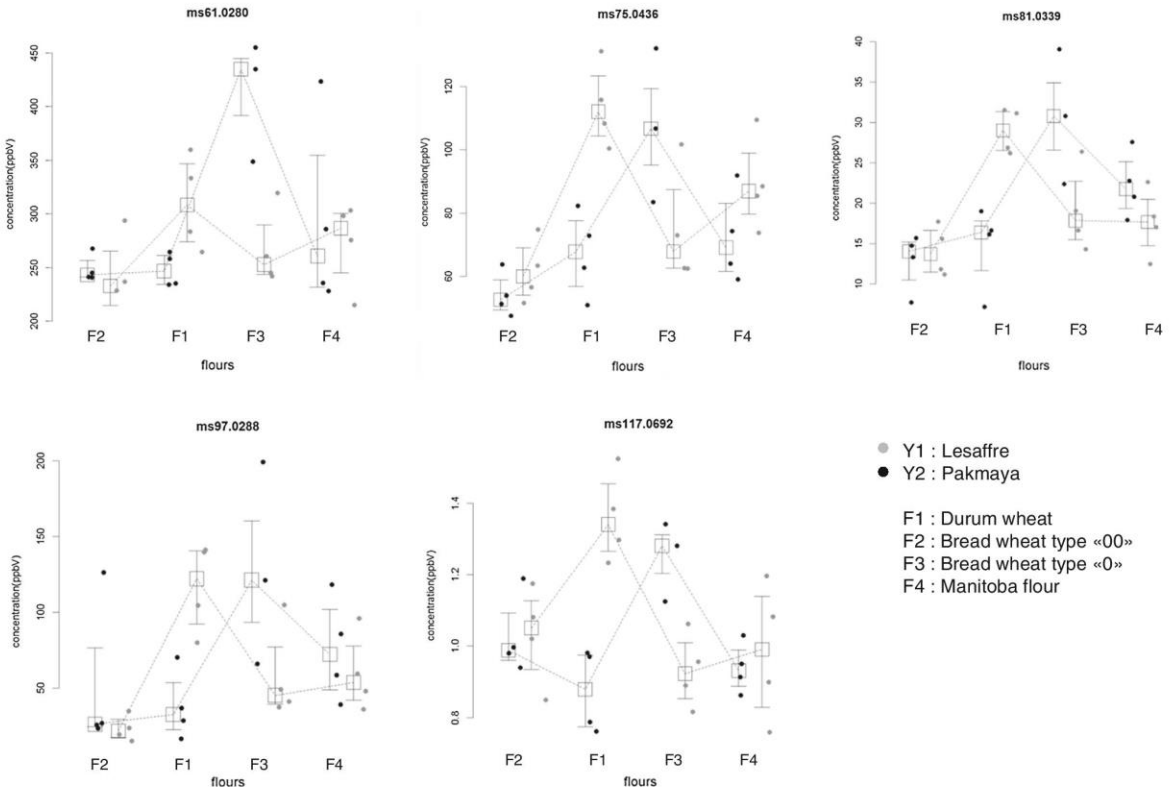

Fig. 5 Disruptive or cross-interaction between flour and yeast for selected peaks showing an inverse volatile productivity upon changing one component

addressable only to the differences in strain metabolic behaviour and not to the concentration of starter added to the dough (Birch et al. 2013b; Randez-Gil et al. 2013). This observation might be connected with differences in the gene-regulating mechanisms and biosynthetic pathways of aroma compound formation (Birch et al. 2013a) and/or with strain-dependent differences in the response to the stressful environment imposed by the food matrix. For example, Erasmus et al. (2003) observed that in *S. cerevisiae* exposed to osmotic stress (a stressor typical of 'dough environment'), many genes (e.g. oxidative and non-oxidative branches of the pentose phosphate pathway and structural genes involved in the formation of acetic acid from acetaldehyde and succinic acid from glutamate were found upregulated) are highly upregulated with respect to the control (unstressed yeast cells) (Erasmus et al. 2003). The observations related to differences among types of flour provided a possible explanation for differences in sensory profile between white bread and bread obtained from durum wheat. The latter is the case, for example, of Altamura bread with a status of protected designation of origin (Cauvain and Young 2001). In this case, the differences could be mainly addressable to different contents of reducing sugars and/or of protease. These two chemical classes are the key flour constituents susceptible to direct influencing the flavour of the final products (Goesaert et al. 2005). In fact, the levels of reducing sugars and proteases influence the production of Maillard reaction products (in the case of proteases, this influence can be due to the release of free amino acids which will subsequently undergo Maillard reaction), conditioning bread flavour and crust colour (Bowles 1996; Hebeda 1996). We also demonstrated the possibility to monitor ethanol concentrations online, an analytical aspect which is crucial for bioprocess assessment in the case of alcoholic fermentation and the leavening process. In addition, in order to highlight the potential of PTR-ToF-MS, it is crucial to underline that together with this molecule, we were able to measure a large number of mass peaks at the same time.

Concerning the interaction between various types of flour and yeast, we noted, upon baking, a disruptive interaction (also known as cross-interaction observed when, in the presence of two variables, changing one will cause a reverse response) in the case of peak *m/z* 97.028. This can be tentatively assigned to furfural, an important intermediate of the Maillard reaction of pentose or ascorbic acid, relevant in bread aroma and colour (Murata et al. 2007). Two biological mechanisms may be involved in this phenomenon, the pentose utilization

of some strains of *S. cerevisiae* (Hahn-Hägerdal et al. 2007) and the aptitude of *S. cerevisiae* under specific conditions to L-ascorbic acid accumulated intracellularly in significant amounts (Sauer et al. 2004). Similar trends were observed for peaks 61.028, 75.044, 101.096, 117.091 tentatively identified as acetic acid/acetate ester, propionic acid/propanoate ester, hexanal and hexanoic acid/methylpropyl acetate, respectively (Aprea et al. 2007). These compounds, tentatively identified, are characteristic of bread aroma, recently reported with odours ranging from 'green' (Hexanal) to fruity (esters), through pungent (acids) (Birch et al. 2013b). The differences in yeast/flavour interactions could be not necessarily connected with a different content of precursors/specific chemicals, but might also be related to the general dissimilarities in flour chemical constituents susceptible to directly or indirectly influence the yeast fermentation behaviour. For instance, Boyacioglu and D'Appolonia (Boyacioglu and D'Appolonia 1994) found that durum wheat samples contained a slightly higher content of protein and a higher content of sugars than that of metabolism wheat flours. These changes in the chemical composition may lead to changes in yeast metabolites.It is the case, to provide you an example, of the starch addition to liquid fermentation systems simulating sourdough inoculated with *S. cerevisiae* leads to changes in the production of selected metabolites (Vernocchi et al. 2008; Birch et al. 2013b). With regard to possible influence on the bread aroma of positive/negative yeast/flour interactions, it is important to underline how furfural and some esters were encompassed among the most frequent volatile organic compounds in bread crumb (Birch et al. 2013b) and that esters, in particular, detain a huge potential in improving bread aroma as having pleasant and fruity odours (Birch et al. 2013a). Our findings on yeast/flour interaction shed a new light on the potential use of PTR-MS for the online monitoring of food fermentations, underlining phenomena of interest both from a biological and industrial point of view. Intriguingly, we found phenomena of interaction in volatile esters, which are suggested to belong to the domestication phenotype of *S. cerevisiae*. Indeed, *S. cerevisiae* strains used in food fermentations generally release more volatile acetate esters than their wild counterparts (Steensels et al. 2014). A synergistic interaction has also been observed for formic acid, a 'pungent' volatile organic acid rarely described in bread VOC analysis (Gelinas and Lachance 1995), and a constituent of ginger-bread, formed by the baking process (Ayuto and Rohns 1984).

PTR-ToF-MS is proven to be a fast high-throughput tool for the study of interactions between yeast and flour. It may enable manufacturers to easily choose the combination of ingredients able to yield the production of certain selected volatiles serving as flavour precursors in the final baked product. In this contest, PTR-ToF-MS may offer to bread makers the possibility of optimizing their recipes increasing favoured aroma precursors and depriving them of unwanted off-odours. The next studies will be focused on the reciprocal interaction of flour, yeast and bacteria, considering a sourdough-like environment. In our opinion, the analysis of yeast/flour interactions in terms of VOC release is a good model to demonstrate the potential of PTR-ToF-MS in the study of the existing wide range of protechnological microbes/food matrices couples. Moreover, considering the increasing interest in improving bread qualities (e.g. Demirkesen et al. 2013; Różyło 2014) and the number of possible variables that may influence the sensory quality (e.g. Kiskini et al. 2012; Di Monaco et al. 2015; Soukoulis et al. 2013), PTR-MS appears to be a suitable tool to rapidly test the effect of new biotechnological/technological applications on process efficiency, product quality and product shelf-life.

Conclusions

Concluding, in addition to the variances in volatile productivity by different *S. cerevisiae* strains shown in previous works, we reported that the effect of yeast is more pronounced than that of flour types. The peak-by-peak monitoring followed by a tailored statistical approach revealed not only the effect of changing ingredients but also different kinds of yeast/flour interaction. For this reason, we underline the importance on the selection of ingredients for each bread recipe depending on the desired volatile profile of the baked product. PTR-ToF-MS is proven to be a fast high-throughput tool for the study of bread bioprocess technology monitoring volatile compounds and in analysing protechnological microbes/matrix interaction during food fermentations.

Acknowledgments The support of the Autonomous Province of Trento (PAT-ADP 2014) is acknowledged. Giuseppe Spano is supported by MIUR [PON02_00186_2937475] in the framework of the project named 'Protocolli innovativi per lo sviluppo di alimenti funzionali' [Pro.Ali.Fun.].

References

Annett, L. E., Spaner, D., & Wismer, W. V. (2007). Sensory profiles of bread made from paired samples of organic and conventionally grown wheat grain. *Journal of Food Science*, *72*(4), S254–S260.

Aprea, E., Biasioli, F., Märk, T. D., & Gasperi, F. (2007). PTR-MS study of esters in water and water/ethanol solutions: fragmentation patterns and partition coefficients. *International Journal of Mass Spectrometry*, *262*(1–2), 114–121.

Ayuto, M., & Rohns, G. (1984). Formic acid in ginger bread–an adulterant? *Zeitschrift für Lebensmittel-Untersuchung und -Forschung*, *179*(3), 243–244.

Biasioli, F., Gasperi, F., Yeretzian, C., & Märk, T. D. (2011). PTR-MS monitoring of VOCs and BVOCs in food science and technology. *TrAC, Trends in Analytical Chemistry*, *30*(7), 968–977.

Birch, A. N., Petersen, M. A., Arneborg, N., & Hansen, Å. S. (2013a). Influence of commercial baker's yeasts on bread aroma profiles. *Food Research International*, *52*(1), 160–166.

Birch, A. N., Petersen, M. A., & Hansen, Å. S. (2013b). Review: Aroma of wheat bread crumb. *Cereal Chemistry Journal.*, *91*(2), 105–114.

Birch, A. N., van den Berg, F. W. J., & Hansen, Ã. S. (2013c). Expansion profiles of wheat doughs fermented by seven commercial baker's yeasts. *Journal of Cereal Science*, *58*(2), 318–323.

Bowles, L. K. (1996). *Amylolytic enzymes. Food Science and Technology* (pp. 105–130). New York:Marcel Dekker.

Boyacioglu, M., & D'Appolonia, B. (1994). Characterization and utilization of durum wheat for breadmaking. I. Comparison of chemical, rheological, and baking properties between bread wheat flours and durum wheat flours. *Cereal Chemistry*, *71*(1), 21–27.

Capozzi, V., Menga, V., Diges, A. M., De Vita, P., van Sinderen, D., Cattivelli, L., Fares, C., & Spano, G. (2011). Biotechnological production of vitamin B2-enriched bread and pasta. *Journal of Agricultural and Food Chemistry*, *59*(14), 8013–8020.

Cappellin, L., Biasioli, F., Fabris, A., Schuhfried, E., Soukoulis, C., Märk, T. D., & Gasperi, F. (2010). Improved mass accuracy in PTR-TOF-MS: another step towards better compound identification in PTR-MS. *International Journal of Mass Spectrometry*, *290*(1), 60–63.

Cappellin, L., Biasioli, F., Granitto, P. M., Schuhfried, E., Soukoulis, C., Costa, F., Märk, T. D., & Gasperi, F. (2011). On data analysis in PTR-TOF-MS: from raw spectra to data mining. *Sensors and Actuators B: Chemical*, *155*(1), 183–190.

Cappellin, L., Karl, T., Probst, M., Ismailova, O., Winkler, P. M., Soukoulis, C., Aprea, E., Märk, T. D., Gasperi, F., & Biasioli, F. (2012). On quantitative determination of volatile organic compound concentrations using proton transfer reaction time-of-flight mass spectrometry. *Environmental Science and Technology*, *46*(4), 2283–2290.

Cauvain, S. P., & Young, L. S. (2001). *Baking problems solved*. Boca Raton:CRC Press.

Cho, I., & Peterson, D. (2010). Chemistry of bread aroma: a review. *Food Science and Biotechnology*, *19*(3), 575–582.

Demirkesen, I., Sumnu, G., & Sahin, S. (2013). Quality of gluten-free bread formulations baked in different ovens. *Food and Bioprocess Technology*, *6*(3), 746–753.

Di Monaco, R., Torrieri, E., Pepe, O., Masi, P., & Cavella, S. (2015). Effect of sourdough with exopolysaccharide (EPS)-producing lactic acid bacteria (LAB) on sensory quality of bread during shelf life. *Food and Bioprocess Technology*, *8*(3), 691–701.

Dueñas-Sánchez, R., Pérez, A. G., Codón, A. C., Benítez, T., & Rincón, A. M. (2014). Overproduction of 2-phenylethanol by industrial yeasts to improve organoleptic properties of bakers' products. *International Journal of Food Microbiology*, *180*, 7–12.

Erasmus, D. J., Merwe, G. K., & Vuuren, H. J. (2003). Genome-wide expression analyses: metabolic adaptation of Saccharomyces cerevisiae to high sugar stress. *FEMS Yeast Research*, *3*(4), 375–399.

Feldman, M., Levy, A. A., Fahima, T., & Korol, A. (2012). Genomic asymmetry in allopolyploid plants: wheat as a model. *Journal of Experimental Botany*, *63*(14), 5045–5059.

Gassenmeier, K., & Schieberle, P. (1995). Potent aromatic compounds in the crumb of wheat bread (French-type) â€" influence of pre-ferments and studies on the formation of key odorants during dough processing. *Zeitschrift fur Lebensmittel-Untersuchung und Forschung*, *201*(3), 241–248.

Gelinas, P. (2009). Inventions on baker's yeast strains and specialty ingredients. *Recent Patents on Food, Nutrition & Agriculture*, *1*(2), 104–132.

Gélinas, P. (2012). In search of perfect growth media for baker's yeast production: mapping patents. *Comprehensive Reviews in Food Science and Food Safety*, *11*(1), 13–33.

Gelinas, P., & Lachance, O. (1995). Development of fermented dairy ingredients as flavor enhancers for bread. *Cereal Chemistry*, *72*(1), 17–21.

Goesaert, H., Brijs, K., Veraverbeke, W. S., Courtin, C. M., Gebruers, K., & Delcour, J. A. (2005). Wheat flour constituents: how they impact bread quality, and how to impact their functionality. *Trends in Food Science and Technology*, *16*(1–3), 12–30.

Hahn-Hägerdal, B., Karhumaa, K., Jeppsson, M., & Gorwa-Grauslund, M. (2007). Metabolic engineering for pentose utilization in Saccharomyces cerevisiae. In L. Olsson (Ed.), *Biofuels, vol 108. Advances in biochemical engineering/biotechnology* (pp. 147–177). Berlin: Springer.

Hansen, Å., & Hansen, B. (1994). Influence of wheat flour type on the production of flavour compounds in wheat sourdoughs. *Journal of Cereal Science*, *19*(2), 185–190.

Hebeda, R. (1996). *Baked goods freshness: technology, evaluation, and inhibition of staling, vol 75*. Boca Raton:CRC Press.

Heenan, S. P., Dufour, J.-P., Hamid, N., Harvey, W., & Delahunty, C. M. (2009). Characterisation of fresh bread flavour: relationships between sensory characteristics and volatile composition. *Food Chemistry*, *116*(1), 249–257.

Hui, Y. H. (2008). *Bakery products: science and technology*. Hoboken: John Wiley & Sons.

Jordan, A., Haidacher, S., Hanel, G., Hartungen, E., Märk, L., Seehauser, H., Schottkowsky, R., Sulzer, P., & Märk, T. D. (2009). A high resolution and high sensitivity proton-transfer-reaction time-of-flight mass spectrometer (PTR-TOF-MS). *International Journal of Mass Spectrometry*, *286*(2–3), 122–128.

Kiskini, A., Kapsokefalou, M., Yanniotis, S., & Mandala, I. (2012). Effect of iron fortification on physical and sensory quality of gluten-free bread. *Food and Bioprocess Technology*, *5*(1), 385–390.

Kulp, K., & Lorenz, K. (2003). *Handbook of dough fermentations, vol 127*. Boca Raton:CRC Press.

Lindinger, W., Hansel, A., & Jordan, A. (1998). On-line monitoring of volatile organic compounds at pptv levels by means of proton-transfer-reaction mass spectrometry (PTR-MS) medical applications, food control and environmental research. *International Journal of Mass Spectrometry and Ion Processes*, *173*(3), 191–241.

Makhoul, S., Romano, A., Cappellin, L., Spano, G., Capozzi, V., Benozzi, E., Märk, T. D., Aprea, E., Gasperi, F., El-Nakat, H., Guzzo, J., & Biasioli, F. (2014). Proton-transfer-reaction mass spectrometry for the study of the production of volatile compounds by bakery yeast starters. *Journal of Mass Spectrometry*, *49*(9), 850–859.

Martins, S. I. F. S., Jongen, W. M. F., & van Boekel, M. A. J. S. (2000). A review of Maillard reaction in food and implications to kinetic modelling. *Trends in Food Science and Technology*, *11*(9–10), 364–373.

Mathewson, P. (2000). Enzymatic activity during bread baking. *Cereal Foods World*, *45*(3), 98–101.

Murata, M., Totsuka, H., & Ono, H. (2007). Browning of furfural and amino acids, and a novel yellow compound, furpipate, formed from lysine and furfural. *Bioscience, Biotechnology, and Biochemistry*, *71*(7), 1717–1723.

Onishi, M., Inoue, M., Araki, T., Iwabuchi, H., & Sagara, Y. (2012). A PTR-MS-based protocol for simulating bread aroma during mastication. *Food and Bioprocess Technology*, *5*(4), 1228–1237.

Paraskevopoulou, A., Chrysanthou, A., & Koutidou, M. (2012). Characterisation of volatile compounds of lupin protein isolate-enriched wheat flour bread. *Food Research International*, *48*(2), 568–577.

Patel, B. K., Waniska, R. D., & Seetharaman, K. (2005). Impact of different baking processes on bread firmness and starch properties in breadcrumb. *Journal of Cereal Science*, *42*(2), 173–184.

Poinot, P., Gl, A., Jl, G.-P., De, C., Fillonneau, C., Le Bail, A., & Prost, C. (2008). Influence of formulation and process on the aromatic profile

and physical characteristics of bread. *Journal of Cereal Science*, *48*(3), 686–697.

Purlis, E., & Salvadori, V. O. (2009). Modelling the browning of bread during baking. *Food Research International*, *42*(7), 865–870.

Randez-Gil, F., Córcoles-Sáez, I., & Prieto, J. A. (2013). Genetic and phenotypic characteristics of baker's yeast: relevance to baking. *Annual Review of Food Science and Technology.*, *4*, 191–214.

Rega, B., Al, G., Delarue, J., Maire, M., & Giampaoli, P. (2009). On-line dynamic HS-SPME for monitoring endogenous aroma compounds released during the baking of a model cake. *Food Chemistry*, *112*(1), 9–17.

Romano, A., Capozzi, V., Spano, G., & Biasioli, F. (2015). Proton transfer reaction-mass spectrometry: online and rapid determination of volatile organic compounds of microbial origin. *Applied Microbiology and Biotechnology, 99*(9), 3787–3795. doi:10.1007/s00253-015-6528-y

Różyło, R. (2014). Effect of process modifications in two cycles of dough mixing on physical properties of wheat bread baked from weak flour. *Food and Bioprocess Technology*, *7*(3), 774–783.

Salovaara, H., & Valjakka, T. (1987). The effect of fermentation temperature, flour type, and starter on the properties of sour wheat bread. *International Journal of Food Science and Technology*, *22*(6), 591–597.

Sauer, M., Branduardi, P., Valli, M., & Porro, D. (2004). Production of l-ascorbic acid by metabolically engineered Saccharomyces cerevisiae and Zygosaccharomyces bailii. *Applied and Environmental Microbiology*, *70*(10), 6086–6091.

Shevchenko, A., Yang, Y., Knaust, A., Thomas, H., Jiang, H., Lu, E., Wang, C., & Shevchenko, A. (2014). Proteomics identifies the composition and manufacturing recipe of the 2500-year old sourdough bread from Subeixi cemetery in China. *Journal of Proteomics*, *105*, 363–371.

Soukoulis, C., Cappellin, L., Aprea, E., Costa, F., Viola, R., Märk, T., Gasperi, F., & Biasioli, F. (2013). PTR-ToF-MS, a novel, rapid, high sensitivity and non-invasive tool to monitor volatile compound release during fruit post-harvest storage: the case study of apple ripening. *Food and Bioprocess Technology*, *6*(10), 2831–2843.

Steensels, J., Meersman, E., Snoek, T., Saels, V., & Verstrepen, K. J. (2014). Large-scale selection and breeding to generate industrial yeasts with superior aroma production. *Applied and Environmental Microbiology*, *80*(22), 6965–6975.

Van Boekel M & Brands C (1998) Heating of sugar-casein solutions: isomerization and Maillard reactions. *The Maillard Reaction in Foods and Medicine*, 154–159.

Vernocchi, P., Ndagijimana, M., Serrazanetti, D., Gianotti, A., Vallicelli, M., & Guerzoni, M. E. (2008). Influence of starch addition and dough microstructure on fermentation aroma production by yeasts and lactobacilli. *Food Chemistry*, *108*(4), 1217–1225.

After underlining the importance of selecting the ingredients for each bread recipe depending on the desired volatile profile of the baked product, and after proving that PTR-ToF-MS is able to analyze protechnological microbes/matrix interaction during food fermentations, we were interested in investigating microbe/microbe interaction in the same matrix. A third *ProBake* paper, currently being reviewed by the co-authors, explains our findings.

3.4 *Saccharomyces cerevisiae* and *Lactobacillus sanfranciscensis* 'volatomes' and the study of VOCs associated with their interaction in sourdough

Salim Makhoul[1,2,3], Andrea Romano[4], Vittorio Capozzi[1,4,5], Giuseppe Spano[5], Eugenio Aprea[1], Luca Cappellin[1], Elisabetta Benozzi[1,6], Matteo Scampicchio[4], Tilmann D. Märk[6], Flavia Gasperi[1], Hanna El-Nakat[2], Jean Guzzo[3], and Franco Biasioli[1]

[1] Department of Food Quality and Nutrition, Research and Innovation Centre, Fondazione Edmund Mach (FEM), via E. Mach 1, 38010 San Michele all'Adige (TN), Italy

[2] Department of Chemistry, University of Balamand, P. O. Box 100, Tripoli, Lebanon

[3] UMR PAM – équipe VALMIS, IUVV, 1 rue Claude Ladrey, 21078 Dijon Cedex, France

[4] Faculty of Science and Technology, Free University of Bolzano, 39100, Bolzano, Italy

[5] Department of Agriculture, Food and Environment Sciences, University of Foggia, via Napoli 25, 71122 Foggia, Italy

[6] Institut für Ionenphysik und Angewandte Physik, Leopold-Franzens Universität Innsbruck, Technikerstr. 25, 6020 Innsbruck, Austria

Abstract

The high-throughput analytical approaches able to provide a snapshot of the volatile organic compounds (VOCs) released in association of a given metabolism has been receiving increasing interesting in reason of the biological and applicative relevance. The 'volatome' perspective cast a new light on the advantages of direct injection mass spectrometry (DIMS) among the analytical approaches to study VOCs content associated with biological systems. Here, using PTR-ToF-MS, we study i) the VOCs associated with *Saccharomyces cerevisiae* and *Lactobacillus sanfranciscensis* growth in microbiological media , ii) the 'volatomes' associated with dough, and iii) the VOCs associate with *S. cerevisiae* and *L. sanfranciscensis* interaction in a sourdough model and in the corresponding bread. To the best of our knowledge, we report for the first time the application of PTR-MS in order to study the evolution of 'volatome' associated with microbial growth in laboratory media and, concurrently, in a food matrix. In addition, it is the first report on the impact of *S. cerevisiae* and *L. sanfranciscensis* interactions on the VOCs associated with the bread headspaces.

Keywords: *PTR-MS; VOCs; bread; yeast; bacteria; sourdough.*

Introduction

Foods are a complex and dynamic environment in which an extended diversity of microorganisms (bacteria, yeasts and fungi) can coexist. One of the big efforts of modern food microbiology is to develop models able to consider possible interactions that take place among different microbes in these food ecosystems. The interactions among protechnological microbes, in particular, are of outstanding interest in reason of the impact on final food quality and safety (Ivey, Massel, & Phister, 2013). Although a rich literature described the microbial successions in various matrices/fermentations, a limited number of studies exploring the mechanisms of interaction of microbes participating in a given fermentation are known about how the microbes present interact. In general, 'omics' and untargeted approaches can provide a better insight into the complexity of industrial microorganisms' interactions in food matrices. The principal industrial microorganisms in the food sectors are generally considered to be the yeast species *Saccharomyces cerevisiae* and the heterogeneous class of lactic acid bacteria (with *Lactobacillus sanfranciscensis* as the most representative prokaryote belonging to this heterogeneous class), microbes which have been selected over millennia in reason of their contribution to the quality of fermented foods, undergoing a complex series of genetic rearrangements typical of domestication processes in nutrient-rich food environments (Douglas & Klaenhammer, 2010). Mixed populations of *S. cerevisiae* yeasts and lactic acid bacteria are present in many fermented foods and beverages. With a yeast/LAB ratio of generally 1:100 (M. Gobbetti, 1998) and with a clear coexistence in the dough, sourdough represent an interesting model to study the interaction between yeasts and lactic acid bacteria. Sourdough fermentation, one of the oldest food biotechnologies, improving sensory, structural, nutritional and shelf life properties of leavened baked goods, has been receiving considerable attention for a long time, with increasing interest in the modern food industry. This influence on dough and on baked foods' characteristics is achieved upon different levels of acidification, proteolysis and

activation of a number of enzymatic activities (Marco Gobbetti, Rizzello, Di Cagno, & De Angelis, 2014). In fact, enzymatic and microbial conversion of flour components during bread-making deeply influence bread quality (Gänzle, 2014), with consistent strain- or species-specific features (Gänzle, Vermeulen, & Vogel, 2007; M. Gobbetti, De Angelis, Corsetti, & Di Cagno, 2005).

Among the other 'omics', the volatome, the volatile metabolome, is of outstanding interest also in the sourdough environment giving that: i) it analyzes an important subset of molecular basis of sensory properties of fermented foods (Pico, Bernal, & Gómez, 2015) and, at the same time, ii) it studies a crucial class of 'infochemicals' in microbial interaction during fermentations (M. Gobbetti, De Angelis, Di Cagno, Minervini, & Limitone, 2007); a class of chemicals generally described as organic volatiles with low molecular weight (<300 Da) and high vapor pressure at ambient temperatures (Romano, Capozzi, Spano, & Biasioli, 2015a).

Proton transfer reaction mass spectrometry (PTR-MS) is an established method for the rapid, direct and non-invasive on-line monitoring of volatile organic compounds in food without the need of any sample pretreatment, basically based on the hydronium ion protonation of neutral compounds (M) according to the following reaction:

$$H_3O^+ + M \rightarrow H_2O + MH^+$$

PTR-MS is characterized by short response times and high sensitivity with limits of detection in the parts per trillion by volume range (Soukoulis et al., 2010). The coupling of proton transfer ionization with Time-of-Flight (ToF) mass spectrometers offers several advantages related to high time and mass resolution. While a previous study defined a PTR-MS-based protocol only for simulating bread aroma during mastication (Onishi, Inoue, Araki, Iwabuchi, & Sagara, 2012), only recently, PTR-ToF-MS found application to the monitoring this food bioprocess through the on-line monitoring of yeast in volatile production during the leavening process of

the dough and upon baking (Makhoul, Romano, Cappellin, Spano, Capozzi, Benozzi, Märk, Aprea, Gasperi, El-Nakat, et al., 2014).

In this paper, we study i) the VOCs associated with *Saccharomyces cerevisiae* and *Lactobacillus sanfranciscensis* growth in Yeast Peptone Dextrose (YPD) medium and in de Man, Rogosa and Sharpe (MRS) medium, respectively, ii) the 'volatomes' associated with dough environment, and iii) the VOCs associate with *S. cerevisiae* and *L. sanfranciscensis* interaction in a sourdough model and in the corresponding bread.

Materials and methods:

Sample preparation

Four different experimental types of dough samples were prepared from one strain of *S. cerevisiae* yeast and one strain of *L. sanfranciscensis* bacteria. The samples were prepared according to the procedure described in in the American Association of Cereal Chemists AACC 10-10B was applied (Approved Methods of the AACC, 10th ed.; American Association of Cereal Chemists: St. Paul, MN, 2000), according to Capozzi et al. (Capozzi et al., 2011), with minor modifications in order to prepare a sourdough model. The basic dough control (D1) was obtained by mixing 100g of bread wheat flour (type '00',Granoro, Italy), 1.5g of sodium chloride (Sigma Aldrich, St Louis, MO), 6g of sucrose (Sigma Aldrich), 3g of animal fat (Casa Modena, Modena, Italy), 4mg of ascorbic acid (Sigma Aldrich) and 60mL of distilled water. The preparation was carried out using a bread homemaker machine (Princess Household Appliances, Lainate, Italia). The control samples were supplemented with one of these three preparations, either yeast alone (D2), or bacteria alone (D3), or a mixture of both (D4). The yeast preparation was added in the amount of 10^6 CFU/g dough, 10^8 CFU/g dough for the bacteria, and 10^6 CFU/g dough to 10^8 CFU/g dough for the sourdough-like model, achieving a ratio of 1:100 of *S. cerevisiae* to *L. sanfranciscensis*. The dough was divided into 1.0 g pieces

(stored in 22 mL vials). During preparation, the dough was kept at 4 °C in order to reduce the fermentation process. Then the samples were transferred at 30 °C for the whole duration of the experiment (approximately 17 hours). Seven replicates of each dough sample were analyzed (along with 4 empty vials, resulting in a total of 32 vials) and the entire experiment was repeated twice.

For baked bread analysis, the same experiment was repeated with D1, D2, D3 and D4 dough types. After 17 hours of leavening, the average time needed for traditional sourdough preparation, the vials were taken out. Caps were removed and vials were transferred to a kitchen oven and baked for 8 minutes at 220 °C. Around this temperature, Maillard reactions, condensation reactions, take place between amino acids and sugars creating flavor, aroma and color of the bread crust. Thus it is considered an important biochemical process (Cho & Peterson, 2010). It is important to note that prior to the analysis, we accurately cleaned the oven and turned it on for one hour with ventilation to be sure to avoid residual VOCs from other preparations. To confirm the absence of residual VOCs, an empty vial was introduced in the oven during baking and later used as a blank control.

Microbial counts

For microbiological analyses, 10 g of each sample was homogenized in a stomacher bag with10 mL of a saline peptone water for 4 min, after which serial dilutions were prepared. For the count of LAB, MRS agar containing 100 mg/L cycloheximide was used, and the plates were incubated under anaerobic conditions (BBL, GasPack-System) at 30 °C for 72 h. For the count of yeasts, YPD agar containing 10 mg/L chloramphenicol was used, and the plates were incubated at 30 °C for 48 h.

PTR-TOF-MS analysis:

In order to measure the headspace of the dough and bread samples, a commercial PTR-TOF-MS 8000 apparatus from Ionicon Analytik GmbH (Innsbruck, Austria), was used in its standard configuration (V mode). The ionization conditions in the drift tube were the following: 110°C drift tube temperature, 2.30 mbar drift pressure, 550 V drift voltage. This led to an E/N ratio of about 140 Townsend (1 Td = 10^{-17} cm^2 V^{-1} s^{-1}). The inlet line consisted of a PEEK capillary tube (internal diameter 0.40 mm) heated at 110°C. The inlet flow was set at 120 sccm and 40 sccm for dough and bread measurements, respectively.

The automation used for the leavening experiments was the same as the one described in previous works by Makhoul et al. (Makhoul, Romano, Cappellin, Spano, Capozzi, Benozzi, Märk, Aprea, Gasperi, El-Nakat, et al., 2014) using an autosampler (Gerstel, Mulheim am Main, Germany) especially adapted to PTR-MS analyses. At the beginning of the experiment, the robotic arm moved the sample from a cooling tray where it was kept at 4°C, to the incubation tray, whose temperature was set at 30°C. Vials were then moved to the temperature-controlled purging site, connected to the PTR-ToF-MS inlet, and where the headspace analysis took place for 30 seconds with an acquisition rate of one spectrum per second. After measurement, the vial was moved to the incubation tray and the cycle was repeated on the following sample. This allowed to perform a scan of the tray (32 samples) in approximately one hour (1 cycle = 54 min). During leavening, the scan was repeated 19 times, in order to monitor the fermentation process. Due to the presence of relevant amounts of ethanol (an average of 20 ppmv of ethanol) in the headspace of the samples during leavening, an inert gas dilution was applied in an inert gas to sample ratio of 2:1. This permitted to prevent primary ion depletion and formation of ethanol clusters which might affect the final quantification of volatiles (Aprea, Biasioli, Märk,

& Gasperi, 2007). In fact, at all times, the ionisation should be carried out by the H_3O^+ primary ions. If at any point, the levels of ethanol or ethanol clusters exceed that of H_3O^+, the latter will not remain the primary ionizing ion which will lead to errors in data analysis afterwards.

The headspace of micro-loaves obtained after baking was measured as before. Prior to analysis, samples were flushed with a stream of clean air (200 mL/min for 30 seconds), as generated by a Gas Calibration Unit apparatus (Ionicon Analytik GmbH), then incubated at 30 °C for 30 minutes and finally analyzed for 30 seconds at one spectrum per second. No dilution of the headspace was required in this case.

Data analysis

Dead time correction, internal calibration of mass spectral data and peak extraction were performed according to a procedure described in the works of Cappellin et al. (Cappellin et al., 2010; Cappellin et al., 2011), using a modified Gaussian peak shape. Peak intensity in ppbv was estimated using the formula described in literature (W. Lindinger et al., 1998), using a constant value for the reaction rate constant coefficient ($k = 2.10^{-9}$ cm^3 s^{-1}). This introduces a systematic error for the absolute concentration for each compound that is in most cases below 30% and could be accounted for if the actual rate constant coefficient is available(Cappellin, Karl, et al., 2012).

All data detected and recorded by the PTR-TOF-MS were processed and analyzed using MATLAB (MathWorks, Natick, MA) and in-house developed scripts written in R programming language (R Foundation for Statistical Computing, Vienna, Austria).

Results

Saccharomyces cerevisiae and Lactobacillus sanfranciscensis 'volatomes'

The volatome of *Saccharomyces cerevisiae* and *Lactobacillus sanfranciscensis* were realized upon the on-line monitoring of the cultured microorganisms, over many days. More than 300 mass peaks were obtained. **Tables 3 and 4** summarize VOCs detected at the main log1, log2, lag1, lag2 and stat cycles, after applying a 1ppbv threshold, keeping only the peaks pertaining to the yeast/bacteria and not the medium, and eliminating isotopologues.

Table 3. Simplified *Saccharomyces cerevisiae* volatome

Mass peak	lag 1	lag 2	log 1	log 2	stat	Tent. Ident.
41.039	14 ± 5	13 ± 6	30 ± 27	104 ± 104	126 ± 127	Alkylic fragment
42.010				18 ± 19	20 ± 20	non identified
43.018	47 ± 23	111 ± 90	142 ± 120	175 ± 123	231 ± 145	
43.055	2 ± 1	2 ± 1	12 ± 12	46 ± 48	59 ± 61	Alkylic fragment
44.980		1.4 ± 0.5	1.3 ± 0.7	1.3 ± 0.8	1.1 ± 0.6	
44.998		1.2 ± 0.3	5 ± 5	6 ± 7	1.6 ± 0.7	
47.047	3 ± 3	22 ± 22	487 ± 515	2056 ± 2314	2842 ± 3010	Ethanol
49.028			1 ± 1	2 ± 2	2 ± 2	
49.053			1 ± 1	5 ± 6	7 ± 7	
57.070	10 ± 3	8 ± 2	17 ± 15	100 ± 103	127 ± 132	
61.028	6 ± 2	5 ± 2	6 ± 3	39 ± 38	54 ± 52	Acetic Acid
65.059				3 ± 3	4 ± 5	
69.070	5 ± 2	5 ± 3	5 ± 4	4 ± 3	3 ± 2	fragment (pentanal)
71.085			6 ± 6	28 ± 30	31 ± 32	
73.065	10 ± 4	12 ± 6	32 ± 32	37 ± 32	17 ± 10	n-butyraldehyde/methylpropanal
75.080				3 ± 3	4 ± 5	
87.081	2.3 ± 0.8	2 ± 1	2.3 ± 1.8	2 ± 2	1.4 ± 0.9	isoveraldehyde/2-methylbutanal/pentanal
89.059				6 ± 7	10 ± 10	2-Methyl propanoic acid/ethyl acetate
93.087				3 ± 3	4 ± 4	

Table 4. Simplified *Lactobacillus sanfranciscensis* volatome

Mass peak	lag 1	lag 2	log 1	log 2	Tent. Ident.
42.010	1.0 ± 0.1	1.3 ± 0.1	10.1 ± 0.4	7.3 ± 2.5	non identified
43.055	1.7 0.1	1.3 ± 0.1	3.5 ± 0.6	3.7 ± 0.7	Alkylic fragment
44.980			1.0 ± 0.1		
44.998		2.9 ± 0.1	6.1 ± 0.3	1.9 ± 0.4	
45.034	56.9 ± 2.3	81.5 ± 2.5	668.0 ± 44.5	273.9 ± 128.6	
46.995			1.1 ± 0.1		
47.047	22.8 ± 1	42.2 ± 1.5	445.1 ± 34.8	294.8 ± 67.3	Ethanol
49.011			1.8 ± 0.1		
49.028			0.9 ± 0.1		
49.053			1.0 ± 0.1		

Note that the lag, logarithmic and stationary phases correspond to the main phases of the microbial grotta curve.

Automated monitoring of the leavening process

After setting up both the PTR-ToF-MS and the autosampler, the leavening process was launched, allowing the samples to be incubated at 30 °C for thirty minutes, and then their headspace was analyzed every 54 minutes. This generated up to twenty time points during the course of a typical leavening experiment. The whole dataset consisted of seven replicates for each experimental mode, obtained by aggregating two distinct biological replicates.

Volatile profile of the samples during the leavening process

More than 400 peaks were detected during each cycle of this leavening process, and upon baking. A 1 ppbv concentration threshold filter was applied on the results in order to exclude the peaks which have no or poor contribution to the experimental modes. Further analysis and filtering, including the elimination of peaks belonging to isotopes, reduced more the number of

peaks in the database, to reach an average of 30 peaks per cycle for the leavening and 58 remaining peaks for the baked results.

Figure 22 illustrates the evolution of some chosen peaks throughout the leavening process. Three timepoints were chosen as examples of the early stage of the experiment (cycle 5 corresponding to four hours after the launching of the leavening process), the middle stage (cycle 15 corresponding to thirteen hours) and the last stage of leavening (cycle 19 corresponding to seventeen hours). Different interactions can be observed throughout the course of the experiment. For example the sourdough model showed an amplified production of peak m/z 41.039 (identified as an alkylic fragment) in cycle 5, while later (in cycles 15 and 19) the activity of the yeast is suppressed by the presence of the bacteria and the production of this peak in Dough 4 (sourdough model) is much less than in Dough 2 (Yeast alone), but still higher than that in Dough 3 (inoculated only with bacteria). The same applies for m/z 45.033 identified as acetaldehyde. For this peak, the sourdough model (D4) has the highest productivity at the beginning of the leavening process, then D2 overtakes D3 and D4 which have similar productivity. In the case of m/z 43.018, an ester fragment, the sourdough model (D4) had the highest productivity followed by D3, then D2, with D2 having almost the same productivity as that of D1 which is the basic dough without any inoculations. Another example is m/z 59.050 identified as acetone, D3 produced the most during the first two chosen timepoints, while D2 overtakes at the end of the leavening process, and a limited productivity is observed in the sourdough-model (D4). Finally, the maximum productivity of m/z 61.028, identified as acetic acid, was observed in D4 at all times, followed by D3 then D2 similar to D1 with no inoculations.

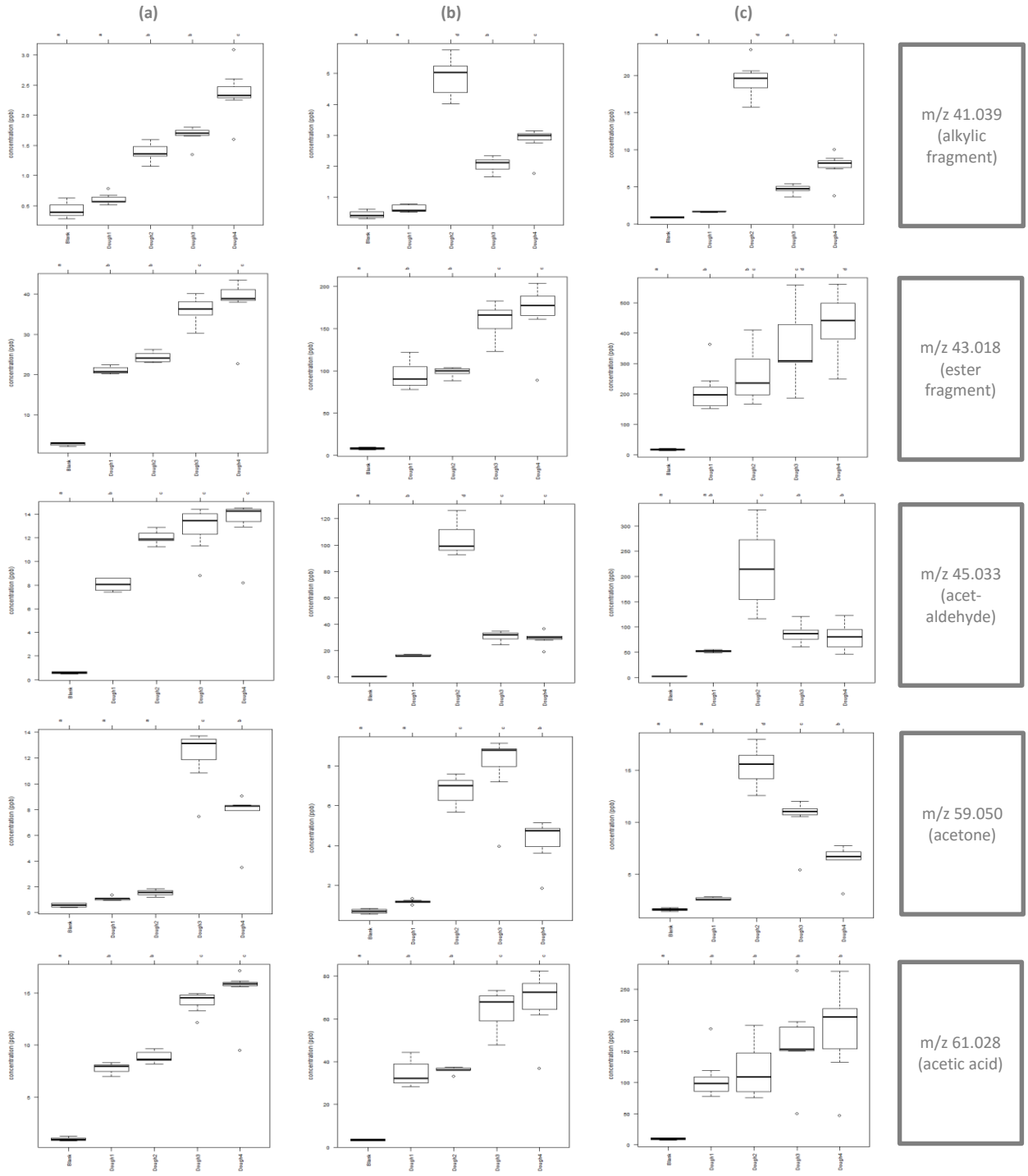

Figure 22. Selected volatiles emitted from the different dough samples at the first stage (a), middle stage (b), and at the end (c) of the experiment. Boxplots represent medians, upper and lower quartile, maximum and minimum for the selected masses

Volatile profile of the baked samples

After baking, the headspace analysis of the obtained micro-loaves revealed the productivity of 58 mass peaks kept after applying the 1 ppbv threshold. **Appendix 3** depicts the significantly different results, expressed in terms of productivity in ppbv per hour. One-way ANOVA ($p < 0.05/58 = 0.0009$ with Bonferroni correction) shows differences between experimental modes for 39 relevant peaks. In 20 out of these 39 peaks, B2 (the bread inoculated with yeast) showed the highest productivity followed by B4 (the sourdough model), while the latter (B4) showed the highest productivity for 6 peaks. B2 and B4 showed similar productivity for 10 peaks, B4 and B3 (the bread inoculated with bacteria) for 1 peak, and B1 (the bread control without any inoculations) and B4 showed similar productivity for 1 peak. Finally, for 1 peak B2, B3 and B4 showed a higher productivity than B1. We did not observe any difference in yeast count between the two preparations (data not shown). The observations in VOCs changes reported for the dough have a particular relevance if we consider that the production of dehydrated dough/sourdoughs is a business having worldwide diffusion, as these are generally added as ingredient to several bakery productions (Kulp & Lorenz, 2003).

In-depth analysis of volatile profile of the sourdough model

Differences between the different types of dough prepared, throughout the entire process, were observed by means of Principal Component Analysis (PCA), with each point representing a distinct sampling point (**Figure 23**). It was clear that all three preparations were able to perform fermentation (as observed by the evident increase in dough volume) and displayed a clear evolution of the VOCs profiles. The score plots for the first and third principal components, which comprised 85.0% of the overall variability, had different starting and ending points and the shading consistently varied over time. The results were repeatable also between the two

distinct biological replicates and an overall time evolution, which sums up the various kinetics, was visible having similar overall trends.

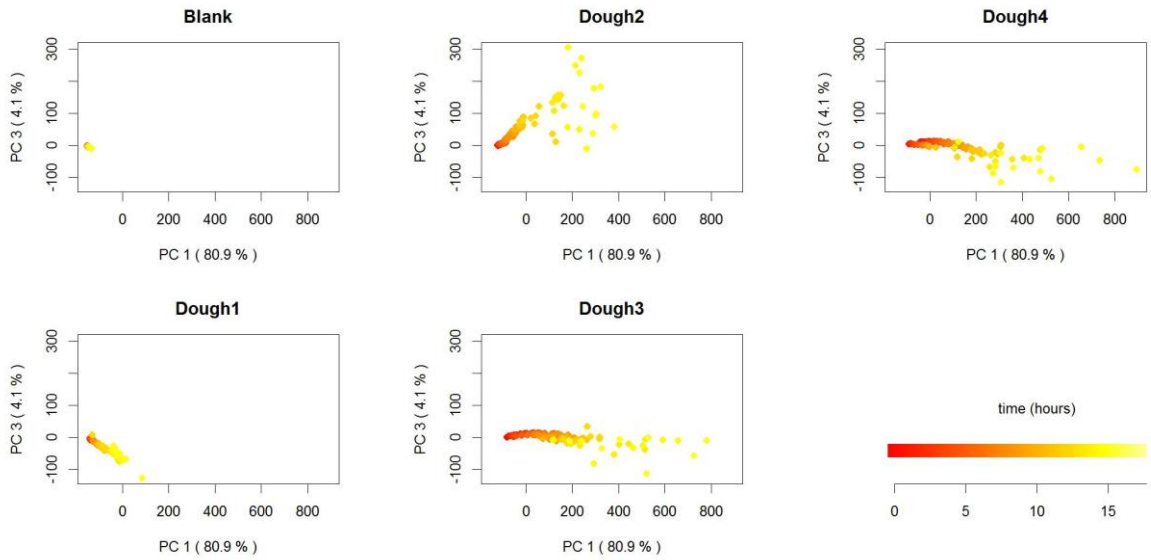

Figure 23. Volatile emission during leavening: Principal Component Analysis of the data. Score plots for the first and third principal components for the four types of prepared dough are depicted.

We can notice differences between the dough inoculated with the yeast preparation (D2) on one hand and the dough inoculated with the microbial preparation (D3) and the sourdough model (D4) on the other hand. Minor differences can be noticed between D3 and D4, however further investigation is needed to study the effect of adding yeast and bacteria together. Furthermore, it is possible to observe for D1, after no VOCs production during the first hours of the leavening (darker points), a limited volatile release pattern is detected at later stages around the end of the experiment. It seems to be driven by the spontaneous fermentation of the virtuous microflora naturally present in the flour (M. Gobbetti, Corsetti, La Rosa, & De Vincenzi, 1994) in addition to the microorganisms present in the surrounding preparation area. However, it requires several days, with frequent backslopping, to reach a sufficient concentration to perform an efficient sourdough fermentation (Makhoul, Romano, Cappellin, Spano, Capozzi, Benozzi, Märk, Aprea, Gasperi, El-Nakat, et al., 2014), and this can be verified when D1 is compared to the remaining preparations.

In-depth analysis of volatile profile of the baked sourdough model

Upon baking, the score plots for the first two principal components, which comprised 97.9% of the overall variability (**Figure 24**), shows a clear separation of the samples based on the type of inoculation added.

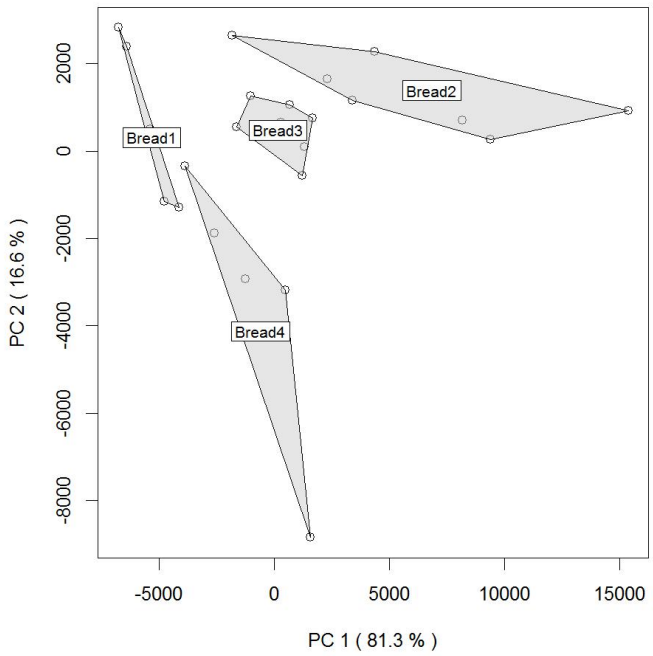

Figure 24. Volatile emission upon baking: Principal Component Analysis of the data. Score plots for the first two principal components for the four types of bread are depicted.

Discussion and conclusion

The high-throughput analytical approaches able to provide a snapshot of the volatile organic compounds (VOCs) released in association of a given metabolism has been receiving increasing interesting in reason of the biological and applicative relevance. As already mentioned, this sum of volatile organic metabolites is also indicated with the term ‘volatome’. Among the techniques for VOCs determination, the ‘volatome’ perspective cast a new light on the advantages of direct injection mass spectrometry (DIMS). In fact, while gas chromatography–mass spectrometry

(GC-MS) remains a standard for targeted VOCs analysis, DIMS, allowing direct analysis of headspace associated with a specific matrix/organism with no prior separation, offers intriguing application due to the possibility of on-line monitoring without samples destruction. Among DIMS techniques, proton transfer reaction–mass spectrometry (PTR-MS) couples simplicity of analysis and the control of the ionization conditions. The food sector provides us several examples of 'volatomic' applications of considerable interest for both biological and applicative relevance. In particular, considering fermentations, i) the food matrices could be consider specific environments, ii) the yeasts, molds, and bacteria designated organisms, and iii) the volatiles, at the same time, part of microbial metabolic interaction and molecular basis of food flavour. Fermented foods as interesting products for sensory innovation, fermented foods as treasured models to simplify processes in less manageable biological systems (Wolfe & Dutton, 2015).

In this study, to the best of our knowledge, we report for the first time the application of PTR-MS in order to study the evolution of 'volatome' associated with microbial growth in laboratory media and, concurrently, in a food matrix. In particular, we studied the 'volatome' associated with laboratory cultures of *Saccharomyces cerevisiae* and *Lactobacillus sanfranciscensis*, respectively grown in Yeast Peptone Dextrose (YPD) medium and in de Man, Rogosa and Sharpe (MRS) medium. Moreover, we described volatiles released by *Saccharomyces cerevisiae* and by *Lactobacillus sanfranciscensis* during their separate development in a dough for bread-making.

These two microorganisms represent the most important domesticated eukaryotic and prokaryotic organisms in the sourdough environment. *S. cerevisiae* has been used for thousands years by mankind to perform the alcoholic fermentation in food and beverages such as bread, beer, and wine, showing an evolutionary history associated with these fermentative processes

(Sicard & Legras, 2011). With its smaller genome in size (1.23 Mb) among available *Lactobacillus* genome sequences (Sun et al., 2015), *L. sanfranciscensis* represents a worthy example of specialized adaptation to dough environment (e.g. it preferentially catabolizes maltose, the principal sugar of the dough) (Suzzi, 2011).

In our study, we confirmed that the production of VOCs depends on the nutritional environment. In particular, while Heddergott et al (Heddergott, Calvo, & Latgé, 2014) demonstrated this feature using *Aspergillus fumigatus* as model organism and *in vitro* conditions (three defined media), we reported this evidence using yeast and bacterial model comparing *in vitro* (laboratory media) and *in vivo* (dough environment) conditions .

With concern of the studied microbial interaction, in 2007, Guerzoni et al. used individual cultures and co-cultures of *L. sanfranciscensis* and *S. cerevisiae* as model of the metabolite-mediated interactions lactobacilli and yeasts in model and real systems (Guerzoni, Vernocchi, Ndagijimana, Gianotti, & Lanciotti, 2007). These researchers employed GC as analytical techniques for their investigations, while we adopted a PTR-based approach. Consequently, we explored the volatiles arena using 'analytical lens' that privilege sensitivity and the monitoring in the time, implying a certain loss in identification power (Romano et al., 2015b). In addition, for the first time, we considered the repercussions of *S. cerevisiae* and *L. sanfranciscensis* interactions on the VOCs associated with the headspaces of corresponding loaves.

Considering possible future perspectives, it appears interesting i) to increase the diversity of protechnological microbes studied in the sourdough environment and ii) to compare VOCs patterns associated with single-specie cultures with the VOCs profile linked to real sourdough fermentations in order to understand , as recently done to assess the *S. cerevisiae* contribute to kefir volatome (Hu, Gunathilake, Chen, & Urban, 2014).

3.5 Summary of the *ProBake* results, ongoing research and future prospects

The findings recorded during the *ProBake* project, were summarized in the following paper (Vittorio Capozzi et al., 2015) presented by our group during the International Conference on Food and Biosystems Engineering, which took place in May 2015, in Greece.

This paper describes our investigations on the possible application of the comprehensive methodology we had elaborated (automatic sampling, PTR-ToF-MS analysis and tailored data handling and analysis) for the monitoring of fermentation in two foods, bread and yogurt, as models to respectively study the diversity of yeast (*Saccharomyces cerevisiae*) and bacterial (lactic acid bacteria) SCs. Note that yogurt is the topic of a parallel study conducted by our group in order to test the same methodology (Benozzi et al., 2015). The paper provided further insights on both projects and PTR-ToF-MS was once again proven to be a fast high-throughput tool for the study of food bioprocesses. In addition, this approach, allowed us to select a panel of VOCs as potential markers for the rapid screening of starter cultures in the food industry.

Finally, our approach was deemed useful in the selection of volatiles associated with flavors, off-flavors, desired (undesired) technological properties which are relevant for the industrial food manufacturing process. More generally, microbial-associated VOCs represent a fascinating field for the formulation of new hypotheses in fundamental biology and in the discovery of new and/or improved products and solutions for human exploitation.

International Conference on Food and Biosystems Engineering, 28-31 May 2015, Mykonos island,
FaBE2015 168

PTR-ToF-MS and food bioprocesses: potential in monitoring VOCs release by starter cultures during food fermentation

Vittorio Capozzi[1,2], Salim Makhoul[1,3,4], Andrea Romano[2], Giuseppe Spano[5], Eugenio Aprea[1], Luca Cappellin[1], Tilmann D. Mark[6], Hanna El-Nakat[4], Jean Guzzo[3], Flavia Gasperi[1], Matteo Scampicchio[2], Franco Biasioli[1]*

[1]Dept. of Food Quality and Nutrition, Research and Innovation Centre, (FEM), San Michele all Adige, Italy
[2]Faculty of Science and Technology, Free University of Bolzano, 39100, Bolzano, Italy
[3]UMR PAM-EquIpe VALMIS, IUVV, 1 rue Claude Ladrey, 21078 Dijon Cedex, France
[4]Dept. of Chemistry, University of Balamand, P. O. Box 100, Tripoli, Lebanon
[5]Dept. of Agriculture, Food and Environmental Sciences, University of Foggia, Foggia, Italy
[6]Institut fur Ionenphysik und Angewandte Physik, Leopold-Franzens Universitat, Innsbruck, Austria

Abstract

In the modern agro-industry, food fermentations are usually achieved by the supplementing the row materials with starter cultures (SCs) (a microbial preparation of large numbers of cells of selected microorganisms). This practices ensures a number of benefits, including the possibility to enhance and standardize the sensory quality of fermented foods. In fact, microbes produce VOCs (volatile organic compounds) which contribute to, and often dominate, the perceived quality of food and drive consumer preference. Among the methods to monitor VOC release, Proton Transfer Reaction Time of Flight Mass Spectrometry (PTR-ToF-MS) is particularly interesting because of its high sensitivity and non-invasive analysis. Moreover, thanks to the high mass resolution, it provides in a split second highly informative spectra. A further development is the coupling of PTR-ToF-MS with an auto-sampler and with tailored data analysis tools. This paper describes our recently investigations on the possible application of this comprehensive methodology (automatic sampling, PTR-ToF-MS analysis and tailored data handling and analysis) to the monitoring of fermentation in two foods, bread and yogurt, as models to respectively study the diversity of yeast (Saccharomyces cerevisiae) and bacterial (lactic acid bacteria) SCs. PTR-ToF-MS is proven to be a fast high-throughput tool for the study of food bioprocesses. In fact, the employment of PTR-ToF-MS, integrated

*Corresponding author e-mail: franco

International Conference on Food and Biosystems Engineering, 28-31 May 2015, Mykonos island,
FaBE2015 168

with a multifunctional auto-sampler, allowed us to measure the time evolution of several mass peaks and highlighted reproducible differences among diverse commercial SCs with a minimal need for manual operation and in a short time. We selected a panel of VOCs as potential markers for the rapid screening of SCs in relation with flavor, off-flavor and technological properties which are relevant for the bakery and the yogurt industry.

Keywords: PTR-MS, VOCs, bread, yogurt, yeast, bacteria, aroma, bioprocess

Fermented foods are consumable products that are generated from thermally treated or untreated food raw materials of plant or animal origin They have characteristic sensory and nutritional value as well as properties determining shelf life, hygiene or practical value that are decisively affected by microorganisms and/or enzymes (from the raw material) (Vogel et al 2011). It exists a wide arena of edible fermented products, largely deriving from traditional fermented foods and beverages (Capozzi and Spano 2011). In this range of products the fermentative step influences sensory characteristics, nutritional value, shelf life and safety. This noticeable led the modern food industry to develop strategies to manage food fermentation. The principal solution foresee the inoculum of the raw material with a microbial preparation adequate in quantity and quality to steer fermentative processes. This microbial biomass is named 'starter culture', and is defined as a 'preparation of live microorganisms or their resting forms, whose metabolic activity has desired effects in the fermentation substrate, the food' (Vogel et al 2011). The use of starter cultures in the management of food fermentations represents a practices that imply an articulate panel of benefices for producers and consumers, including improved shelf-life, optimization of fermentation time, increased level of standardization of product qualities, and the food safety risk reductions. Together with these benefits, this practices ensures including the possibility to enhance and standardize the sensory quality of fermented foods. A certain quantity of microbial metabolites susceptible to influence food properties belong to the class of volatile organic compounds (VOCs), molecules defined as low molecular weight (<300 Da) carbon-based solids and liquids that readily enter the gas phase by vaporizing at 0.01 kPa at a temperature of approximately 20 °C (Pagans et al. 2006). In reason of these physical characteristics, VOCs generally can pass through cross cellular membranes, with the subsequent release into the matrix/environment, contributing to (and often dominating) the perceived sensory quality of food and driving consumer preference.

Since the first description of volatile production by a bacterium (Zoller and Clark 1921), several microbial VOCs have been characterized, belonging to different chemical classes (e.g. fatty acid derivatives, aromatic compounds, nitrogen-containing compounds, sulfur compounds, terpenoids, metalloid compounds) (Schulz and Dickschat 2007). The reference approach in terms VOCs identification and quantification is gas chromatography-mass spectrometry (GC-MS). To explicate these potentialities GC-MS require a pre-concentration phase and a time ranging from few minutes to more than one hour for chromatographic analysis. However, due to diversity of microbial strains/species and food matrices involved, in reason of the number of possible applications and environmental conditions, there is clearly a mounting request for new analytical technologies allowing to detect microbial VOCs in rapid and non-invasive fashion, allowing us to perform massive screenings and bioprocess on-line monitoring (Romano et al. 2015). From this point of view, Direct Injection Mass Spectrometry (DIMS) techniques provides an alternative approach to VOCs identification and quantification. In particular, Proton-Transfer-

International Conference on Food and Biosystems Engineering, 28-31 May 2015, Mykonos island, FaBE2015 168

Reaction Mass Spectrometry (PTR-MS), combining high sensitivity, rapid examination, and direct analysis on the sample headspace, represents a suitable analytical technique for microbial VOC analysis during food processing. In particular, PTR-MS coupled with Time-of-Flight (ToF) mass analyzers enhanced analytical information provided (improved mass resolution) (Fabris et al. 2010).

Here we report recent investigations on the possible application of this comprehensive methodology (automatic sampling, PTR-ToF-MS analysis and tailored data handling and analysis) to the monitoring of fermentation in two foods, bread and yogurt, as models to respectively study the diversity of yeast (*Saccharomyces cerevisiae*) and bacterial (lactic acid bacteria) starter cultures.

I. Proton transfer Reaction-Mass Spectrometry (PTR-MS): A Brief Outline and Experimental Conditions

PTR-MS is a DIMS technique based on the ionization of neutral VOC molecules with hydronium ions (H_3O^+) produced by a hollow cathode discharge on water vapors, according to the following reaction:

$$H_3O^+ + M \rightarrow H_2O + MH^+.$$

This proton transfer reaction belongs to the so called 'soft ionization' methods, since the excess energy of the reaction is reduced, leading to a very limited fragmentation of the VOCs associated ions.

1.1. PTR-ToF-MS analysis. Measurements of the headspace of the yogurt, dough and bread samples were performed with a commercial PTR-ToF 8000 apparatus from Ionicon Analytik GmbH (Innsbruck, Austria), in its standard configuration (V mode). The ionization conditions in the drift tube were the following: 110 °C drift tube temperature, 2.30 mbar drift pressure, 550 V drift voltage. This led to an E/N ratio of about 140 Townsend (1 Td = 10^{-17} cm^2 V^{-1} s^{-1}). The inlet line consisted of a PEEK capillary tube (internal diameter 0.40 mm) heated at 110 °C. The inlet flow was set at 120 sccm for dough and 40 sccm for bread and yogurt measurements.

1.2. PTR-ToF-MS and multifunctional autosampler. The automation used for the leavening experiments was obtained using an autosampler (Gerstel, Mulheim am Main, Germany) especially adapted to PTR-MS analyses. At the beginning of the experiment, the robotic arm moved the sample from a cooling tray where it was kept at 4 °C, to the incubation tray, whose temperature was set at 30 °C. Vials were then moved to the temperature-controlled purging site, connected to the PTR-ToF-MS inlet, and where the headspace analysis took place for 30 seconds with an acquisition rate of one spectrum per second. After measurement, the vial was moved to the incubation tray and the cycle was repeated on the following sample. This allowed to perform a scan of the tray in approximately one hour. During leavening, the scan was repeated 16 to 20 times, in order to monitor the fermentation process.

1.3. Data analysis. Dead time correction, internal calibration of mass spectral data and peak extraction were performed according to a procedure described in the works of Cappellin et al. (Cappellin et al. 2010; Cappellin et al. 2011), using a modified Gaussian peak shape. Peak intensity in ppbV was estimated using the formula described in literature (Lindinger et al. 1998), using a constant value for the reaction rate constant coefficient (k = 2.10^{-9} cm^3 s^{-1}). This introduces a systematic error for the absolute concentration for each compound that is in most cases below 30% and could be accounted for if the actual rate constant coefficient is available (Cappellin et al. 2012).

All data detected and recorded by the PTR-ToF-MS were processed and analysed using MATLAB (MathWorks, Natick, MA) and in-house developed scripts written in R programming language (R Foundation for Statistical Computing, Vienna, Austria).

International Conference on Food and Biosystems Engineering, 28-31 May 2015, Mykonos island,
FaBE2015 168

II. Bread Bioprocess Monitoring and Yeast Starter Cultures

2.1. Bread bioprocess VOCs monitoring. Bread was prepared according to the procedure described in AACC 10^{-10B}(Approved Methods of the AACC, 10th ed.; American Association of Cereal Chemists: St. Paul, MN, 2000), with minor modifications (Capozzi et al. 2011), by mixing the following ingredients in a bread homemaker machine (Princess Household Appliances, Lainate, Italia): 200 g of flour, 3g of sodium chloride, 12g of sucrose, 6g of animal, 8 mg of ascorbic acid, and 120 mL of distilled water. The dough samples were supplemented with a yeast preparation following the manufacturer's recommendations. We sampled 1.0 g pieces from each dough that we put in 22 mL vial. Four replicates of each dough sample were analyzed and the entire experiment was repeated twice. During preparation, the dough was kept at 4 °C in order to reduce the fermentation process. During the whole duration of the experiment the samples were incubated at 30 °C.

For baked bread analysis, after the leavening time, the vials were taken out. Caps were removed and vials were transferred to a kitchen oven and baked for 8 minutes at 220 °C. We accurately cleaned the oven prior to the analysis and turned it on for one hour with ventilation to avoid residual VOCs. An empty vial was introduced in the oven during baking and later used as a blank control. Due to the presence of relevant amounts of ethanol (an average of 20 ppmv of ethanol) in the headspace of the samples during leavening, an inert gas dilution was applied (inert gas to sample ratio of 2:1). This permitted to prevent primary ion depletion and formation of ethanol clusters which might affect the final quantification of volatiles (Aprea et al. 2007).

Prior to analysis, samples were flushed with a stream of clean air (200 mL/min for 30 seconds), as generated by a Gas Calibration Unit apparatus (Ionicon Analytik GmbH), then incubated at 30 °C for 30 minutes and finally analyzed. No dilution of the headspace was required in this case.

2.2. The effect of different yeast starter cultures. We recently demonstrated the applicability of our comprehensive methodology (automatic sampling, PTR-ToF-MS analysis and tailored data handling and analysis) to online study volatile organic compound production during the bread leavening process, and for the differentiation of bakery yeast starter cultures in reason of their release of volatile compounds (Makhoul et al. 2014). In particular, Makhoul et al. (2014) compared uninoculated dough (dough1) with doughs respectively inoculated with three yeast commercial preparations (Y1, Y2 and Y3) from three different manufacturers (dough 2, dough 3, dough 4) and a so called 'natural yeast' preparation (dough 5) (e.g. in Figure 1 a commercial yeast starter cultures and the corresponding inoculated dough prepared according to the reported procedure).

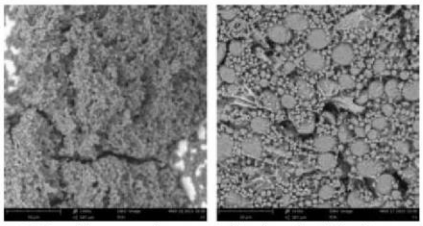

Figure 1. Yeast biomass and corresponding inoculated dough preparation observed by scanning electron microscopy (SEM, Phenom proX, Phenom-World B.V., Netherlands) (magnification 1450X).

The dough headspace (Figure 2) displayed more than 400 distinct peaks. Even if ethanol (peak at nominal mass 47) was the second peak in terms of relative abundance, it is important to underline that no depletion of the primary ion (monitored using peak at m/z 21) was observed. In general, we observed that mass peaks with average concentrations below 1 ppbv showed little or no difference with respect to the different experimental modes. Hence, using a minimum threshold of 1 ppbv (average concentration), we filtered the data set, obtaining a panel of 72 mass peaks. We detected the maximum expansion in the cycle 3 (about 2 h and 42 min of leavening).

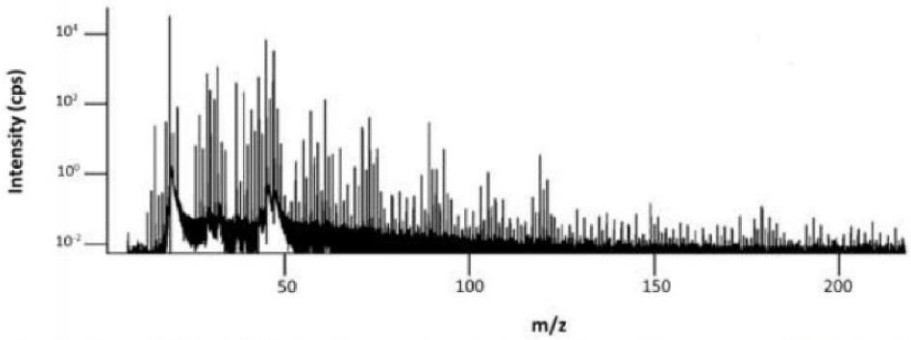

Figure 2. Average PTR-ToF-MS mass spectra of dough, obtained by averaging over 150–750 s of measurement.

For each of these mass peaks we provided a tentative identification. From a biotechnological perspective, observing the ethanol concentration, we have a direct analytic determination to monitor yeast primary metabolic activity in the dough (during alcoholic fermentation sugars are fermented by yeast into CO_2, ethanol and other organic materials), while the standard bakery determination of leavening activity is indirectly determined using the dough volume expansion (an indirect empiric measure of CO_2 released by yeast in the dough).

In figure 3, we show the results obtained for the five experimental modes were visualized by means of principal component analysis (PCA), with each point representing a distinct sampling. The three yeast preparations were able to perform fermentation and displayed a clear evolution of the VOC profile, in which the elbow-like disposition of the points reveals that different VOCs reached highest concentrations at different time points during the experiment.

On the contrary, the dough 1 and the dough 5 and showed a limited release of VOCs and slow fermentation performances (in the case of dough 1 the slow fermentation is due to the presence of autochthonous microbes in the flours, while in the case of dough 5 it is important to underline that we are talking of a dried sourdough, so a dried dough containing a mixture of yeast and bacteria in a 1/100 ratio that normally require a longer leavening time in reason of the low fermentation rate).

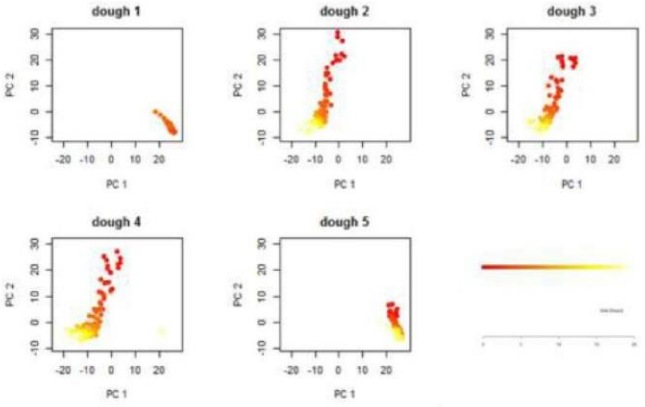

Figure 3. Principal component analysis of the volatile release during leavening. Different colors represent time evolution, according to the legend.

We choose the data corresponding to the maximum in volume expansion for the three preparation Y1, Y2, and Y3, for an in-depth comparison of leavening associated volatiles. One-way analysis of variance (ANOVA) ($p<0.05$) showed significant differences for 16 peaks, indicating a clear impact of the yeast on the volatile pattern of the fermented dough.

Analyzing the corresponding bread, mass spectral data yielded about 400 mass peaks overall. Similarly to the dough analysis, we filtered the data on a 1 -ppbv threshold, obtaining 64 mass peaks. One-way analysis of variance (ANOVA) ($p<0.05$) showed significant differences in concentration for 8 peaks, confirming the impact of the different experimental modes on the volatile pattern also at the level of finished products (the concentrations for one of these peaks is reported in Figure 4).

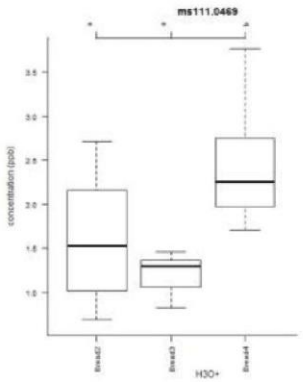

Figure 4. Exemplificative volatile emitted from dough after about 3 h of fermentation. Labels depict statistically significant differences (one-way ANOVA, $p<0.05$ and Tukey's test).

Recently, this same strategy (PTR-ToF-MS coupled with an auto-sampler and with tailored data analysis tools) has been used to analyze the effect on VOCs productivity of i) *Saccharomyces cerevisiae* strains as well as the type of wheat flour used in the bread-making (Makhoul et al. unpublished results), ii) the interaction between *S. cerevisiae* and *Lactobacillus sanfranciscensis* (Makhoul et al. unpublished results), iii) different commercial aromatic yeast starter cultures for bakery (Capozzi et al. unpublished results), iv) of different regional artisanal sourdough preparations (Capozzi et al. unpublished results).

III. Yoghurt Bioprocess Monitoring and Bacterial Starter Culture

3.1. Yoghurt bioprocess VOCs monitoring. Yoghurt was prepared using ultra-high-temperature low-fat milk (1.5% milk fat, 8.5% solids non-fat). Each vial (22 mL vial) were filled with 5 ml milk. The content was heat-treated at 80 °C for 30 min in a water bath and, successively, fast cooled to 45 °C in a cooler (4 °C). The yogurt starter culture was added to the milk in the vial and the samples were placed in a tray with controlled temperature (45 °C) for lactic acid fermentation. The robotic arm of the autosampler carried out the inoculation of all vials (except blanks) at a final starter concentration suggested by the manufacturer. The incubation time was set to 240 minutes, (Routray and Mishra, 2011). The autosampler has been used in this step as well, to monitor VOCs concentrations over time. For each experimental mode (the different starters additions and uninoculated blanks as well), twelve vials were employed. The whole experiment has been performed in three replicates, on separate days, differently randomizing the sample order in each day.

3.2. Yoghurt bioprocess and the effect of different bacterial starter cultures. PTR-ToF-MS coupled with an automated sampling system and with a tailored statistical tools led us to detect, during the monitoring lactic acid fermentation of yoghurt, more than 300 mass peaks, tentatively identifying all major yoghurt aroma volatiles (in Table 1 an exemplificative list).

Table 1. An exemplificative list of mass peaks associated to sum formulas and tentative identifications according to Cheng 2010 (1) and/or Soukoulis et al., 2010 (2).

Meas. mass	Theor. mass	Sum formula	Tentative identification	Ref.
46.037	46.037	C[13]CH5O+	isotope C13 of acetaldehyde	1,2
47.013	47.013	CH3O2+	formic acid	1,2
47.047	47.047	C2H7O+	ethanol	1,2
63.026	63.029	C2H7S+	dimetyl sulfide	1,2
73.065	73.064	C4H9O+	2-butanone/butanal/cyclobutanol	1,2
87.044	87.044	C4H7O2+	dyacetil	1,2
89.059	89.060	C4H9O2+	acetoin	1,2
97.028	97.028	C5H5O2+	furfural	1,2
125.060	125.059	C7H9O2+	guaiacol	1
137.132	137.132	C10H17+	R-α-pinene/3-carene/D-limonene	1,2

For each mass peaks we were able to report the evolution of the associated volatile during lactic acid fermentation in yoghurt (e.g. in Figure 5 we report this evolution for the mass peak m/z 43.018, sum formula $C_2H_3O^+$, tentatively identified as a fragment of acetic acid and/or a fragment of 2-heptanone).

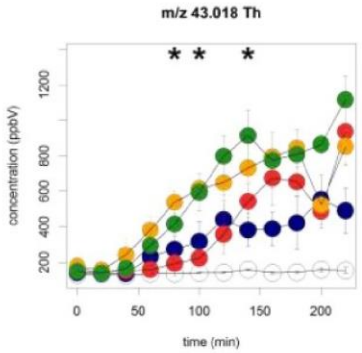

Figure 5. Fermentation kinetics of mass peak mz 43.018.
Different colors of the circles correspond to different starter cultures.
The blank circles correspond to uninoculated samples.

Recently, we use PTR-ToF-MS (coupled with an auto-sampler and with tailored data analysis tools) to monitor lactic fermentation driven by different yoghurt commercial starter cultures (freeze-dried direct-vat-set (DVS) yogurt cultures containing *Streptococcus thermophilus* and *Lactobacillus delbrueckii*subsp. *bulgaricus*) (Benozzi et al. unpublished results).

IV. The Impact of our Proposed Approach

4.1. Food bioprocessing. PTR-ToF-MS is proven to be a fast high-throughput tool for the study of food bioprocesses.

In fact, the employment of PTR-ToF-MS, integrated with a multifunctional auto-sampler, allowed us to measure the time evolution of several mass peaks and highlighted reproducible differences among diverse commercial starter cultures with a minimal need for manual operation and in a short time.

In general, this approach, allowed us to selected a panel of VOCs as potential markers for the rapid screening of starter cultures in food industry.

4.2. Other possible applications. Our ap-

proach might be useful in the selection of volatiles associated with flavors, off-flavors, desired(undesired) technological properties which are relevant for the industrial food manufacturing process. More generally, microbial-associated VOCs represent an fascinating field for the formulation of new hypotheses in fundamental biology and in the discovery of new and/or improved products and solutions for human exploitation.

References

[1] Capozzi, V., Menga, V., Digesu, A.M., De Vita, P., van Sinderen, D., Cattivelli, L., et al. (2011) Biotechnological production of vitamin B2-enriched bread and pasta. J. Agric. Food Chem. 59: 8013-8020.

[2] Capozzi, V. and Spano, G. (2011) Food Microbial Biodiversity and Microbes of Protected Origin. Front Microbiol 2:

[3] Cappellin, L., Biasioli, F., Fabris, A., Schuhfried, E., Soukoulis, C., Mark, T.D., and Gasperi, F. (2010) Improved mass accuracy in PTR-ToF-MS: Another step towards better compound identification in PTR-MS. International Journal of Mass Spectrometry 290: 60-63.

[4] Cappellin, L., Biasioli, F., Granitto, P.M., Schuhfried, E., Soukoulis, C., Costa, F., et al. (2011) On data analysis in PTR-TOF-MS: From raw spectra to data mining. Sensors and Actuators B: Chemical 155: 183-190.

[5] Cappellin, L., Karl, T., Probst, M., Ismailova, O., Winkler, P.M., Soukoulis, C., et al. (2012) On Quantitative Determination of Volatile Organic Compound Concentrations Using Proton Transfer Reaction Time-of-Flight Mass Spectrometry. Environ. Sci. Technol. 46: 2283-2290.

[6] Cappellin, L., Loreto, F., Aprea, E., Romano, A., del Pulgar, J.S., Gasperi, F., and Biasioli, F. (2013) PTR-MS in Italy: a multipurpose sensor with applications in environmental, agri-food and health science. Sensors (Basel) 13: 11923-11955.

[7] Cheng, H. (2010) Volatile flavor compounds in yogurt: a review. Crit Rev Food Sci Nutr 50: 938-950.

[8] Fabris, A., Biasioli, F., Granitto, P.M., Aprea, E., Cappellin, L., Schuhfried, E., et al. (2010) PTR-TOF-MS and data-mining methods for rapid characterisation of agro-industrial samples: influence of milk storage conditions on the volatile compounds profile of Trentingrana cheese. J. Mass Spectrom. 45: 1065-1074.

[9] Lindinger, W., Hansel, A., and Jordan, A. (1998) On-line monitoring of volatile organic compounds at pptv levels by means of proton-transfer-reaction mass spectrometry (PTR-MS) medical applications, food control and environmental research. International Journal of Mass Spectrometry and Ion Processes 173: 191-241.

[10] Makhoul, S., Romano, A., Cappellin, L., Spano, G., Capozzi, V., Benozzi, E., et al. (2014) Proton-transfer-reaction mass spectrometry for the study of the production of volatile compounds by bakery yeast starters. J Mass Spectrom 49: 850-859.

[11] Romano, A., Capozzi, V., Spano, G., and Biasioli, F. (2015) Proton transfer reaction-mass spectrometry: online and rapid determination of volatile organic compounds of microbial origin. Appl. Microbiol. Biotechnol. 99: 3787-3795.

[12] Routray, W. and Mishra, H.N. (2011) Scientific and technical aspects of yogurt aroma and taste: a review. Comprehensive Reviews in Food Science and Food Safety 10: 208-220.

[13] Schulz, S. and Dickschat, J.S. (2007) Bacterial volatiles: the smell of small organisms. Nat Prod Rep 24: 814-842.

[14] Soukoulis, C., Aprea, E., Biasioli, F., Cappellin, L., Schuhfried, E., MÃd'rk, T.D., and Gasperi, F. (2010) Proton Transfer Reaction Time-of-Flight Mass Spectrometry monitoring of the evolution of volatile compounds during lactic acid fermentation of milk. Rapid Commun. Mass Spectrom. 24: 2127-3134.

[15] Vogel, R.F., Hammes, W.P., Habermeyer, M., Engel, K.-H., Knorr, D., and Eisenbrand, G. (2011) Microbial food cultures-opinion of the Senate Commission on Food Safety (SKLM) of the German Research Foundation (DFG). Mol. Nutr. Food Res. 55: 654-662.

[16] Zoller, H.F. and Clark, W.M. (1921) The production of volatile fatty acids by bacteria of the dysentery group. J. Gen. Physiol. 3: 325-330.

Conclusion

4. Conclusion

VOCs are organic compounds of interest in many fields of study, namely bioprocesses. Various detection techniques have been applied so far in order to detect, identify and quantify them. Each technique has many advantages as well as some limitations mainly in terms of resolution, sensitivity and time-consumption. PTR-MS, being a relatively newly-developed DIMS technique, is recommended in this thesis as an answer for these limitations.

Numerous upgrades and add-ons were introduced to the PTR device in order to improve its performance, and data-mining as well as multivariate analysis tools were also established and tested first on a simple model molecule, ethylene, and later on a more complex matrix: the bread bioprocess (the *ProBake* project). The results of the ethylene study confirmed the high capacity of the SRI-MS technique in detecting this VOC, specifically using O_2^+ as a primary reagent ion.

As for the results of the *ProBake* project, we were able to conceive a tailored approach in order to maximize the potential of PTR-ToF-MS in studying the complicated bread-making bioprocess. The full automaton was achieved, the effect of each ingredient was studied. Moreover, ingredient/microbe as well as microbe/microbe interactions were elucidated. The main achievements realized in this thesis are summarized in the following abstract, presented during the 27th International Conference on Yeast Genetics and Molecular Biology, and published by *Wiley Publishers* in October 2015, and present a promising basis for future endeavors.

Finally, it is important to highlight the following points regarding the importance of our approach and its future applications:

i. Using starter culture applications in bread making as a model, we demonstrated the great analytical potential of PTR-ToF-MS coupled with an autosampler and tailored data analysis in food bioprocess monitoring.

ii. The impressive rapidity of the analysis and the consistent degree of automation are features of outstanding importance in a field with great number of variables (variety of matrices, heterogeneity of protechnological microbes, number of ingredients and additives, physical-chemical variables, different regimen of technologies, …) and in massive screening of microbial biotypes.

iii. The wide number of possible applications dealing with VOCs monitoring (e.g. molecular basis of sensory properties, markers of technological phases, biomarker for spoilage microbes/pathogens detection, monitoring of shelf-life, biological investigations) testifies the relevance of our analytical approach.

iv. Our methodology can be easily adapted to industrial applications and to consumer-oriented innovations.

27th International Conference on Yeast Genetics and Molecular Biology **S247**
Poster Session 15: New tools in yeast research

PS15-5: PTR-ToF-MS and bioprocesses: Potential in monitoring VOCs release by eukaryotic microbes

Vittorio Capozzi[1,2], Salim Makhoul[1,3,4], Luca Cappellin[1], Andrea Romano[2], Giuseppe Spano[5], Eugenio Aprea[1], Tilmann D. Märk[6], Flavia Gasperi[1], Matteo Scampicchio[2], Franco Biasioli[1]

[1]Department of Food Quality and Nutrition, Research and Innovation Centre, Fondazione Edmund Mach (FEM), via E. Mach 1, 38010 San Michele all'Adige (TN), Italy; [2]Faculty of Science and Technology, Free University of Bolzano, 39100, Bolzano, Italy; [3]UMR PAM – équipe VALMIS, IUVV, 1 rue Claude Ladrey, 21078 Dijon Cedex, France; [4]Department of Chemistry, University of Balamand, P. O. Box 100, Tripoli, Lebanon; [5]Department of Agriculture, Food and Environmental Sciences, University of Foggia, via Napoli 25, 71122 Foggia, Italy; [6]Institut für Ionenphysik und Angewandte Physik, Leopold-Franzens Universität Innsbruck, Technikerstr. 25, 6020 Innsbruck, Austria

The release of volatile organic compounds (VOCs) by eukaryotic microbes is of interest for several fields, comprising food, environmental, biotechnological and medical applications. In addition, it represents an intriguingly opportunity to conceive and to confirm new hypotheses in fundamental biology and in breeding sciences. For example, VOCs studies in an -omics perspective are generally defined as volatome, indicating with this terms the organic volatile subset of metabolome. The various techniques for VOC analysis generally aim to combine either sample throughput or analytical insight. From this point of view, Proton Transfer Reaction Time of Flight Mass Spectrometry (PTR-ToF-MS) represents a valid compromise, with the advantages of on-line process monitoring and non-invasive analysis. In order to maximize the advantages of on-line bioprocess monitoring, we coupled PTR-ToF-MS with an auto-sampler, adding a tailored data analysis tools. We demonstrated the applicability of our comprehensive methodology (automatic sampling, PTR-ToF-MS analysis and tailored data handling and analysis) the study *Saccharomyces cerevisiae* volatile organic compounds released during alcoholic fermentations. In particular, considering bread-making bioprocess, we use this approach i) to differentiate bakery yeast starter cultures in reason of their release of VOCs and to analyze the effect on VOCs productivity as a function of ii) different bakery yeast starter cultures/flour combinations, ii) the interaction between *S. cerevisiae* and *Lactobacillus sanfranciscensis* as model microorganisms in the sourdough environment, iv) different commercial aromatic yeast starter cultures for bakery.

LIST OF REFERENCES

Adams, N., & Smith, D. (1976). The selected ion flow tube (SIFT); a technique for studying ion-neutral reactions. *International Journal of Mass Spectrometry and Ion Physics, 21*(3), 349-359.

Agarwal, B. (2012). Proton transfer reaction time-of-flight mass spectrometry advancement in detection of hazardous substances.

Annett, L. E., Spaner, D., & Wismer, W. V. (2007). Sensory profiles of bread made from paired samples of organic and conventionally grown wheat grain. *Journal of Food Science, 72*(4), S254-260. doi: 10.1111/j.1750-3841.2007.00331.x

Aprea, E., Biasioli, F., Märk, T. D., & Gasperi, F. (2007). PTR-MS study of esters in water and water/ethanol solutions: Fragmentation patterns and partition coefficients. *International Journal of Mass Spectrometry, 262*(1–2), 114-121. doi: http://dx.doi.org/10.1016/j.ijms.2006.10.016

Arena, M. P., Caggianiello, G., Russo, P., Albenzio, M., Massa, S., Fiocco, D., . . . Spano, G. (2015). Functional Starters for Functional Yogurt. *Foods, 4*(1), 15-33.

Arena, M. P., Russo, P., Capozzi, V., López, P., Fiocco, D., & Spano, G. (2014). Probiotic abilities of riboflavin-overproducing Lactobacillus strains: a novel promising application of probiotics. *Applied Microbiology and Biotechnology, 98*(17), 7569-7581.

Art, H. W. (1993). *Dictionary of ecology and environmental science*: H. Holt.

Arthur, C. L., & Pawliszyn, J. (1990). Solid phase microextraction with thermal desorption using fused silica optical fibers. *Analytical chemistry, 62*(19), 2145-2148.

Ballabio, D., Cosio, M. S., Mannino, S., & Todeschini, R. (2006). A chemometric approach based on a novel similarity/diversity measure for the characterisation and selection of electronic nose sensors. *Analytica chimica acta, 578*(2), 170-177.

Bean, H. D., Mellors, T. R., Zhu, J., & Hill, J. E. (2015). Profiling Aged Artisanal Cheddar Cheese Using Secondary Electrospray Ionization Mass Spectrometry. *Journal of Agricultural and Food Chemistry, 63*(17), 4386-4392.

Benozzi, E., Romano, A., Capozzi, V., Makhoul, S., Cappellin, L., Khomenko, I., . . . Märk, T. D. (2015). Monitoring of lactic fermentation driven by different starter cultures via direct injection mass spectrometric analysis of flavour-related volatile compounds. *Food Research International*.

Berchtold, C., Bosilkovska, M., Daali, Y., Walder, B., & Zenobi, R. (2014). Real-time monitoring of exhaled drugs by mass spectrometry. *Mass Spectrometry Reviews, 33*(5), 394-413.

Bergamaschi, M., Aprea, E., Betta, E., Biasioli, F., Cipolat-Gotet, C., Cecchinato, A., . . . Gasperi, F. (2015). Effects of dairy system, herd within dairy system, and individual cow characteristics on the volatile organic compound profile of ripened model cheeses. *Journal of Dairy Science, 98*(4), 2183-2196.

Berger, R. G. (2007). *Flavours and fragrances: chemistry, bioprocessing and sustainability*: Springer Science & Business Media.

Biasioli, F., Gasperi, F., Yeretzian, C., & Märk, T. D. (2011). PTR-MS monitoring of VOCs and BVOCs in food science and technology. *TrAC Trends in Analytical Chemistry, 30*(7), 968-977. doi: 10.1016/j.trac.2011.03.009

Biasioli, F., Yeretzian, C., Märk, T. D., Dewulf, J., & Van Langenhove, H. (2011). Direct-injection mass spectrometry adds the time dimension to (B) VOC analysis. *TrAC Trends in Analytical Chemistry, 30*(7), 1003-1017.

Bisson, L. F. (2012). Geographic origin and diversity of wine strains of saccharomyces. *American Journal of Enology and Viticulture, 63*(2), 165-176.

Blake, R. S., Monks, P. S., & Ellis, A. M. (2009). Proton-transfer reaction mass spectrometry. *Chemical reviews, 109*(3), 861-896.

Bohme, D. K., Dunkin, D., Fehsenfeld, F., & Ferguson, E. (1969). Flowing Afterglow Studies of Ion–Molecule Association Reactions. *The Journal of Chemical Physics, 51*(3), 863-872.

Booth, H., & Campbell, M. (1929). Studies of Anesthetic Ethylene: I. The Odor of Ethylene. *Anesthesia & Analgesia, 8*(4), 221-226.

Boscaini, E., Van Ruth, S., Biasioli, F., Gasperi, F., & Märk, T. D. (2003). Gas chromatography-olfactometry (GC-O) and proton transfer reaction-mass spectrometry (PTR-MS) analysis of the flavor profile of Grana Padano, Parmigiano Reggiano, and Grana Trentino cheeses. *Journal of Agricultural and Food Chemistry*, *51*(7), 1782-1790.

Botre, B., Gharpure, D., Shaligram, A., & Sadistap, S. (2009). *Semiconductor sensor array based electronic nose for milk, rancid milk and yoghurt odors identification.* Paper presented at the OLFACTION AND ELECTRONIC NOSE: Proceedings of the 13th International Symposium on Olfaction and Electronic Nose.

Bovolenta, S., Saccà, E., Corazzin, M., Gasperi, F., Biasioli, F., & Ventura, W. (2008). Effects of stocking density and supplement level on milk production and cheese characteristics in Brown cows grazing on mountain pasture. *Journal of dairy research, 75*(03), 357-364.

Budding Yeast. (2015/11/25/01:09:09). from http://users.rcn.com/jkimball.ma.ultranet/BiologyPages/Y/Yeast.html

Buhr, K., van Ruth, S., & Delahunty, C. (2002). Analysis of volatile flavour compounds by Proton Transfer Reaction-Mass Spectrometry: fragmentation patterns and discrimination between isobaric and isomeric compounds. *International Journal of Mass Spectrometry, 221*(1), 1-7. doi: 10.1016/S1387-3806(02)00896-5

C Borresen, E., J Henderson, A., Kumar, A., L Weir, T., & P Ryan, E. (2012). Fermented foods: patented approaches and formulations for nutritional supplementation and health promotion. *Recent patents on food, nutrition & agriculture, 4*(2), 134-140.

Campbell-Platt, G. (1987). *Fermented foods of the world. A dictionary and guide*: Butterworths.

Campbell-Platt, G. (1994). Fermented foods—a world perspective. *Food Research International, 27*(3), 253-257.

Caplice, E., & Fitzgerald, G. F. (1999). Food fermentations: role of microorganisms in food production and preservation. *International Journal of Food Microbiology, 50*(1), 131-149.

Capozzi, V., Makhoul, S., Cappellin, L., Romano, A., Spano, G., Aprea, E., . . . Biasioli, F. (2015). *PTR-ToF-MS and bioprocesses: Potential in monitoring VOCs release by eukaryotic microbes.* Paper presented at the YEAST.

Capozzi, V., Makhoul, S., Romano, A., Spano, G., Aprea, E., Cappellin, L., . . . Biasioli, F. (2015). *PTR-ToF-MS and food bioprocesses: potential in monitoring VOCs release by starter cultures during food fermentation.* Paper presented at the International Conference on Food and Biosystems Engineering, Mykonos, Greece.

Capozzi, V., Menga, V., Digesù, A. M., De Vita, P., van Sinderen, D., Cattivelli, L., . . . Spano, G. (2011). Biotechnological Production of Vitamin B2-Enriched Bread and Pasta. *Journal of Agricultural and Food Chemistry, 59*(14), 8013-8020. doi: 10.1021/jf201519h

Capozzi, V., Russo, P., Dueñas, M. T., López, P., & Spano, G. (2012). Lactic acid bacteria producing B-group vitamins: a great potential for functional cereals products. *Applied Microbiology and Biotechnology, 96*(6), 1383-1394.

Capozzi, V., Russo, P., Ladero, V., Fernández, M., Fiocco, D., Alvarez, M. A., . . . Spano, G. (2012). Biogenic amines degradation by Lactobacillus plantarum: toward a potential application in wine. *Frontiers in Microbiology, 3*.

Capozzi, V., Russo, P., & Spano, G. (2012). Microbial information regimen in EU Geographical Indications. *World Patent Information, 34*(3), 229-231.

Capozzi, V., & Spano, G. (2011). Food Microbial Biodiversity and "Microbes of Protected Origin". *Frontiers in Microbiology, 2*. doi: 10.3389/fmicb.2011.00237

Capozzi, V., Spano, G., & Fiocco, D. (2012). Transdisciplinarity and microbiology education. *Journal of Microbiology & Biology Education: JMBE, 13*(1), 70.

Cappellin, L., Biasioli, F., Fabris, A., Schuhfried, E., Soukoulis, C., Märk, T. D., & Gasperi, F. (2010). Improved mass accuracy in PTR-TOF-MS: Another step towards better compound identification in PTR-MS. *International Journal of Mass Spectrometry, 290*(1), 60-63. doi: 10.1016/j.ijms.2009.11.007

Cappellin, L., Biasioli, F., Granitto, P. M., Schuhfried, E., Soukoulis, C., Costa, F., . . . Gasperi, F. (2011). On data analysis in PTR-TOF-MS: From raw spectra to data mining. *Sensors and Actuators B: Chemical, 155*(1), 183-190. doi: 10.1016/j.snb.2010.11.044

Cappellin, L., Karl, T., Probst, M., Ismailova, O., Winkler, P. M., Soukoulis, C., . . . Biasioli, F. (2012). On Quantitative Determination of Volatile Organic Compound Concentrations Using Proton Transfer Reaction Time-of-Flight Mass Spectrometry. *Environmental Science & Technology, 46*(4), 2283-2290. doi: 10.1021/es203985t

Cappellin, L., Loreto, F., Aprea, E., Romano, A., del Pulgar, J. S., Gasperi, F., & Biasioli, F. (2013). PTR-MS in Italy: a multipurpose sensor with applications in environmental, agri-food and health science. *Sensors, 13*(9), 11923-11955.

Cappellin, L., Makhoul, S., Schuhfried, E., Romano, A., del Pulgar, J. S., Aprea, E., . . . Biasioli, F. (2014). Ethylene: Absolute real-time high-sensitivity detection with PTR/SRI-MS. The example of fruits, leaves and bacteria. *International Journal of Mass Spectrometry, 365*, 33-41.

Cappellin, L., Soukoulis, C., Aprea, E., Granitto, P., Dallabetta, N., Costa, F., . . . Biasioli, F. (2012). PTR-ToF-MS and data mining methods: a new tool for fruit metabolomics. *Metabolomics, 8*(5), 761-770.

Castada, H. Z., Wick, C., Taylor, K., & Harper, W. J. (2014). Analysis of Selected Volatile Organic Compounds in Split and Nonsplit Swiss Cheese Samples Using Selected-Ion Flow Tube Mass Spectrometry (SIFT-MS). *Journal of Food Science, 79*(4), C489-C498.

Chialva, F., Gabri, G., Liddle, P., & Ulian, F. (1982). Qualitative evaluation of aromatic herbs by direct head space (GC) 2 analysis. Applications of the method and comparison with the traditional analysis of essential oils *Aromatic Plants* (pp. 183-195): Springer.

Cho, I., & Peterson, D. (2010). Chemistry of bread aroma: A review. *Food Science and Biotechnology, 19*(3), 575-582. doi: 10.1007/s10068-010-0081-3

Das, A., Raychaudhuri, U., & Chakraborty, R. (2012). Cereal based functional food of Indian subcontinent: a review. *Journal of food science and technology, 49*(6), 665-672.

Dickschat, J. S., Martens, T., Brinkhoff, T., Simon, M., & Schulz, S. (2005). Volatiles released by a Streptomyces species isolated from the North Sea. *Chemistry & biodiversity, 2*(7), 837-865.

Douglas, G. L., & Klaenhammer, T. R. (2010). Genomic evolution of domesticated microorganisms. *Annual review of food science and technology, 1*, 397-414. doi: 10.1146/annurev.food.102308.124134

Edtbauer, A., Hartungen, E., Jordan, A., Hanel, G., Herbig, J., Jürschik, S., . . . Sulzer, P. (2014). Theory and practical examples of the quantification of CH 4, CO, O 2, and CO 2 with an advanced proton-transfer-reaction/selective-reagent-ionization instrument (PTR/SRI-MS). *International Journal of Mass Spectrometry, 365*, 10-14.

Ellis, A. M., & Mayhew, C. A. (2013). *Proton transfer reaction mass spectrometry: principles and applications*: John Wiley & Sons.

Fabris, A., Biasioli, F., Granitto, P. M., Aprea, E., Cappellin, L., Schuhfried, E., . . . Endrizzi, I. (2010). PTR-TOF-MS and data-mining methods for rapid characterisation of agro-industrial samples: influence of milk storage conditions on the volatile compounds profile of Trentingrana cheese. *Journal of Mass Spectrometry, 45*(9), 1065-1074.

Ferguson, E. E. (1992). A personal history of the early development of the flowing afterglow technique for ion-molecule reaction studies. *Journal of the American Society for Mass Spectrometry, 3*(5), 479-486.

Franz, C. M., Huch, M., Mathara, J. M., Abriouel, H., Benomar, N., Reid, G., . . . Holzapfel, W. H. (2014). African fermented foods and probiotics. *International Journal of Food Microbiology, 190*, 84-96.

Frédéric Leroy, L. D. V. (2004). Lactic acid bacteria as functional starter cultures for the food fermentation industry. *Trends in Food Science & Technology*(2), 67-78. doi: 10.1016/j.tifs.2003.09.004

Gallardo-Escamilla, F., Kelly, A., & Delahunty, C. (2007). Mouthfeel and flavour of fermented whey with added hydrocolloids. *International Dairy Journal, 17*(4), 308-315.

Gallardo-Escamilla, F. J., Kelly, A. L., & Delahunty, C. M. (2005). Influence of Starter Culture on Flavor and Headspace Volatile Profiles of Fermented Whey and Whey Produced from Fermented Milk. *Journal of Dairy Science, 88*(11), 3745-3753. doi: 10.3168/jds.S0022-0302(05)73060-5

Galle, S. A., Koot, A., Soukoulis, C., Cappellin, L., Biasioli, F., Alewijn, M., & van Ruth, S. M. (2011). Typicality and geographical origin markers of protected origin cheese from the Netherlands revealed by PTR-MS. *Journal of Agricultural and Food Chemistry, 59*(6), 2554-2563.

Gänzle, M. G. (2014). Enzymatic and bacterial conversions during sourdough fermentation. *Food Microbiology, 37*(0), 2-10. doi: http://dx.doi.org/10.1016/j.fm.2013.04.007

Gänzle, M. G., Vermeulen, N., & Vogel, R. F. (2007). Carbohydrate, peptide and lipid metabolism of lactic acid bacteria in sourdough. *Food Microbiology, 24*(2), 128-138. doi: 10.1016/j.fm.2006.07.006

Gassenmeier, K., & Schieberle, P. (1995). Potent aromatic compounds in the crumb of wheat bread (French-type) — influence of pre-ferments and studies on the formation of key odorants during dough processing. *Zeitschrift für Lebensmittel-Untersuchung und Forschung, 201*(3), 241-248. doi: 10.1007/BF01192996

Gobbetti, M. (1998). The sourdough microflora: Interactions of lactic acid bacteria and yeasts. *Trends in Food Science & Technology, 9*(7), 267-274. doi: http://dx.doi.org/10.1016/S0924-2244(98)00053-3

Gobbetti, M., Corsetti, A., La Rosa, F., & De Vincenzi, S. (1994). Identification and clustering of lactic acid bacteria and yeasts from wheat sourdoughs of central Italy. *Italian J Food Sci, 1*, 85-94.

Gobbetti, M., De Angelis, M., Corsetti, A., & Di Cagno, R. (2005). Biochemistry and physiology of sourdough lactic acid bacteria. *Trends in Food Science & Technology, 16*(1–3), 57-69. doi: http://dx.doi.org/10.1016/j.tifs.2004.02.013

Gobbetti, M., De Angelis, M., Di Cagno, R., Minervini, F., & Limitone, A. (2007). Cell-cell communication in food related bacteria. *International Journal of Food Microbiology, 120*(1-2), 34-45. doi: 10.1016/j.ijfoodmicro.2007.06.012

Gobbetti, M., Rizzello, C. G., Di Cagno, R., & De Angelis, M. (2014). How the sourdough may affect the functional features of leavened baked goods. *Food Microbiology, 37*(0), 30-40. doi: http://dx.doi.org/10.1016/j.fm.2013.04.012

Grimm, C., Lloyd, S. W., Miller, J., & Spanier, A. (1997). *The analysis of food volatiles using direct thermal desorption*: Dekker: New York.

Gross, J. H. (2011). *Mass Spectrometry*: Springer.

Guerzoni, M. E., Vernocchi, P., Ndagijimana, M., Gianotti, A., & Lanciotti, R. (2007). Generation of aroma compounds in sourdough: Effects of stress exposure and lactobacilli–yeasts interactions. *Food Microbiology, 24*(2), 139-148. doi: http://dx.doi.org/10.1016/j.fm.2006.07.007

Guilhaus, M. (1995). Principles and instrumentation in time-of-flight mass spectrometry. *J. Mass Spectrom, 30*(11), 1519-1532.

Hamamatsu. MCP guide. In H. PHOTONICS (Ed.). Japan.

Hansel, A., Jordan, A., Holzinger, R., Prazeller, P., Vogel, W., & Lindinger, W. (1995). Proton transfer reaction mass spectrometry: on-line trace gas analysis at the ppb level. *International Journal of Mass Spectrometry and Ion Processes, 149–150,* 609-619. doi: 10.1016/0168-1176(95)04294-U

Harrison, A. G. (1992). *Chemical ionization mass spectrometry*: CRC press.

Heddergott, C., Calvo, A., & Latgé, J. (2014). The volatome of Aspergillus fumigatus. *Eukaryotic cell, 13*(8), 1014-1025.

House, E. (2009). Refinement of ptr-ms methodology and application to the measurement of (o) vocs from cattle slurry.

Hu, J.-B., Gunathilake, S., Chen, Y.-C., & Urban, P. L. (2014). On the dynamics of kefir volatome. *RSC Advances, 4*(55), 28865-28870. doi: 10.1039/C4RA02990A

Hui, Y. H. (2008). *Bakery Products: Science and Technology*: John Wiley & Sons.

Hutkins, R. W. (2008). *Microbiology and technology of fermented foods* (Vol. 22): John Wiley & Sons.

Inomata, S., Tanimoto, H., Aoki, N., Hirokawa, J., & Sadanaga, Y. (2006). A novel discharge source of hydronium ions for proton transfer reaction ionization: design, characterization, and performance. *Rapid Communications in Mass Spectrometry, 20*(6), 1025-1029.

Ionicon website. Retrieved 23/11/2015, from http://www.ionicon.com/product/accessories/fastgc

ISO 16000-6:2011 - Indoor air -- Part 6: Determination of volatile organic compounds in indoor and test chamber air by active sampling on Tenax TA sorbent, thermal desorption and gas chromatography using MS or MS-FID. (2015/11/11/15:43:05). from http://www.iso.org/iso/catalogue_detail.htm?csnumber=52213

Ivey, M., Massel, M., & Phister, T. G. (2013). Microbial interactions in food fermentations. *Annual review of food science and technology, 4*, 141-162. doi: 10.1146/annurev-food-022811-101219

Jordan, A., Haidacher, S., Hanel, G., Hartungen, E., Herbig, J., Märk, L., . . . Märk, T. D. (2009). An online ultra-high sensitivity Proton-transfer-reaction mass-spectrometer combined with switchable reagent ion capability (PTR + SRI − MS). *International Journal of Mass Spectrometry, 286*(1), 32-38. doi: 10.1016/j.ijms.2009.06.006

Jordan, A., Haidacher, S., Hanel, G., Hartungen, E., Märk, L., Seehauser, H., . . . Märk, T. D. (2009). A high resolution and high sensitivity proton-transfer-reaction time-of-flight mass spectrometer (PTR-TOF-MS). *International Journal of Mass Spectrometry, 286*(2–3), 122-128. doi: 10.1016/j.ijms.2009.07.005

Kabak, B., & Dobson, A. D. (2011). An introduction to the traditional fermented foods and beverages of Turkey. *Critical reviews in food science and nutrition, 51*(3), 248-260.

Kaban, G. (2013). Sucuk and pastırma: Microbiological changes and formation of volatile compounds. *Meat science, 95*(4), 912-918.

Kai, M., Effmert, U., Berg, G., & Piechulla, B. (2007). Volatiles of bacterial antagonists inhibit mycelial growth of the plant pathogen Rhizoctonia solani. *Archives of Microbiology, 187*(5), 351-360.

Karasek, F. W., & Clement, R. E. (2012). *Basic gas chromatography-mass spectrometry: principles and techniques*: Elsevier.

Karl, M., Guenther, A., Köble, R., Leip, A., & Seufert, G. (2009). A new European plant-specific emission inventory of biogenic volatile organic compounds for use in atmospheric transport models. *Biogeosciences, 6*(6), 1059-1087.

Karl, T., Hansel, A., Cappellin, L., Kaser, L., Herdlinger-Blatt, I., & Jud, W. (2012). Selective measurements of isoprene and 2-methyl-3-buten-2-ol based on NO^{+$} ionization mass spectrometry. *Atmospheric Chemistry and Physics, 12*(24), 11877-11884. doi: 10.5194/acp-12-11877-2012

Kawai, Y., Yamaguchi, S., Okada, Y., & TAKEUCHI, K. (2004). Reactions of Protonated Water Clusters H+ (H2O) n (n= 2 and 4) with D20, Acetonitrile, Acetone, DMS, DMSO, and Pyridine. *Journal of the Mass Spectrometry Society of Japan, 52*(5), 271-276.

Klee, H. J. (2010). Improving the flavor of fresh fruits: genomics, biochemistry, and biotechnology. *New Phytologist, 187*(1), 44-56.

Kulp, K., & Lorenz, K. (2003). *Handbook of dough fermentations* (Vol. 127): CRC Press.

Lagg, A., Taucher, J., Hansel, A., & Lindinger, W. (1994). Applications of proton transfer reactions to gas analysis. *International Journal of Mass Spectrometry and Ion Processes, 134*(1), 55-66.

Langford, V. S., Reed, C. J., Milligan, D. B., McEwan, M. J., Barringer, S. A., & Harper, W. J. (2012). Headspace analysis of Italian and New Zealand parmesan cheeses. *Journal of Food Science, 77*(6), C719-C726.

Lanza, M., Acton, W. J., Breiev, K., Jürschik, S., Gutmann, R., Jordan, A., . . . Märk, L. (2015). *SELECTIVE-REAGENT-IONIZATION MASS SPECTROMETRY (SRI-MS): ADVANCEMENTS IN INSTRUMENTATION AND NOVEL APPLICATIONS.* Paper presented at the 20 th Symposium on Application of Plasma Processes.

Leroy, F., & De Vuyst, L. (2004). Lactic acid bacteria as functional starter cultures for the food fermentation industry. *Trends in Food Science & Technology, 15*(2), 67-78.

Lincoln, R. J., Boxshall, G. A., & Clark, P. F. (1998). *A dictionary of ecology, evolution and systematics*: Cambridge University Press Cambridge.

Lindinger, W., Fall, R., & Karl, T. (2001). *Environmental, food and medical applications of proton-transfer-reaction mass spectrometry (PTR-MS)* (Vol. 4): Elsevier: Amsterdam, The Netherlands.

Lindinger, W., Hansel, A., & Jordan, A. (1998). On-line monitoring of volatile organic compounds at pptv levels by means of proton-transfer-reaction mass spectrometry (PTR-MS) medical applications, food control and environmental research. *International Journal of Mass Spectrometry and Ion Processes, 173*(3), 191-241. doi: 10.1016/S0168-1176(97)00281-4

López-Feria, S., Cárdenas, S., & Valcárcel, M. (2008). Simplifying chromatographic analysis of the volatile fraction of foods. *TrAC Trends in Analytical Chemistry, 27*(9), 794-803.

Makhoul, S., Romano, A., Capozzi, V., Spano, G., Aprea, E., Cappellin, L., . . . Gasperi, F. (2015). Volatile Compound Production During the Bread-Making Process: Effect of Flour, Yeast and Their Interaction. *Food and Bioprocess Technology, 8*(9), 1925-1937.

Makhoul, S., Romano, A., Cappellin, L., Spano, G., Capozzi, V., Benozzi, E., . . . Biasioli, F. (2014). Proton-transfer-reaction mass spectrometry for the study of the production of

volatile compounds by bakery yeast starters. *Journal of Mass Spectrometry, 49*(9), 850-859. doi: 10.1002/jms.3421

Makhoul, S., Romano, A., Cappellin, L., Spano, G., Capozzi, V., Benozzi, E., . . . El-Nakat, H. (2014). Proton-transfer-reaction mass spectrometry for the study of the production of volatile compounds by bakery yeast starters. *Journal of Mass Spectrometry, 49*(9), 850-859.

Marsili, R. (1999a). Comparison of Solid-Phase Microextraction and Dynamic Headspace Methods for the Gas Chromatographic—Mass Spectrometric Analysis of Light-Induced Lipid Oxidation Products in Milk. *Journal of chromatographic science, 37*(1), 17-23.

Marsili, R. (1999b). SPME-MS-MVA as an electronic nose for the study of off-flavors in milk. *Journal of Agricultural and Food Chemistry, 47*(2), 648-654.

Martins, S. I. F. S., Jongen, W. M. F., & van Boekel, M. A. J. S. (2000). A review of Maillard reaction in food and implications to kinetic modelling. *Trends in Food Science & Technology, 11*(9–10), 364-373. doi: 10.1016/S0924-2244(01)00022-X

Matlab, M. (1999). Natick, MA: Mathworks.

Mei, J. B., Reineccius, G. A., Knighton, W. B., & Grimsrud, E. P. (2004). Influence of strawberry yogurt composition on aroma release. *Journal of Agricultural and Food Chemistry, 52*(20), 6267-6270.

Murooka, Y., & Yamshita, M. (2008). Traditional healthful fermented products of Japan. *Journal of industrial microbiology & biotechnology, 35*(8), 791-798.

Nickerson, G. B., & Likens, S. (1966). Gas chromatography evidence for the occurrence of hop oil components in beer. *Journal of Chromatography A, 21*, 1-5.

Nout, M. R. (2009). Rich nutrition from the poorest–Cereal fermentations in Africa and Asia. *Food Microbiology, 26*(7), 685-692.

Olivares, A., Dryahina, K., Navarro, J. L., Smith, D., Španěl, P., & Flores, M. (2011). SPME-GC-MS versus selected ion flow tube mass spectrometry (SIFT-MS) analyses for the study of volatile compound generation and oxidation status during dry fermented sausage processing. *Journal of Agricultural and Food Chemistry, 59*(5), 1931-1938.

Onishi, M., Inoue, M., Araki, T., Iwabuchi, H., & Sagara, Y. (2012). A PTR-MS-Based Protocol for Simulating Bread Aroma During Mastication. *Food and Bioprocess Technology, 5*(4), 1228-1237. doi: 10.1007/s11947-010-0422-5

Pagans, E., Font, X., & Sánchez, A. (2006). Emission of volatile organic compounds from composting of different solid wastes: abatement by biofiltration. *Journal of hazardous materials, 131*(1), 179-186.

Paraskevopoulou, A., Chrysanthou, A., & Koutidou, M. (2012). Characterisation of volatile compounds of lupin protein isolate-enriched wheat flour bread. *Food Research International, 48*(2), 568-577. doi: 10.1016/j.foodres.2012.05.028

Patel, B. K., Waniska, R. D., & Seetharaman, K. (2005). Impact of different baking processes on bread firmness and starch properties in breadcrumb. *Journal of Cereal Science, 42*(2), 173-184. doi: 10.1016/j.jcs.2005.04.007

Pecsok, R. L. (1959). Principles and practice of gas chromatography. *Principles and practice of gas chromatography*.

Pérès, C., Begnaud, F., & Berdagué, J.-L. (2002). Fast characterization of Camembert cheeses by static headspace–mass spectrometry. *Sensors and Actuators B: Chemical, 87*(3), 491-497.

Pfeifer, M., Kugler, K. G., Sandve, S. R., Zhan, B., Rudi, H., Hvidsten, T. R., . . . Olsen, O.-A. (2014). Genome interplay in the grain transcriptome of hexaploid bread wheat. *Science, 345*(6194). doi: 10.1126/science.1250091

Pico, J., Bernal, J., & Gómez, M. (2015). Wheat bread aroma compounds in crumb and crust: A review. *Food Research International, 75*(0), 200-215. doi: http://dx.doi.org/10.1016/j.foodres.2015.05.051

Poinot, P., Arvisenet, G. l., Grua-Priol, J. l., Colas, D. e., Fillonneau, C., Le Bail, A., & Prost, C. (2008). Influence of formulation and process on the aromatic profile and physical characteristics of bread. *Journal of Cereal Science, 48*(3), 686-697.

Reale, A., Di Renzo, T., Succi, M., Tremonte, P., Coppola, R., & Sorrentino, E. (2013). Microbiological and Fermentative Properties of Baker's Yeast Starter Used in Breadmaking. *Journal of Food Science, 78*(8), M1224-M1231. doi: 10.1111/1750-3841.12206

Romano, A., Capozzi, V., Spano, G., & Biasioli, F. (2015a). Proton transfer reaction-mass spectrometry: online and rapid determination of volatile organic compounds of microbial origin. *Applied Microbiology and Biotechnology, 99*(9), 3787-3795. doi: 10.1007/s00253-015-6528-y

Romano, A., Capozzi, V., Spano, G., & Biasioli, F. (2015b). Proton transfer reaction–mass spectrometry: online and rapid determination of volatile organic compounds of microbial origin. *Applied Microbiology and Biotechnology, 99*(9), 3787-3795.

Romano, A., Fischer, L., Herbig, J., Campbell-Sills, H., Coulon, J., Lucas, P., . . . Biasioli, F. (2014). Wine analysis by FastGC proton-transfer reaction-time-of-flight-mass spectrometry. *International Journal of Mass Spectrometry, 369*, 81-86.

Ross, C. F. (2009). Sensory science at the human–machine interface. *Trends in Food Science & Technology, 20*(2), 63-72.

Ross, R. P., Morgan, S., & Hill, C. (2002). Preservation and fermentation: past, present and future. *International Journal of Food Microbiology, 79*(1), 3-16.

Rudduck, J., Harris, S., & Wallace, G. (1994). 'Coherence'and students' experience of learning in the secondary school. *Cambridge Journal of Education, 24*(2), 197-211.

Russo, P., Capozzi, V., Arena, M. P., Spadaccino, G., Dueñas, M. T., López, P., . . . Spano, G. (2014). Riboflavin-overproducing strains of Lactobacillus fermentum for riboflavin-enriched bread. *Applied Microbiology and Biotechnology, 98*(8), 3691-3700.

Saint-Eve, A., Martin, N., Guillemin, H., Sémon, E., Guichard, E., & Souchon, I. (2006). Flavored yogurt complex viscosity influences real-time aroma release in the mouth and sensory properties. *Journal of Agricultural and Food Chemistry, 54*(20), 7794-7803.

Salim ur, R., Paterson, A., & Piggott, J. R. (2006). Flavour in sourdough breads: a review. *Trends in Food Science & Technology, 17*(10), 557-566. doi: 10.1016/j.tifs.2006.03.006

Satish Kumar, R., Kanmani, P., Yuvaraj, N., Paari, K., Pattukumar, V., & Arul, V. (2013). Traditional Indian fermented foods: a rich source of lactic acid bacteria. *International Journal of Food Sciences and Nutrition, 64*(4), 415-428.

Schulz, S., & Dickschat, J. S. (2007). Bacterial volatiles: the smell of small organisms. *Natural product reports, 24*(4), 814-842.

SHIMADZU CORPORATION. (2015/11/21/07:50:49). from http://www.shimadzu.com/

Sicard, D., & Legras, J.-L. (2011). Bread, beer and wine: yeast domestication in the Saccharomyces sensu stricto complex. *Comptes rendus biologies, 334*(3), 229-236.

Smith, D., & Adams, N. (1987). The selected ion flow tube (SIFT): studies of ion-neutral reactions. *Adv. Atom. Mol. Phys, 24*, 1-49.

Sõukand, R., Pieroni, A., Biró, M., Dénes, A., Doğan, Y., Hajdari, A., . . . Nedelcheva, A. (2015). An ethnobotanical perspective on traditional fermented plant foods and beverages in Eastern Europe. *Journal of ethnopharmacology*.

Soukoulis, C., Aprea, E., Biasioli, F., Cappellin, L., Schuhfried, E., Märk, T. D., & Gasperi, F. (2010). Proton transfer reaction time-of-flight mass spectrometry monitoring of the

evolution of volatile compounds during lactic acid fermentation of milk. *Rapid Communications in Mass Spectrometry, 24*(14), 2127-2134. doi: 10.1002/rcm.4617

Spanel, P., & Smith, D. (1997). SIFT studies of the reactions of H 3 O+, NO+ and O 2+ with a series of alcohols. *International Journal of Mass Spectrometry and Ion Processes, 167*, 375-388.

Španěl, P., & Smith, D. (1998). Selected ion flow tube studies of the reactions of H 3 O+, NO+, and O 2+ with several aromatic and aliphatic hydrocarbons. *International Journal of Mass Spectrometry, 181*(1), 1-10.

Steinkraus, K. H. (2002). Fermentations in world food processing. *Comprehensive Reviews in food science and food safety, 1*(1), 23-32.

Sulzer, P., Edtbauer, A., Hartungen, E., Jürschik, S., Jordan, A., Hanel, G., . . . Märk, T. D. (2012). From conventional proton-transfer-reaction mass spectrometry (PTR-MS) to universal trace gas analysis. *International Journal of Mass Spectrometry, 321*, 66-70.

Sun, Z., Harris, H. M., McCann, A., Guo, C., Argimón, S., Zhang, W., . . . Kagawa, T. F. (2015). Expanding the biotechnology potential of lactobacilli through comparative genomics of 213 strains and associated genera. *Nature communications, 6*.

Survey, U. S. G. WATER RESOURCES DATA—STATE, 2005.

Suzzi, G. (2011). From wild strain to domesticated strain: the philosophy of microbial diversity in foods. *Frontiers in Microbiology, 2*.

Swain, M. R., Anandharaj, M., Ray, R. C., & Parveen Rani, R. (2014). Fermented fruits and vegetables of Asia: a potential source of probiotics. *Biotechnology research international, 2014*.

Taylor, A. (2010). Linforth (Editörler). Food Flavor Technology: Wiley-Blackwell Publishing, Chichester, W. Sussex, UK.

Taylor, A., Linforth, R., Harvey, B., & Blake, A. (2000). Atmospheric pressure chemical ionisation mass spectrometry for in vivo analysis of volatile flavour release. *Food Chemistry, 71*(3), 327-338.

Taylor, K., Wick, C., Castada, H., Kent, K., & Harper, W. J. (2013). Discrimination of Swiss cheese from 5 different factories by high impact volatile organic compound profiles determined by odor activity value using selected ion flow tube mass spectrometry and odor threshold. *Journal of Food Science, 78*(10), C1509-C1515.

Team, R. C. (2014). R: A language and environment for statistical computing. R Foundation for Statistical Computing, Vienna, Austria, 2012: ISBN 3-900051-07-0.

Tsevdou, M., Soukoulis, C., Cappellin, L., Gasperi, F., Taoukis, P. S., & Biasioli, F. (2013). Monitoring the effect of high pressure and transglutaminase treatment of milk on the evolution of flavour compounds during lactic acid fermentation using PTR-ToF-MS. *Food Chemistry, 138*(4), 2159-2167.

Vacuum Technology & Vacuum Pumps from the leading manufacturer Pfeiffer Vacuum. (2015/11/28/14:05:07). from https://www.pfeiffer-vacuum.com/en/

Van Kerrebroeck, S., Vercammen, J., Wuyts, R., & De Vuyst, L. (2015). Selected Ion Flow Tube–Mass Spectrometry for Online Monitoring of Submerged Fermentations: A Case Study of Sourdough Fermentation. *Journal of Agricultural and Food Chemistry, 63*(3), 829-835.

Vera, L., Mestres, M., Boqué, R., Busto, O., & Guasch, J. (2010). Use of synthetic wine for models transfer in wine analysis by HS-MS e-nose. *Sensors and Actuators B: Chemical, 143*(2), 689-695.

Watson, T. H. (2009). *THE FLOWING AFTERGLOW AS A CHEMICAL REACTIONMASS SPECTROMETER: ACCURACY DETERMINATIONS AND REAGENT IONDEVELOPMENT*. University of Pittsburgh.

Werkhoff, P., & Bretschneider, W. (1987). Dynamic headspace gas chromatography: concentration of volatile components after thermal desorption by intermediate cryofocusing in a cold trap: I. Principle and applications. *Journal of Chromatography A, 405*, 87-98.

Weurman, C. (1969). Isolation and concentration of volatiles in food odor research. *Journal of Agricultural and Food Chemistry, 17*(2), 370-384.

Wisthaler, A., Apel, E., Bossmeyer, J., Hansel, A., Junkermann, W., Koppmann, R., . . . Steinbrecher, R. (2008). Technical Note: Intercomparison of formaldehyde measurements at the atmosphere simulation chamber SAPHIR. *Atmospheric Chemistry and Physics, 8*(8), 2189-2200.

Wiza, J. L. (1979). Microchannel plate detectors. *Nuclear Instruments and Methods, 162*(1), 587-601.

Wolfe, B. E., & Dutton, R. J. (2015). Fermented Foods as Experimentally Tractable Microbial Ecosystems. *Cell, 161*(1), 49-55.

Yang, Y., Xu, R.-m., Song, J., & Wang, W.-m. (2010). High Throughput Biotechnology in Traditional Fermented Food Industry. *Recent patents on food, nutrition & agriculture, 2*(3), 251-257.

Yener, S., Romano, A., Cappellin, L., Märk, T. D., Sánchez del Pulgar, J., Gasperi, F., . . . Biasioli, F. (2014). PTR-ToF-MS characterisation of roasted coffees (C. arabica) from different geographic origins. *Journal of Mass Spectrometry, 49*(9), 929-935.

Zogorski, J. S., Carter, J. M., Ivahnenko, T., Lapham, W. W., Moran, M. J., Rowe, B. L., . . . Toccalino, P. L. (2006). Volatile organic compounds in the nation's ground water and drinking-water supply wells. *US Geological Survey Circular, 1292*, 101.

Zohora, S. E., Khan, A., Srivastava, A., & Hundewale, N. (2013). Electronic Noses Application to Food Analysis Using Metal Oxide Sensors: A Review. *International Journal of Soft Computing and Engineering (IJSCE), 3*.

Zoller, H. F., & Clark, W. M. (1921). The production of volatile fatty acids by bacteria of the dysentery group. *The Journal of general physiology, 3*(3), 325.

Appendices

Appendix 1. List of VOCs studied by PTR-MS along with their formula, proton affinity, mass and protonated mass.

No.	Name	Formel	PA (kcal/mol)	Masse	prot mass
				0,0000	
1	Hydrogen	(H2)	100,9	2,0157	3,0235
2	Helium	(He)	42,5	4,0026	5,0104
3	Lithium hydride	(HLi)	244,2	8,0238	9,0317
4	Nitrogen atom	(N)	81,8	14,0031	15,0109
5	Oxygen, atomic	(O)	116,0	15,9949	17,0027
6	NH2	(H2N)	184,8	16,0187	17,0265
7	Methane	(CH4)	129,9	16,0313	17,0391
8	Ammonia	(H3N)	204,1	17,0265	18,0344
9	Water	(H2O)	165,2	18,0106	19,0184
10	Fluorine atom	(F)	81,3	18,9984	20,0062
11	Neon	(Ne)	48,6	19,9924	21,0003
12	Hydrogen fluoride	(HF)	115,7	20,0062	21,0141
13	Magnesium	(Mg)	195,9	23,9850	24,9929
14	LiOH	(HLiO)	241,0	24,0187	25,0266
15	Ethynyl radical	(C2H)	183,3	25,0078	26,0157
16	Acetylene	(C2H2)	153,3	26,0157	27,0235
17	Diborane(6)	(H6B2)	147,0	26,0728	27,0806
18	Hydrogen cyanide	(CHN)	170,4	27,0109	28,0187
19	Hydrogen isocyanide	(CHN)	184,6	27,0109	28,0187
20	Vinyl radical	(C2H3)	180,5	27,0235	28,0313
21	Silicon	(Si)	200,0	27,9769	28,9848
22	Carbon monoxide	(CO)	141,7	27,9949	29,0027
23	Nitrogen	(N2)	118,0	28,0061	29,0140
24	Ethylene	(C2H4)	162,6	28,0313	29,0391
25	Formyl radical	(CHO)	152,0	29,0027	30,0106
26	Methanimine	(CH3N)	203,8	29,0265	30,0344
27	Ethyl radical	(C2H5)	147,2	29,0391	30,0470
28	Silylene	(H2Si)	200,2	29,9926	31,0004
29	Nitric oxide	(NO)	109,0	29,9980	31,0058
30	Formaldehyde	(CH2O)	170,4	30,0106	31,0184
31	HCOH (hydroxymethylene)	(CH2O)	230,9	30,0106	31,0184
32	Diimide	(H2N2)	191,9	30,0218	31,0296
33	CH2NH2	(CH4N)	203,0	30,0344	31,0422
34	Ethane	(C2H6)	142,5	30,0470	31,0548
35	Phosphorus atom	(P)	149,8	30,9738	31,9816
36	Hydroxymethyl radical	(CH3O)	166,1	31,0184	32,0262
37	Methylamine	(CH5N)	214,9	31,0422	32,0500
38	Sulfur atom	(S)	158,8	31,9721	32,9799
39	Phosphinidene	(HP)	160,2	31,9816	32,9894
40	Oxygen	(O2)	100,6	31,9898	32,9977
41	Fluoromethylene	(CHF)	190,4	32,0062	33,0141
42	Silane	(H4Si)	152,9	32,0082	33,0161
43	Methyl alcohol	(CH4O)	180,3	32,0262	33,0340
44	Hydrazine	(H4N2)	203,9	32,0374	33,0453
45	Phosphino radical	(H2P)	169,5	32,9894	33,9972
46	Hydroperoxy radical	(HO2)	157,7	32,9977	34,0055
47	Hydrogen sulfide	(H2S)	168,5	33,9877	34,9955
48	Phosphine	(H3P)	187,6	33,9972	35,0051
49	Hydrogen peroxide	(H2O2)	161,4	34,0055	35,0133
50	Methyl fluoride	(CH3F)	143,0	34,0219	35,0297
51	Chlorine atom	(Cl)	122,8	34,9689	35,9767
52	Oxygen monofluoride	(FO)	121,6	34,9933	36,0011
53	Argon	(Ar)	88,2	35,9675	36,9754
54	Hydrogen chloride	(HCl)	133,1	35,9767	36,9845
55	Carbon trimer	(C3)	183,3	36,0000	37,0078
56	Cyclopropenylidene	(C3H2)	227,4	38,0157	39,0235
57	Cyclopropenyl radical	(C3H3)	175,7	39,0235	40,0313
58	Propargyl radical	(C3H3)	177,1	39,0235	40,0313
59	Magnesium monoxide	(MgO)	236,1	39,9800	40,9878
60	Sodium hydroxide	(HNaO)	248,0	39,9925	41,0003
61	Dicarbon monoxide	(C2O)	185,2	39,9949	41,0027
62	(CD3)2O	(C2D6O)	186,9	39,9949	41,0027
63	Propyne	(C3H4)	178,8	40,0313	41,0391
64	1,2-Propadiene	(C3H4)	185,3	40,0313	41,0391
65	Cyclopropene	(C3H4)	197,3	40,0313	41,0391
66	Acetonitrile	(C2H3N)	186,2	41,0265	42,0344

No.	Name	Formel	PA (kcal/mol)	Masse	prot mass
67	Methane, isocyano-	(C2H3N)	199,0	41,0265	42,0344
68	Cyclopropyl radical	(C3H5)	175,8	41,0391	42,0470
69	Allyl radical	(C3H5)	175,9	41,0391	42,0470
70	Lithium chloride	(ClLi)	197,7	41,9849	42,9927
71	Ketene	(C2H2O)	197,3	42,0106	43,0184
72	Cyanamide	(CH2N2)	192,6	42,0218	43,0296
73	Methane, diazo-	(CH2N2)	205,4	42,0218	43,0296
74	Cyclopropane	(C3H6)	179,3	42,0470	43,0548
75	Propene	(C3H6)	179,6	42,0470	43,0548
76	SiNH	(HNSi)	203,2	42,9878	43,9957
77	Isocyanic acid	(CHNO)	180,0	43,0058	44,0136
78	Fulminic acid	(CHNO)	181,2	43,0058	44,0136
79	Boron oxide hydroxide	(HBO2)	182,4	43,0106	44,0184
80	Hydrogen azide	(HN3)	180,5	43,0170	44,0249
81	Acetyl radical	(C2H3O)	156,1	43,0184	44,0262
82	CH2CHO	(C2H3O)	185,0	43,0184	44,0262
83	N-Methyl methanimine	(C2H5N)	211,5	43,0422	44,0500
84	Acetaldimine	(C2H5N)	211,7	43,0422	44,0500
85	Ethenamine	(C2H5N)	214,9	43,0422	44,0500
86	Ethylenimine	(C2H5N)	216,7	43,0422	44,0500
87	Isopropyl radical	(C3H7)	160,5	43,0548	44,0626
88	Silicon monoxide	(OSi)	185,7	43,9718	44,9797
89	Carbon monosulfide	(CS)	189,2	43,9721	44,9799
90	Methinophosphide	(CHP)	167,1	43,9816	44,9894
91	Carbon dioxide	(CO2)	129,2	43,9898	44,9977
92	Nitrous oxide	(N2O)	137,5	44,0011	45,0089
93	Ethyne, fluoro-	(C2HF)	164,0	44,0062	45,0141
94	Acetaldehyde	(C2H4O)	183,8	44,0262	45,0340
95	Ethylene oxide	(C2H4O)	184,9	44,0262	45,0340
96	Methyl diazene	(CH4N2)	202,0	44,0374	45,0453
97	Propane	(C3H8)	150,5	44,0626	45,0704
98	Phosphorus mononitride	(NP)	188,6	44,9768	45,9847
99	SiOH	(HOSi)	185,3	44,9797	45,9875
100	HSiO	(HOSi)	193,6	44,9797	45,9875
101	Hydrocarboxyl radical	(CHO2)	149,0	44,9977	46,0055
102	Scandium	(Sc)	218,5	45,0000	46,0078
103	Cyanogen fluoride	(CFN)	151,1	45,0015	46,0093
104	Formamide	(CH3NO)	196,5	45,0215	46,0293
105	CH2CH2OH	(C2H5O)	178,1	45,0340	46,0419
106	Ethylamine	(C2H7N)	217,9	45,0578	46,0657
107	Methanamine, N-methyl-	(C2H7N)	222,2	45,0578	46,0657
108	HSiOH	(H2OSi)	200,8	45,9875	46,9953
109	H2SiO	(H2OSi)	201,0	45,9875	46,9953
110	Thioformaldehyde	(CH2S)	181,6	45,9877	46,9955
111	Nitrogen dioxide	(NO2)	141,1	45,9929	47,0007
112	Formic acid	(CH2O2)	177,3	46,0055	47,0133
113	Ethene, fluoro-	(C2H3F)	174,2	46,0219	47,0297
114	Ethanol	(C2H6O)	185,6	46,0419	47,0497
115	Dimethyl ether	(C2H6O)	189,3	46,0419	47,0497
116	Hydrazine, methyl-	(CH6N2)	214,1	46,0531	47,0609
117	Phosphorus monoxide	(OP)	163,0	46,9687	47,9765
118	H3SiO	(H3OSi)	167,3	46,9953	48,0031
119	H2SiOH	(H3OSi)	176,4	46,9953	48,0031
120	Hydroxylamine, o-methyl-	(CH5NO)	202,0	47,0371	48,0449
121	Magnesium dimer	(Mg2)	219,6	47,9701	48,9779
122	Chloromethylene	(CHCl)	208,6	47,9767	48,9845
123	Ozone	(O3)	149,5	47,9847	48,9926
124	Titanium	(Ti)	209,4	48,0000	49,0078
125	H3SiOH	(H4OSi)	178,4	48,0031	49,0110
126	Methanethiol	(CH4S)	184,8	48,0034	49,0112
127	Phosphine, methyl-	(CH5P)	203,6	48,0129	49,0207
128	Ethane, fluoro-	(C2H5F)	163,5	48,0375	49,0454
129	Tetraborane(8)	(H8B4)	187,6	48,1143	49,1222
130	Chromium	(Cr)	189,1	49,9460	50,9539
131	Methyl chloride	(CH3Cl)	154,9	49,9923	51,0002
132	Difluoromethylene	(CF2)	182,8	49,9968	51,0046
133	1,3-Butadiyne	(C4H2)	175,8	50,0157	51,0235

No.	Name	Formel	PA (kcal/mol)	Masse	prot mass
134	Tetraborane(10)	(H10B4)	144,6	50,1300	51,1378
135	Vanadium	(V)	205,4	51,0000	52,0078
136	Propiolonitrile	(C3HN)	179,6	51,0109	52,0187
137	CCCO	(C3O)	210,4	51,9949	53,0027
138	Cyanogen	(C2N2)	162,0	52,0061	53,0140
139	Methane, difluoro-	(CH2F2)	148,2	52,0125	53,0203
140	2-Propenenitrile	(C3H3N)	187,5	53,0265	54,0344
141	Iron	(Fe)	180,2	53,9396	54,9474
142	2-Butyne	(C4H6)	185,6	54,0470	55,0548
143	1,2-Butadiene	(C4H6)	186,3	54,0470	55,0548
144	1,3-Butadiene	(C4H6)	187,1	54,0470	55,0548
145	Cyclobutene	(C4H6)	190,3	54,0470	55,0548
146	1-Methylcyclopropene	(C4H6)	204,9	54,0470	55,0548
147	Manganese	(Mn)	190,6	55,0000	56,0078
148	Propanenitrile	(C3H5N)	189,8	55,0422	56,0500
149	Ethane, isocyano-	(C3H5N)	203,6	55,0422	56,0500
150	1-Azabicyclo[1.1.0]butane	(C3H5N)	211,5	55,0422	56,0500
151	Propargylamine	(C3H5N)	212,2	55,0422	56,0500
152	vinylimine	(C3H5N)	218,1	55,0422	56,0500
153	2-Methylallyl radical	(C4H7)	185,9	55,0548	56,0626
154	C2S	(C2S)	207,8	55,9721	56,9799
155	2-Propenal	(C3H4O)	190,5	56,0262	57,0340
156	Methylketene	(C3H4O)	199,4	56,0262	57,0340
157	NCCH2NH2	(C2H4N2)	197,2	56,0374	57,0453
158	2-Butene, (E)-	(C4H8)	178,5	56,0626	57,0704
159	1-Propene, 2-methyl-	(C4H8)	191,7	56,0626	57,0704
160	Methane, isocyanato-	(C2H3NO)	182,7	57,0215	58,0293
161	Methyl azide	(CH3N3)	199,1	57,0327	58,0405
162	CH2COCH3	(C3H5O)	196,0	57,0340	58,0419
163	Cyclopropylamine	(C3H7N)	216,4	57,0578	58,0657
164	2-Propen-1-amine	(C3H7N)	217,5	57,0578	58,0657
165	Aziridine, 2-methyl-	(C3H7N)	219,2	57,0578	58,0657
166	Aziridine, 1-methyl-	(C3H7N)	222,1	57,0578	58,0657
167	2-Propanimine	(C3H7N)	223,2	57,0578	58,0657
168	1-Methylethenylamine	(C3H7N)	225,1	57,0578	58,0657
169	Azetidine	(C3H7N)	225,8	57,0578	58,0657
170	Thioketene	(C2H2S)	197,5	57,9877	58,9955
171	Nickel	(Ni)	176,1	58,0000	59,0078
172	Propanal	(C3H6O)	187,6	58,0419	59,0497
173	Oxetane	(C3H6O)	191,6	58,0419	59,0497
174	Acetone	(C3H6O)	194,1	58,0419	59,0497
175	Propylene oxide	(C3H6O)	194,2	58,0419	59,0497
176	Ethene, methoxy-	(C3H6O)	205,2	58,0419	59,0497
177	(E)-Dimethyldiazene	(C2H6N2)	207,2	58,0531	59,0609
178	Diazene, dimethyl-	(C2H6N2)	211,0	58,0531	59,0609
179	CH3C(=NH)NH2	(C2H6N2)	232,1	58,0531	59,0609
180	Isobutane	(C4H10)	161,5	58,0783	59,0861
181	B5H8	(B5H8)	182,5	58,1273	59,1351
182	Cobalt	(Co)	177,5	58,9332	59,9410
183	Formamide, N-methyl-	(C2H5NO)	203,5	59,0371	60,0449
184	Acetamide	(C2H5NO)	206,5	59,0371	60,0449
185	CH2CH2CH2OH	(C3H7O)	175,9	59,0497	60,0575
186	1-Propanamine	(C3H9N)	219,4	59,0735	60,0813
187	2-Propanamine	(C3H9N)	220,8	59,0735	60,0813
188	Ethanamine, N-methyl-	(C3H9N)	225,4	59,0735	60,0813
189	Trimethylamine	(C3H9N)	226,8	59,0735	60,0813
190	Pentaborane(9)	(H9B5)	167,3	59,1351	60,1429
191	Silicon monosulfide	(SSi)	163,2	59,9490	60,9568
192	SiS	(SSi)	169,7	59,9490	60,9568
193	Carbonyl sulfide	(COS)	150,2	59,9670	60,9748
194	Thiirane	(C2H4S)	193,4	60,0034	61,0112
195	Phosphirane	(C2H5P)	191,7	60,0129	61,0207
196	Acetic acid	(C2H4O2)	186,9	60,0211	61,0290
197	Methyl formate	(C2H4O2)	187,0	60,0211	61,0290
198	1-Propanol	(C3H8O)	188,2	60,0575	61,0653
199	Isopropyl alcohol	(C3H8O)	190,1	60,0575	61,0653
200	Ethane, methoxy-	(C3H8O)	193,4	60,0575	61,0653

No.	Name	Formel	PA (kcal/mol)	Masse	prot mass
201	Hydrazine, 1,1-dimethyl-	(C2H8N2)	221,5	60,0687	61,0766
202	Ethylenediamine	(C2H8N2)	227,2	60,0687	61,0766
203	Cyanogen chloride	(CClN)	172,6	60,9719	61,9798
204	Methane, nitro-	(CH3NO2)	179,9	61,0164	62,0242
205	Methyl nitrite	(CH3NO2)	191,0	61,0164	62,0242
206	HCOONH2	(CH3NO2)	199,6	61,0164	62,0242
207	H3BO3 (B(OH)3)	(BH3O3)	174,5	61,0212	62,0290
208	Ethanolamine	(C2H7NO)	222,3	61,0528	62,0606
209	CH2=S=O	(CH2OS)	191,0	61,9826	62,9905
210	H2N-NO2	(H2N2O2)	181,0	62,0116	63,0195
211	Ethanethiol	(C2H6S)	188,6	62,0190	63,0268
212	Dimethyl sulfide	(C2H6S)	198,6	62,0190	63,0268
213	Phosphine, dimethyl-	(C2H7P)	217,2	62,0285	63,0364
214	1,2-Ethanediol	(C2H6O2)	195,1	62,0368	63,0446
215	Copper	(Cu)	156,6	62,9296	63,9374
216	Phosphorus monosulfide	(PS)	166,8	62,9458	63,9537
217	Nitric acid	(HNO3)	179,6	62,9956	64,0035
218	Ethylamine, 2-fluoro-	(C2H6FN)	213,4	63,0484	64,0563
219	Sulfur dioxide	(O2S)	160,5	63,9619	64,9697
220	Osmium tetraoxide	(O4Os)	161,8	63,9797	64,9875
221	Zinc	(Zn)	145,5	64,0000	65,0078
222	Ethyl chloride	(C2H5Cl)	165,9	64,0080	65,0158
223	Ethene, 1,2-difluoro-, (E)-	(C2H2F2)	164,8	64,0125	65,0203
224	Ethene, 1,1-difluoro-	(C2H2F2)	175,4	64,0125	65,0203
225	Ethanol, 2-fluoro-	(C2H5FO)	171,0	64,0324	65,0403
226	Cyclopentadienyl radical	(C5H5)	198,8	65,0391	66,0470
227	Chlorofluoromethylene	(CClF)	184,6	65,9673	66,9751
228	Carbonic difluoride	(CF2O)	159,6	65,9917	66,9995
229	Malononitrile	(C3H2N2)	173,2	66,0218	67,0296
230	1,3-Cyclopentadiene	(C5H6)	196,5	66,0470	67,0548
231	Cyanoketene	(C3HNO)	187,4	67,0058	68,0136
232	HNCCCO	(C3HNO)	205,8	67,0058	68,0136
233	Cyclopropanecarbonitrile	(C4H5N)	193,5	67,0422	68,0500
234	Pyrrole	(C4H5N)	209,2	67,0422	68,0500
235	Iron, methylene-	(CH2Fe)	222,8	67,9553	68,9631
236	C3S	(C3S)	223,0	67,9721	68,9799
237	Furan	(C4H4O)	190,4	68,0262	69,0340
238	1H-Pyrazole	(C3H4N2)	213,4	68,0374	69,0453
239	1H-Imidazole	(C3H4N2)	225,2	68,0374	69,0453
240	Cyclopentene	(C5H8)	183,0	68,0626	69,0704
241	2-Pentyne	(C5H8)	193,8	68,0626	69,0704
242	Ethenylcyclopropane	(C5H8)	195,2	68,0626	69,0704
243	1-Butyne, 3-methyl-	(C5H8)	196,5	68,0626	69,0704
244	1,3-Butadiene, 2-methyl-	(C5H8)	198,9	68,0626	69,0704
245	1,3-Pentadiene, (E)-	(C5H8)	200,5	68,0626	69,0704
246	Cyclobutene, 1-methyl-	(C5H8)	202,2	68,0626	69,0704
247	Cyclopropene, 3,3-dimethyl-	(C5H8)	203,3	68,0626	69,0704
248	CH3COCN propanenitrile, 2-oxo	(C3H3NO)	178,5	69,0215	70,0293
249	Isoxazole	(C3H3NO)	202,8	69,0215	70,0293
250	Oxazole	(C3H3NO)	209,5	69,0215	70,0293
251	1H-1,2,3-Triazole	(C2H3N3)	210,0	69,0327	70,0405
252	1H-1,2,4-Triazole	(C2H3N3)	211,8	69,0327	70,0405
253	Butanenitrile	(C4H7N)	191,2	69,0578	70,0657
254	Propanenitrile, 2-methyl-	(C4H7N)	192,1	69,0578	70,0657
255	Propane, 1-isocyano-	(C4H7N)	204,7	69,0578	70,0657
256	Iron monoxide	(FeO)	216,8	69,9345	70,9424
257	Methane, trifluoro-	(CHF3)	147,9	70,0030	71,0109
258	Cyclobutanone	(C4H6O)	191,8	70,0419	71,0497
259	2-Propenal, 2-methyl-	(C4H6O)	193,3	70,0419	71,0497
260	Furan, 2,5-dihydro-	(C4H6O)	196,8	70,0419	71,0497
261	2-Butenal	(C4H6O)	198,7	70,0419	71,0497
262	Methyl vinyl ketone	(C4H6O)	199,5	70,0419	71,0497
263	Furan, 2,3-dihydro-	(C4H6O)	207,3	70,0419	71,0497
264	Cyanamide, dimethyl-	(C3H6N2)	203,7	70,0531	71,0609
265	CH3NHCH2CN	(C3H6N2)	206,5	70,0531	71,0609
266	H2NCH2CH2CN	(C3H6N2)	207,2	70,0531	71,0609
267	2-Butene, 2-methyl-	(C5H10)	193,3	70,0783	71,0861

No.	Name	Formel	PA (kcal/mol)	Masse	prot mass
268	1,6-Dicarbahexaborane(6)	(C2H6B4)	206,5	70,0987	71,1065
269	Nitrogen trifluoride	(F3N)	135,7	70,9983	72,0061
270	Methoxyacetonitrile	(C3H5NO)	181,4	71,0371	72,0449
271	2-Azetidinone	(C3H5NO)	204,0	71,0371	72,0449
272	Acrylamide	(C3H5NO)	208,0	71,0371	72,0449
273	ethyl azide	(C2H5N3)	209,8	71,0483	72,0562
274	Azetidine, N-methyl-	(C4H9N)	210,9	71,0735	72,0813
275	2-Propen-1-amine, 2-methyl-	(C4H9N)	217,7	71,0735	72,0813
276	Ethanamine, N-ethylidene	(C4H9N)	223,6	71,0735	72,0813
277	Pyrrolidine	(C4H9N)	226,8	71,0735	72,0813
278	(CH3)2NCH=CH2	(C4H9N)	228,7	71,0735	72,0813
279	2-Silaisobutene	(C3H8Si)	227,0	72,0395	73,0474
280	Butanal	(C4H8O)	189,5	72,0575	73,0653
281	Propanal, 2-methyl-	(C4H8O)	190,7	72,0575	73,0653
282	Furan, tetrahydro-	(C4H8O)	196,4	72,0575	73,0653
283	2-Butanone	(C4H8O)	197,8	72,0575	73,0653
284	Ethene, ethoxy-	(C4H8O)	207,9	72,0575	73,0653
285	1-Propene, 2-methoxy-	(C4H8O)	213,9	72,0575	73,0653
286	CoCH2	(CH2Co)	222,8	72,9489	73,9567
287	Thiocyanic acid, methyl ester	(C2H3NS)	190,7	72,9986	74,0064
288	Methane, isothiocyanato-	(C2H3NS)	191,3	72,9986	74,0064
289	Formamide, N,N-dimethyl-	(C3H7NO)	211,8	73,0528	74,0606
290	Acetamide, N-methyl-	(C3H7NO)	212,5	73,0528	74,0606
291	1-Propanamine, 2-methyl-	(C4H11N)	220,2	73,0891	74,0970
292	1-Butanamine	(C4H11N)	220,2	73,0891	74,0970
293	2-Butanamine	(C4H11N)	221,0	73,0891	74,0970
294	2-Propanamine, 2-methyl-	(C4H11N)	223,9	73,0891	74,0970
295	2-Propanamine, N-methyl-	(C4H11N)	227,0	73,0891	74,0970
296	Ethanamine, N-ethyl-	(C4H11N)	227,6	73,0891	74,0970
297	Ethanamine, N,N-dimethyl-	(C4H11N)	229,7	73,0891	74,0970
298	Thietane	(C3H6S)	199,1	74,0190	75,0268
299	Thiirane, methyl-	(C3H6S)	200,4	74,0190	75,0268
300	Methyl vinyl sulfide	(C3H6S)	205,1	74,0190	75,0268
301	Propanoic acid	(C3H6O2)	190,6	74,0368	75,0446
302	Formic acid, ethyl ester	(C3H6O2)	191,3	74,0368	75,0446
303	Acetic acid, methyl ester	(C3H6O2)	196,7	74,0368	75,0446
304	1-Butanol	(C4H10O)	188,7	74,0732	75,0810
305	1-Propanol, 2-methyl-	(C4H10O)	189,7	74,0732	75,0810
306	Ethanol, 1,1-dimethyl-	(C4H10O)	192,9	74,0732	75,0810
307	2-Butanol	(C4H10O)	194,8	74,0732	75,0810
308	Methyl propyl ether	(C4H10O)	194,9	74,0732	75,0810
309	Propane, 2-methoxy-	(C4H10O)	197,6	74,0732	75,0810
310	Ethoxy ethane	(C4H10O)	198,0	74,0732	75,0810
311	1,3-Propanediamine	(C3H10N2)	235,8	74,0844	75,0922
312	Acetonitrile, chloro-	(C2H2ClN)	178,3	74,9876	75,9954
313	Ethanethioamide	(C2H5NS)	211,4	75,0143	76,0221
314	Ethane, nitro-	(C2H5NO2)	183,0	75,0320	76,0399
315	Nitrous acid, ethyl ester	(C2H5NO2)	195,9	75,0320	76,0399
316	Acetamide,N-hydroxy	(C2H5NO2)	204,1	75,0320	76,0399
317	Glycine	(C2H5NO2)	211,8	75,0320	76,0399
318	Ethanamine, 2-methoxy-	(C3H9NO)	221,6	75,0684	76,0762
319	1-Propanol, 3-amino-	(C3H9NO)	230,2	75,0684	76,0762
320	Methanamine, N,N-dimethyl-, N-oxide	(C3H9NO)	235,0	75,0684	76,0762
321	Carbon disulfide	(CS2)	163,2	75,9441	76,9520
322	Thiourea	(CH4N2S)	214,2	76,0095	77,0173
323	F(CH3)Si=CH2	(C2H5FSi)	184,4	76,0145	77,0223
324	Benzyne	(C6H4)	201,0	76,0313	77,0391
325	2-Propanone, 1-fluoro-	(C3H5FO)	190,2	76,0324	77,0403
326	1-Propanethiol	(C3H8S)	189,7	76,0347	77,0425
327	2-Propanethiol	(C3H8S)	192,2	76,0347	77,0425
328	Ethane, (methylthio)-	(C3H8S)	202,2	76,0347	77,0425
329	Phosphine, trimethyl-	(C3H9P)	229,2	76,0442	77,0520
330	Ethanol, 2-methoxy-	(C3H8O2)	183,7	76,0524	77,0603
331	1,3-Propanediol	(C3H8O2)	209,2	76,0524	77,0603
332	Methyl nitrate	(CH3NO3)	175,6	77,0113	78,0191
333	1,5-hexadiyn-3-yl radical	(C6H5)	179,3	77,0391	78,0470
334	CH3-CC-CC-CH2 (2,4-hexadiyn-1-yl radical)	(C6H5)	195,9	77,0391	78,0470

No.	Name	Formel	PA (kcal/mol)	Masse	prot mass
335	Phenyl radical	(C6H5)	211,3	77,0391	78,0470
336	FCH2CH2CH2NH2	(C3H8FN)	218,4	77,0641	78,0719
337	B-Borazinyl radical	(B3H5N3)	192,0	77,0872	78,0950
338	Arsine	(H3As)	178,8	77,9451	78,9529
339	Disiloxane	(H6OSi2)	179,0	77,9957	79,0035
340	Acetic acid, fluoro-	(C2H3FO2)	183,0	78,0117	79,0195
341	Dimethyl sulfoxide	(C2H6OS)	211,4	78,0139	79,0218
342	Germane	(H4Ge)	170,5	78,0313	79,0391
343	Benzene	(C6H6)	179,3	78,0470	79,0548
344	Borazine	(H6B3N3)	191,8	78,0950	79,1028
345	Bromine	(Br)	132,5	78,9183	79,9262
346	Pyridine	(C5H5N)	222,3	79,0422	80,0500
347	Hydrogen bromide	(HBr)	139,6	79,9262	80,9340
348	Sulfur trioxide	(O3S)	140,5	79,9568	80,9646
349	F2Si=CH2	(CH2F2Si)	177,2	79,9894	80,9972
350	Ethanol, 2-chloro-	(C2H5ClO)	183,1	80,0029	81,0107
351	Pyrazine	(C4H4N2)	209,5	80,0374	81,0453
352	1,3-Diazine	(C4H4N2)	212,6	80,0374	81,0453
353	Pyridazine	(C4H4N2)	216,8	80,0374	81,0453
354	1,4-Cyclohexadiene	(C6H8)	200,0	80,0626	81,0704
355	1,3-Cyclohexadiene	(C6H8)	200,0	80,0626	81,0704
356	1-Methyl-3-methylenecyclobutene	(C6H8)	212,3	80,0626	81,0704
357	NCC(CH3)CO	(C4H3NO)	190,7	81,0215	82,0293
358	CH3NCCCO	(C4H3NO)	219,9	81,0215	82,0293
359	1,3,5-Triazine	(C3H3N3)	202,9	81,0327	82,0405
360	Ethylamine, 2,2-difluoro-	(C2H5F2N)	208,1	81,0390	82,0468
361	2,4-Dicarbaheptaborane(7)	(C2H7B5)	167,1	81,1195	82,1273
362	Dichloromethylene	(CCl2)	205,8	81,9377	82,9455
363	H3PO3	(H3O3P)	196,3	81,9820	82,9898
364	Ethene, trifluoro-	(C2HF3)	167,3	82,0030	83,0109
365	Hydrogen selenide	(H2Se)	170,4	82,0157	83,0235
366	CF2HCH2OH	(C2H4F2O)	174,0	82,0230	83,0308
367	Furan, 3-methyl-	(C5H6O)	203,6	82,0419	83,0497
368	Furan, 2-methyl-	(C5H6O)	206,9	82,0419	83,0497
369	3(5)-methylpyrazole	(C4H6N2)	216,8	82,0531	83,0609
370	4-methylpyrazole	(C4H6N2)	217,0	82,0531	83,0609
371	1-methylpyrazole	(C4H6N2)	217,9	82,0531	83,0609
372	4-Methylimidazole	(C4H6N2)	227,8	82,0531	83,0609
373	1H-Imidazole, 1-methyl-	(C4H6N2)	229,3	82,0531	83,0609
374	1H-Imidazole, 2-methyl-	(C4H6N2)	230,3	82,0531	83,0609
375	Cyclohexene	(C6H10)	187,5	82,0783	83,0861
376	Cyclopentene, 1-methyl-	(C6H10)	194,6	82,0783	83,0861
377	Cyclopentane, methylene-	(C6H10)	199,0	82,0783	83,0861
378	1,3-Butadiene, 2,3-dimethyl-	(C6H10)	200,6	82,0783	83,0861
379	1,2-Dimethylcyclobutene	(C6H10)	201,4	82,0783	83,0861
380	CH3CH=C(CH3)CH=CH2	(C6H10)	204,2	82,0783	83,0861
381	Cyclopropane, 1-ethenyl-1-methyl-	(C6H10)	204,9	82,0783	83,0861
382	1,3-Pentadiene, 2-methyl-	(C6H10)	206,7	82,0783	83,0861
383	Cyclopropane, (1-methylethenyl)-	(C6H10)	208,6	82,0783	83,0861
384	1,3,3-Trimethylcyclopropene	(C6H10)	213,1	82,0783	83,0861
385	4-NH2-pyrazole	(C3H5N3)	217,2	83,0483	84,0562
386	3(5)-aminopyrazole	(C3H5N3)	220,1	83,0483	84,0562
387	Pentanenitrile	(C5H9N)	191,8	83,0735	84,0813
388	Propanenitrile, 2,2-dimethyl-	(C5H9N)	193,5	83,0735	84,0813
389	Tert-butyl isocyanide	(C5H9N)	208,0	83,0735	84,0813
390	2-Propyn-1-amine, N,N-dimethyl-	(C5H9N)	224,8	83,0735	84,0813
391	Krypton	(Kr)	101,5	83,9115	84,9193
392	Thiophene	(C4H4S)	194,9	84,0034	85,0112
393	Cyclopentanone	(C5H8O)	196,9	84,0575	85,0653
394	2-pentenal(E)	(C5H8O)	200,7	84,0575	85,0653
395	3-Buten-2-one, 3-methyl-	(C5H8O)	201,5	84,0575	85,0653
396	2-Butenal,2-methyl-(Z)-	(C5H8O)	201,6	84,0575	85,0653
397	2-Butenal,2-methyl-(Z)-	(C5H8O)	201,6	84,0575	85,0653
398	Ethanone, 1-cyclopropyl-	(C5H8O)	204,3	84,0575	85,0653
399	3-methyl-2-butenal	(C5H8O)	204,6	84,0575	85,0653
400	3-Penten-2-one	(C5H8O)	206,6	84,0575	85,0653
401	2H-Pyran, 3,4-dihydro-	(C5H8O)	207,0	84,0575	85,0653

No.	Name	Formel	PA (kcal/mol)	Masse	prot mass
402	4-Methyl-2,3-dihydrofuran	(C5H8O)	207,5	84,0575	85,0653
403	Furan, 2,3-dihydro-5-methyl-	(C5H8O)	216,7	84,0575	85,0653
404	Acetonitrile, (dimethylamino)-	(C4H8N2)	211,5	84,0687	85,0766
405	1,4,5,6-tetrahydropyrimdine	(C4H8N2)	239,4	84,0687	85,0766
406	Cyclohexane	(C6H12)	164,3	84,0939	85,1017
407	2-Pentene, 2-methyl-	(C6H12)	194,1	84,0939	85,1017
408	CH3CH=C(CH3)C2H5	(C6H12)	194,3	84,0939	85,1017
409	2-Butene, 2,3-dimethyl-	(C6H12)	194,5	84,0939	85,1017
410	Thiazole	(C3H3NS)	216,1	84,9986	86,0064
411	CH3COOCN carbonocyanic acid, methyl ester	(C3H3NO2)	178,1	85,0164	86,0242
412	Methacrylamide	(C4H7NO)	210,4	85,0528	86,0606
413	2H-Azetidin-2-one, 2-methyl-	(C4H7NO)	210,9	85,0528	86,0606
414	2-butenamide	(C4H7NO)	211,8	85,0528	86,0606
415	Piperidine	(C5H11N)	228,0	85,0891	86,0970
416	N,N-Dimethylallyl amine	(C5H11N)	228,9	85,0891	86,0970
417	(CH3)2C=NC2H5	(C5H11N)	229,5	85,0891	86,0970
418	Pyrrolidine, 1-methyl-	(C5H11N)	231,0	85,0891	86,0970
419	CH3CH=CHN(CH3)2	(C5H11N)	231,1	85,0891	86,0970
420	Ethanamine, N-(2-propylidene)	(C5H11N)	232,6	85,0891	86,0970
421	Lithium bromide	(BrLi)	195,7	85,9343	86,9422
422	4-fluoropyrazole	(C3H3FN2)	206,3	86,0280	87,0359
423	2,3-Butanedione	(C4H6O2)	192,1	86,0368	87,0446
424	Acetic acid ethenyl ester	(C4H6O2)	194,4	86,0368	87,0446
425	2-Propenoic acid, 2-methyl-	(C4H6O2)	194,8	86,0368	87,0446
426	Crotonic acid	(C4H6O2)	195,5	86,0368	87,0446
427	Cyclopropanecarboxylic acid	(C4H6O2)	196,8	86,0368	87,0446
428	1,4-Dioxin, 2,3-dihydro-	(C4H6O2)	197,1	86,0368	87,0446
429	2-Propenoic acid, methyl ester	(C4H6O2)	197,4	86,0368	87,0446
430	Isocrotonic acid	(C4H6O2)	197,4	86,0368	87,0446
431	g-Butyrolactone	(C4H6O2)	200,9	86,0368	87,0446
432	Pentanal	(C5H10O)	190,7	86,0732	87,0810
433	2H-Pyran, tetrahydro-	(C5H10O)	196,7	86,0732	87,0810
434	C2H5OCH2CH=CH2	(C5H10O)	199,5	86,0732	87,0810
435	2-Butanone, 3-methyl-	(C5H10O)	200,0	86,0732	87,0810
436	3-Pentanone	(C5H10O)	200,0	86,0732	87,0810
437	Furan, tetrahydro-2-methyl-	(C5H10O)	201,6	86,0732	87,0810
438	C2H5OCH=CHCH3	(C5H10O)	209,5	86,0732	87,0810
439	trans-CH3CH=CH-OC2H5	(C5H10O)	209,6	86,0732	87,0810
440	c-C(CH3)(C2H5)NHNH	(C4H10N2)	214,7	86,0844	87,0922
441	Piperazine	(C4H10N2)	224,5	86,0844	87,0922
442	CH3NHCH2CH2NHCH3	(C4H10N2)	236,4	86,0844	87,0922
443	(CH3)2N-CH=N-CH3	(C4H10N2)	239,6	86,0844	87,0922
444	CH3SCH2CN	(C3H5NS)	187,7	87,0143	88,0221
445	1,4-Dioxyl radical	(C4H7O2)	192,1	87,0446	88,0524
446	n-C3H7NHCHO	(C4H9NO)	209,6	87,0684	88,0762
447	Acetamide, N-ethyl-	(C4H9NO)	214,7	87,0684	88,0762
448	Acetamide, N,N-dimethyl-	(C4H9NO)	217,1	87,0684	88,0762
449	Propanamide, N-methyl-	(C4H9NO)	220,1	87,0684	88,0762
450	Morpholine	(C4H9NO)	220,7	87,0684	88,0762
451	1-Pentanamine	(C5H13N)	220,4	87,1048	88,1126
452	Neopentylamine	(C5H13N)	221,9	87,1048	88,1126
453	2-Butanamine, 2-methyl-	(C5H13N)	225,0	87,1048	88,1126
454	(C2H5)(i-C3H7)NH	(C5H13N)	229,4	87,1048	88,1126
455	(CH3)2(n-C3H7)N	(C5H13N)	230,1	87,1048	88,1126
456	Ethanamine, N-ethyl-N-methyl-	(C5H13N)	232,3	87,1048	88,1126
457	2-Propanamine, N,N-dimethyl-	(C5H13N)	232,3	87,1048	88,1126
458	Phosphorus trifluoride	(F3P)	166,5	87,9690	88,9768
459	Carbon tetrafluoride	(CF4)	126,2	87,9936	89,0014
460	Ethylene carbonate	(C3H4O3)	194,7	88,0160	89,0239
461	Thiophene, tetrahydro-	(C4H8S)	203,0	88,0347	89,0425
462	CH2=C(CH3)-SCH3	(C4H8S)	212,4	88,0347	89,0425
463	1,4-Dioxane	(C4H8O2)	190,7	88,0524	89,0603
464	Formic acid, propyl ester	(C4H8O2)	193,3	88,0524	89,0603
465	Formic acid, 1-methylethyl ester	(C4H8O2)	193,9	88,0524	89,0603
466	1,3-Dioxane	(C4H8O2)	196,4	88,0524	89,0603
467	Propanoic acid, methyl ester	(C4H8O2)	198,5	88,0524	89,0603
468	Ethyl acetate	(C4H8O2)	199,7	88,0524	89,0603

No.	Name	Formel	PA (kcal/mol)	Masse	prot mass
469	Ethene, 1,1-dimethoxy-	(C4H8O2)	228,8	88,0524	89,0603
470	Urea, N,N'-dimethyl-	(C3H8N2O)	216,1	88,0637	89,0715
471	1-Propanol, 2,2-dimethyl-	(C5H12O)	190,1	88,0888	89,0966
472	Butane, 1-methoxy-	(C5H12O)	196,2	88,0888	89,0966
473	Propane, 2-methoxy-2-methyl-	(C5H12O)	200,6	88,0888	89,0966
474	Propane, 2-ethoxy-	(C5H12O)	201,4	88,0888	89,0966
475	Tetramethylhydrazine	(C4H12N2)	226,8	88,1000	89,1079
476	1,4-butanediamine	(C4H12N2)	240,1	88,1000	89,1079
477	Yttrium	(Y)	231,1	89,0000	90,0078
478	Cl(CH2)2CN	(C3H4ClN)	184,9	89,0032	90,0111
479	Methanethioamide, N,N-dimethyl-	(C3H7NS)	217,1	89,0299	90,0377
480	C6H5CD3	(C7H5D3)	188,7	89,0391	90,0470
481	Iso-propyl nitrite	(C3H7NO2)	202,1	89,0477	90,0555
482	Acetamide, N-hydroxy-N-methyl	(C3H7NO2)	209,4	89,0477	90,0555
483	Acetamide, N-methoxy	(C3H7NO2)	209,9	89,0477	90,0555
484	Alanine	(C3H7NO2)	215,5	89,0477	90,0555
485	Sarcosine	(C3H7NO2)	220,3	89,0477	90,0555
486	NH2(CH2)4OH	(C4H11NO)	235,3	89,0841	90,0919
487	Ethanethioic acid, s-methyl ester	(C3H6OS)	198,3	90,0139	91,0218
488	CH3C(=S)OCH3	(C3H6OS)	202,2	90,0139	91,0218
489	Carbonic acid, dimethyl ester	(C3H6O3)	198,5	90,0317	91,0395
490	Methanamine, N-methyl-N-nitro-	(C2H6N2O2)	198,1	90,0429	91,0508
491	Silanol, trimethyl	(C3H10OSi)	194,8	90,0501	91,0579
492	1-Butanethiol	(C4H10S)	191,7	90,0503	91,0581
493	1-Propanethiol, 2-methyl-	(C4H10S)	191,9	90,0503	91,0581
494	2-Butanethiol	(C4H10S)	194,3	90,0503	91,0581
495	2-Propanethiol, 2-methyl-	(C4H10S)	195,1	90,0503	91,0581
496	Diethyl sulfide	(C4H10S)	204,5	90,0503	91,0581
497	Ethane, 1,2-dimethoxy-	(C4H10O2)	205,1	90,0681	91,0759
498	1,4-Butanediol	(C4H10O2)	218,5	90,0681	91,0759
499	Benzyl radical	(C7H7)	198,7	91,0548	92,0626
500	Cycloheptatrienyl radical	(C7H7)	199,0	91,0548	92,0626
501	Carbon monoselenide	(CSe)	198,8	92,0000	93,0078
502	FCO2C2H5	(C3H5FO2)	181,0	92,0274	93,0352
503	Trimethylphosphine oxide	(C3H9OP)	217,6	92,0391	93,0469
504	1,2,3-Propanetriol	(C3H8O3)	209,1	92,0473	93,0552
505	Anilino radical	(C6H6N)	227,1	92,0500	93,0578
506	Toluene	(C7H8)	187,4	92,0626	93,0704
507	2,5-Norbornadiene	(C7H8)	204,0	92,0626	93,0704
508	Phenoxy radical	(C6H5O)	204,8	93,0340	94,0419
509	Aniline	(C6H7N)	210,9	93,0578	94,0657
510	2-Propyn-1-amine, N-2-propynyl-	(C6H7N)	217,6	93,0578	94,0657
511	Pyridine, 3-methyl-	(C6H7N)	225,6	93,0578	94,0657
512	Pyridine, 4-methyl-	(C6H7N)	226,4	93,0578	94,0657
513	Pyridine, 2-methyl-	(C6H7N)	226,6	93,0578	94,0657
514	Methyl bromide	(CH3Br)	158,7	93,9418	94,9496
515	Acetic acid, chloro-	(C2H3ClO2)	183,0	93,9822	94,9900
516	Disulfide, dimethyl	(C2H6S2)	195,0	93,9911	94,9989
517	Formaldehyde, seleno-	(CH2Se)	183,1	94,0157	95,0235
518	CFH2COCFH2	(C3H4F2O)	182,5	94,0230	95,0308
519	1-Propyne, 3,3'-oxybis-	(C6H6O)	187,5	94,0419	95,0497
520	Phenol	(C6H6O)	195,0	94,0419	95,0497
521	3-Pyridinamine	(C5H6N2)	220,8	94,0531	95,0609
522	2-Pyridinamine	(C5H6N2)	223,7	94,0531	95,0609
523	4-Pyridinamine	(C5H6N2)	234,8	94,0531	95,0609
524	2-Norbornene	(C7H10)	199,4	94,0783	95,0861
525	Acetonitrile, trifluoro-	(C2F3N)	164,8	94,9983	96,0061
526	Pyridine, 1-oxide	(C5H5NO)	220,7	95,0371	96,0449
527	1H-Pyrrole, 2,5-dimethyl-	(C6H9N)	219,7	95,0735	96,0813
528	Methanesulfonic acid	(CH4O3S)	182,0	95,9881	96,9959
529	Phosphabenzene	(C5H5P)	195,6	96,0129	97,0207
530	2(1H)-Pyrimidinone	(C4H4N2O)	208,9	96,0324	97,0402
531	Benzene, fluoro-	(C6H5F)	180,7	96,0375	97,0454
532	Bicyclo[2.2.1]hept-2-ene, 7-oxa-	(C6H8O)	200,2	96,0575	97,0653
533	Furan, 2,5-dimethyl-	(C6H8O)	208,0	96,0575	97,0653
534	3,4-dimethylfuran	(C6H8O)	208,1	96,0575	97,0653
535	2,4-Dimethylfuran	(C6H8O)	213,6	96,0575	97,0653

No.	Name	Formel	PA (kcal/mol)	Masse	prot mass
536	trans-dimethylamino acrylonitrile	(C5H8N2)	214,4	96,0687	97,0766
537	3(5),4-dimethylpyrazole	(C5H8N2)	221,6	96,0687	97,0766
538	1,4-Dimethylpyrazole	(C5H8N2)	222,0	96,0687	97,0766
539	1,3-Dimethylpyrazole	(C5H8N2)	223,3	96,0687	97,0766
540	1,5-Dimethylpyrazole	(C5H8N2)	223,4	96,0687	97,0766
541	1H-Pyrazole, 3,5-dimethyl-	(C5H8N2)	223,5	96,0687	97,0766
542	1,4-Dimethylimidazole	(C5H8N2)	233,4	96,0687	97,0766
543	1,5-Dimethylimidazole	(C5H8N2)	233,7	96,0687	97,0766
544	1H-Imidazole, 1,2-dimethyl-	(C5H8N2)	235,3	96,0687	97,0766
545	Cyclopentene, 1,2-dimethyl-	(C7H12)	196,7	96,0939	97,1017
546	Cyclohexene, 1-methyl-	(C7H12)	197,3	96,0939	97,1017
547	(CH3)2C=CHC(CH3)=CH2	(C7H12)	211,2	96,0939	97,1017
548	4-NO2-pyrazole	(C3H3N3O)	196,7	97,0276	98,0354
549	2-Fluoropyridine	(C5H4FN)	211,5	97,0328	98,0406
550	3-F-pyridine	(C5H4FN)	215,7	97,0328	98,0406
551	4-F-pyridine	(C5H4FN)	218,0	97,0328	98,0406
552	N'-cyano-N,N-dimethyl formamidine	(C4H7N3)	212,3	97,0640	98,0718
553	1-methyl-3-aminopyrazole	(C4H7N3)	224,5	97,0640	98,0718
554	1-methyl-5-aminopyrazole	(C4H7N3)	226,9	97,0640	98,0718
555	2-Propen-1-amine, N-2-propenyl-	(C6H11N)	227,0	97,0891	98,0970
556	Sulfuric acid	(H2O4S)	166,9	97,9674	98,9752
557	CF3CHO	(C2HF3O)	164,5	97,9979	99,0058
558	Thiophene, 2-methyl-	(C5H6S)	205,3	98,0190	99,0268
559	(CH3)2NCOCN	(C4H6N2O)	198,2	98,0480	99,0558
560	(CH2=CHCH2)2O	(C6H10O)	197,8	98,0732	99,0810
561	Cyclohexanone	(C6H10O)	201,1	98,0732	99,0810
562	7-Oxabicyclo[2.2.1]heptane	(C6H10O)	201,9	98,0732	99,0810
563	Cyclohexene oxide	(C6H10O)	202,7	98,0732	99,0810
564	3-hexen-2-one(E)	(C6H10O)	207,3	98,0732	99,0810
565	3-methyl-3-penten-2-one(Z)	(C6H10O)	207,4	98,0732	99,0810
566	3-Penten-2-one, 4-methyl-	(C6H10O)	210,0	98,0732	99,0810
567	4,4-dimethyl-2-imidazoline	(C5H10N2)	236,4	98,0844	99,0922
568	(CH3)2N-CH=N-(2-propenyl)	(C6H12N)	240,2	98,0970	99,1048
569	2-Pentene, 2,4-dimethyl-	(C7H14)	194,1	98,1096	99,1174
570	Trifluoronitrosomethane	(CF3NO)	168,2	98,9932	100,0010
571	2-Methylthiazole	(C4H5NS)	222,5	99,0143	100,0221
572	2,2,2-Trifluoroethylamine	(C2H4F3N)	202,7	99,0296	100,0374
573	NCCOOC2H5	(C4H5NO2)	178,4	99,0320	100,0399
574	Pentanenitrile, 3-ethoxy	(C5H9NO)	193,3	99,0684	100,0762
575	2-propenamide, N,N-dimethyl	(C5H9NO)	216,3	99,0684	100,0762
576	2-Pyrrolidinone, 1-methyl-	(C5H9NO)	220,5	99,0684	100,0762
577	c-C4H6N(2-OCH3)	(C5H9NO)	226,8	99,0684	100,0762
578	Cyclohexanamine	(C6H13N)	223,3	99,1048	100,1126
579	Ethanamine, N-butylidene-	(C6H13N)	225,3	99,1048	100,1126
580	1H-Azepine, hexahydro-	(C6H13N)	228,7	99,1048	100,1126
581	1-Propen-1-amine, N,N,2-trimethyl-	(C6H13N)	231,1	99,1048	100,1126
582	Piperidine, 1-methyl-	(C6H13N)	232,2	99,1048	100,1126
583	(CH3)2NC(CH3)=CHCH3	(C6H13N)	240,6	99,1048	100,1126
584	2-Aminothiazole	(C3H4N2S)	222,5	100,0095	101,0173
585	Ethanol, 2,2,2-trifluoro-	(C2H3F3O)	167,8	100,0136	101,0214
586	CF3OCH3	(C2H3F3O)	172,9	100,0136	101,0214
587	Cyclobutane carboxylic acid	(C5H8O2)	195,5	100,0524	101,0603
588	2-methyl-2-butenoic acid(Z)	(C5H8O2)	196,6	100,0524	101,0603
589	2-Butenoic acid, 3-methyl-	(C5H8O2)	196,7	100,0524	101,0603
590	trans-Alpha,beta-penteneoic acid	(C5H8O2)	196,9	100,0524	101,0603
591	2-Propenoic acid, 2-methyl-, methyl ester	(C5H8O2)	198,9	100,0524	101,0603
592	Cyclopropanecarboxylic acid, methyl ester	(C5H8O2)	201,7	100,0524	101,0603
593	2-Butenoic acid, methyl ester, (E)-	(C5H8O2)	203,5	100,0524	101,0603
594	Acetylacetone	(C5H8O2)	208,7	100,0524	101,0603
595	Silane, ethenyltrimethyl-	(C5H12Si)	199,1	100,0708	101,0787
596	Oxepane	(C6H12O)	198,9	100,0888	101,0966
597	2-Butanone, 3,3-dimethyl-	(C6H12O)	200,8	100,0888	101,0966
598	3-Hexanone	(C6H12O)	201,5	100,0888	101,0966
599	2,2-Dimethyltetrahydrofuran	(C6H12O)	202,6	100,0888	101,0966
600	Pyrazolidine, 1,2-dimethyl-	(C5H12N2)	229,4	100,1000	101,1079
601	(CH3)2N-CH=N-C2H5	(C5H12N2)	241,1	100,1000	101,1079
602	(CH3)2N-C(CH3)=NCH3	(C5H12N2)	244,5	100,1000	101,1079

No.	Name	Formel	PA (kcal/mol)	Masse	prot mass
603	1-Hexanamine	(C6H15N)	220,1	101,1204	102,1283
604	1-Propanamine, n-propyl-	(C6H15N)	230,0	101,1204	102,1283
605	N,N-Dimethyl isobutylamine	(C6H15N)	231,5	101,1204	102,1283
606	1-Butanamine, N,N-dimethyl-	(C6H15N)	231,6	101,1204	102,1283
607	2-Propanamine, N-(1-methylethyl)-	(C6H15N)	232,3	101,1204	102,1283
608	(sec-C4H9)(CH3)2N	(C6H15N)	233,2	101,1204	102,1283
609	2-Propanamine, N,N,2-trimethyl-	(C6H15N)	234,0	101,1204	102,1283
610	Triethylamine	(C6H15N)	234,7	101,1204	102,1283
611	Sulfuryl fluoride	(F2O2S)	144,6	101,9587	102,9665
612	SiF3OH	(F3HOSi)	153,3	101,9749	102,9827
613	4-Cl-pyrazole	(C3H3ClN2)	207,8	101,9985	103,0063
614	Ruthenium	(Ru)	185,0	102,0000	103,0078
615	2-Imidazolidinethione	(C3H6N2S)	220,9	102,0252	103,0330
616	Phenylacetylene	(C8H6)	199,6	102,0470	103,0548
617	2H-Thiopyran, tetrahydro-	(C5H10S)	204,6	102,0503	103,0581
618	Formic acid, butyl ester	(C5H10O2)	192,4	102,0681	103,0759
619	Butanoic acid, methyl ester	(C5H10O2)	200,0	102,0681	103,0759
620	Acetic acid, 1-methylethyl ester	(C5H10O2)	200,0	102,0681	103,0759
621	Propanoic acid, 2-methyl-, methyl ester	(C5H10O2)	200,0	102,0681	103,0759
622	n-Propyl acetate	(C5H10O2)	200,2	102,0681	103,0759
623	cis-1,2-Cyclopentanediol	(C5H10O2)	211,8	102,0681	103,0759
624	(CH3)2N-CH=N-OCH3	(C4H10N2O)	226,7	102,0793	103,0871
625	Propane, 1-methoxy-2,2-dimethyl-	(C6H14O)	197,5	102,1045	103,1123
626	Di-n-propyl ether	(C6H14O)	200,3	102,1045	103,1123
627	Diisopropyl ether	(C6H14O)	204,7	102,1045	103,1123
628	Propane, 2-ethoxy-2-methyl-	(C6H14O)	204,7	102,1045	103,1123
629	Methanediamine, N,N,N',N'-tetramethyl-	(C5H14N2)	227,6	102,1157	103,1235
630	1,5-Diaminopentane	(C5H14N2)	239,3	102,1157	103,1235
631	1,3-Propanediamine, N,N-dimethyl-	(C5H14N2)	245,3	102,1157	103,1235
632	Rhodium	(Rh)	183,6	103,0000	104,0078
633	Benzonitrile	(C7H5N)	193,8	103,0422	104,0500
634	Benzene, isocyano-	(C7H5N)	207,6	103,0422	104,0500
635	Dimethyl thioacetamide	(C4H9NS)	221,1	103,0456	104,0534
636	(CH3)3CONO	(C4H9NO2)	206,5	103,0633	104,0712
637	(CH3)2NCOOCH3	(C4H9NO2)	210,4	103,0633	104,0712
638	CH3NHCOOC2H5	(C4H9NO2)	212,5	103,0633	104,0712
639	Boric acid, trimethyl ester	(C3H9BO3)	195,0	103,0681	104,0759
640	1,2-Ethanediamine, N-(2-aminoethyl)-	(C4H13N3)	223,2	103,1109	104,1188
641	Phosphoryl fluoride	(F3OP)	166,1	103,9639	104,9717
642	Methane, chlorotrifluoro-	(CClF3)	136,4	103,9641	104,9719
643	Silicon tetrafluoride	(F4Si)	120,2	103,9705	104,9784
644	Thioacetic acid, o-ethyl ester	(C4H8OS)	206,4	104,0296	105,0374
645	2-Pyridinecarbonitrile	(C6H4N2)	208,6	104,0374	105,0453
646	3-Pyridinecarbonitrile	(C6H4N2)	209,6	104,0374	105,0453
647	4-Pyridinecarbonitrile	(C6H4N2)	210,5	104,0374	105,0453
648	Thiourea, N,N'-dimethyl-	(C3H8N2S)	221,5	104,0408	105,0486
649	C2H5OCOOCH3	(C4H8O3)	201,5	104,0473	105,0552
650	Styrene	(C8H8)	200,3	104,0626	105,0704
651	Cubane	(C8H8)	206,0	104,0626	105,0704
652	o-Xylylene	(C8H8)	214,5	104,0626	105,0704
653	1,4-Cyclohexadiene,3,6-bis(methylene)-	(C8H8)	215,2	104,0626	105,0704
654	Silane, methoxytrimethyl-	(C4H12OSi)	202,5	104,0657	105,0736
655	1-Propanethiol, 2,2-dimethyl-	(C5H12S)	193,6	104,0660	105,0738
656	Propane, 1,3-dimethoxy-	(C5H12O2)	214,5	104,0837	105,0916
657	Cyanogen bromide	(CBrN)	178,8	104,9214	105,9292
658	L-Serine	(C3H7NO3)	218,6	105,0426	106,0504
659	C6H5CH=NH	(C7H7N)	218,0	105,0578	106,0657
660	Pyridine, 4-ethenyl-	(C7H7N)	223,0	105,0578	106,0657
661	2,3-Cyclobutenopyridine	(C7H7N)	223,2	105,0578	106,0657
662	3,4-Cyclobutenopyridine	(C7H7N)	225,7	105,0578	106,0657
663	1-Phenylethyl radical	(C8H9)	199,9	105,0704	106,0783
664	Diethanolamine	(C4H11NO2)	228,0	105,0790	106,0868
665	Methyl dithioacetate	(C3H6S2)	205,7	105,9911	106,9989
666	Palladium	(Pd)	166,3	106,0000	107,0078
667	Benzaldehyde	(C7H6O)	199,6	106,0419	107,0497
668	2,4,6-Cycloheptatrien-1-one	(C7H6O)	220,7	106,0419	107,0497
669	4-Methylene-2,5-cyclohexadiene-1-one	(C7H6O)	221,2	106,0419	107,0497

No.	Name	Formel	PA (kcal/mol)	Masse	prot mass
670	HOCH2CH(OH)CH2CH2OH	(C4H10O3)	216,5	106,0630	107,0708
671	Ethylbenzene	(C8H10)	188,3	106,0783	107,0861
672	p-Xylene	(C8H10)	190,0	106,0783	107,0861
673	Benzene, 1,2-dimethyl-	(C8H10)	190,3	106,0783	107,0861
674	Benzene, 1,3-dimethyl-	(C8H10)	193,8	106,0783	107,0861
675	ClCON(CH3)2	(C3H6ClNO)	202,2	107,0138	108,0216
676	Benzene, nitroso-	(C6H5NO)	204,3	107,0371	108,0449
677	4-Pyridinecarboxaldehyde	(C6H5NO)	215,0	107,0371	108,0449
678	2-Me-phenoxy	(C7H7O)	209,0	107,0497	108,0575
679	3-Me-phenoxy	(C7H7O)	209,7	107,0497	108,0575
680	2-OH-benzyl	(C7H7O)	210,0	107,0497	108,0575
681	4-Me-phenoxy	(C7H7O)	211,4	107,0497	108,0575
682	3-OH-benzyl	(C7H7O)	211,6	107,0497	108,0575
683	4-OH-benzyl	(C7H7O)	214,3	107,0497	108,0575
684	Benzenamine, 2-methyl-	(C7H9N)	213,0	107,0735	108,0813
685	Benzenamine, 3-methyl-	(C7H9N)	214,2	107,0735	108,0813
686	p-Toluidine	(C7H9N)	214,4	107,0735	108,0813
687	Benzylamine	(C7H9N)	218,4	107,0735	108,0813
688	Aniline, N-methyl-	(C7H9N)	219,2	107,0735	108,0813
689	Pyridine, 2,5-dimethyl-	(C7H9N)	225,8	107,0735	108,0813
690	Pyridine, 2,3-dimethyl-	(C7H9N)	226,1	107,0735	108,0813
691	3-(C2H5)-pyridine	(C7H9N)	226,5	107,0735	108,0813
692	Pyridine, 2,4-dimethyl-	(C7H9N)	227,2	107,0735	108,0813
693	4-(C2H5)-pyridine	(C7H9N)	227,2	107,0735	108,0813
694	Pyridine, 2-ethyl-	(C7H9N)	227,6	107,0735	108,0813
695	Pyridine, 3,5-dimethyl-	(C7H9N)	228,1	107,0735	108,0813
696	Pyridine, 2,6-dimethyl-	(C7H9N)	230,1	107,0735	108,0813
697	(iso-C5H11)3N	(C5H33N)	223,0	107,2613	108,2691
698	Ethane, bromo-	(C2H5Br)	166,6	107,9575	108,9653
699	Carbonyl selenide	(COSe)	160,1	107,9949	109,0027
700	Carbonochloridic acid, ethyl ester	(C3H5ClO2)	182,9	107,9978	109,0056
701	p-Benzoquinone	(C6H4O2)	191,0	108,0211	109,0290
702	Benzyl alcohol	(C7H8O)	186,0	108,0575	109,0653
703	Bicyclo[2.2.1]hept-2-en-7-one	(C7H8O)	198,5	108,0575	109,0653
704	Benzene, methoxy-	(C7H8O)	200,7	108,0575	109,0653
705	Bicyclo[2.2.1]hept-2-en-5-one	(C7H8O)	202,1	108,0575	109,0653
706	1,2-Benzenediamine	(C6H8N2)	214,3	108,0687	109,0766
707	1,4-Benzenediamine	(C6H8N2)	216,5	108,0687	109,0766
708	1,3-Benzenediamine	(C6H8N2)	222,3	108,0687	109,0766
709	Bicyclo[2.2.1]hept-2-ene, 2-methyl-	(C8H12)	202,0	108,0939	109,1017
710	2-Methylenebicyclo[2.2.1]-heptane	(C8H12)	205,9	108,0939	109,1017
711	Cyclopropane, 1,1'-ethenylidenebis-	(C8H12)	216,3	108,0939	109,1017
712	3-Fluorobenzyl radical	(C7H6F)	199,9	109,0454	110,0532
713	Phenol, 3-amino-	(C6H7NO)	214,8	109,0528	110,0606
714	Phenol, 2-amino-	(C6H7NO)	214,8	109,0528	110,0606
715	2(1H)-Pyridinone, 1-methyl-	(C6H7NO)	221,5	109,0528	110,0606
716	Pyridine, 2-methoxy-	(C6H7NO)	223,3	109,0528	110,0606
717	Pyridine, 3-methyl-, 1-oxide	(C6H7NO)	223,5	109,0528	110,0606
718	Pyridine, 3-methoxy-	(C6H7NO)	226,0	109,0528	110,0606
719	Pyridine, 4-methoxy-	(C6H7NO)	230,4	109,0528	110,0606
720	Cyclohexanecarbonitrile	(C7H11N)	194,9	109,0891	110,0970
721	1-Azabicyclo[2.2.2]oct-2-ene	(C7H11N)	228,4	109,0891	110,0970
722	Phosphonic acid, dimethyl ester	(C2H7O3P)	214,1	110,0133	111,0211
723	Benzene, 1-fluoro-4-methyl-	(C7H7F)	182,6	110,0532	111,0610
724	Benzene, 1-fluoro-2-methyl-	(C7H7F)	184,8	110,0532	111,0610
725	Benzene, 1-fluoro-3-methyl-	(C7H7F)	187,7	110,0532	111,0610
726	Norbornan-7-one	(C7H10O)	199,0	110,0732	111,0810
727	2-Norbornanone	(C7H10O)	202,6	110,0732	111,0810
728	Methanone, dicyclopropyl-	(C7H10O)	210,7	110,0732	111,0810
729	Piperidine, 1-carbonitrile-	(C6H10N2)	209,3	110,0844	111,0922
730	4-Cyanopiperidine	(C6H10N2)	218,1	110,0844	111,0922
731	3,4,5-Trimethylpyrazole	(C6H10N2)	226,5	110,0844	111,0922
732	1,3,5-Trimethylpyrazole	(C6H10N2)	226,9	110,0844	111,0922
733	(CH3)2N-CH=N-(2-propynyl)	(C6H10N2)	237,4	110,0844	111,0922
734	(CH3)2C=C(CH3)C(CH3)=CH2	(C8H14)	208,7	110,1096	111,1174
735	4-F-phenoxy	(C6H4FO)	204,2	111,0246	112,0324
736	2(1H)-Pyrimidinone, 4-amino-	(C4H5N3O)	227,0	111,0433	112,0511

No.	Name	Formel	PA (kcal/mol)	Masse	prot mass
737	Benzenamine, 3-fluoro-	(C6H6FN)	207,2	111,0484	112,0563
738	p-Fluoroaniline	(C6H6FN)	208,4	111,0484	112,0563
739	(CH3)2N-CH=N-CH2CN	(C5H9N3)	226,7	111,0796	112,0875
740	Histamine	(C5H9N3)	238,8	111,0796	112,0875
741	Exo-2-aminonorbornane	(C7H13N)	221,4	111,1048	112,1126
742	Endo-2-aminonorbornane	(C7H13N)	221,4	111,1048	112,1126
743	Quinuclidine	(C7H13N)	235,3	111,1048	112,1126
744	Benzene, chloro-	(C6H5Cl)	180,1	112,0080	113,0158
745	2-Propanone, 1,1,1-trifluoro-	(C3H3F3O)	173,4	112,0136	113,0214
746	Uracil	(C4H4N2O2)	208,9	112,0273	113,0351
747	1,4-Cyclohexanedione	(C6H8O2)	193,8	112,0524	113,0603
748	c-hexane-1,2-dione	(C6H8O2)	202,4	112,0524	113,0603
749	1,3-Cyclohexanedione	(C6H8O2)	210,6	112,0524	113,0603
750	Cyclohexanone, 4-methyl-	(C7H12O)	201,8	112,0888	113,0966
751	Cycloheptanone	(C7H12O)	202,2	112,0888	113,0966
752	Triethylenediamine	(C6H12N2)	228,5	112,1000	113,1079
753	1H,5H-Pyrazolo[1,2-a]pyrazole,tetrahydro-	(C6H12N2)	233,8	112,1000	113,1079
754	(CH3)2N-CH=N-(c-propyl)	(C6H12N2)	240,5	112,1000	113,1079
755	Pyridine, 3-chloro-	(C5H4ClN)	215,2	113,0032	114,0111
756	Pyridine, 2-chloro-	(C5H4ClN)	215,3	113,0032	114,0111
757	4-Chloropyridine	(C5H4ClN)	218,9	113,0032	114,0111
758	3(5)-nitropyrazole	(C3H3N3O2)	196,2	113,0225	114,0304
759	3-fluoro-pyridine-1-oxide	(C5H4FNO)	215,1	113,0277	114,0355
760	1,1,1-Trifluorotrimethylamine	(C3H6F3N)	192,3	113,0452	114,0531
761	CF3CH2NHCH3	(C3H6F3N)	210,4	113,0452	114,0531
762	Propylamine, 3,3,3-trifluoro-	(C3H6F3N)	212,0	113,0452	114,0531
763	2-propenamide, N,N,2-trimethyl-	(C6H11NO)	218,0	113,0841	114,0919
764	2-Piperidinone, 1-methyl-	(C6H11NO)	219,6	113,0841	114,0919
765	Acetylpyrrolidine	(C6H11NO)	221,7	113,0841	114,0919
766	Butenamide, N,N-dimethyl-	(C6H11NO)	222,7	113,0841	114,0919
767	c-C6H11CH2NH2	(C7H15N)	221,6	113,1204	114,1283
768	(CH3)2NC(C2H5)=CHCH3	(C7H15N)	237,0	113,1204	114,1283
769	Carbonothioic dichloride	(CCl2S)	179,9	113,9098	114,9176
770	Acetic acid, trifluoro-	(C2HF3O2)	170,0	113,9929	115,0007
771	Benzene, 1,4-difluoro-	(C6H4F2)	172,1	114,0281	115,0359
772	Benzene, 1,2-difluoro-	(C6H4F2)	174,8	114,0281	115,0359
773	Benzene, 1,3-difluoro-	(C6H4F2)	179,2	114,0281	115,0359
774	2,2,2-Trifluoroethyl methyl ether	(C3H5F3O)	178,8	114,0292	115,0371
775	cyclopentane carboxylic acic	(C6H10O2)	195,5	114,0681	115,0759
776	CH3COCH2CH2COCH3	(C6H10O2)	213,2	114,0681	115,0759
777	1,3-Dimethyl-2-imidazolidinone	(C5H10N2O)	219,6	114,0793	115,0871
778	Cyclohexanemethanol	(C7H14O)	191,8	114,1045	115,1123
779	1-Methoxycyclohexane	(C7H14O)	201,0	114,1045	115,1123
780	4-Heptanone	(C7H14O)	202,1	114,1045	115,1123
781	3-Pentanone, 2,4-dimethyl-	(C7H14O)	203,2	114,1045	115,1123
782	Pyridazine hexahydro-1,2-dimethyl-	(C6H14N2)	231,0	114,1157	115,1235
783	(CH3)2N-CH=N-(n-propyl)	(C6H14N2)	241,9	114,1157	115,1235
784	(CH3)2N-CH=N-(1-methylethyl)	(C6H14N2)	242,5	114,1157	115,1235
785	(CH3)2N-C(CH3)=NC2H5	(C6H14N2)	245,9	114,1157	115,1235
786	Proline	(C5H9NO2)	220,0	115,0633	116,0712
787	N,N-Dimethylbutyramide	(C6H13NO)	220,4	115,0997	116,1075
788	Acetamide, N,N-diethyl-	(C6H13NO)	221,3	115,0997	116,1075
789	c-C5H10N(2-OCH3)	(C6H13NO)	229,0	115,0997	116,1075
790	Methanehydrazonamide, N,N,N',N'-tetramethyl-	(C5H13N3)	238,0	115,1109	116,1188
791	N,N,N',N'-Tetramethylguanidine	(C5H13N3)	246,6	115,1109	116,1188
792	1-Heptanamine	(C7H17N)	220,4	115,1361	116,1439
793	(CH3)3CCH2N(CH3)2	(C7H17N)	231,7	115,1361	116,1439
794	1-Propanamine, N,N-diethyl-	(C7H17N)	233,9	115,1361	116,1439
795	(t-C5H11)(CH3)2N	(C7H17N)	234,8	115,1361	116,1439
796	(i-C3H7)N(C2H5)2	(C7H17N)	238,0	115,1361	116,1439
797	CF3CFO	(C2F4O)	159,9	115,9885	116,9964
798	3-Methylphenylacetylene	(C9H8)	201,8	116,0626	117,0704
799	Indene	(C9H8)	203,1	116,0626	117,0704
800	Benzene, 1-ethynyl-4-methyl-	(C9H8)	204,6	116,0626	117,0704
801	(CH2)5PCH3	(C6H13P)	231,7	116,0755	117,0833
802	4-Hydroxy-4-methylpentan-2-one	(C6H12O2)	196,7	116,0837	117,0916
803	trans-1,3-cyclohexanol	(C6H12O2)	198,0	116,0837	117,0916

No.	Name	Formel	PA (kcal/mol)	Masse	prot mass
804	Propanoic acid, 2,2-dimethyl-, methyl ester	(C6H12O2)	202,4	116,0837	117,0916
805	cis-1,3-cyclohexandiol	(C6H12O2)	210,5	116,0837	117,0916
806	Urea, tetramethyl-	(C5H12N2O)	222,5	116,0950	117,1028
807	Propane, 2-methyl-2-(1-methylethoxy)-	(C7H16O)	208,0	116,1201	117,1279
808	N,N'-Diethyl-N,N'-dimethylhydrazine	(C6H16N2)	230,4	116,1313	117,1392
809	Propyltrimethylhydrazine	(C6H16N2)	231,2	116,1313	117,1392
810	1,6-Hexanediamine	(C6H16N2)	236,9	116,1313	117,1392
811	1,2-Ethanediamine, N,N,N',N'-tetramethyl-	(C6H16N2)	242,3	116,1313	117,1392
812	Benzeneacetonitrile	(C8H7N)	192,7	117,0578	118,0657
813	4-H2N-C6H4-CCH	(C8H7N)	218,9	117,0578	118,0657
814	Indole	(C8H7N)	223,2	117,0578	118,0657
815	(CH3)2NCOOC2H5	(C5H11NO2)	214,4	117,0790	118,0868
816	Valine	(C5H11NO2)	217,6	117,0790	118,0868
817	(CH3)3SiN(CH3)2	(C5H15NSi)	231,0	117,0974	118,1052
818	NH2(CH2)6OH	(C6H15NO)	228,7	117,1154	118,1232
819	Benzonitrile, 3-amino-	(C7H6N2)	201,3	118,0531	119,0609
820	1H-Indazole	(C7H6N2)	215,5	118,0531	119,0609
821	1H-Pyrrolo[2,3-b]pyridine	(C7H6N2)	224,8	118,0531	119,0609
822	1H-Benzimidazole	(C7H6N2)	228,1	118,0531	119,0609
823	Imidazo[1,2-a]pyridine	(C7H6N2)	232,3	118,0531	119,0609
824	(CH3)2Ge=CH2	(C3H8Ge)	203,6	118,0626	119,0704
825	Benzene, 1-propenyl-, (E)-	(C9H10)	199,5	118,0783	119,0861
826	Benzene, cyclopropyl-	(C9H10)	199,5	118,0783	119,0861
827	(Z)-1-Phenylpropene	(C9H10)	199,9	118,0783	119,0861
828	Benzene, 1-ethenyl-3-methyl-	(C9H10)	203,0	118,0783	119,0861
829	Benzene, 1-ethenyl-2-methyl-	(C9H10)	204,4	118,0783	119,0861
830	Benzene, 1-ethenyl-4-methyl-	(C9H10)	205,9	118,0783	119,0861
831	a-Methylstyrene	(C9H10)	206,4	118,0783	119,0861
832	Propane, 1,1'-thiobis-	(C6H14S)	206,0	118,0816	119,0894
833	Diisopropyl sulfide	(C6H14S)	209,6	118,0816	119,0894
834	Phosphine, triethyl-	(C6H15P)	234,7	118,0911	119,0990
835	CH3O(CH2)4OCH3	(C6H14O2)	222,7	118,0994	119,1072
836	Benzoxazole	(C7H5NO)	213,1	119,0371	120,0449
837	CH3OC(S)N(CH3)2	(C4H9NOS)	214,9	119,0405	120,0483
838	Benzene, azido-	(C6H5N3)	196,0	119,0483	120,0562
839	Threonine	(C4H9NO3)	220,6	119,0582	120,0661
840	Aziridine, 1-phenyl-	(C8H9N)	221,4	119,0735	120,0813
841	5H-1-Pyrindine, 6,7-dihydro-	(C8H9N)	225,6	119,0735	120,0813
842	5H-2-Pyrindine, 6,7-dihydro-	(C8H9N)	226,6	119,0735	120,0813
843	1H-Indole, 2,3-dihydro-	(C8H9N)	228,7	119,0735	120,0813
844	2-Phenyl-2-propyl radical	(C9H11)	201,0	119,0861	120,0939
845	C6H5(CHC2H5) radical	(C9H11)	201,0	119,0861	120,0939
846	Arsine, trimethyl-	(C3H9As)	214,5	119,9920	120,9998
847	2,6,7-Trioxa-1-phosphabicyclo[2.2.1]heptane	(C3H5O3P)	192,3	119,9976	121,0055
848	1,1-(Dimethylthio)ethene	(C4H8S2)	222,6	120,0067	121,0146
849	C2H5S(OCH3)CO	(C4H8O2S)	199,8	120,0245	121,0323
850	4-Pyridinecarbonitrile, 1-oxide	(C6H4N2O)	208,7	120,0324	121,0402
851	3-Pyridinecarbonitrile, 1-oxide	(C6H4N2O)	210,2	120,0324	121,0402
852	3-FC6H4CCH	(C8H5F)	193,3	120,0375	121,0454
853	4-FC6H4CCH	(C8H5F)	198,3	120,0375	121,0454
854	9H-Purine	(C5H4N4)	220,1	120,0436	121,0514
855	3-CH3C6H4CHO	(C8H8O)	200,9	120,0575	121,0653
856	Benzaldehyde, 4-methyl-	(C8H8O)	203,7	120,0575	121,0653
857	Acetophenone	(C8H8O)	205,9	120,0575	121,0653
858	Benzene, propyl-	(C9H12)	188,8	120,0939	121,1017
859	Benzene, (1-methylethyl)-	(C9H12)	189,2	120,0939	121,1017
860	Benzene, 1,3,5-trimethyl-	(C9H12)	199,9	120,0939	121,1017
861	L-Cysteine	(C3H7NO2S)	215,9	121,0197	122,0276
862	Benzamide	(C7H7NO)	213,1	121,0528	122,0606
863	4-Aminobenzenecarbonal	(C7H7NO)	217,7	121,0528	122,0606
864	Ethanone, 1-(4-pyridinyl)-	(C7H7NO)	218,5	121,0528	122,0606
865	Ethanone, 1-(3-pyridinyl)-	(C7H7NO)	218,9	121,0528	122,0606
866	OP(N(CH3)2)(CH3)2	(C4H12NOP)	223,9	121,0657	122,0735
867	3-C2H5C6H4NH2	(C8H11N)	214,6	121,0891	122,0970
868	Benzenamine, 2,6-dimethyl-	(C8H11N)	215,7	121,0891	122,0970
869	Benzenamine, N-ethyl-	(C8H11N)	219,6	121,0891	122,0970
870	Benzeneethanamine	(C8H11N)	223,9	121,0891	122,0970

No.	Name	Formel	PA (kcal/mol)	Masse	prot mass
871	Benzenamine, N,N-dimethyl-	(C8H11N)	224,9	121,0891	122,0970
872	4-(i-C3H7)-C5H4N	(C8H11N)	228,0	121,0891	122,0970
873	2-(C3H7)-pyridine	(C8H11N)	228,2	121,0891	122,0970
874	2-(i-C3H7)-pyridine	(C8H11N)	228,6	121,0891	122,0970
875	Carbonodithioic acid, o,s-dimethyl ester	(C3H6OS2)	206,1	121,9860	122,9938
876	1,3,2-Dioxaphospholane,2-methoxy-	(C3H7O3P)	214,0	122,0133	123,0211
877	Benzoic acid	(C7H6O2)	196,9	122,0368	123,0446
878	CH2=CH-SeCH3	(C3H6Se)	203,2	122,0470	123,0548
879	Niacinamide	(C6H6N2O)	219,1	122,0480	123,0558
880	Benzene, (methoxymethyl)-	(C8H10O)	195,3	122,0732	123,0810
881	N,N-Dimethyl-2-pyridinamine	(C7H10N2)	227,8	122,0844	123,0922
882	N,N-Dimethyl-3-pyridinamine	(C7H10N2)	231,4	122,0844	123,0922
883	4-Pyridinamine, N,N-dimethyl-	(C7H10N2)	238,3	122,0844	123,0922
884	Benzene, nitro-	(C6H5NO2)	191,1	123,0320	124,0399
885	CF2HCON(CH3)2	(C4H7F2NO)	206,6	123,0496	124,0574
886	Benzenamine, 4-methoxy-	(C7H9NO)	215,0	123,0684	124,0762
887	Benzenamine, 2-methoxy-	(C7H9NO)	216,0	123,0684	124,0762
888	Benzenamine, 3-methoxy-	(C7H9NO)	218,2	123,0684	124,0762
889	2-(CH3OCH2)-pyridine	(C7H9NO)	225,8	123,0684	124,0762
890	1-Azabicyclo[2.2.2]octane, 3-methylene	(C8H13N)	229,6	123,1048	124,1126
891	1-Azabicyclo[2.2.2]octane, 3-methylene	(C8H13N)	229,6	123,1048	124,1126
892	Ethanol, 2-bromo-	(C2H5BrO)	183,1	123,9524	124,9602
893	4-Nitropyridine	(C5H4N2O2)	208,8	124,0273	125,0351
894	Phosphorous acid, trimethyl ester	(C3H9O3P)	221,9	124,0289	125,0368
895	3-FC6H4CHO	(C7H5FO)	194,7	124,0324	125,0403
896	Benzaldehyde, 4-fluoro-	(C7H5FO)	197,8	124,0324	125,0403
897	Benzene, (methylthio)-	(C7H8S)	208,7	124,0347	125,0425
898	4H-Pyran-4-one, 2,6-dimethyl-	(C7H8O2)	225,1	124,0524	125,0603
899	O(CH2CH2CN)2	(C6H8N2O)	194,7	124,0637	125,0715
900	2-Cyclohexenone, 5,5-dimethyl-	(C8H12O)	207,8	124,0888	125,0966
901	2,3,4,5-tetramethylfuran	(C8H12O)	219,0	124,0888	125,0966
902	3(5)-t-butylpyrazole	(C7H12N2)	220,6	124,1000	125,1079
903	n-Butylpyrazole	(C7H12N2)	222,1	124,1000	125,1079
904	1-t-Butylimidazole	(C7H12N2)	235,9	124,1000	125,1079
905	1,5-diazabicyclo[4.3.0]non-5-ene	(C7H12N2)	248,1	124,1000	125,1079
906	Pyridine, 2-(methylthio)-	(C6H7NS)	222,3	125,0299	126,0377
907	Pyridine, 3-(methylthio)-	(C6H7NS)	223,9	125,0299	126,0377
908	Pyridine, 4-(methylthio)-	(C6H7NS)	228,3	125,0299	126,0377
909	1-Azabicyclo[2.2.2]octan-3-one	(C7H11NO)	221,7	125,0841	126,0919
910	(CH3)2N-CH=N-CH2CH2CN	(C6H11N3)	233,7	125,0953	126,1031
911	1-Azabicyclo[2.2.2]octane, 4-methyl-	(C8H15N)	234,1	125,1204	126,1283
912	1,4,4-(CH3)3-1,2,3,4-tetrahydropyridine	(C8H15N)	234,2	125,1204	126,1283
913	1-azabicyclo[2.2.2]-octane, 3-methyl	(C8H15N)	234,9	125,1204	126,1283
914	1-azabicyclo[2.2.2]-octane, 2-methyl	(C8H15N)	235,9	125,1204	126,1283
915	Benzene, 1-chloro-4-methyl-	(C7H7Cl)	182,3	126,0236	127,0315
916	Benzene, 1-chloro-2-methyl-	(C7H7Cl)	184,2	126,0236	127,0315
917	Benzene, 1-chloro-3-methyl-	(C7H7Cl)	187,4	126,0236	127,0315
918	Thymine	(C5H6N2O2)	210,5	126,0429	127,0508
919	(c-C3H5)2CS	(C7H10S)	216,9	126,0503	127,0581
920	c-C6H11COCH3	(C8H14O)	201,1	126,1045	127,1123
921	Cyclooctanone	(C8H14O)	203,1	126,1045	127,1123
922	3-Amino-1-azabicyclo[2.2.2]octane	(C7H14N2)	231,3	126,1157	127,1235
923	1,2-Diazabicyclo[2.2.2]octane, 2-methyl-	(C7H14N2)	231,6	126,1157	127,1235
924	2,3-Diazabicyclo[2.2.1]heptane, 2,3-dimethyl-	(C7H14N2)	233,8	126,1157	127,1235
925	(CH3)2N-C(CH3)=N(c-C3H5)	(C7H14N2)	244,7	126,1157	127,1235
926	Iodine atom	(I)	145,4	126,9045	127,9123
927	m-Chloroaniline	(C6H6ClN)	207,8	127,0189	128,0267
928	p-Chloroaniline	(C6H6ClN)	208,9	127,0189	128,0267
929	2-Cl-4-(CH3)-pyridine	(C6H6ClN)	218,4	127,0189	128,0267
930	2-Cl-6-(CH3)-pyridine	(C6H6ClN)	218,6	127,0189	128,0267
931	1-methyl-3-nitropyrazole	(C4H5N3O2)	202,5	127,0382	128,0460
932	1-methyl-5-nitropyrazole	(C4H5N3O2)	203,4	127,0382	128,0460
933	1-Methyl-5-nitroimidizole	(C4H5N3O2)	214,1	127,0382	128,0460
934	Dimethyl(2,2-difluoroethyl)amine	(C4H8F3N)	215,9	127,0609	128,0687
935	4,4,4-Trifluorobutylamine	(C4H8F3N)	215,9	127,0609	128,0687
936	N,3,5-Trimethylpiperidine	(C8H17N)	229,6	127,1361	128,1439
937	N,3,5-Trimethylpiperidine	(C8H17N)	229,6	127,1361	128,1439

No.	Name	Formel	PA (kcal/mol)	Masse	prot mass
938	1,4,4-Trimethylpiperidine	(C8H17N)	230,8	127,1361	128,1439
939	Cyclohexanamine, N,N-dimethyl-	(C8H17N)	232,1	127,1361	128,1439
940	Xenon	(Xe)	118,6	127,9035	128,9114
941	Hydrogen iodide	(HI)	150,0	127,9123	128,9201
942	CF3C(O)OCH3	(C3H3F3O2)	177,1	128,0085	129,0163
943	2,2,2-Trifluoroethyl formate	(C3H3F3O2)	178,4	128,0085	129,0163
944	1,4-Benzenedicarbonitrile	(C8H4N2)	186,2	128,0374	129,0453
945	1,3-Benzenedicarbonitrile	(C8H4N2)	186,3	128,0374	129,0453
946	Ether, ethyl 2,2,2-trifluoroethyl	(C4H7F3O)	182,3	128,0449	129,0527
947	Naphthalene	(C10H8)	191,9	128,0626	129,0704
948	Azulene	(C10H8)	221,1	128,0626	129,0704
949	Cyclohexanecarboxylic acid	(C7H12O2)	197,3	128,0837	129,0916
950	C6H11CH2OCH3	(C8H16O)	198,6	128,1201	129,1279
951	2,2,4-Trimethyl-3-pentanone	(C8H16O)	204,9	128,1201	129,1279
952	1H-1,2-Diazepine, hexahydro-1,2-dimethyl	(C7H16N2)	231,2	128,1313	129,1392
953	(CH3)2N-CH=N-(n-butyl)	(C7H16N2)	242,2	128,1313	129,1392
954	(CH3)2N-CH=N-(2-methylpropyl)	(C7H16N2)	242,7	128,1313	129,1392
955	(CH3)2N-CH=N-(1-methylpropyl)	(C7H16N2)	243,5	128,1313	129,1392
956	(CH3)2N-CH=N(t-C4H9)	(C7H16N2)	244,2	128,1313	129,1392
957	(CH3)2N-C(CH3)=N(n-C3H7)	(C7H16N2)	246,2	128,1313	129,1392
958	(CH3)2N-C(CH3)=N(i-C3H7)	(C7H16N2)	246,5	128,1313	129,1392
959	3-chloro-pyridine-1-oxide	(C5H4ClNO)	215,6	128,9981	130,0060
960	Isoquinoline	(C9H7N)	226,5	129,0578	130,0657
961	Quinoline	(C9H7N)	227,1	129,0578	130,0657
962	N,N,N',N',N''-Pentamethylguanidine	(C6H15N3)	250,4	129,1266	130,1344
963	1-Octanamine	(C8H19N)	220,1	129,1517	130,1596
964	1-Propanamine, 2-methyl-N-(2-methylpropyl)-	(C8H19N)	229,1	129,1517	130,1596
965	1-Butanamine, N-butyl-	(C8H19N)	231,4	129,1517	130,1596
966	2-Butanamine, N-(1-methylpropyl)-	(C8H19N)	234,3	129,1517	130,1596
967	(t-C4H9)2NH	(C8H19N)	235,9	129,1517	130,1596
968	(i-C3H7)2(C2H5)N	(C8H19N)	237,5	129,1517	130,1596
969	2-Propanone, 1,1,3,3-tetrafluoro-	(C3H2F4O)	167,5	130,0042	131,0120
970	Quinoxaline	(C8H6N2)	216,0	130,0531	131,0609
971	Cinnoline	(C8H6N2)	223,8	130,0531	131,0609
972	CH3C(OCH3)=CHCOOCH3	(C6H10O3)	219,1	130,0630	131,0708
973	3,5-(CH3)2-C6H3-CCH	(C10H10)	204,0	130,0783	131,0861
974	CH2=(CH3)OSi(CH3)3	(C6H14OSi)	223,1	130,0814	131,0892
975	c-C6H11CH2SH	(C7H14S)	194,6	130,0816	131,0894
976	Heptamethylenesulfide	(C7H14S)	205,7	130,0816	131,0894
977	c-C6H11SCH3	(C7H14S)	206,7	130,0816	131,0894
978	(CH3)2N-CH=N-(2-methoxyethyl)	(C6H14N2O)	243,8	130,1106	131,1184
979	n-Butyl ether	(C8H18O)	202,2	130,1358	131,1436
980	Di-sec-butyl ether	(C8H18O)	207,0	130,1358	131,1436
981	Di-tert-butyl ether	(C8H18O)	212,2	130,1358	131,1436
982	Tert-butyl trimethylhydrazine	(C7H18N2)	231,6	130,1470	131,1548
983	Butyltrimethylhydrazine	(C7H18N2)	232,1	130,1470	131,1548
984	1,7-Diaminoheptane	(C7H18N2)	238,6	130,1470	131,1548
985	1,3-Propanediamine, N,N,N',N'-tetramethyl-	(C7H18N2)	247,6	130,1470	131,1548
986	Benzonitrile, 4-formyl-	(C8H5NO)	190,6	131,0371	132,0449
987	CH3CONHCH2COOCH3	(C5H9NO3)	213,2	131,0582	132,0661
988	2-Propyn-1-amine, N,N-di-2-propynyl-	(C9H9N)	221,2	131,0735	132,0813
989	Leucine	(C6H13NO2)	218,6	131,0946	132,1025
990	Isoleucine	(C6H13NO2)	219,4	131,0946	132,1025
991	Dimethyl(trimethylsilylmethyl)amine	(C6H17NSi)	232,9	131,1130	132,1209
992	NH2(CH2)3NH(CH2)3NH2	(C6H17N3)	233,2	131,1422	132,1501
993	Arsenic trifluoride	(AsF3)	152,2	131,9168	132,9246
994	CF3COCl	(C2ClF3O)	162,8	131,9590	132,9668
995	Hydrogen telluride	(H2Te)	176,4	132,0157	133,0235
996	1,2,3-Trifluorobenzene	(C6H3F3)	173,4	132,0187	133,0265
997	1,2,4-Trifluorobenzene	(C6H3F3)	174,4	132,0187	133,0265
998	1,3,5-Trifluorobenzene	(C6H3F3)	177,2	132,0187	133,0265
999	L-Asparagine	(C4H8N2O3)	222,0	132,0535	133,0613
1000	2-methylbenzofuran	(C9H8O)	205,3	132,0575	133,0653
1001	4-CH3O-C6H4-CCH	(C9H8O)	212,6	132,0575	133,0653
1002	1-methylindazole	(C8H8N2)	220,4	132,0687	133,0766
1003	2-Methyl-2H-indazole	(C8H8N2)	225,6	132,0687	133,0766
1004	1-methylbenzimidazole	(C8H8N2)	231,2	132,0687	133,0766

No.	Name	Formel	PA (kcal/mol)	Masse	prot mass
1005	5-Methylimidazo(1,2-a)pyridine	(C8H8N2)	236,0	132,0687	133,0766
1006	2-Methylimidazo(1,2-a)pyridine	(C8H8N2)	236,8	132,0687	133,0766
1007	7-Methylimidazo(1,2-a)pyridine	(C8H8N2)	237,7	132,0687	133,0766
1008	Thiourea, tetramethyl-	(C5H12N2S)	226,5	132,0721	133,0799
1009	Tetralin	(C10H12)	193,6	132,0939	133,1017
1010	Benzene, 1-cyclopropyl-3-methyl-	(C10H12)	199,8	132,0939	133,1017
1011	Benzene, 1-cyclopropyl-2-methyl-	(C10H12)	200,9	132,0939	133,1017
1012	Benzene, 1-cyclopropyl-4-methyl-	(C10H12)	202,3	132,0939	133,1017
1013	Benzene, 1-methyl-2-(1-methylethenyl)-	(C10H12)	204,8	132,0939	133,1017
1014	Benzene, 1-methyl-3-(1-methylethenyl)-	(C10H12)	207,1	132,0939	133,1017
1015	3-CH3C6H4C(CH3)=CH2	(C10H12)	208,3	132,0939	133,1017
1016	4-CH3C6H4C(CH3)CH2	(C10H12)	210,9	132,0939	133,1017
1017	(C2H5)3SiOH	(C6H16OSi)	196,4	132,0970	133,1049
1018	(n-C3H7)2(CH3)P	(C7H17P)	235,1	132,1068	133,1146
1019	CH3O(CH2)5OCH3	(C7H16O2)	222,7	132,1150	133,1229
1020	Aspartic acid	(C4H7NO4)	217,2	133,0375	134,0453
1021	2H-Benzotriazole, 2-methyl-	(C7H7N3)	212,6	133,0640	134,0718
1022	1-methylbenzotriazole	(C7H7N3)	222,6	133,0640	134,0718
1023	4-H2NC6H4C(CH3)=CH2	(C9H11N)	222,3	133,0891	134,0970
1024	N-Phenylazetidine	(C9H11N)	223,0	133,0891	134,0970
1025	Quinoline, 5,6,7,8-tetrahydro-	(C9H11N)	227,5	133,0891	134,0970
1026	Isoquinoline, 5,6,7,8-tetrahydro-	(C9H11N)	227,5	133,0891	134,0970
1027	Methyltrioxaphosphabicycloheptane	(C4H7O3P)	197,1	134,0133	135,0211
1028	2,6,7-Trioxa-1-phosphabicyclo[2.2.2]octane	(C4H7O3P)	207,6	134,0133	135,0211
1029	((CH3)2SiH)2O	(C4H14OSi2)	202,1	134,0583	135,0661
1030	1H-Purine, 6-methyl-	(C6H6N4)	225,1	134,0592	135,0671
1031	Benzyl methyl ketone	(C9H10O)	201,4	134,0732	135,0810
1032	1-Propanone, 1-phenyl-	(C9H10O)	207,4	134,0732	135,0810
1033	Ethanone, 1-(3-methylphenyl)-	(C9H10O)	207,6	134,0732	135,0810
1034	Ethanone, 1-(4-methylphenyl)-	(C9H10O)	209,3	134,0732	135,0810
1035	(C2H5)3PO	(C6H15OP)	224,0	134,0861	135,0939
1036	Ethane, 1,1'-oxybis[2-methoxy-	(C6H14O3)	219,8	134,0943	135,1021
1037	Benzene, butyl-	(C10H14)	189,3	134,1096	135,1174
1038	Benzene, 1,2,3,5-tetramethyl-	(C10H14)	202,1	134,1096	135,1174
1039	Adenine	(C5H5N5)	225,3	135,0545	136,0623
1040	Benzamide, 4-methyl-	(C8H9NO)	214,7	135,0684	136,0762
1041	m-Toluamide	(C8H9NO)	214,7	135,0684	136,0762
1042	Acetophenone, 4'-amino-	(C8H9NO)	217,3	135,0684	136,0762
1043	N-Ethyl-N-methylaniline	(C9H13N)	224,5	135,1048	136,1126
1044	Benzenamine, N,N,3-trimethyl-	(C9H13N)	225,3	135,1048	136,1126
1045	Benzenamine, N,N,4-trimethyl-	(C9H13N)	227,1	135,1048	136,1126
1046	Benzenamine, N,N,2-trimethyl-	(C9H13N)	227,4	135,1048	136,1126
1047	Pyridine, 4-(1,1-dimethylethyl)-	(C9H13N)	228,6	135,1048	136,1126
1048	2-(t-C4H9)-pyridine	(C9H13N)	230,1	135,1048	136,1126
1049	Benzenemethanamine, N,N-dimethyl-	(C9H13N)	231,6	135,1048	136,1126
1050	2,6-(C2H5)2-pyridine	(C9H13N)	232,5	135,1048	136,1126
1051	3-ClC6H4CCH	(C8H5Cl)	194,3	136,0080	137,0158
1052	Benzene, 1-chloro-4-ethynyl-	(C8H5Cl)	199,7	136,0080	137,0158
1053	1,3,2-Dioxaphosphorinane,2-methoxy-	(C4H9O3P)	221,2	136,0289	137,0368
1054	Hypoxanthine	(C5H4N4O)	218,2	136,0385	137,0463
1055	Benzoic acid, 3-methyl-	(C8H8O2)	198,5	136,0524	137,0603
1056	Benzoic acid, 4-methyl-	(C8H8O2)	200,0	136,0524	137,0603
1057	Benzoic acid, 2-methyl-	(C8H8O2)	200,6	136,0524	137,0603
1058	Benzaldehyde, 3-methoxy-	(C8H8O2)	201,8	136,0524	137,0603
1059	Benzoic acid, methyl ester	(C8H8O2)	203,2	136,0524	137,0603
1060	Ethanone, 1-(3-hydroxyphenyl)-	(C8H8O2)	206,5	136,0524	137,0603
1061	Benzaldehyde, 4-methoxy-	(C8H8O2)	210,7	136,0524	137,0603
1062	Acetophenone, 4'-hydroxy-	(C8H8O2)	211,3	136,0524	137,0603
1063	CH2=C(CH3)-SeCH3	(C4H8Se)	210,3	136,0626	137,0704
1064	3-NH2-C6H4CONH2	(C7H8N2O)	214,7	136,0637	137,0715
1065	Benzamide, 4-amino-	(C7H8N2O)	221,2	136,0637	137,0715
1066	3-FC6H4C(CH3)=CH2	(C9H9F)	200,8	136,0688	137,0767
1067	4-FC6H4C(CH3)=CH2	(C9H9F)	206,3	136,0688	137,0767
1068	1-azabicyclo[2.2.2]-octane, 2-cyano	(C8H12N2)	221,4	136,1000	137,1079
1069	1-Azabicyclo[2.2.2]octane-4-carbonitrile	(C8H12N2)	223,4	136,1000	137,1079
1070	1-azabicyclo[2.2.2]-octane, 3-cyano	(C8H12N2)	224,0	136,1000	137,1079
1071	1,4-Benzenediamine, N,N-dimethyl-	(C8H12N2)	228,3	136,1000	137,1079

No.	Name	Formel	PA (kcal/mol)	Masse	prot mass
1072	1,5,5-Trimethyl-3-methylenecyclohexene	(C10H16)	215,0	136,1252	137,1330
1073	Benzene, 1-methyl-4-nitro-	(C7H7NO2)	194,8	137,0477	138,0555
1074	p-Aminobenzoic acid	(C7H7NO2)	206,6	137,0477	138,0555
1075	Benzoic acid, 3-amino-	(C7H7NO2)	206,6	137,0477	138,0555
1076	Anthranilic acid	(C7H7NO2)	215,5	137,0477	138,0555
1077	1-(3-pyridinyl-1-oxide)ethanone	(C7H7NO2)	218,2	137,0477	138,0555
1078	Pyridine-4-carboxylic acid, methyl ester	(C7H7NO2)	220,9	137,0477	138,0555
1079	Methyl nicotinate	(C7H7NO2)	220,9	137,0477	138,0555
1080	2-Propen-1-amine, N,N-di-2-propenyl-	(C9H15N)	232,4	137,1204	138,1283
1081	3-ClC6H4CH=CH2	(C8H7Cl)	201,2	138,0236	139,0315
1082	p-Nitroaniline	(C6H6N2O2)	206,8	138,0429	139,0508
1083	Ethanone, 1-(3-fluorophenyl)-	(C8H7FO)	202,2	138,0481	139,0559
1084	Ethanone, 1-(4-fluorophenyl)-	(C8H7FO)	205,3	138,0481	139,0559
1085	Dimethylphenylphosphine	(C8H11P)	231,8	138,0598	139,0677
1086	2-Cyclohexen-1-one, 3,5,5-trimethyl-	(C9H14O)	213,6	138,1045	139,1123
1087	1-methyl-5-t-butylpyrazole	(C8H14N2)	225,0	138,1157	139,1235
1088	1-methyl-3-t-butylpyrazole	(C8H14N2)	225,8	138,1157	139,1235
1089	3(5)-methyl-5(3)-t-butylpyrazole	(C8H14N2)	226,0	138,1157	139,1235
1090	3,5-diethyl-4-methylpyrazole	(C8H14N2)	227,7	138,1157	139,1235
1091	1,5-diazabicyclo[4.4.0]dec-6-ene (DBD)	(C8H14N2)	250,1	138,1157	139,1235
1092	Lanthanum	(La)	242,1	139,0000	140,0078
1093	p-Fluorobenzamide	(C7H6FNO)	209,7	139,0433	140,0512
1094	Benzamide, 3-fluoro-	(C7H6FNO)	209,7	139,0433	140,0512
1095	3-CH3SC6H4NH2	(C7H9NS)	215,6	139,0456	140,0534
1096	N,N-Dimethyl-4-fluoroaniline	(C8H10FN)	221,1	139,0797	140,0876
1097	2-Cyclohexenone,3-amino,5,5-dimethyl-	(C8H13NO)	226,4	139,0997	140,1075
1098	N"", N""-dimethylhistamine	(C7H13N3)	244,3	139,1109	140,1188
1099	N"", N""-dimethylhistamine	(C7H13N3)	244,3	139,1109	140,1188
1100	1,5,7-triazabicyclo[4.4.0]dec-5-ene	(C7H13N3)	252,1	139,1109	140,1188
1101	Piperidine, 1-(2-methyl-1-propenyl)-	(C9H17N)	229,8	139,1361	140,1439
1102	1-Cyclopentylpyrrolidine	(C9H17N)	233,1	139,1361	140,1439
1103	Arsabenzene	(C5H5As)	187,8	139,9607	140,9685
1104	Benzaldehyde, 3-chloro-	(C7H5ClO)	194,4	140,0029	141,0107
1105	Benzaldehyde, 4-chloro-	(C7H5ClO)	198,8	140,0029	141,0107
1106	Pyridine-1-oxide, 4-nitro-	(C5H4N2O3)	207,4	140,0222	141,0300
1107	Phosphoric acid, trimethyl ester	(C3H9O4P)	213,0	140,0238	141,0317
1108	4-(C2H5COO)-pyrazole	(C6H8N2O2)	210,5	140,0586	141,0664
1109	(CH3)2N-CH=N-CH2CF3	(C5H9F3N)	231,3	140,0687	141,0765
1110	Cyclononanone	(C9H16O)	203,9	140,1201	141,1279
1111	1,6-Diazabicyclo[4.4.0]decane	(C8H16N2)	234,0	140,1313	141,1392
1112	N,N'-Bipyrrolidine	(C8H16N2)	234,2	140,1313	141,1392
1113	2,3-Diazabicyclo[2.2.2]octane, 2,3-dimethyl-	(C8H16N2)	234,4	140,1313	141,1392
1114	CF3CON(CH3)2	(C4H6F3NO)	203,0	141,0401	142,0480
1115	trans-3-Aminobicyclo[2.2.2]octan-2-ol	(C8H15NO)	223,0	141,1154	142,1232
1116	cis-3-Aminobicyclo[2.2.2]octan-2-ol	(C8H15NO)	226,8	141,1154	142,1232
1117	Piperidine, 1-(2-methylpropyl)-	(C9H19N)	232,9	141,1517	142,1596
1118	c-C6H11CH2N(CH3)2	(C9H19N)	233,2	141,1517	142,1596
1119	Piperidine, 2,2,6,6-tetramethyl-	(C9H19N)	235,7	141,1517	142,1596
1120	Methyl iodide	(CH3I)	165,7	141,9279	142,9358
1121	CTe	(CTe)	213,2	142,0000	143,0078
1122	Acetic acid, trifluoro-, ethyl ester	(C4H5F3O2)	181,5	142,0242	143,0320
1123	Naphthalene, 2-methyl-	(C11H10)	198,9	142,0783	143,0861
1124	Naphthalene, 1-methyl-	(C11H10)	199,6	142,0783	143,0861
1125	c-C6H11COOCH3	(C8H14O2)	202,3	142,0994	143,1072
1126	5-Nonanone	(C9H18O)	203,5	142,1358	143,1436
1127	3-Pentanone, 2,2,4,4-tetramethyl-	(C9H18O)	206,0	142,1358	143,1436
1128	(CH3)2N-CH=N(n-C5H11)	(C8H18N2)	243,5	142,1470	143,1548
1129	(CH3)2N-CH=N-(1,1-dimethylpropyl)	(C8H18N2)	244,4	142,1470	143,1548
1130	(CH3)2N-C(C2H5)=N(i-C3H7)	(C8H18N2)	247,8	142,1470	143,1548
1131	(CH3)2N-C(CH3)=N(t-C4H9)	(C8H18N2)	248,1	142,1470	143,1548
1132	Acetonitrile, trichloro-	(C2Cl3N)	173,4	142,9096	143,9175
1133	Pyridine, 2-chloro-6-methoxy-	(C6H6ClNO)	216,6	143,0138	144,0216
1134	6-Chloro-1-methyl-2(1H)pyridinone	(C6H6ClNO)	218,8	143,0138	144,0216
1135	1-Naphthalenamine	(C10H9N)	216,9	143,0735	144,0813
1136	neo-C5H11CON(CH3)2	(C8H17NO)	221,8	143,1310	144,1388
1137	(CH3)2N-CH=N(CH2)2N(CH3)2	(C7H17N3)	245,9	143,1422	144,1501
1138	((CH3)2N)2C=NC2H5	(C7H17N3)	251,3	143,1422	144,1501

No.	Name	Formel	PA (kcal/mol)	Masse	prot mass
1139	Neopentyl, t-butyl amine	(C9H21N)	233,6	143,1674	144,1752
1140	(t-C4H9)C(CH3)2N(CH3)2	(C9H21N)	234,9	143,1674	144,1752
1141	1-Propanamine, N,N-dipropyl-	(C9H21N)	237,1	143,1674	144,1752
1142	Dithiouracil	(C4H4N2S2)	218,0	143,9816	144,9894
1143	CF3COSCH3	(C3H3F3OS)	183,0	143,9857	144,9935
1144	H2C=Te	(CH2Te)	190,2	144,0157	145,0235
1145	CF3CH2SC2H5	(C4H7F3S)	190,8	144,0221	145,0299
1146	4-(C6H5)-pyrazole	(C9H8N2)	216,7	144,0687	145,0766
1147	3(5)-phenylpyrazole	(C9H8N2)	218,5	144,0687	145,0766
1148	(CH3)2N-C(CH3)=N(CH2)2OCH3	(C7H16N2O)	247,6	144,1263	145,1341
1149	Tetraethylhydrazine	(C8H20N2)	228,8	144,1626	145,1705
1150	Hydrazine, 1,2-dimethyl-1,2-dipropyl	(C8H20N2)	232,3	144,1626	145,1705
1151	(CH3)2N(CH2)4N(CH3)2	(C8H20N2)	250,1	144,1626	145,1705
1152	C2F5CN	(C3F5N)	165,7	144,9951	146,0029
1153	3-CN-C6H4-COCH3	(C9H7NO)	197,2	145,0528	146,0606
1154	Benzonitrile, 4-acetyl-	(C9H7NO)	197,7	145,0528	146,0606
1155	Quinoline, 1-oxide	(C9H7NO)	225,5	145,0528	146,0606
1156	4-Chloro-1-azabicyclo[2.2.2]octane	(C7H12ClN)	226,9	145,0658	146,0737
1157	1-azabicyclo[2.2.2]-octane, 2-chloro	(C7H12ClN)	227,2	145,0658	146,0737
1158	3-Chloro-1-azabicyclo[2.2.2]octane	(C7H12ClN)	227,9	145,0658	146,0737
1159	CH3CONHCH(CH3)COOCH3(N-Acetyl-L-alaninemethylester)	(C6H11NO3)	224,4	145,0739	146,0817
1160	(CH3)3Si(CH2)2N(CH3)2	(C7H19NSi)	234,4	145,1287	146,1365
1161	Acetaldehyde, trichloro-	(C2HCl3O)	172,7	145,9093	146,9171
1162	Sulfur hexafluoride	(F6S)	137,3	145,9625	146,9703
1163	L-Glutamine	(C5H10N2O3)	224,1	146,0691	147,0770
1164	Benzonitrile, 4-(dimethylamino)-	(C9H10N2)	212,6	146,0844	147,0922
1165	3-(CH3)2NC6H4CN	(C9H10N2)	213,9	146,0844	147,0922
1166	2,5-Dimethylimidazo(1,2-a)pyridine	(C9H10N2)	238,1	146,0844	147,0922
1167	2,3-Dimethylimidazo(1,2-a)pyridine	(C9H10N2)	238,6	146,0844	147,0922
1168	2,7-Dimethylimidazo(1,2-a)pyridine	(C9H10N2)	239,1	146,0844	147,0922
1169	Lysine	(C6H14N2O2)	238,0	146,1055	147,1134
1170	Di-n-butyl sulfide	(C8H18S)	208,5	146,1129	147,1207
1171	Di-tert-butyl sulfide	(C8H18S)	213,7	146,1129	147,1207
1172	2-(CF3)-pyridine	(C6H4F3N)	212,1	147,0296	148,0374
1173	3-(CF3)-pyridine	(C6H4F3N)	213,3	147,0296	148,0374
1174	Pyridine, 4-trifluoromethyl-	(C6H4F3N)	213,6	147,0296	148,0374
1175	L-Glutamic acid	(C5H9NO4)	218,2	147,0532	148,0610
1176	c-C5H9N,2-CH2Cl,1-CH3	(C7H14ClN)	227,2	147,0815	148,0893
1177	N-Phenylpyrrolidine	(C10H13N)	225,0	147,1048	148,1126
1178	Methane, bromotrifluoro-	(CBrF3)	138,5	147,9135	148,9214
1179	Ethanol, 2,2,2-trichloro-	(C2H3Cl3O)	174,5	147,9249	148,9328
1180	Benzonitrile, 4-nitro-	(C7H4N2O2)	185,1	148,0273	149,0351
1181	Benzonitrile, 3-nitro-	(C7H4N2O2)	186,8	148,0273	149,0351
1182	4-Methyl-2,6,7-trioxa-1-phosphabicyclo[2.2.2]octane	(C5H9O3P)	211,0	148,0289	149,0368
1183	4-CH3S-C6H4-CCH	(C9H8S)	212,2	148,0347	149,0425
1184	Di(1-pyrazolyl)methane	(C7H8N4)	221,1	148,0749	149,0827
1185	c-P(O)CH3N(CH3)CH2CH2N(CH3)	(C5H13N2OP)	226,4	148,0765	149,0844
1186	2,6-(CH3)=C6H3-COCH3	(C10H12O)	205,0	148,0888	149,0966
1187	3-CH3OC6H4C(CH3)=CH2	(C10H12O)	208,7	148,0888	149,0966
1188	2,5-(CH3)=C6H3-COCH3	(C10H12O)	208,8	148,0888	149,0966
1189	2,3-(CH3)=C6H3-COCH3	(C10H12O)	209,0	148,0888	149,0966
1190	3,5-(CH3)=C6H3-COCH3	(C10H12O)	209,4	148,0888	149,0966
1191	2,4-(CH3)=C6H3-COCH3	(C10H12O)	210,9	148,0888	149,0966
1192	3,4-(CH3)=C6H3-COCH3	(C10H12O)	211,1	148,0888	149,0966
1193	4-CH3OC6H4C(CH3)=CH2	(C10H12O)	217,9	148,0888	149,0966
1194	nornicotine	(C9H12N2)	230,3	148,1000	149,1079
1195	(CH3)2N-CH=N-phenyl	(C9H12N2)	235,2	148,1000	149,1079
1196	Benzene, pentamethyl-	(C11H16)	203,3	148,1252	149,1330
1197	L-Methionine	(C5H11NO2S)	223,2	149,0510	150,0589
1198	Benzaldehyde, 4-(dimethylamino)-	(C9H11NO)	221,1	149,0841	150,0919
1199	Benzamide, N,N-dimethyl-	(C9H11NO)	223,0	149,0841	150,0919
1200	Benzenamine, N,N,2,6-tetramethyl-	(C10H15N)	228,0	149,1204	150,1283
1201	Benzenamine, N,N,3,5-tetramethyl-	(C10H15N)	228,5	149,1204	150,1283
1202	Benzenamine, N,N-diethyl-	(C10H15N)	229,4	149,1204	150,1283
1203	CF3SO3H	(CHF3O3S)	167,3	149,9598	150,9677
1204	Benzene, 1,2,3,4-tetrafluoro-	(C6H2F4)	167,8	150,0093	151,0171
1205	Benzene, 1,2,4,5-tetrafluoro-	(C6H2F4)	178,4	150,0093	151,0171

No.	Name	Formel	PA (kcal/mol)	Masse	prot mass
1206	Benzene, 1,2,3,5-tetrafluoro-	(C6H2F4)	178,6	150,0093	151,0171
1207	3-F-4-CH3O-C6H3-CCH	(C9H7FO)	208,7	150,0481	151,0559
1208	Benzoic acid, 3-methyl-, methyl ester	(C9H10O2)	204,5	150,0681	151,0759
1209	Benzoic acid, 2-methyl-, methyl ester	(C9H10O2)	204,9	150,0681	151,0759
1210	Benzoic acid, 4-methyl-, methyl ester	(C9H10O2)	205,4	150,0681	151,0759
1211	Ethanone, 1-(3-methoxyphenyl)-	(C9H10O2)	208,3	150,0681	151,0759
1212	Acetophenone, 4'-methoxy-	(C9H10O2)	213,8	150,0681	151,0759
1213	Pentamethylphosphonic diamide	(C5H15N2OP)	227,4	150,0922	151,1000
1214	3-(CH2Cl)-C6H4-CN	(C8H6ClN)	194,0	151,0189	152,0267
1215	4-(CH2Cl)-C6H4-CN	(C8H6ClN)	194,3	151,0189	152,0267
1216	Benzaldehyde, 4-nitro-	(C7H5NO3)	190,1	151,0269	152,0348
1217	6H-Purin-6-one, 2-amino-1,7-dihydro-	(C5H5N5O)	229,2	151,0494	152,0572
1218	Benzene, 2,4-dimethyl-1-nitro-	(C8H9NO2)	198,6	151,0633	152,0712
1219	Benzoic acid, 4-amino-, methyl ester	(C8H9NO2)	211,1	151,0633	152,0712
1220	p-Methoxybenzamide	(C8H9NO2)	214,5	151,0633	152,0712
1221	m-Methoxybenzamide	(C8H9NO2)	214,7	151,0633	152,0712
1222	N,N,N',N'-Tetramethylphosphorotriamide	(C4H14N3OP)	226,3	151,0874	152,0953
1223	3-Methoxy-N,N-dimethylbenzenamine	(C9H13NO)	220,1	151,0997	152,1075
1224	Benzenamine, 4-methoxy-N,N-dimethyl-	(C9H13NO)	226,8	151,0997	152,1075
1225	Tricyclo[3.3.1.1(3,7)]decane-1-amine	(C10H17N)	226,8	151,1361	152,1439
1226	4-ClC6H4C(CH3)=CH2	(C9H9Cl)	204,3	152,0393	153,0471
1227	3-HO-C6H4-COOCH3	(C8H8O3)	202,9	152,0473	153,0552
1228	4-HO-C6H4-COOCH3	(C8H8O3)	206,2	152,0473	153,0552
1229	Benzenamine, N-methyl-4-nitro-	(C7H8N2O2)	213,2	152,0586	153,0664
1230	Biphenylene	(C12H8)	202,8	152,0626	153,0704
1231	Camphor	(C10H16O)	205,4	152,1201	153,1279
1232	1,8-diazabicyclo[5.4.0]undec-7-ene	(C9H16N2)	250,4	152,1313	153,1392
1233	h5-Cyclopentadienylnitrosylnickel	(C5H5NNiO)	198,8	153,0371	154,0449
1234	4-NO2-C6H4CH2OH	(C7H7NO3)	193,7	153,0426	154,0504
1235	4-Trifluoromethylpiperidine	(C6H10F3N)	221,0	153,0765	154,0844
1236	7-methyl-1,5,7-triazabicyclo[4.4.0]dec-5-ene	(C8H15N3)	253,9	153,1266	154,1344
1237	1-Azabicyclo[3.3.3]undecane	(C10H19N)	230,6	153,1517	154,1596
1238	6-Chloropurine	(C5H3ClN4)	208,9	154,0046	155,0124
1239	Acetophenone, 3'-chloro-	(C8H7ClO)	202,5	154,0185	155,0264
1240	Ethanone, 1-(4-chlorophenyl)-	(C8H7ClO)	204,9	154,0185	155,0264
1241	3-F-C6H4-COOCH3	(C8H7FO2)	198,9	154,0430	155,0508
1242	4-F-C6H4-COOCH3	(C8H7FO2)	201,0	154,0430	155,0508
1243	(CH3)2(C6H5)PO	(C8H11OP)	217,4	154,0548	155,0626
1244	3(5)-methyl-5(3)-ethoxycarbonylpyrazole	(C7H10N2O2)	215,9	154,0742	155,0821
1245	Biphenyl	(C12H10)	194,5	154,0783	155,0861
1246	Acenaphthene	(C12H10)	203,7	154,0783	155,0861
1247	2-Cyclohexen-1-one,3-methoxy,5,5-dimethyl-	(C9H14O2)	220,6	154,0994	155,1072
1248	1,5-Diazabicyclo[3.3.3]undecane	(C9H18N2)	232,2	154,1470	155,1548
1249	1-Azabicyclo[2.2.2]octane,4-N,N-dimethylamino-	(C9H18N2)	235,2	154,1470	155,1548
1250	(CH3)2N-CH=N-(c-hexyl)	(C9H18N2)	244,0	154,1470	155,1548
1251	Methyl rhenium pentacarbonyl	(C6H3O5Re)	186,2	154,9980	156,0059
1252	Benzamide, 4-chloro-	(C7H6ClNO)	209,7	155,0138	156,0216
1253	3-Chlorobenzamide	(C7H6ClNO)	209,7	155,0138	156,0216
1254	Benzenamine, 4-chloro-N,N-dimethyl-	(C8H10ClN)	220,7	155,0502	156,0580
1255	L-Histidine	(C6H9N3O2)	236,1	155,0695	156,0773
1256	Iodoethane	(C2H5I)	173,2	155,9436	156,9514
1257	Benzene, bromo-	(C6H5Br)	180,2	155,9575	156,9653
1258	o,o',o''-Trimethyl thiophosphate	(C3H9O3PS)	211,3	156,0010	157,0088
1259	Sulfone, methyl phenyl	(C7H8O2S)	194,3	156,0245	157,0323
1260	CF3CO2(n-C3H7)	(C5H7F3O2)	182,7	156,0398	157,0476
1261	CF3CH2COOC2H5	(C5H7F3O2)	190,7	156,0398	157,0476
1262	1-Piperidinyloxy, 2,2,6,6-tetramethyl-	(C9H18NO)	210,6	156,1388	157,1467
1263	(CH3)2N-CH=N-(n-hexyl)	(C9H20N2)	243,3	156,1626	157,1705
1264	(CH3)2N-C(CH3)=N(n-C5H11)	(C9H20N2)	247,2	156,1626	157,1705
1265	(C2H5)2N-C(CH3)=N(n-C3H7)	(C9H20N2)	248,0	156,1626	157,1705
1266	(CH3)2N-C(C2H5)=N(t-C4H9)	(C9H20N2)	249,3	156,1626	157,1705
1267	Pyridine, 2-bromo-	(C5H4BrN)	214,9	156,9527	157,9605
1268	Pyridine, 3-bromo-	(C5H4BrN)	215,8	156,9527	157,9605
1269	4-Bromopyridine	(C5H4BrN)	217,7	156,9527	157,9605
1270	(CH3)2NC(CH3)=N(CH2)2N(CH3)2	(C8H19N3)	250,5	157,1579	158,1657
1271	((CH3)2N)2C=N(i-C3H7)	(C8H19N3)	252,3	157,1579	158,1657
1272	(CH3)2N-CH=N-(CH2)3N(CH3)2	(C8H19N3)	252,7	157,1579	158,1657

No.	Name	Formel	PA (kcal/mol)	Masse	prot mass
1273	1-Decanamine	(C10H23N)	220,4	157,1830	158,1909
1274	3,5-dinitropyrazole	(C3H2N4O4)	181,5	158,0076	159,0154
1275	3-Chloro-5,5-dimethylcyclohex-2-enone	(C8H11ClO)	207,5	158,0498	159,0577
1276	3(5)-methyl-5(3)-phenylpyrazole	(C10H10N2)	223,1	158,0844	159,0922
1277	1-methyl-3-phenylpyrazole	(C10H10N2)	223,2	158,0844	159,0922
1278	1-methyl-5-phenylpyrazole	(C10H10N2)	223,6	158,0844	159,0922
1279	1,8-Naphthalenediamine	(C10H10N2)	225,7	158,0844	159,0922
1280	(t-C4H9)2CS	(C9H18S)	210,6	158,1129	159,1207
1281	Pentane, 1,1'-oxybis-	(C10H22O)	203,7	158,1671	159,1749
1282	2H-1,4-Ethanoquinoline, 3,4-dihydro-	(C11H13N)	234,4	159,1048	160,1126
1283	(CH3)2(t-C4H9)SiN(CH3)2	(C8H21NSi)	231,9	159,1443	160,1522
1284	(CH3)3Si(CH2)3N(CH3)2	(C8H21NSi)	234,4	159,1443	160,1522
1285	CCl3COCH3	(C3H3Cl3O)	183,7	159,9249	160,9328
1286	CF3COOCH2CH2F	(C4H4F4O2)	176,1	160,0147	161,0226
1287	2,8,9-Trioxa-1-phosphadamantane	(C6H9O3P)	214,9	160,0289	161,0368
1288	2,3,5-Trimethylimidazo(1,2-a)-pyridine	(C10H12N2)	240,7	160,1000	161,1079
1289	Benzene, (2,2-dimethyl-1-methylenepropyl)-	(C12H16)	205,1	160,1252	161,1330
1290	3-CF3C6H4NH2	(C7H6F3N)	204,8	161,0452	162,0531
1291	4-Cyanobenzoic acid methyl ester	(C9H7NO2)	195,1	161,0477	162,0555
1292	3-CN-C6H4-COOCH3	(C9H7NO2)	195,2	161,0477	162,0555
1293	Tricyclo[3.3.1.13,7]decane-1-carbonitrile	(C11H15N)	199,6	161,1204	162,1283
1294	Pyrrolidine, 1-(4-methylphenyl)	(C11H15N)	217,5	161,1204	162,1283
1295	3-(CH3)2NC6H4C(CH3)=CH2	(C11H15N)	226,2	161,1204	162,1283
1296	N-Phenylpiperidine	(C11H15N)	227,8	161,1204	162,1283
1297	4-(CH3)2NC6H4C(CH3)=CH2	(C11H15N)	230,5	161,1204	162,1283
1298	Acetic acid, trichloro-	(C2HCl3O2)	184,1	161,9042	162,9120
1299	3-CH3CO-C6H4-COCH3	(C10H10O2)	203,5	162,0681	163,0759
1300	Ethanone, 1,1'-(1,4-phenylene)bis-	(C10H10O2)	203,5	162,0681	163,0759
1301	1-(2,3-dihydro-5-benzofuranyl)-ethanone	(C10H10O2)	215,8	162,0681	163,0759
1302	Disiloxane, hexamethyl-	(C6H18OSi2)	202,2	162,0896	163,0974
1303	nicotine	(C10H14N2)	230,4	162,1157	163,1235
1304	(CH3)2N-CH=N-(4-methylphenyl)	(C10H14N2)	236,4	162,1157	163,1235
1305	(CH3)2N-CH=N-(phenylmethyl)	(C10H14N2)	242,5	162,1157	163,1235
1306	(CH3)2N-C(C6H5)=NCH3	(C10H14N2)	246,9	162,1157	163,1235
1307	Benzene, hexamethyl-	(C12H18)	205,7	162,1409	163,1487
1308	3-(NO2)C6H4C(CH3)=CH2	(C9H9NO2)	194,2	163,0633	164,0712
1309	4-(NO2)C6H4C(CH3)=CH2	(C9H9NO2)	195,0	163,0633	164,0712
1310	N,N,4-Trimethyl benzamide	(C10H13NO)	220,9	163,0997	164,1075
1311	3-CH3-C6H4CON(CH3)2	(C10H13NO)	220,9	163,0997	164,1075
1312	3-(CH3)2NC6H4COCH3	(C10H13NO)	221,9	163,0997	164,1075
1313	4-N,N-Dimethylaminoacetophenone	(C10H13NO)	222,7	163,0997	164,1075
1314	Phosphorous triamide, hexamethyl-	(C6H18N3P)	222,3	163,1238	164,1317
1315	Benzenamine, N,N-diethyl-4-methyl-	(C11H17N)	230,1	163,1361	164,1439
1316	2-C6H13(c-C5H4N)	(C11H17N)	230,3	163,1361	164,1439
1317	Benzenamine, N,N-diethyl-3-methyl-	(C11H17N)	230,4	163,1361	164,1439
1318	2,6-(i-C3H7)2-pyridine	(C11H17N)	234,2	163,1361	164,1439
1319	4-HC(O)-C6H4-COOCH3	(C9H8O3)	198,9	164,0473	165,0552
1320	1,3,2-Dioxaphosphorinane,2-methoxy-4,6-dimethyl-(2b,4a,6a)-	(C6H13O3P)	226,3	164,0602	165,0681
1321	1,3,2-Dioxaphosphorinane,2-methoxy-4,6-dimethyl-(2a,4a,6a)-	(C6H13O3P)	227,4	164,0602	165,0681
1322	(CH3)2Sn=CH2	(C3H8Sn)	214,5	164,0626	165,0704
1323	2,6-(CH3)2-C6H3-COOCH3	(C10H12O2)	204,4	164,0837	165,0916
1324	3,5-(CH3)2-C6H3-COOCH3	(C10H12O2)	206,0	164,0837	165,0916
1325	2,5-(CH3)2-C6H3-COOCH3	(C10H12O2)	206,3	164,0837	165,0916
1326	2,3-(CH3)2-C6H3-COOCH3	(C10H12O2)	206,3	164,0837	165,0916
1327	2,4-(CH3)2-C6H3-COOCH3	(C10H12O2)	207,1	164,0837	165,0916
1328	3-NH2-C6H4CON(CH3)2	(C9H12N2O)	225,8	164,0950	165,1028
1329	4-NH2-C6H4CON(CH3)2	(C9H12N2O)	227,2	164,0950	165,1028
1330	1,2-Benzenediamine, N,N,N',N'-tetramethyl-	(C10H16N2)	234,9	164,1313	165,1392
1331	Acetophenone, 4'-nitro-	(C8H7NO3)	197,1	165,0426	166,0504
1332	3-Nitroacetophenone	(C8H7NO3)	197,5	165,0426	166,0504
1333	Benzene, 1,3,5-trimethyl-2-nitro-	(C9H11NO2)	197,0	165,0790	166,0868
1334	L-Phenylalanine	(C9H11NO2)	220,6	165,0790	166,0868
1335	2-Propanone, 1,1,1,3,3,3-hexafluoro-	(C3F6O)	160,2	165,9853	166,9932
1336	3-Cl-4-CH3O-C6H3-CCH	(C9H7ClO)	208,7	166,0185	167,0264
1337	Benzamide, 4-nitro-	(C7H6N2O3)	202,1	166,0378	167,0457
1338	Benzamide, 3-nitro-	(C7H6N2O3)	204,3	166,0378	167,0457
1339	3-CH3S-C6H4-COCH3	(C9H10OS)	207,2	166,0452	167,0531

No.	Name	Formel	PA (kcal/mol)	Masse	prot mass
1340	4-CH3S-C6H4-COCH3	(C9H10OS)	212,1	166,0452	167,0531
1341	3-CH3O-C6H4-COOCH3	(C9H10O3)	204,6	166,0630	167,0708
1342	Benzoic acid, 4-methoxy-, methyl ester	(C9H10O3)	207,9	166,0630	167,0708
1343	Benzenamine, N,N-dimethyl-4-nitro-	(C8H10N2O2)	213,7	166,0742	167,0821
1344	Benzenamine, N,N-dimethyl-3-nitro-	(C8H10N2O2)	213,8	166,0742	167,0821
1345	Fluorene	(C13H10)	199,6	166,0783	167,0861
1346	Adamantylmethylether	(C11H18O)	205,7	166,1358	167,1436
1347	4-Methylcamphor	(C11H18O)	206,4	166,1358	167,1436
1348	N,N-Dimethyl p-fluorobenzamide	(C9H10FNO)	221,2	167,0746	168,0825
1349	3-F-C6H4CON(CH3)2	(C9H10FNO)	221,2	167,0746	168,0825
1350	N,N,2,6-Tetramethylaniline,4-fluoro	(C10H14FN)	225,5	167,1110	168,1189
1351	tricyclo[4.4.0.03,8]decan-4-ol-5-amino, stereoisomer	(C10H17NO)	221,9	167,1310	168,1388
1352	tricyclo[4.4.0.03,8]decan-4-ol-5-amino, stereoisomer	(C10H17NO)	226,4	167,1310	168,1388
1353	tricyclo[4.4.0.03,8]decan-4-ol-5-amino, stereoisomer	(C10H17NO)	226,9	167,1310	168,1388
1354	2-Cyclohexenone,3-(N,N-dimethylamino)-5,5-dimethyl-	(C10H17NO)	235,1	167,1310	168,1388
1355	7-ethyl-1,5,7-triazabicyclo[4.4.0]dec-5-ene (ETBD)	(C9H17N3)	255,3	167,1422	168,1501
1356	Benzene, pentafluoro-	(C6HF5)	165,4	167,9998	169,0077
1357	2-Propanol, 1,1,1,3,3,3-hexafluoro-	(C3H2F6O)	164,2	168,0010	169,0088
1358	1,3,5-Trimethoxybenzene	(C9H12O3)	221,6	168,0786	169,0865
1359	1,3-dimethyl-5-ethoxycarbonylpyrazole	(C8H12N2O2)	221,2	168,0899	169,0977
1360	1,5-dimethyl-3-ethoxycarbonylpyrazole	(C8H12N2O2)	223,4	168,0899	169,0977
1361	Diphenylmethane	(C13H12)	191,8	168,0939	169,1017
1362	1,1'-Biphenyl, 2-methyl-	(C13H12)	195,0	168,0939	169,1017
1363	1,1'-Biphenyl, 4-methyl-	(C13H12)	195,5	168,0939	169,1017
1364	1,1'-Biphenyl, 3-methyl-	(C13H12)	197,9	168,0939	169,1017
1365	thiocamphor	(C10H16S)	211,2	168,0973	169,1051
1366	1,1'-Bipiperidine	(C10H20N2)	234,6	168,1626	169,1705
1367	Pyridine, pentafluoro-	(C5F5N)	182,9	168,9951	170,0029
1368	CF3CONH(n-C4H9)	(C6H10F3NO)	203,4	169,0714	170,0793
1369	2-Naphthalenol, 3-aminodecahydro-(2 ,3$, 4"", 8""$)	(C10H19NO)	226,4	169,1467	170,1545
1370	Benzene, 1-bromo-4-methyl-	(C7H7Br)	185,3	169,9731	170,9809
1371	Benzene, 1-bromo-2-methyl-	(C7H7Br)	185,3	169,9731	170,9809
1372	Benzene, 1-bromo-3-methyl-	(C7H7Br)	186,9	169,9731	170,9809
1373	Nickel tetracarbonyl	(C4NiO4)	177,5	169,9797	170,9875
1374	3-Cl-C6H4-COOCH3	(C8H7ClO2)	199,5	170,0135	171,0213
1375	4-Chlorobenzoic acid methyl ester	(C8H7ClO2)	201,1	170,0135	171,0213
1376	3-CF3-C6H4-CCH	(C9H5F3)	193,0	170,0343	171,0422
1377	CF3CO2(n-C4H9)	(C6H9F3O2)	182,9	170,0555	171,0633
1378	(CH3)2N-C(CH3)=N(n-C6H13)	(C10H22N2)	246,9	170,1783	171,1861
1379	(CH3)2N-C(C2H5)=N(n-C5H11)	(C10H22N2)	248,0	170,1783	171,1861
1380	3-BrC6H4NH2	(C6H6BrN)	208,7	170,9684	171,9762
1381	4-Trifluoromethylbenzoic acid nitrile	(C8H4F3N)	188,0	171,0296	172,0374
1382	3-(CF3)-C6H4-CN	(C8H4F3N)	189,1	171,0296	172,0374
1383	((CH3)2N)2C=N(t-C4H9)	(C9H21N3)	253,8	171,1735	172,1814
1384	(CH3)2NC(CH3)=N-(CH2)3N(CH3)2	(C9H21N3)	257,5	171,1735	172,1814
1385	Carbon diselenide	(CSe2)	173,3	172,0000	173,0078
1386	1-methyl-3,5-dinitropyrazole	(C4H4N4O4)	188,3	172,0233	173,0311
1387	3-CF3C6H4CH=CH2	(C9H7F3)	193,9	172,0500	173,0578
1388	3(5)-ethyl-5(3)-phenylpyrazole	(C11H12N2)	224,1	172,1000	173,1079
1389	1,5-dimethyl-3-phenylpyrazole	(C11H12N2)	227,8	172,1000	173,1079
1390	1,3-dimethyl-5-phenylpyrazole	(C11H12N2)	228,4	172,1000	173,1079
1391	Hydrazine, N,N'-dibutyl-N,N'-dimethyl-	(C10H24N2)	233,2	172,1939	173,2018
1392	Hydrazine, 1,2-di-isobutyl 1,2-dimethyl-	(C10H24N2)	234,2	172,1939	173,2018
1393	(CH3)2N(CH2)6N(CH3)2	(C10H24N2)	248,0	172,1939	173,2018
1394	(CH3)2N-CH=N-(4-cyanophenyl)	(C10H11N3)	227,5	173,0953	174,1031
1395	Ethanone, 2,2,2-trifluoro-1-phenyl-	(C8H5F3O)	191,2	174,0292	175,0371
1396	p-CF3C6H4CHO	(C8H5F3O)	192,5	174,0292	175,0371
1397	l-Arginine	(C6H14N4O2)	251,2	174,1117	175,1195
1398	N,N,2,6-Tetramethyl-4-cyanoaniline	(C11H14N2)	218,4	174,1157	175,1235
1399	""-t-butylstyrene,3-CH3	(C13H18)	207,1	174,1409	175,1487
1400	""-t-butylstyrene,4-CH3	(C13H18)	208,8	174,1409	175,1487
1401	CCl3CH2N(CH3)2	(C4H8Cl3N)	218,2	174,9722	175,9801
1402	Lutetium	(Lu)	237,1	175,0000	176,0078
1403	1-H-Azepine, hexahydro-1-phenyl	(C12H17N)	228,6	175,1361	176,1439
1404	Silane,trimethyl(1-phenylethenyl)-	(C11H16Si)	205,8	176,1021	177,1100
1405	12-Crown-4	(C8H16O4)	221,6	176,1049	177,1127
1406	Ethanone, 1-[4-(1,1-dimethylethyl)phenyl]-	(C12H16O)	211,0	176,1201	177,1279

No.	Name	Formel	PA (kcal/mol)	Masse	prot mass
1407	(CH3)2N-C(4-CH3-C6H4)=NCH3	(C11H16N2)	248,0	176,1313	177,1392
1408	OP(n-C3H7)3	(C9H21OP)	226,6	176,1330	177,1408
1409	(i-C3H7)3PO	(C9H21OP)	228,1	176,1330	177,1408
1410	c-OP[N(CH3)2]N(CH3)CH2CH2N(CH3)	(C6H16N3OP)	230,0	177,1031	178,1109
1411	Pyrrolidine, 1-(4-methoxyphenyl)	(C11H15NO)	229,7	177,1154	178,1232
1412	(CH3)2NC6H4(t-C4H9)	(C12H19N)	230,0	177,1517	178,1596
1413	N,N-Di-(n-propyl)benzenamine	(C12H19N)	230,1	177,1517	178,1596
1414	4-CH3COO-C6H4-COCH3	(C10H10O3)	203,7	178,0630	179,0708
1415	4-CH3SC6H4C(CH3)=CH2	(C10H12NS)	226,1	178,0690	179,0769
1416	Phenanthrene	(C14H10)	197,3	178,0783	179,0861
1417	Anthracene	(C14H10)	208,0	178,0783	179,0861
1418	2,4,6-(CH3)3-C6H2-COOCH3	(C11H14O2)	206,9	178,0994	179,1072
1419	Nikethamide	(C10H14N2O)	225,0	178,1106	179,1184
1420	""-t-butylstyrene,3-F	(C12H15F)	200,3	178,1158	179,1236
1421	2,5,8,11-Tetraoxadodecane	(C8H18O4)	226,5	178,1205	179,1283
1422	1-Adamantyl methyl ketone	(C12H18O)	206,1	178,1358	179,1436
1423	Acridine	(C13H9N)	232,5	179,0735	180,0813
1424	4-(CH3)2NC6H4COOCH3	(C10H13NO2)	220,1	179,0946	180,1025
1425	3-CH3O-C6H4CON(CH3)2	(C10H13NO2)	220,9	179,0946	180,1025
1426	3-(CH3)2NC6H4COOCH3	(C10H13NO2)	222,4	179,0946	180,1025
1427	N,N-Dimethyl 4-methoxybenzamide	(C10H13NO2)	226,7	179,0946	180,1025
1428	OP(N(CH3)2)3	(C6H18N3OP)	229,1	179,1187	180,1266
1429	Tris(2-methylallyl)amine	(C12H21N)	230,3	179,1674	180,1752
1430	N,N-Dimethyladamantylamine	(C12H21N)	237,5	179,1674	180,1752
1431	Phenazine	(C12H8N2)	224,3	180,0687	181,0766
1432	Stannane, tetramethyl-	(C4H12Sn)	196,7	180,0939	181,1017
1433	Ethylene, 1,1-diphenyl-	(C14H12)	211,6	180,0939	181,1017
1434	4-Ethylcamphor	(C12H20O)	206,9	180,1514	181,1592
1435	Furan, 2,5-bis(1,1-dimethylethyl)-	(C12H20O)	214,0	180,1514	181,1592
1436	3,5-di-t-butylpyrazole	(C11H20N2)	227,4	180,1626	181,1705
1437	4-(CH3SO2)-C6H4-CN	(C8H7NO2S)	191,1	181,0197	182,0276
1438	3-(CH3SO2)-C6H4-CN	(C8H7NO2S)	191,3	181,0197	182,0276
1439	(CF3CH2)2NH	(C4H5F6N)	200,4	181,0326	182,0404
1440	4-Nitrobenzoic acid methyl ester	(C8H7NO4)	194,2	181,0375	182,0453
1441	3-O2N-C6H4-COOCH3	(C8H7NO4)	194,7	181,0375	182,0453
1442	Pyrrolidine, 1-(4-chlorophenyl)	(C10H12ClN)	224,0	181,0658	182,0737
1443	Tyrosine	(C9H11NO3)	221,3	181,0739	182,0817
1444	7-isopropyl-1,5,7-triazabicyclo[4.4.0]dec-5-ene (ITBD)	(C10H19N3)	256,1	181,1579	182,1657
1445	3-BrC6H4CH=CH2	(C8H7Br)	196,7	181,9731	182,9809
1446	4-BrC6H4CH=CH2	(C8H7Br)	200,5	181,9731	182,9809
1447	3-Cl-4-CH3S-C6H3-CCH	(C9H7ClS)	207,9	181,9957	183,0035
1448	(CF3)2C(CH3)OH	(C4H4F6O)	165,5	182,0166	183,0245
1449	(CF3CH2)2O	(C4H4F6O)	168,9	182,0166	183,0245
1450	3-CH3S-C6H4-COOCH3	(C9H10O2S)	203,8	182,0402	183,0480
1451	4-CH3S-C6H4-COOCH3	(C9H10O2S)	206,5	182,0402	183,0480
1452	Triethyl phosphate	(C6H15O4P)	217,4	182,0708	183,0786
1453	Benzophenone	(C13H10O)	210,9	182,0732	183,0810
1454	Bibenzyl	(C14H14)	191,7	182,1096	183,1174
1455	N,N-Dimethyl p-chlorobenzamide	(C9H10ClNO)	221,2	183,0451	184,0529
1456	3-Cl-C6H4CON(CH3)2	(C9H10ClNO)	221,2	183,0451	184,0529
1457	Phenyl 3-pyridyl ketone	(C12H9NO)	222,7	183,0684	184,0762
1458	4-ClC6H4N(C2H5)2	(C10H14ClN)	222,5	183,0815	184,0893
1459	Ferrocene	(C10H10Fe)	206,4	184,0179	185,0257
1460	3-Cl-4-CH3O-C6H3-COCH3	(C9H9ClO2)	211,3	184,0291	185,0369
1461	Tributylamine	(C12H27N)	238,6	185,2143	186,2222
1462	Benzene, hexafluoro-	(C6F6)	154,7	185,9904	186,9982
1463	3-CF3C6H4C(CH3)=CH2	(C10H9F3)	197,0	186,0656	187,0735
1464	4-CF3C6H4C(CH3)CH2	(C10H9F3)	197,4	186,0656	187,0735
1465	N,N'-Dimethyl-1,8-naphthalenediamine	(C12H14N2)	229,6	186,1157	187,1235
1466	N,N'-Dimethyl-1,8-naphthalenediamine	(C12H14N2)	229,6	186,1157	187,1235
1467	Anthracene, 1,2,3,4,5,6,7,8-octahydro-	(C14H18)	202,2	186,1409	187,1487
1468	Phenanthrene, 1,2,3,4,5,6,7,8-octahydro-	(C14H18)	202,3	186,1409	187,1487
1469	4-CF3-C6H4-COCH3	(C9H7F3O)	199,5	188,0449	189,0527
1470	3-CF3-C6H4-COCH3	(C9H7F3O)	199,8	188,0449	189,0527
1471	Nickelocene	(C10H10Ni)	224,0	188,0783	189,0861
1472	""-t-butylstyrene,3,5-dimethyl	(C14H20)	208,8	188,1565	189,1643
1473	4-CF3-C6H4CONH2	(C8H6F3NO)	206,2	189,0401	190,0480

No.	Name	Formel	PA (kcal/mol)	Masse	prot mass
1474	3-CF3-C6H4CONH2	(C8H6F3NO)	207,3	189,0401	190,0480
1475	triglycine	(C6H11N3O4)	231,1	189,0750	190,0828
1476	4-CF3C6H4N(CH3)2	(C9H10F3N)	216,0	189,0765	190,0844
1477	3-CF3C6H4N(CH3)2	(C9H10F3N)	217,2	189,0765	190,0844
1478	Acetic acid, trichloro-, ethyl ester	(C4H5Cl3O2)	189,0	189,9355	190,9433
1479	Iron,methyldicarbonyl-h5-cyclopentadienyl	(C8H8FeO2)	189,4	189,9920	190,9999
1480	(CH3)2N-CH=N-(4-acetylphenyl)	(C11H14N2O)	234,2	190,1106	191,1184
1481	3-CH3-C6H4-C(Si(CH3)3)=CH2	(C12H18Si)	207,6	190,1178	191,1256
1482	4-CH3-C6H4-C(Si(CH3)3)=CH2	(C12H18Si)	209,6	190,1178	191,1256
1483	Silane, trimethyl(3-phenyl-2-propenyl)-	(C12H18Si)	210,1	190,1178	191,1256
1484	4-((CH3)3Si)C6H4C(CH3)=CH2	(C12H18Si)	210,1	190,1178	191,1256
1485	""-t-butylstyrene, 4-methoxy	(C13H18O)	214,1	190,1358	191,1436
1486	((CH3)2N)2C=N-C6H5	(C11H17N3)	248,2	191,1422	192,1501
1487	2,6-(t-C4H9)2-pyridine	(C13H21N)	234,9	191,1674	192,1752
1488	2,4-(t-C4H9)2 -pyridine	(C13H21N)	235,0	191,1674	192,1752
1489	Anthracene, 2-methyl-	(C15H12)	212,1	192,0939	193,1017
1490	Anthracene, 9-methyl-	(C15H12)	213,9	192,0939	193,1017
1491	2,3,5,6-(CH3)4-C6H-COOCH3	(C12H16O2)	207,0	192,1150	193,1229
1492	4-Tert-butylbenzoic acid methyl ester	(C12H16O2)	207,2	192,1150	193,1229
1493	(CH3)2N-CH=N-(4-nitrophenyl)	(C9H11N3O2)	227,3	193,0851	194,0930
1494	5,5-Dimethyl-3-pyrrolidino-cyclohex-2-en-1-one	(C12H19NO)	239,3	193,1467	194,1545
1495	Iron pentacarbonyl	(C5FeO5)	199,1	193,9142	194,9220
1496	1,4-Benzenedicarboxylic acid dimethyl ester	(C10H10O4)	201,6	194,0579	195,0657
1497	1,4-Benzenedicarboxylic acid dimethyl ester	(C10H10O4)	201,6	194,0579	195,0657
1498	1,3-Benzenedicarboxylic acid dimethyl ester	(C10H10O4)	201,8	194,0579	195,0657
1499	Benzamide, N,N-dimethyl-4-nitro-	(C9H10N2O3)	214,7	194,0691	195,0770
1500	3-NO2-C6H4CON(CH3)2	(C9H10N2O3)	214,7	194,0691	195,0770
1501	""-t-butylstyrene,3-Cl	(C12H15Cl)	200,5	194,0862	195,0941
1502	4-F-C6H4-C(Si(CH3)3)=CH2	(C11H15FSi)	205,2	194,0927	195,1005
1503	N,N,2,6-Tetramethyl-4-nitroaniline	C10H14N2O2	219,6	194,1055	195,1134
1504	Tricyclo[3.3.1.13,7]decane-1-carboxylic acid, methyl ester	(C12H18O2)	206,6	194,1307	195,1385
1505	3,5-di-t-butyl-4-methylpyrazole	(C12H22N2)	231,2	194,1783	195,1861
1506	1-methyl-3,5-di-t-butylpyrazole	(C12H22N2)	232,1	194,1783	195,1861
1507	C3F7CN	(C4F7N)	166,0	194,9919	195,9997
1508	Phosphorothioic triamide, hexamethyl-	(C6H18N3PS)	225,2	195,0959	196,1037
1509	3-Amino-tricyclo[7.3.0.04,8]dodecan-2-ol	(C12H21NO)	221,4	195,1623	196,1701
1510	5,5-Dimethyl-3-(diethylamino)-cyclohex-2-en-1-one	(C12H21NO)	239,3	195,1623	196,1701
1511	1-Azabicyclo[4.4.4]tetradecane	(C13H25N)	214,5	195,1987	196,2065
1512	Methane, trifluoroiodo-	(CF3I)	149,5	195,8997	196,9075
1513	Hydromanganese pentacarbonyl	(C5HMnO5)	199,8	195,9824	196,9902
1514	Benzene, 1,1'-(1,3-propanediyl)bis-	(C15H16)	196,1	196,1252	197,1330
1515	Benzene,1-methyl-3-(2-phenylethyl)-	(C15H16)	199,3	196,1252	197,1330
1516	1,6-Diazabicyclo[4.4.4]tetradecane	(C12H24N2)	226,4	196,1939	197,2018
1517	2,6-Di-t-butylpiperidine	(C13H27N)	237,2	197,2143	198,2222
1518	Azulene, 1,4-dimethyl-7-(1-methylethyl)-	(C15H18)	235,0	198,1409	199,1487
1519	3-Cl-4-CH3S-C6H3-COCH3	(C9H9ClOS)	209,8	200,0063	201,0141
1520	3-Cl-4-CH3O-C6H3-COOCH3	(C9H9ClO3)	205,0	200,0240	201,0318
1521	Phosphine, methyldiphenyl-	(C13H13P)	232,5	200,0755	201,0833
1522	N,N,N'-Trimethyl-1,8-naphthalenediamine	(C13H16N2)	235,3	200,1313	201,1392
1523	Hydrazine, N,N'-dimethyl-N,N'-dipentyl-	(C12H28N2)	233,4	200,2252	201,2331
1524	Hydrazine, 1,2-dimethyl 1,2-dineopentyl-	(C12H28N2)	233,8	200,2252	201,2331
1525	Chromium,dicarbonyl(h5-2,4-cyclopentadien-1-yl)nitrosyl-	(C7H5CrNO3)	195,9	200,9730	201,9808
1526	Fluoranthene	(C16H10)	198,9	202,0783	203,0861
1527	Pyrene	(C16H10)	207,8	202,0783	203,0861
1528	4-(1-adamantyl)-pyrazole	(C13H18N2)	218,2	202,1470	203,1548
1529	1-(1-adamantyl)pyrazole	(C13H18N2)	228,1	202,1470	203,1548
1530	4-CF3-C6H4-COOCH3	(C9H7F3O2)	197,4	204,0398	205,0476
1531	3-CF3-C6H4-COOCH3	(C9H7F3O2)	197,7	204,0398	205,0476
1532	Glycyl phenylalanyl	C11H12N2O2	226,5	204,0899	205,0977
1533	1,3-di-(t-C4H9)-5-CH3-C6H3	(C15H24)	204,1	204,1878	205,1956
1534	((CH3)2N)2C=N-(4-CH3-C6H4)	(C12H19N3)	249,6	205,1579	206,1657
1535	4-(n-C8H17)C6H4NH2	(C14H23N)	214,0	205,1830	206,1909
1536	4-CH3O-C6H4-C(Si(CH3)3)=CH2	(C12H18OSi)	215,8	206,1127	207,1205
1537	""-t-butylstyrene,4-CH3S	(C13H18S)	213,7	206,1129	207,1207
1538	(CH3)2N-CH=N-(tricyclo[3.3.1.1]dec-1-yl-)	(C13H22N2)	247,0	206,1783	207,1861
1539	N,N,2,6-Tetramethylaniline,4-carboxylic acid, methyl ester	(C12H17NO2)	226,1	207,1259	208,1338
1540	5,5-Dimethyl-3-(piperidino)cyclohex-2-en-1-one	(C13H21NO)	239,2	207,1623	208,1701

→ α-farnesen

No.	Name	Formel	PA (kcal/mol)	Masse	prot mass
1541	15,16-diazatricyclo[8.4.1.13,8]hexadeca-1,3,5,7,9,11,13-heptaene	(C14H12N2)	235,3	208,1000	209,1079
1542	Benzene, 1,1'-ethenylidenebis-[4-methyl-	(C16H16)	215,2	208,1252	209,1330
1543	1,4-dimethyl-3,5-di-t-butylpyrazole	(C13H24N2)	234,1	208,1939	209,2018
1544	3,3,6,9,9-pentamethyl-2,10-diazabicyclo[4.4.0]dec-1-ene	(C13H24N2)	248,3	208,1939	209,2018
1545	((CH3)2N)2C=N(4-FC6H4)	(C11H16FN3)	246,2	209,1328	210,1407
1546	Manganese, pentacarbonylmethyl-	(C6H3MnO5)	182,8	209,9980	211,0059
1547	Benzene, 1,1'-(1,4-butanediyl)bis-	(C16H18)	196,5	210,1409	211,1487
1548	1-Methyl-2,6-t-butylpiperidine	(C14H29N)	241,7	211,2300	212,2378
1549	3,5-diethoxycarbonylpyrazole	(C9H12N2O4)	210,7	212,0797	213,0875
1550	(C5H5)Cr(CO)3CH3	(C9H8CrO3)	205,6	213,9934	215,0012
1551	4-CH3SO2-C6H4-COOCH3	(C9H10O4S)	197,9	214,0300	215,0378
1552	3-CH3SO2-C6H4-COOCH3	(C9H10O4S)	198,6	214,0300	215,0378
1553	1,8-Naphthalenediamine, N,N,N',N'-tetramethyl-	(C14H18N2)	245,8	214,1470	215,1548
1554	3-Cl-4-CH3S-C6H3-COOCH3	(C9H9ClO2S)	204,5	216,0012	217,0090
1555	CH2=C(SeCH3)2	(C4H8Se2)	219,3	216,0626	217,0704
1556	CH3(C6H5)2PO	(C13H13OP)	217,2	216,0704	217,0782
1557	3(5)-phenyl-5(3)-ethoxycarbonylpyrazole	C12H12N2O2	215,1	216,0899	217,0977
1558	N,N-Dimethyl-p-trifluorobenzamide	C10H10F3NO	215,5	217,0714	218,0793
1559	3-CF3-C6H4CON(CH3)2	C10H10F3NO	216,2	217,0714	218,0793
1560	Chromium hexacarbonyl	(C6CrO6)	176,8	217,9155	218,9234
1561	Benzene, 1-iodo-2-methyl-	(C7H7I)	186,5	217,9592	218,9671
1562	4-SO2F-C6H4-COOCH3	(C8H7FO4S)	191,8	218,0049	219,0127

No.	Name	Formel	PA (kcal/mol)	Masse	prot mass
1563	3-SO2F-C6H4-COOCH3	(C8H7FO4S)	192,7	218,0049	219,0127
1564	Manganese, tricarbonyl[(1,2,3,4,5-h5)-1-methyl-2,4-cyclopentadien-1-yl]-	(C9H7MnO3)	199,4	218,0395	219,0473
1565	3-IC6H4NH2	(C6H6IN)	210,0	218,9545	219,9623
1566	(CO)6V	(C6O6V)	191,3	218,9695	219,9773
1567	9,5-metheno-5H,7H-pyrimido[1,6-a:3,4-a']bisazepine	(C15H12N2)	222,5	220,1000	221,1079
1568	3,5-diphenylpyrazole	(C15H12N2)	226,1	220,1000	221,1079
1569	15-Crown-5	(C10H20O5)	225,6	220,1311	221,1389
1570	(CH3)2NC(CH3)=N(1-Adam)	(C14H24N2)	251,1	220,1939	221,2018
1571	((CH3)2N)2C=N-(4-CH3O-C6H4)	(C12H19N3O)	250,4	221,1528	222,1606
1572	OP(CH2N(CH3)2)3	(C9H24N3OP)	238,5	221,1657	222,1735
1573	C6H5COCCl3	(C8H5Cl3O)	195,8	221,9406	222,9484
1574	CH3O[CH2CH2O]4CH3	(C10H22O5)	228,0	222,1467	223,1545
1575	(h5-Cyclopentadienyl)dicarbonylrhodium	(C7H5O2Rh)	211,5	224,0290	225,0368
1576	""-t-butylstyrene, 4-CH3O, 3-Cl	(C13H17ClO)	210,9	224,0968	225,1046
1577	C6H5(CH2)5C6H5	(C17H20)	194,7	224,1565	225,1643
1578	(C6H5CH2)Cr(CO)3	(C10H7CrO3)	203,8	224,9856	225,9934
1579	((CH3)2N)2C=N(4-ClC6H4)	(C11H16ClN3)	245,7	225,1033	226,1111
1580	(CH3)2N-CH=N-(4-bromophenyl)	(C9H11BrN2)	234,5	226,0106	227,0184
1581	1-methyl-3,5-diethoxycarbonylpyrazole	C10H14N2O4	218,2	226,0954	227,1032
1582	N,N,2,6-Tetramethylaniline,4-bromo-	(C10H14BrN)	223,7	227,0310	228,0388
1583	Deoxycytidine	(C9H13N3O4)	236,4	227,0906	228,0984
1584	triamylamine	(C15H33N)	223,5	227,2613	228,2691
1585	Triphenylene	(C18H12)	195,8	228,0939	229,1017
1586	Chrysene	(C18H12)	201,1	228,0939	229,1017
1587	Naphthacene	(C18H12)	216,5	228,0939	229,1017
1588	""-t-butylstyrene,4-CF3	(C13H15F3)	197,0	228,1126	229,1204
1589	""-t-butylstyrene,3-CF3	(C13H15F3)	198,4	228,1126	229,1204
1590	Stibine, triphenyl-	(C18H15Sb)	202,1	231,1174	232,1252
1591	Mercury, dimethyl-	(C2H6Hg)	184,4	232,0470	233,0548
1592	Ruthenium, bis(h5-cyclopentadienyl)	(C10H10Ru)	217,1	232,0783	233,0861
1593	N,N-Dimethylbenzenamine,2,4-di-t-butyl	(C16H27N)	232,6	233,2143	234,2222
1594	1-methyl-3,5-diphenylpyrazole	(C16H14N2)	229,0	234,1157	235,1235
1595	10,5-metheno-5H-bisazepino[1,2-d:2',1'-g][1,4]diazepine,7,8-dihydro	(C16H14N2)	230,1	234,1157	235,1235
1596	Perfluoro-tert-butylamine	(C4H2F9N)	188,0	235,0044	236,0122
1597	guanosine	C10H13N5O2	237,7	235,1069	236,1147
1598	Perfluoro-tert-butanol	(C4HF9O)	162,5	235,9884	236,9962
1599	15,16-diazatricyclo[8.4.1.13,8]hexadeca-1,3,5,7,9,11,13-heptaene,15,16-	(C16H16N2)	235,3	236,1313	237,1392
1600	trans-1,4-diphenylcyclohexane	(C18H20)	192,2	236,1565	237,1643
1601	Uranium	(U)	237,9	238,0000	239,0078
1602	C6H5(CH2)6C6H5	(C18H22)	195,1	238,1722	239,1800
1603	Thymidine	C10H14N2O5	226,8	242,0903	243,0981
1604	Cytidine	(C9H13N3O5)	234,8	243,0855	244,0933
1605	Tris(dimethylamino)phosphine selenide	C6H18N3PSe	223,1	243,1238	244,1317
1606	Uridine	(C9H12N2O6)	226,5	244,0695	245,0774
1607	i-C3H7(C6H5)2PO	(C15H17OP)	217,2	244,1017	245,1095
1608	Benzenamine, N,N-diphenyl-	(C18H15N)	217,2	245,1204	246,1283
1609	5,6-Dihydrouridine	(C9H14N2O6)	209,0	246,0852	247,0930
1610	tetraglycine	(C8H14N4O5)	232,7	246,0964	247,1042
1611	Benzene, 1,3,5-tri-tert-butyl-	(C18H30)	202,9	246,2348	247,2426
1612	11,5-metheno-5H,7H-bisazepino[1,2-a:2',1'-d][1,5]diazocine,8,9-dihydro	(C17H16N2)	233,0	248,1313	249,1392
1613	Deoxyadenosine	C10H13N5O3	237,2	251,1018	252,1097
1614	(CH3)2Pb=CH2	(C3H8Pb)	225,1	252,0626	253,0704
1615	Perylene	(C20H12)	212,4	252,0939	253,1017
1616	3,5-(CF3)2C6H3N(CH3)2	(C10H9F6N)	211,6	257,0639	258,0717
1617	t-C4H9(C6H5)2PO	(C16H19OP)	217,2	258,1174	259,1252
1618	dodecahedrane	(C20H20)	201,6	260,1565	261,1643
1619	Phosphine, triphenyl-	(C18H15P)	232,5	262,0911	263,0990
1620	12,5-metheno-5H-bisazepino[1,2-a:2',1'-d][1,5]diazonine,7,8,9,10-tetrahy	(C18H18N2)	232,6	262,1470	263,1548
1621	OP(N(C2H5)2)3	C12H30N3OP	232,9	263,2126	264,2205
1622	1,4,7,10,13,16-Hexaoxacyclooctadecane	(C12H24O6)	231,4	264,1573	265,1651
1623	trans-1,4-dibenzylcyclohexane	(C20H24)	192,7	264,1878	265,1956
1624	Molybdenum hexacarbonyl	(C6MoO6)	182,4	265,9695	266,9773
1625	adenosine	C10H13N5O4	236,6	267,0968	268,1046
1626	Deoxyguanosine	C10H13N5O4	238,2	267,0968	268,1046
1627	CTe2	(CTe2)	184,3	272,0000	273,0078
1628	Methyldodecahedrane	(C21H22)	204,5	274,1722	275,1800
1629	Benzo[ghi]perylene	(C22H12)	209,4	276,0939	277,1017

No.	Name	Formel	PA (kcal/mol)	Masse	prot mass
1630	13,5-metheno-5H,7H-bisazepino[1,2-a:2',1'-d][1,5]diazecine,8,9,10,11-te	(C19H20N2)	237,3	276,1626	277,1705
1631	(C6H5)3PO	(C18H15OP)	216,6	278,0861	279,0939
1632	Picene	(C22H14)	203,6	278,1096	279,1174
1633	2',3'-O-Isopropylideneuridine	C12H16N2O6	209,0	284,1008	285,1087
1634	1,16-Dimethyldodecahedrane	(C22H24)	209,5	288,1878	289,1956
1635	14,5-metheno-5H-bisazepino[1,2-a:2',1'-d][1,5]diazacycloundecine,7,8,9,	(C20H22N2)	233,9	290,1783	291,1861
1636	(C6H5)3PS	(C18H15PS)	216,6	294,0632	295,0710
1637	(1-adamytyl)2CO	(C21H30O)	213,8	298,2297	299,2375
1638	Coronene	(C24H12)	205,9	300,0939	301,1017
1639	Arsine, triphenyl-	(C18H15As)	217,2	306,0390	307,0468
1640	(1-adamantyl)2CS	(C21H30S)	218,1	314,2068	315,2146
1641	[(C5H5)(CO)Fe]2(:-CO)(:-C=CH2)	(C15H12Fe2O	234,8	315,9680	316,9759
1642	(C6H5)3AsO	(C18H15AsO)	216,6	322,0339	323,0417
1643	Tungsten hexacarbonyl	(C6O6W)	181,3	351,9695	352,9773
1644	(C12H25(OC2H4)7OH	(C26H54O8)	240,6	494,3819	495,3897
1645	3(5)-phenyl-5(3)-ethoxycarbonylpyrazole	(C12H	215,1	#WERT!	#WERT!

Supplementary material

Table 1 (Extended):

Meas.Mass	Theor.Mass	Sum Formula	Flour Types																		Yeasts							Tentative Identification	Ref.
			Concentration (ppb)																p-value		Concentration (ppb)						p-value		
			F1			F2			F3			F4									Y1			Y2					
			Mean		S.D.		C.V.	Mean		S.D.		C.V.	Mean		S.D.		C.V.	Mean		S.D.		C.V.								
41.038	41.039	$C_3H_5^+$	92.1	±	26.1	a	0.3	87.1	±	25.8	a	0.3	88.8	±	23.7	a	0.3	104.1	±	42.9	a	0.4	0.693	81.2	±	17.4	a	0.2	105.9	±	35.6	a	0.3	**0.02**	alkylic fragment (diverse origin)	(Makhoul et al. 2014)
42.01	n.a.	n.i.	4	±	2.1	a	0.5	3.7	±	2.2	a	0.6	3.1	±	1.8	a	0.6	2.8	±	1.6	a	0.6	0.574	4.1	±	1.9	a	0.5	2.8	±	1.7	a	0.6	0.061		
42.043	n.a.	n.i.	3.6	±	1.3	a	0.4	3.4	±	0.9	a	0.3	3.5	±	1	a	0.3	4.1	±	1.6	a	0.4	0.635	3.1	±	0.7	a	0.2	4.2	±	1.4	a	0.3	**0.011**		
43.054	43.054	$C_3H_7^+$	50.9	±	12.8	a	0.3	45.3	±	6.4	a	0.1	41.7	±	5.3	a	0.1	38.1	±	6.2	a	0.2	**0.033**	45.1	±	7.1	a	0.2	43	±	11.3	a	0.3	0.547	alkylic fragment (diverse origin)	
47.013	47.013	$CH_3O_2^+$	28.3	±	5.4	a	0.2	37.9	±	19	a	0.5	32.5	±	11	a	0.3	27.2	±	12.1	a	0.4	0.354	38.9	±	13.9	b	0.4	23.5	±	4.7	a	0.2	**0**		(Makhoul et al. 2014)
51.94	n.a.	n.i.	1.8	±	0.1	a	0.1	1.8	±	0.1	a	0.1	1.8	±	0.1	a	0.1	1.9	±	0.1	a	0.1	0.301	1.8	±	0.1	a	0.1	1.9	±	0.1	a	0.1	**0.013**		
53.038	n.a.	n.i.	1.9	±	0.3	a	0.2	2.1	±	0.3	a	0.1	2.3	±	0.6	a	0.3	2.5	±	0.8	a	0.3	0.147	2	±	0.3	a	0.2	2.5	±	0.7	a	0.3	**0.028**		
55.054	55.054	$C_4H_7^+$	18.8	±	5.8	a	0.3	18.2	±	6.8	a	0.4	22.8	±	10.1	a	0.4	29	±	15.3	a	0.5	0.154	17.3	±	5.7	a	0.3	27.4	±	12.3	b	0.4	**0.006**	fragment (butenal)	(Buhr et al. 2002)
55.934	n.a.	n.i.	5	±	0.3	a	0.1	5.1	±	0.3	a	0.1	5.2	±	0.3	a	0.1	5.3	±	0.3	a	0.1	0.231	5.1	±	0.3	a	0.1	5.3	±	0.3	a	0.1	0.063		
58.04	n.a.	n.i.	2.9	±	1	a	0.3	3.4	±	1.5	a	0.4	4.4	±	2.3	a	0.5	6.5	±	4.7	a	0.7	0.074	2.9	±	1.1	a	0.4	5.8	±	3.6	b	0.6	**0.005**		
59.049	59.049	$C_3H_7O^+$	104.6	±	37.1	a	0.4	142.9	±	51.1	a	0.4	125.3	±	59.7	a	0.5	136.7	±	64	a	0.5	0.512	136.5	±	65.4	a	0.5	117.8	±	35.7	a	0.3	0.339	Acetone	(Kohn et al. 1960)
61.028	61.028	$C_2H_5O_2^+$	244.3	±	27.4	a	0.1	279	±	45.2	a	0.2	329.2	±	88.4	a	0.3	283	±	65.7	a	0.2	0.079	272.4	±	44.2	a	0.2	293.1	±	80.7	a	0.3	0.379	Acetic acid	(Paraskevopoulou et al. 2012; Kohn et al. 1960)
67.055	67.054	$C_5H_7^+$	1.2	±	0.5	a	0.4	1.2	±	0.6	a	0.5	1.5	±	0.7	a	0.5	2.1	±	1.5	a	0.7	0.198	1.1	±	0.5	a	0.5	1.9	±	1.2	a	0.6	**0.012**	fragment (pentenal)	(Buhr et al. 2002; Paraskevopoulou et al. 2012)
69.033	69.033	$C_4H_5O^+$	7	±	2.1	a	0.3	10.8	±	4.4	a	0.4	12.9	±	5.4	a	0.4	10	±	2.4	a	0.2	**0.039**	10.4	±	4.1	a	0.4	9.8	±	4.3	a	0.4	0.733		(Makhoul et al. 2014)
69.07	69.07	$C_5H_9^+$	21.5	±	11.6	a	0.5	22.1	±	20.3	a	0.9	26.6	±	14.1	a	0.5	25.5	±	13.4	a	0.5	0.891	17.1	±	11	a	0.6	31.1	±	14.9	b	0.5	0.006	fragment (pentanal)	(Buhr et al. 2002; Makhoul et al. 2014)
71.049	71.049	$C_4H_7O^+$	142.3	±	33.2	b	0.2	122.8	±	15.4	b	0.1	110.1	±	13.1	ab	0.1	88.5	±	23	a	0.3	**0.001**	122.8	±	24.6	a	0.2	109	±	33.6	a	0.3	0.197	butenal	(Paraskevopoulou et al. 2012)
73.065	73.065	$C_4H_9O^+$	213.8	±	70.3	a	0.3	201.7	±	76.8	a	0.4	230.4	±	105.3	a	0.5	252.7	±	107.3	a	0.4	0.705	181.7	±	69.6	a	0.4	270	±	85.2	b	0.3	**0.004**	n-butyraldehyde/methylpropanal	(Kohn et al. 1960) (Paraskevopoulou et al. 2012)
75.044	75.044	$C_3H_7O_2^+$	57.8	±	8.9	a	0.2	90.6	±	27.9	a	0.3	88.9	±	25.9	a	0.3	80.8	±	16.4	a	0.2	**0.017**	84.9	±	23.9	a	0.3	73.1	±	23.3	a	0.3	0.174	Propionic acid	(Annan et al. 2003; Kohn et al. 1960)
81.034	81.034.	$C_5H_5O^+$	13.5	±	3.2	a	0.2	21.8	±	8.5	a	0.4	24.1	±	8.7	a	0.4	19.9	±	4.5	a	0.2	**0.024**	19.9	±	6.7	a	0.3	19.4	±	8.4	a	0.4	0.859	cyclopentadienone	
81.069	81.07	$C_6H_9^+$	1.3	±	0.2	a	0.2	1.3	±	0.2	a	0.2	1.4	±	0.1	a	0.1	1.2	±	0.1	a	0.1	0.154	1.2	±	0.1	a	0.1	1.3	±	0.2	a	0.2	**0.02**	fragment (hexenal)	(Buhr et al. 2002; Aprea et al. 2007)
83.086	83.086	$C_6H_{11}^+$	1.8	±	0.5	a	0.3	1.5	±	0.5	a	0.3	2.9	±	1.1	b	0.4	2.3	±	0.6	ab	0.3	**0.002**	2.1	±	0.7	a	0.3	2.1	±	1	a	0.5	0.966	hexanol fragment	(Buhr et al. 2002)
85.028	85.028	$C_4H_5O_2^+$	3.2	±	1.2	a	0.4	4.3	±	1.6	a	0.4	5.5	±	1.9	a	0.3	4.6	±	1	a	0.2	**0.041**	4.5	±	1.2	a	0.3	4.2	±	1.9	a	0.5	0.64	2-(5H)-furanone	(Paraskevopoulou et al. 2012; Buhr et al. 2002)
85.065	n.a.	$C_5H_9O^+$	1.9	±	0.5	a	0.3	2.1	±	0.7	a	0.3	2.1	±	0.6	a	0.3	2.1	±	0.6	a	0.3	0.947	2.3	±	0.7	a	0.3	1.8	±	0.4	a	0.2	**0.041**	Cyclopentanone/ 3-Penten-2-one/ 2-Pentenal/ 2,3-Dihydro-4H-pyran	(Aprea et al. 2007)
87.081	87.08	$C_5H_{11}O^+$	20.2	±	12.4	a	0.6	21.2	±	17.5	a	0.8	29	±	19.7	a	0.7	49.6	±	45	a	0.9	0.132	16.2	±	10.7	a	0.7	44.8	±	33.9	b	0.8	**0.003**	isovaleraldehyde/2-,methylbutanal/pentanal	(Kohn et al. 1960; Paraskevopoulou et al. 2012; Schieberle and Grosch 1985)
89.06	89.06	$C_4H_9O_2^+$	200	±	46.5	b	0.2	172.7	±	19.2	b	0.1	157	±	18.3	ab	0.1	126.2	±	35.4	a	0.3	**0.001**	176.3	±	33.1	a	0.2	151.3	±	46.3	a	0.3	0.094	2-Methyl -propanoic acid/ethyl acetate	(Hansen and Hansen 1994b; Paraskevopoulou et al. 2012)
90.95	n.a.	n.i.	1.2	±	0	a	0.0	1.2	±	0.1	a	0.1	1.3	±	0.1	a	0.1	1.3	±	0.1	a	0.1	**0.03**	1.2	±	0.1	a	0.1	1.3	±	0.1	a	0.1	0.581		
93.038	93.037.	$C_3H_9OS^+$	9.2	±	0.5	b	0.1	8.2	±	0.3	a	0.0	7.6	±	0.7	a	0.1	7.3	±	0.8	a	0.1	**0**	8.1	±	0.8	a	0.1	8.1	±	1.1	a	0.1	0.948	3-(methylthio)-1-propanol	from methionine metabolism	
103.076	103.075	$C_5H_{11}O_2^+$	5.5	±	2.1	a	0.4	4.8	±	2.1	a	0.4	5.8	±	1.4	a	0.2	5.9	±	2.4	a	0.4	0.765	6.8	±	1.6	b	0.2	4.1	±	1.4	a	0.3	**0**	2-Methyl-butanoic acid /pentanoic acid/ethylpropionate	(Annan et al. 2003; Paraskevopoulou et al. 2012)

Table 2 (extended):

Meas.Mass	Theor.Mass	Sum Formula	Flour Types																						Yeasts								Tentative Identification	Ref.
			Concentration (ppb)																				p-value		Concentration (ppb)								p-value		
			F1				F2				F3				F4										Y1				Y2						
			Mean		S.D.		C.V.	Mean		S.D.		C.V.	Mean		S.D.		C.V.	Mean		S.D.		C.V.			Mean		S.D.		C.V.	Mean		S.D.		C.V.			
41.038	41.039	$C_3H_5^+$	92.1	±	26.1	a	0.3	87.1	±	25.8	a	0.3	88.8	±	23.7	a	0.3	104.1	±	42.9	a	0.4	0.693	81.2	±	17.4	a	0.2	105.9	±	35.6	a	0.3	**0.02**	alkylic fragment (diverse origin)	(Makhoul et al. 2014)
42.01	n.a.	non identified	4	±	2.1	a	0.5	3.7	±	2.2	a	0.6	3.1	±	1.8	a	0.6	2.8	±	1.6	a	0.6	0.574	4.1	±	1.9	a	0.5	2.8	±	1.7	a	0.6	0.061		
42.043	n.a.	non identified	3.6	±	1.3	a	0.4	3.4	±	0.9	a	0.3	3.5	±	1	a	0.3	4.1	±	1.6	a	0.4	0.635	3.1	±	0.7	a	0.2	4.2	±	1.4	a	0.3	**0.011**		
43.054	43.054	$C_3H_7^+$	50.9	±	12.8	a	0.3	45.3	±	6.4	a	0.1	41.7	±	5.3	a	0.1	38.1	±	6.2	a	0.2	**0.033**	45.1	±	7.1	a	0.2	43	±	11.3	a	0.3	0.547	alkylic fragment (diverse origin)	
47.013	47.013	$CH_3O_2^+$	28.3	±	5.4	a	0.2	37.9	±	19	a	0.5	32.5	±	11	a	0.3	27.2	±	12.1	a	0.4	0.354	38.9	±	13.9	b	0.4	23.5	±	4.7	a	0.2	**0**		(Makhoul et al. 2014)
51.94	n.a.	non identified	1.8	±	0.1	a	0.1	1.8	±	0.1	a	0.1	1.8	±	0.1	a	0.1	1.9	±	0.1	a	0.1	0.301	1.8	±	0.1	a	0.1	1.9	±	0.1	a	0.1	**0.013**		
53.038	n.a.	non identified	1.9	±	0.3	a	0.2	2.1	±	0.3	a	0.1	2.3	±	0.6	a	0.3	2.5	±	0.8	a	0.3	0.147	2	±	0.3	a	0.2	2.5	±	0.7	a	0.3	**0.028**		
55.054	55.054	$C_4H_7^+$	18.8	±	5.8	a	0.3	18.2	±	6.8	a	0.4	22.8	±	10.1	a	0.4	29	±	15.3	a	0.5	0.154	17.3	±	5.7	a	0.3	27.4	±	12.3	b	0.4	**0.006**	fragment (butenal)	(Buhr et al. 2002)
55.934	n.a.	non identified	5	±	0.3	a	0.1	5.1	±	0.3	a	0.1	5.2	±	0.3	a	0.1	5.3	±	0.3	a	0.1	0.231	5.1	±	0.3	a	0.1	5.3	±	0.3	a	0.1	0.063		
58.04	n.a.	non identified	2.9	±	1	a	0.3	3.4	±	1.5	a	0.4	4.4	±	2.3	a	0.5	6.5	±	4.7	a	0.7	0.074	2.9	±	1.1	a	0.4	5.8	±	3.6	b	0.6	**0.005**		
59.049	59.049	$C_3H_7O^+$	104.6	±	37.1	a	0.4	142.9	±	51.1	a	0.4	125.3	±	59.7	a	0.5	136.7	±	64	a	0.5	0.512	136.5	±	65.4	a	0.5	117.8	±	35.7	a	0.3	0.339	Acetone	(Kohn et al. 1960)
61.028	61.028	$C_2H_5O_2^+$	244.3	±	27.4	a	0.1	279	±	45.2	a	0.2	329.2	±	88.4	a	0.3	283	±	65.7	a	0.2	0.079	272.4	±	44.2	a	0.2	293.1	±	80.7	a	0.3	0.379	Acetic acid	(Paraskevopoulou et al. 2012; Kohn et al. 1960)
67.055	67.054	$C_5H_7^+$	1.2	±	0.5	a	0.4	1.2	±	0.6	a	0.5	1.5	±	0.7	a	0.5	2.1	±	1.5	a	0.7	0.198	1.1	±	0.5	a	0.5	1.9	±	1.2	a	0.6	**0.012**	fragment (pentenal)	(Buhr et al. 2002; Paraskevopoulou et al. 2012)
69.033	69.033	$C_4H_5O^+$	7	±	2.1	a	0.3	10.8	±	4.4	a	0.4	12.9	±	5.4	a	0.4	10	±	2.4	a	0.2	**0.039**	10.4	±	4.1	a	0.4	9.8	±	4.3	a	0.4	0.733		(Makhoul et al. 2014)
69.07	69.07	$C_5H_9^+$	21.5	±	11.6	a	0.5	22.1	±	20.3	a	0.9	26.6	±	14.1	a	0.5	25.5	±	13.4	a	0.5	0.891	17.1	±	11	a	0.6	31.1	±	14.9	b	0.5	0.006	fragment (pentanal)	(Buhr et al. 2002; Makhoul et al. 2014)
71.049	71.049	$C_4H_7O^+$	142.3	±	33.2	b	0.2	122.8	±	15.4	b	0.1	110.1	±	13.1	ab	0.1	88.5	±	23	a	0.3	**0.001**	122.8	±	24.6	a	0.2	109	±	33.6	a	0.3	0.197	butenal	(Paraskevopoulou et al. 2012)
73.065	73.065	$C_4H_9O^+$	213.8	±	70.3	a	0.3	201.7	±	76.8	a	0.4	230.4	±	105.3	a	0.5	252.7	±	107.3	a	0.4	0.705	181.7	±	69.6	a	0.4	270	±	85.2	b	0.3	**0.004**	n-butyraldehyde/methylpropanal	(Kohn et al. 1960) (Paraskevopoulou et al. 2012)
75.044	75.044	$C_3H_7O_2^+$	57.8	±	8.9	a	0.2	90.6	±	27.9	a	0.3	88.9	±	25.9	a	0.3	80.8	±	16.4	a	0.2	**0.017**	84.9	±	23.9	a	0.3	73.1	±	23.3	a	0.3	0.174	Propionic acid	(Annan et al. 2003; Kohn et al. 1960)
81.034	81.034.	$C_5H_5O^+$	13.5	±	3.2	a	0.2	21.8	±	8.5	a	0.4	24.1	±	8.7	a	0.4	19.9	±	4.5	a	0.2	**0.024**	19.9	±	6.7	a	0.3	19.4	±	8.4	a	0.4	0.859	cyclopentadienone	
81.069	81.07	$C_6H_9^+$	1.3	±	0.2	a	0.2	1.3	±	0.2	a	0.2	1.4	±	0.1	a	0.1	1.2	±	0.1	a	0.1	0.154	1.2	±	0.1	a	0.1	1.3	±	0.2	a	0.2	**0.02**	fragment (hexenal)	(Buhr et al. 2002; Aprea et al. 2007)
83.086	83.086	$C_6H_{11}^+$	1.8	±	0.5	a	0.3	1.5	±	0.5	a	0.3	2.9	±	1.1	b	0.4	2.3	±	0.6	ab	0.3	**0.002**	2.1	±	0.7	a	0.3	2.1	±	1	a	0.5	0.966	hexanol fragment	(Buhr et al. 2002)
85.028	85.028	$C_4H_5O_2^+$	3.2	±	1.2	a	0.4	4.3	±	1.6	a	0.4	5.5	±	1.9	a	0.3	4.6	±	1	a	0.2	**0.041**	4.5	±	1.2	a	0.3	4.2	±	1.9	a	0.5	0.64	2-(5H)-furanone	(Paraskevopoulou et al. 2012; Buhr et al. 2002)
85.065	n.a.	$C_5H_9O^+$	1.9	±	0.5	a	0.3	2.1	±	0.7	a	0.3	2.1	±	0.6	a	0.3	2.1	±	0.6	a	0.3	0.947	2.3	±	0.7	a	0.3	1.8	±	0.4	a	0.2	**0.041**	Cyclopentanone/ 3-Penten-2-one/ 2-Pentenal/ 2,3-Dihydro-4H-pyran	(Aprea et al. 2007)
87.081	87.08	$C_5H_{11}O^+$	20.2	±	12.4	a	0.6	21.2	±	17.5	a	0.8	29	±	19.7	a	0.7	49.6	±	45	a	0.9	0.132	16.2	±	10.7	a	0.7	44.8	±	33.9	b	0.8	**0.003**	isovaleraldehyde/2-,methylbutanal/pentanal	(Kohn et al. 1960; Paraskevopoulou et al. 2012; Schieberle and Grosch 1985)
89.06	89.06	$C_4H_9O_2^+$	200	±	46.5	b	0.2	172.7	±	19.2	b	0.1	157	±	18.3	ab	0.1	126.2	±	35.4	a	0.3	**0.001**	176.3	±	33.1	a	0.2	151.3	±	46.3	a	0.3	0.094	2-Methyl -propanoic acid/ethyl acetate	(Hansen and Hansen 1994b; Paraskevopoulou et al. 2012)
90.95	n.a.	non identified	1.2	±	0	a	0.0	1.2	±	0.1	a	0.1	1.3	±	0.1	a	0.1	1.3	±	0.1	a	0.1	**0.03**	1.2	±	0.1	a	0.1	1.3	±	0.1	a	0.1	0.581		
93.038	93.037.	$C_3H_9OS^+$	9.2	±	0.5	b	0.1	8.2	±	0.3	a	0.0	7.6	±	0.7	a	0.1	7.3	±	0.8	a	0.1	**0**	8.1	±	0.8	a	0.1	8.1	±	1.1	a	0.1	0.948	3-(methylthio)-1-propanol from methionine metabolism	
103.076	103.075	$C_5H_{11}O_2^+$	5.5	±	2.1	a	0.4	4.8	±	2.1	a	0.4	5.8	±	1.4	a	0.2	5.9	±	2.4	a	0.4	0.765	6.8	±	1.6	b	0.2	4.1	±	1.4	a	0.3	**0**	2-Methyl-butanoic acid /pentanoic acid/ethylpropionate	(Annan et al. 2003; Paraskevopoulou et al. 2012)

Loadings :

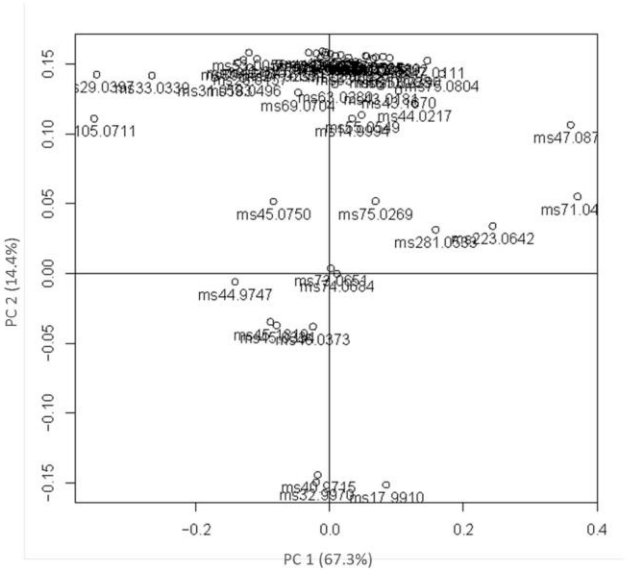
PC 2 (14.4%)
PC 1 (67.3%)
0.15
0.10
0.05
0.00
−0.05
−0.10
−0.15
−0.2
0.0
0.2
0.4
ms69.0704
ms44.0217
ms47.087
ms45.0750
ms75.0269
ms71.04
ms223.0642
ms44.9747
ms74.0684
ms45.0373
ms17.9910

PC variance :

	PC1	PC2	PC3	PC4	PC5	PC6	PC7	PC8	PC9
Variation	67.34%	14.44%	7.18%	2.38%	1.68%	1.32%	0.88%	0.77%	0.53%
Cumulative Variation	67.34%	81.78%	88.96%	91.34%	93.02%	94.34%	95.22%	95.98%	96.51%
	PC10	**PC11**	**PC12**	**PC13**	**PC14**	**PC15**	**PC16**	**PC17**	**PC18**
Variation	0.44%	0.39%	0.31%	0.27%	0.24%	0.21%	0.17%	0.15%	0.12%
Cumulative Variation	96.95%	97.34%	97.64%	97.91%	98.15%	98.37%	98.53%	98.69%	98.81%
	PC19	**PC20**	**PC21**	**PC22**	**PC23**	**PC24**	**PC25**	**PC26**	**PC27**
Variation	0.12%	0.10%	0.10%	0.09%	0.08%	0.07%	0.06%	0.05%	0.05%
Cumulative Variation	98.93%	99.03%	99.13%	99.21%	99.29%	99.36%	99.42%	99.47%	99.52%
	PC28	**PC29**	**PC30**	**PC31**	**PC32**	**PC33**	**PC34**	**PC35**	**PC36**
Variation	0.04%	0.04%	0.04%	0.03%	0.03%	0.03%	0.03%	0.02%	0.02%
Cumulative Variation	99.56%	99.60%	99.64%	99.67%	99.70%	99.73%	99.76%	99.78%	99.80%
	PC37	**PC38**	**PC39**	**PC40**	**PC41**	**PC42**	**PC43**	**PC44**	**PC45**
Variation	0.02%	0.02%	0.02%	0.02%	0.02%	0.01%	0.01%	0.01%	0.01%
Cumulative Variation	99.83%	99.84%	99.86%	99.88%	99.90%	99.91%	99.93%	99.94%	100%

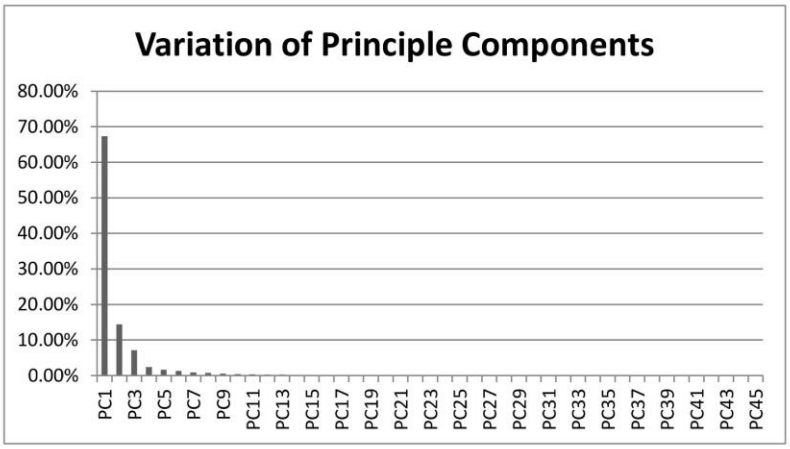

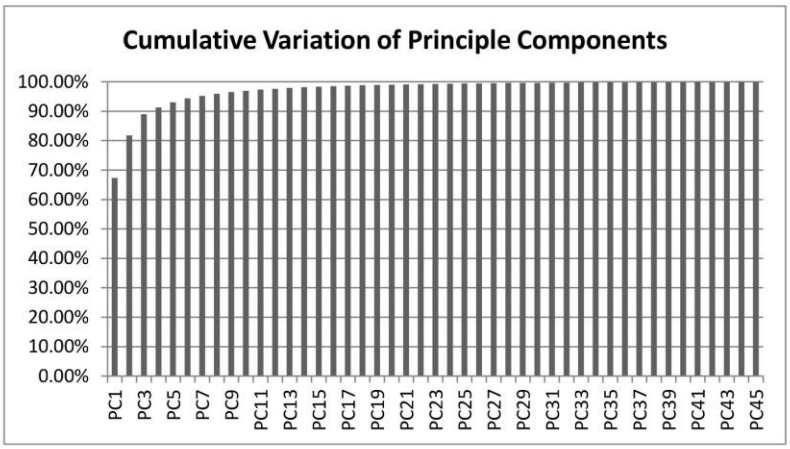

Appendix 3. ANOVA table of baked bread samples (section 3.4)

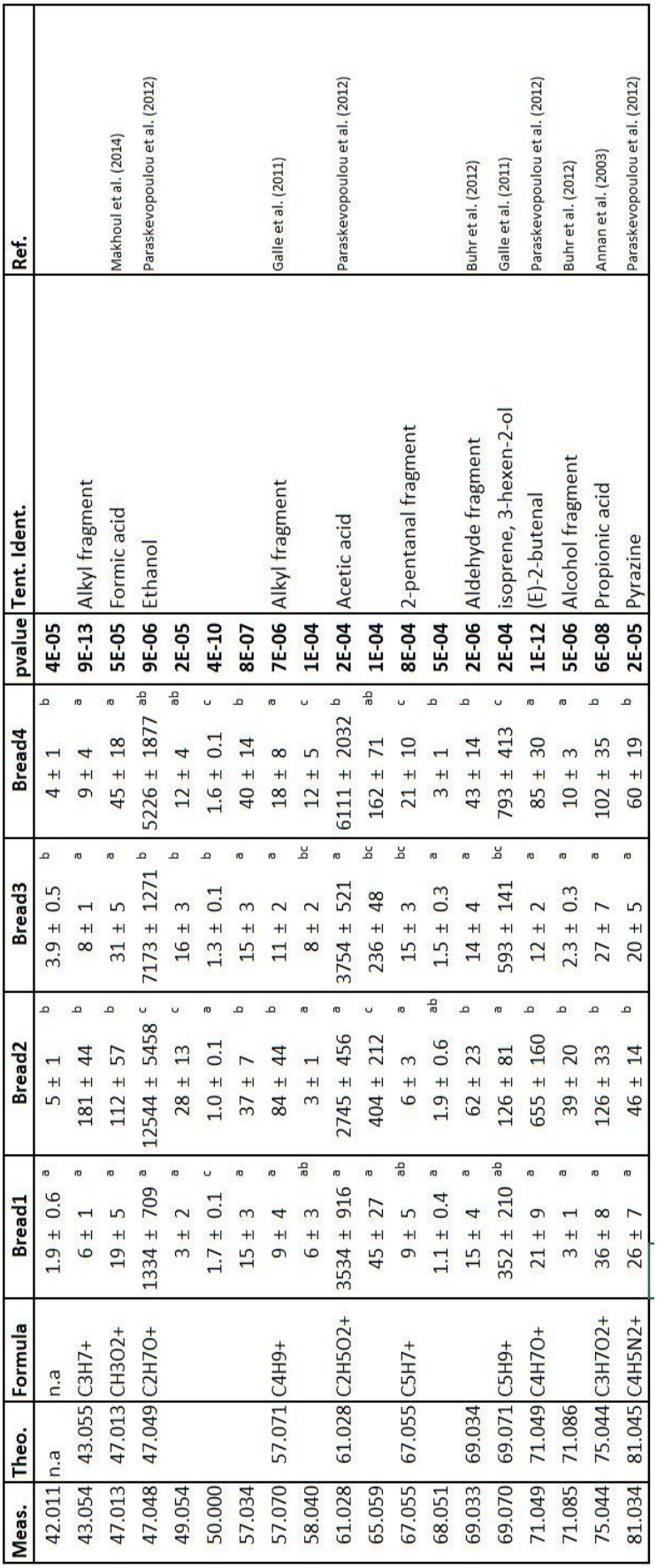

Meas.	Theo.	Formula	Bread1		Bread2		Bread3		Bread4		pvalue	Tent. Ident.	Ref.
42.011	n.a	n.a	1.9 ± 0.6	a	5 ± 1	b	3.9 ± 0.5	b	4 ± 1	b	4E-05		
43.054	43.055	C3H7+	6 ± 1	a	181 ± 44	b	8 ± 1	a	9 ± 4	a	9E-13	Alkyl fragment	
47.013	47.013	CH3O2+	19 ± 5	a	112 ± 57	b	31 ± 5	a	45 ± 18	a	5E-05	Formic acid	Makhoul et al. (2014)
47.048	47.049	C2H7O+	1334 ± 709	a	12544 ± 5458	c	7173 ± 1271	b	5226 ± 1877	ab	9E-06	Ethanol	Paraskevopoulou et al. (2012)
49.054			3 ± 2	a	28 ± 13	c	16 ± 3	b	12 ± 4	ab	2E-05		
50.000			1.7 ± 0.1	c	1.0 ± 0.1	a	1.3 ± 0.1	b	1.6 ± 0.1	c	4E-10		
57.034			15 ± 3	a	37 ± 7	b	15 ± 3	a	40 ± 14	b	8E-07		
57.070	57.071	C4H9+	9 ± 4	a	84 ± 44	b	11 ± 2	a	18 ± 8	a	7E-06	Alkyl fragment	Galle et al. (2011)
58.040			6 ± 3	ab	3 ± 1	a	8 ± 2	bc	12 ± 5	c	1E-04		
61.028	61.028	C2H5O2+	3534 ± 916	a	2745 ± 456	a	3754 ± 521	a	6111 ± 2032	b	2E-04	Acetic acid	Paraskevopoulou et al. (2012)
65.059			45 ± 27	a	404 ± 212	c	236 ± 48	bc	162 ± 71	ab	1E-04		
67.055	67.055	C5H7+	9 ± 5	ab	6 ± 3	a	15 ± 3	bc	21 ± 10	c	8E-04	2-pentanal fragment	
68.051			1.1 ± 0.4	a	1.9 ± 0.6	ab	1.5 ± 0.3	a	3 ± 1	b	5E-04		
69.033	69.034		15 ± 4	a	62 ± 23	b	14 ± 4	a	43 ± 14	b	2E-06	Aldehyde fragment	Buhr et al. (2012)
69.070	69.071	C5H9+	352 ± 210	ab	126 ± 81	a	593 ± 141	bc	793 ± 413	c	2E-04	isoprene, 3-hexen-2-ol	Galle et al. (2011)
71.049	71.049	C4H7O+	21 ± 9	a	655 ± 160	b	12 ± 2	a	85 ± 30	a	1E-12	(E)-2-butenal	Paraskevopoulou et al. (2012)
71.085	71.086		3 ± 1	a	39 ± 20	b	2.3 ± 0.3	a	10 ± 3	a	5E-06	Alcohol fragment	Buhr et al. (2012)
75.044	75.044	C3H7O2+	36 ± 8	a	126 ± 33	b	27 ± 7	a	102 ± 35	b	6E-08	Propionic acid	Annan et al. (2003)
81.034	81.045	C4H5N2+	26 ± 7	a	46 ± 14	b	20 ± 5	a	60 ± 19	b	2E-05	Pyrazine	Paraskevopoulou et al. (2012)

Appendix 3. (continued)

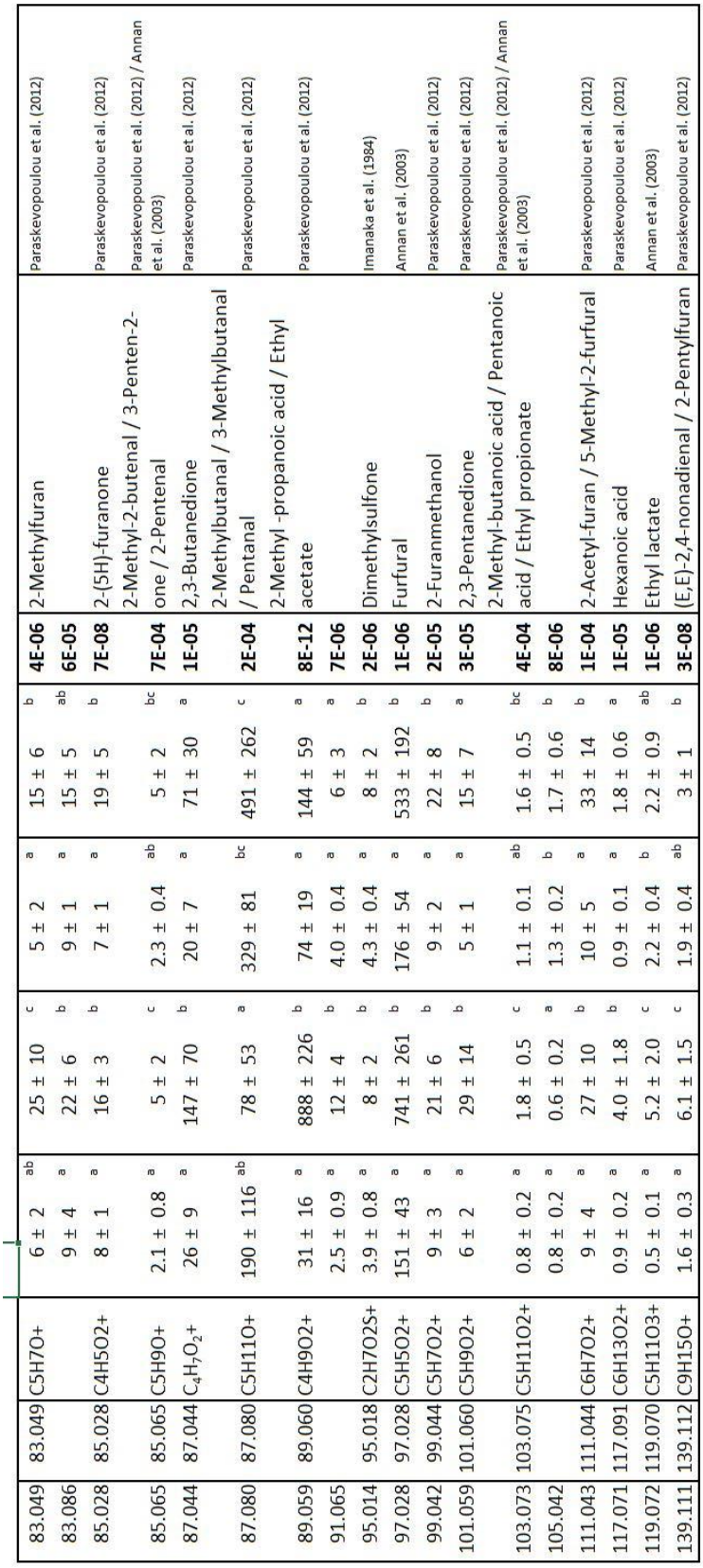

83.049	83.049	C5H7O+	6 ± 2	ab	25 ± 10	c	5 ± 2	a	15 ± 6	b	4E-06	2-Methylfuran	Paraskevopoulou et al. (2012)
83.086			9 ± 4	a	22 ± 6	b	9 ± 1	a	15 ± 5	ab	6E-05		
85.028	85.028	C4H5O2+	8 ± 1	a	16 ± 3	b	7 ± 1	a	19 ± 5	b	7E-08	2-(5H)-furanone	Paraskevopoulou et al. (2012)
85.065	85.065	C5H9O+	2.1 ± 0.8	a	5 ± 2	c	2.3 ± 0.4	ab	5 ± 2	bc	7E-04	2-Methyl-2-butenal / 3-Penten-2-one / 2-Pentenal	Paraskevopoulou et al. (2012) / Annan et al. (2003)
87.044	87.044	$C_4H_7O_2$+	26 ± 9	a	147 ± 70	b	20 ± 7	a	71 ± 30	a	1E-05	2,3-Butanedione	Paraskevopoulou et al. (2012)
87.080	87.080	C5H11O+	190 ± 116	ab	78 ± 53	a	329 ± 81	bc	491 ± 262	c	2E-04	2-Methylbutanal / 3-Methylbutanal / Pentanal	Paraskevopoulou et al. (2012)
89.059	89.060	C4H9O2+	31 ± 16	a	888 ± 226	b	74 ± 19	a	144 ± 59	a	8E-12	2-Methyl -propanoic acid / Ethyl acetate	Paraskevopoulou et al. (2012)
91.065			2.5 ± 0.9	a	12 ± 4	b	4.0 ± 0.4	a	6 ± 3	a	7E-06		
95.014	95.018	C2H7O2S+	3.9 ± 0.8	a	8 ± 2	b	4.3 ± 0.4	a	8 ± 2	b	2E-06	Dimethylsulfone	Imanaka et al. (1984)
97.028	97.028	C5H5O2+	151 ± 43	a	741 ± 261	b	176 ± 54	a	533 ± 192	b	1E-06	Furfural	Annan et al. (2003)
99.042	99.044	C5H7O2+	9 ± 3	a	21 ± 6	b	9 ± 2	a	22 ± 8	b	2E-05	2-Furanmethanol	Paraskevopoulou et al. (2012)
101.059	101.060	C5H9O2+	6 ± 2	a	29 ± 14	b	5 ± 1	a	15 ± 7	a	3E-05	2,3-Pentanedione	Paraskevopoulou et al. (2012)
103.073	103.075	C5H11O2+	0.8 ± 0.2	a	1.8 ± 0.5	c	1.1 ± 0.1	ab	1.6 ± 0.5	bc	4E-04	2-Methyl-butanoic acid / Pentanoic acid / Ethyl propionate	Paraskevopoulou et al. (2012) / Annan et al. (2003)
105.042			0.8 ± 0.2	a	0.6 ± 0.2	a	1.3 ± 0.2	b	1.7 ± 0.6	b	8E-06		
111.043	111.044	C6H7O2+	9 ± 4	a	27 ± 10	b	10 ± 5	a	33 ± 14	b	1E-04	2-Acetyl-furan / 5-Methyl-2-furfural	Paraskevopoulou et al. (2012)
117.071	117.091	C6H13O2+	0.9 ± 0.2	a	4.0 ± 1.8	b	0.9 ± 0.1	a	1.8 ± 0.6	a	1E-05	Hexanoic acid	Paraskevopoulou et al. (2012)
119.072	119.070	C5H11O3+	0.5 ± 0.1	a	5.2 ± 2.0	c	2.2 ± 0.4	b	2.2 ± 0.9	ab	1E-06	Ethyl lactate	Annan et al. (2003)
139.111	139.112	C9H15O+	1.6 ± 0.3	a	6.1 ± 1.5	c	1.9 ± 0.4	ab	3 ± 1	b	3E-08	(E,E)-2,4-nonadienal / 2-Pentylfuran	Paraskevopoulou et al. (2012)

Appendix 4. International Conferences where our results were shared and discussed with the scientific community

November 2015 7th **RAFA International Conference (Czech Republic)**
International Symposium on the Recent Advances in Food Analysis, organized by the University of Chemistry and Technology in Prague and Rikilt Wageningen.
Oral presentation: Proton-Transfer-Reaction Mass Spectrometry for the Study of the Production of Volatile Compounds and the Effect of Flour, Yeast and their Interaction During the Bread-making Process.

October 2013 **4th MS Food Day (Italy)**
Organized by D.A.Re. – Agrofood Technology Cluster, the Division of Mass Spectrometry of the Italian Chemical Society, Bonassisa Lab srl, the Institute of Sciences of Food Production of the NRC and the University of Foggia.
Oral presentation: Rapid Non-Invasive Quality Control of Semi-Finished Products for the Food Industry by Direct Injection Mass Spectrometry Headspace Analysis: the Case of Milk Powder, Whey Powder, and Anhydrous Milk Fat
Oral presentation: Characterization of the Volatile Compounds Constituting Mascarpone Cheese Aroma

September 2015 **YEAST 2015 Conference (Italy)**
27th International Conference on Yeast Genetics and Molecular Biology
Oral presentation: PTR-ToF-MS and bioprocesses: Potential in monitoring VOCs release by eukaryotic microbes

June 2015 **MASSA 2015 International Conference (Italy)**
Organized by the Italian Society of Mass Spectrometry, fellowship awarded.
Oral presentation: Advances in PTR-MS.
Poster: Ethylene: Absolute real-time high-sensitivity detection with PTR/SRI-MS.

May 2015 **FABE 2015 International Conference (Greece)**
International Conference on Food and Biosystems Engineering,
Oral presentation: PTR-ToF-MS and food bioprocesses: potential in monitoring VOCs release by starter cultures during food fermentation

October 2013 **3rd MS Food Day (Italy)**
Organized by the Fondazione Edmund Mach
Poster: Ethylene: Absolute real-time high-sensitivity detection with PTR/SRI-MS.
Poster: Proton-transfer-reaction mass spectrometry for the study of the production of volatile compounds by bakery yeast starters

Appendix 5. Certificates of main training courses and prizes received during my PhD

PROTON TRANSFER REACTION – MASS SPECTROMETRY

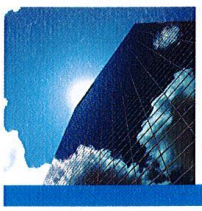

HANDS-ON PTR-MS 2013

> PTR-MS Training Certificate

The 2nd PIMMS PTR-MS training course, 3. - 4. 10. 2013, Innsbruck, Austria.

IONICON hereby certifies that

Salim Makhoul

has participated in a comprehensive PTR-MS training, covering the following subjects:

Theory on
Analytical Mass Spectrometry
PTR-MS and Related Topics

Practice on
Professional Maintenance Training,
Measurement, Calibration and
Instrument Optimization

Innsbruck, October 4, 2013

Dr. Philipp Sulzer

Head of Applied Science Team
IONICON Analytik GmbH

THE SOLUTION FOR REAL-TIME TRACE GAS ANALYSIS

IONICON

Droevendaalsesteeg 1
6708 PB Wageningen
Netherlands

May 13, 2015

To whom it may concern:

Herewith I confirm that Salim Makhoul, PhD student at the Fondazione Edmund Mach, has attended the course "Experimental design and linear modelling", held in 2013 in San Michele all'Adige. The six-hour course (three sessions of two hours) gave a very short introduction to the basic statistical topics mentioned in the title. No exam was taken.

Kind regards,

Ron Wehrens
Business Manager Biometris
Wageningen UR
Netherlands

FONDAZIONE EDMUND MACH

Certificate of Attendance

PTR-MS DATA ANALYSIS AND MULTIVARIATE STATISTICS COURSE
October 7-8, 2013, San Michele all'Adige – Italy

We hereby Certify that

Salim Makhoul

attended
the PTR-MS DATA ANALYSIS AND MULTIVARIATE STATISTICS COURSE
that was held in San Michele all'Adige (Italy) on October 9-11, 2013.

For and on behalf of the Organising Committee
[Luca Cappellin]

Certificate of attendance

To Whom it may concern,

herewith I confirm that **Salim Makhoul**, PhD student at the University of Burgundy and the University of Balamand, has attended the course "***Data Mining: learning from large datasets***", held in 2015 at the University of Innsbruck. The *24*-hour course gave an insight on experimental design, parametric and non-parametric statistical tests, p-values, multiple testing corrections, correlation, chi-squred test, simple and multiple linear regression, principal components analysis. No exam was taken.

Kind regards,
Luca Cappellin, PhD

CENTRO RICERCA e INNOVAZIONE
Fondazione Edmund Mach

University of Burgundy and the University of Balamand

Trento, May 14^{th} 2015

To whom it may concern,

With this present letter I declare that **Salim Makhoul** attended the following training seminars at the Research and Innovation Centre - Fondazione Edmund Mach

- "PTR-MS data analysis and Multivariate Statistics" - October 8^{th} 2013 - 3 hours
- "Exploratory Multivariate Analysis" - June $4/11/18^{th}$ 2013 - 6 hours

Yours Sincerely,

Pietro Franceschi, PhD

Research and Innovation Centre - Fondazione Edmund Mach - Biostatistics and Data Management
Via E. Mach, 1 38010 S. Michele all'Adige (TN) - ITALY
pietro.franceschi@fmach.it - tel: +39-0461-615556
http://cri.fmach.eu/

SRA Instruments S.p.A. • Viale Assunta, 101 • 20063 Cernusco sul Naviglio (MI)

Certificate of training:

This certificate is awarded to:

Makhoul Salim

Has partecipated at the training to: **GCxGC analytical technique with flow modulator, Software Analysis Qualitative and Quantitative GC Image and GC Projects** from January 21,2015 to January 22, 2015 (16 hours).

San Michele All'Adige 22 January 2015

Trainer
Dr. Daniele Morosini
SRA Instruments S.p.A.
Post Sales Technical Engineer
Application Specialist

SRA INSTRUMENTS Micro-GC & GC Solutions

Agilent Technologies
Channel Partner

Waiting for Fame RESEARCHER OPEN MIC

Premio Giuria Popolare

Attestato di Partecipazione

Researcher Open Mic

Salim Makhoul

San. Michele a/A , 19 febbraio 2013

Complimenti, sei pronto per FameLab... partecipa anche tu!

museo delle scienze · FONDAZIONE EDMUND MACH · FONDAZIONE BRUNO KESSLER · UNIVERSITÀ DEGLI STUDI DI TRENTO · COSBI · CENTRO SERVIZI CULTURALI S.CHIARA · ITAS ASSICURAZIONI · Rai Sede di Trento